

University of St Andrews



Full metadata for this thesis is available in
St Andrews Research Repository
at:

<http://research-repository.st-andrews.ac.uk/>

This thesis is protected by original copyright

The expression and activities of histone deacetylase
HDACm through oogenesis and early embryogenesis
of *Xenopus laevis*.

By

James T. P. Ryan

School of Biology, Division of Cell and Molecular Biology
University of St. Andrews

Submitted for the degree of Ph.D.

On 29-08-2000

Supervisor: Dr. John Sommerville



Declarations

I, James Ryan, hereby certify that this thesis, which is approximately 48 000 words in length, has been written by me, that it is the record of work carried out by me and that it has not been submitted in any previous application for a higher degree.

date 29-8-00 signature of candidate

I was admitted as a research student in September, 1997 and as a candidate for the degree of PhD in September, 1998; the higher study for which this is a record was carried out in the University of St. Andrews between 1997 and 2000.

date 29-8-00 signature of candidate

I hereby certify that the candidate has fulfilled the conditions of the resolutions and regulations appropriate for the degree of PhD in the University of St. Andrews and that the candidate is qualified to submit this thesis in application for that degree.

date 29/8/00 signature of supervisor

In submitting this thesis to the University of St. Andrews I understand that I am giving permission for it to be made available for use in accordance with the regulations of the University Library for the time being in force, subject to any copyright vested in the work not being affected thereby. I also understand that the title and abstract will be published, and that a copy of the work may be made and supplied to any *bona fide* library or research worker.

date 29-8-00 signature of candidate

Acknowledgements

I would like to thank my supervisor, John Sommerville, for his continual help, and David Smillie for his practical suggestions. Additional thanks go to my family and friends for their support and encouragement over the past three years.

Index – Table of Contents

| | Page no. |
|--|----------|
| Figure Index | vii |
| Abbreviations | x |
| Abstract | xv |
| 1. Introduction | 1 |
| 1.1. Chromatin | 2 |
| 1.1.1. Histone proteins | 4 |
| 1.1.2. The nucleosome | 6 |
| 1.1.3. Nucleosome formation | 10 |
| 1.1.4. Histone-fold/DNA interactions within the nucleosome | 11 |
| 1.2. Histone modifications | 12 |
| 1.2.1. Acetylation state of histone proteins and the condition of chromatin | 15 |
| 1.3. Control of acetylation state | 20 |
| 1.3.1. Histone acetyltransferases | 20 |
| 1.3.2. Histone deacetylases | 22 |
| (i) Inhibitors of histone deacetylases | 24 |
| (ii) Sub-cellular localization | 26 |
| (iii) Histone deacetylase complexes and associated proteins | 31 |
| (A) Euchromatin and heterochromatin; histone proteins, deacetylation, silencing proteins and their roles in the transition between chromatin states. | 31 |
| (B) Histone deacetylase and transient inhibition of Transcription. | 37 |
| (C) Histone deacetylase and stable inheritance of transcriptional repression | 43 |
| 1.4. Synthesis and incorporation of histone isoforms during early <i>Xenopus</i> development | 45 |
| 1.5. <i>Xenopus</i> histone deacetylase, HDACm | 49 |
| 1.5.1. Aims of the project | 50 |

2. Materials & Methods

| | |
|---|-----|
| 2.1. <i>Xenopus laevis</i>, bacteria, plasmids and fusion proteins | 51 |
| 2.1.1. <i>Xenopus laevis</i> | 51 |
| 2.1.2. Bacteria | 55 |
| 2.1.3. Plasmid vectors | 57 |
| 2.2. Plasmid DNA extraction, purifications and insertion of foreign DNA. Use of plasmid DNA to transform bacterial cells and express inserted DNA. | 64 |
| 2.2.1. Preparation of plasmid DNA by alkaline lysis | 64 |
| 2.2.2. Preparation of Plasmid DNA with the Wizard [®] <i>Plus</i> DNA purification system | 66 |
| 2.2.3a. Polymerase chain reaction | 68 |
| 2.2.3b. Site-Directed mutagenesis by PCR. | 69 |
| 2.2.4. Restriction digest of DNA | 70 |
| 2.2.5. Agarose gel electrophoresis | 71 |
| 2.2.6. Purification of DNA excised from DNA gels | 72 |
| 2.2.7. Ligation of DNA fragments | 74 |
| 2.2.8. Transformation of competent cells | 74 |
| 2.2.9. Synthesis of capped mRNA from plasmid DNA | 75 |
| 2.2.10. Denaturing RNA gel | 76 |
| 2.3. Protein sources, treatments, separation and detection | 78 |
| 2.3.1. Expression and purification of fusion proteins | 78 |
| 2.3.2. Expression of mRNA in rabbit reticulocyte lysate system | 81 |
| 2.3.3. Oocytes | 82 |
| 2.3.4. Collection of embryos | 84 |
| 2.3.5. Fractionation of oocytes | 84 |
| 2.3.6. Freon extraction of yolk protein and lipid from oocytes and fractions | 87 |
| 2.3.7. Progesterone induction of oocyte maturation | 88 |
| 2.3.8. Dephosphorylation of oocyte material | 88 |
| 2.3.9. Extracting histones from oocytes and embryos | 89 |
| 2.3.10. Characterisation of HDACm, its activity, post-translational modifications & partner proteins | 89 |
| 2.3.11. SDS PAGE | 98 |
| 2.3.12a. Visualisation of proteins by Coomassie staining | 100 |
| 2.3.12b. Visualisations of proteins by silver staining | 101 |
| 2.3.13. Western blotting | 101 |
| 2.3.14. Antibodies | 104 |
| 2.3.15. Extracting IgG from serum | 106 |
| 2.3.16. Immunostaining of ovarian and embryo sections | 106 |
| 2.3.17. Whole mount immunostaining of oocytes and nuclei | 108 |
| 2.3.18. Immunostaining lampbrush chromosomes | 109 |
| 2.3.19. Immunostaining of karyomeres | 111 |

| | |
|--|-----|
| 3. Results | |
| 4. 3.1. HDACm and oocytes | 113 |
| 3.1.1. Sequence, size and levels of HDACm protein | 114 |
| 3.1.2. Sub-cellular location of HDACm protein in oocytes | 116 |
| 3.1.3. HDACm is a component of a multimolecular complex | 122 |
| 3.1.4. Examination of the interactions of HDACm with previously identified deacetylase partners | 126 |
| 3.1.5. Histone deacetylase activity in the <i>Xenopus</i> oocyte nucleus | 135 |
| 3.1.6. Acylation of <i>Xenopus</i> histone deacetylase HDACm | 142 |
| 3.2. HDACm and embryos | 147 |
| 3.2.1. Expression of HDACm and RbAp48 in early embryos | 149 |
| 3.2.2. Location of HDACm and candidate deacetylase associated proteins within the embryo | 152 |
| 3.2.3. HDACm is a component of a multimolecular complex that changes in size through blastula | 158 |
| 3.2.4. Detection of <i>in vivo</i> HDACm activity | 163 |
| 3.3. Expression of recombinant HDACm in oocytes | 171 |
| 3.3.1. Injection of HDACm (Ab21) mRNA and protein | 173 |
| 3.3.2. Injection of T7 epitope tagged HDACm DNA | 181 |
| 3.3.3. Injection of DNA and protein from Ab21 sub-clones | 187 |
| 3.4. Phosphorylation of HDACm | 196 |
| 3.4.1. GST- ΔV phosphorylation, nuclear import and α -importin | 201 |
| 3.4.2. GST- ΔV and phosphorylation. Point mutation analysis of the <i>in vitro</i> and <i>in vivo</i> roles of phosphorylation on nuclear import and protein-protein interactions of GST- ΔV . | 207 |
| 4. Discussion | 217 |
| 4.1. HDACm and its activity in early development | 222 |
| 4.1.1. HDACm activity in oogenesis and pre-MBT embryogenesis | 222 |
| 4.1.2. HDACm activity in post-MBT embryogenesis | 225 |
| 4.2. HDACm complex through early development | 227 |
| 4.2.1. HDAC complexes in early <i>Xenopus</i> development | 228 |
| 4.2.2. The RbAp48 and HDACm interaction | 229 |
| (A) HDACm interacts with two molecules of RbAp48. | 230 |
| (B) The interaction of HDACm and RbAp48 is dependant on zinc. | 233 |
| 4.2.3. <i>Xenopus</i> oocyte HDAC complexes | 235 |
| (A) Differences in opinion | 235 |
| (B) Differences resolved | 239 |
| 4.3. Regulation of HDACm nuclear import in oocytes | 243 |
| 4.3.1. Acylation and cytoplasmic retention | 244 |
| 4.3.2. Phosphorylation and nuclear uptake | 245 |
| 4.4. Over-expressing HDACm during oogenesis | 253 |
| 4.5. Summary | 255 |
| 4.6. Further work | 259 |

Appendices

| | |
|--|-----|
| Appendix A: HDACm amino acid and DNA sequences | 261 |
| Appendix B: <i>Xenopus</i> RbAp48 amino acid and DNA sequences | 262 |
| Appendix C: <i>Xenopus</i> MeCP2 amino acid and DNA sequences | 263 |
| Appendix D: <i>Xenopus</i> Sin3 amino acid and DNA sequences | 264 |
| Appendix E: <i>Xenopus</i> importin- α amino acid and DNA sequences | 266 |
| Appendix F: <i>Xenopus</i> RPD3 amino acid and DNA sequences | 267 |

Bibliography

268

Figure Index

| | Page no. |
|---|----------|
| Figure 1: The histone fold | 3 |
| Figure 2: Representation of the molecular structure of histone proteins and their interactions with each other and the DNA backbone. | 5 |
| Figure 3: Nucleosome core particle | 7 |
| Figure 4: Tripartite organisation of the nucleosome and its interactions with histone H1 and DNA. | 9 |
| Figure 5: N-terminal tails of the core histones | 13 |
| Figure 6: Model of the protein-DNA interactions that take place at the yeast silent mating-type loci. | 33 |
| Figure 7: Model of the mechanism by which CAF-1 contributes to formation of stable heterochromatin. | 35 |
| Figure 8: Histone deacetylase can be found in complexes of differing composition. | 39 |
| Figure 9: <i>Xenopus</i> oocyte stages and summary of key features of each stage. | 52 |
| Figure 10: Sequence of intracellular signals that accompany resumption of meiosis and egg activation <i>Xenopus</i> oocytes | 54 |
| Figure 11: The main histological stages in early <i>Xenopus</i> embryogenesis. | 56 |
| Figure 12: Composition of pBluescript plasmid. | 58 |
| Figure 13: Composition of pGEX 4T plasmid series. | 60 |
| Figure 14: Composition of GFP plasmid pCS2*mycGFP-NOTb4-tail. | 62 |
| Figure 15: Composition and derivation of pCGT7 plasmid. | 63 |
| Figure 16: Peptides used to produce polyclonal antisera. | 105 |
| Figure 17: Sequence and size of HDACm protein. | 115 |
| Figure 18: Levels of HDACm protein at different stages of development. | 117 |
| Figure 19: Analysis of antibody specificity. | 119 |
| Figure 20: Characterisation of sub-cellular localisation of HDACm protein in oocytes. | 121 |
| Figure 21: HDACm is found in complexes of increasing size as oocytes mature. | 123 |

| | Page no. |
|---|----------|
| Figure 22: Investigation of the interactions of HDACm with previously identified HDAC partners. | 125 |
| Figure 23: RbAp48 interacts with diacetylated histone H4 in the oocyte nucleus. | 129 |
| Figure 24: Components of the HDACm complex in stage VI oocyte nuclei. | 134 |
| Figure 25: Characterisation of HDACm enzyme activity in oocytes and embryos. | 137 |
| Figure 26: Histone acetylation and protection from histone deacetylase activity in the oocyte nucleus. | 140 |
| Figure 27: HDACm exists in a modified form in the oocyte cytoplasm. | 144 |
| Figure 28: The cytoplasmic modification of HDACm is removed by treatment with hydroxylamine. | 146 |
| Figure 29: Levels of HDACm and RbAp48 proteins in early embryos. | 151 |
| Figure 30: Localisation of nuclear proteins in mid-blastula embryos. | 155 |
| Figure 31: Localisation of nuclear proteins in individual karyomeres of mid-blastula embryos. | 157 |
| Figure 32: HDACm is found in complexes of differing sizes through blastula. | 160 |
| Figure 33: Co-precipitation of proteins associated with HDACm in embryos | 162 |
| Figure 34: Histone acetylation state during early development. | 166 |
| Figure 35: <i>In vivo</i> assay of histone deactylase activity in early embryos | 170 |
| Figure 36: Map of AB21 cDNA and its sub-clones. | 172 |
| Figure 37: Nuclear import of exogenous HDACm (AB21 protein). | 174 |
| Figure 38: Interaction of exogenous ³⁵ S-labelled AB21 protein in the oocyte nucleus. | 177 |
| Figure 39: Morphology and immunostaining of lampbrush chromosomes isolated from AB21 and ΔH injected stage IV oocytes. | 179 |
| Figure 40: Nuclear import of T7-AB21 protein and its incorporation into protein complexes. | 182 |
| Figure 41: Nuclear location of T7-AB21 protein. | 185 |

| | Page no. |
|--|----------|
| Figure 42: Nuclear import of GST- Δ V fusion protein and its incorporation into protein complexes. | 190 |
| Figure 43: Cellular location of GST- Δ V and GFP- Δ V fusion proteins. | 193 |
| Figure 44: Nuclear import of GST- Δ V is dependent upon α importin. | 195 |
| Figure 45: HDACm is phosphorylated in the nucleus of large oocytes. it is dephosphorylated as the oocyte matures in response to progesterone. | 197 |
| Figure 46: <i>In vitro</i> phosphorylation of HDACm fusion proteins. | 199 |
| Figure 47: Peptide sequence of protein digest fragments of GST- Δ V that are phosphorylated <i>in vitro</i> . | 202 |
| Figure 48: Sequence of bacterially expressed GST- Δ V fusion protein and the location of functional sequences within this protein. | 204 |
| Figure 49: Nuclear import of GST- Δ V and the release of GST- Δ V from α -importin is dependent upon phosphorylation. | 206 |
| Figure 50: <i>In vitro</i> and <i>in vivo</i> phosphorylation of GST- Δ V fusion proteins. | 208 |
| Figure 51: Mutant GST- Δ V fusion proteins can be components of multi-molecular complexes. | 212 |
| Figure 52: Mutant GST- Δ V fusion proteins and their interaction with RbAp48. | 214 |
| Figure 53: The relationship between gene expression, histone H4 acetylation and linker histone type during early <i>Xenopus</i> development. | 219 |
| Figure 54: The domains of HDACm that interact with RbAp48 compared with the domains of xRPD3 that interact with RbAp48. | 231 |
| Figure 55: Comparison of amino acid sequence of <i>Xenopus</i> histone deacetylase HDACm with xRPD3. | 237 |
| Figure 56: Mechanisms by which nuclear factors may be retained in the cytoplasm. | 246 |
| Figure 57: Regulation of HDACm nuclear import and importin- α binding by acylation, phosphorylation and acetylation. | 254 |

Abbreviations

| | |
|------|---|
| AL | Annulate lamellae |
| Amps | Amperes |
| AMPS | Ammonium per(oxy)sulphate |
| AP | Alkaline phosphatase |
| ATP | Adenosine triphosphate |
| bHLH | Basic Helix-Loop-Helix |
| bp | base pair(s) |
| BSA | Bovine serum albumin |
| cDNA | Complimentary DNA (synthesised from mRNA) |
| CAC | Chromatin assembly complex |
| CAF | Chromatin assembly factor |
| CER | Cortical endoplasmic reticulum |
| CG | Chorionic Gonadotrophin |
| Ci | Curie |
| CKII | Protein kinase CKII (casein kinase II) |
| CMFM | Calcium and magnesium free medium |
| CMV | Cytomegalovirus |
| cpm | Counts per minute |
| CT | Carboxy terminal |
| CTP | Cytidine triphosphate |
| °C | Degrees centigrade |
| DAPI | 4,6-diamidino-2phenylindole dihydrochloride |
| dATP | Deoxy adenosine triphosphate |
| dCTP | Deoxy cytidine triphosphate |
| dGTP | Deoxy guanosine triphosphate |
| dTTP | Deoxy thymidine triphosphate |
| DNA | Deoxyribonucleic acid |

| | |
|-------------------|--|
| DNase | Deoxyribonuclease |
| DEPC | Diethylpyrocarbonate |
| dpm | Disintegrations per minute |
| dH ₂ O | Distilled water |
| DMSO | Dimethylsulphoxide |
| DTT | Dithiothreitol |
| E | Eluted |
| ECL | Enhanced chemiluminescence |
| EDTA | Ethylenediaminetetraacetic acid |
| FCS | Foetal calf serum |
| FITC | Fluorescein isothiocyanate |
| g | Grammes |
| GFP | Green fluorescent protein |
| GST | Glutathione S-transferase |
| GTP | Guanosine triphosphate |
| GVBD | Germinal vesicle break down |
| h | hour(s) |
| HA | Hydroxalamine |
| HAT | Histone acetyltransferase |
| HDAC | Histone deacetylase |
| HDACm | Histone deacetylase expressed during early development of <i>Xenopus</i> from a stored maternal message. |
| HEPES | N-[2-hydroxyethyl]piperazine-N'[2-sulphonic acid] |
| HMG | High mobility group protein |
| HP1 | Heterochromatin protein 1 |
| IgG | Immunoglobulin G |
| IPTG | Isopropyl- β -D-thiogalactopyranoside |
| K | Lysine |

| (k/m/ μ /n/p) | (kilo/milli/micro/nano/pico) |
|-------------------|--------------------------------------|
| kb | kilobase |
| kD | Kilo dalton |
| λ | Lambda |
| l | Litre |
| LB | Luria broth |
| LTR | Long terminal repeat |
| M | Molar concentration |
| MAT | Mating type locus (yeast) |
| MBT | Mid-blastula transition |
| MECP2 | Methyl CpG binding protein 2 |
| min | minute |
| MMTV | Mouse mammary tumour virus |
| MOPS | 3[N Morpholin] propanesulphonic acid |
| mRNA | Messenger RNA |
| MS222 | Tricane-methane sulphonate |
| NLS | Nuclear localisation signal |
| NP-40 | Nonidet P-40 |
| NPC | Nuclear pore complex |
| NT | Amino terminus |
| OD | Optical density |
| ORC | Origin of replication complex |
| ORF | Open reading frame |
| PAGE | Polyacrylamide gel electrophoresis |
| PBS | Phosphate buffered saline |
| PcG | Polycomb-group |
| PCR | Polymerase chain reaction |
| PEV | Position effect variegation |
| PKC | Protein kinase C |

| | |
|-----------------------|--|
| PMSF | Phenylmethylsulphonyl fluoride |
| PVP | Polyvinylpyrrolidon |
| R | Retained |
| ΔR | GST-HD ΔR fusion protein, subclone of HDACm |
| $\Delta R / \Delta H$ | GST-HD $\Delta R / \Delta H$ fusion protein, subclone of |
| RB | Retinoblastoma protein |
| RbAp48/46 | Retinoblastoma associated protein 48/46 |
| RNA | Ribonucleic acid |
| RNase | Ribonuclease |
| RPD3 | Reduced potassium dependence protein 3 (HDAC) |
| SDS | Sodium dodecylsulphate |
| sec | Second(s) |
| SN | Supernatant |
| SNF | Sucrose non-fermenting |
| SIN3 | SWI independent protein 3 |
| SIR | Silent information regulator |
| SU | Subunit |
| SWI | Switch (yeast ATPase) |
| TAE | Tris-acetate EDTA buffer |
| TB | Terrific broth |
| TBS | Tris buffered saline |
| TBST | Tris buffered saline with Tween-20 |
| TCA | Trichloroacetic acid |
| TE | Tris EDTA buffer |
| TEMED | N,N,N',N'-tetramethylenediamide |
| TRITC | Rhodamine isothiocyanate |
| TSA | Trichostatin A |
| Tween-20 | Polyoxyethylene-sorbitan monolaurate |
| UB | Unbound |

| | |
|------------|---|
| UTP | Uridine triphosphate |
| UTR | Untranslated region |
| UV | Ultra violet |
| ΔV | GST-HD ΔV fusion protein, subclone of HDACm |
| V | Volts |
| XTC | <i>Xenopus</i> tadpole cell line |

Abstract

The *Xenopus laevis* histone deacetylase, HDACm, is a 57 kD protein that is 91% identical human HDAC 1 and exhibits histone deacetylase activity and inhibitor sensitivity similar to that of a class 1 HDAC. This protein is expressed from a maternal message synthesized in the oocyte. The protein is expressed throughout early development.

The aims of this investigation were to analyse the role of HDACm in chromatin remodelling during early development and how this enzyme is regulated. By using a wide variety of biochemical and immunological means it has been possible to demonstrate that this enzyme is a nuclear protein. Nuclear import is mediated through importin- α and a putative bipartite NLS found in the C-terminal domain of HDACm. In the oocyte nucleus and the nuclei of cells in early embryos, HDACm is retained at the internal margin of the nuclear envelope, this separates the active HDACm complex from its major substrate.

The enzyme has *in vivo* activity. Endogenous HDACm activity is not detected until the mid-blastula transition. Over-expression of HDACm in oocytes results in the formation of a complex that binds chromatin and results in its premature condensation. Enzyme activity is associated with multimolecular complexes. The size of the complex varies between approximately 300 kD in large oocytes and approximately 600 kD in mid-blastula embryos. The retinoblastoma associated protein 48 (RbAp48) has been identified as a partner of HDACm in these complexes.

Post-transcriptional modifications of HDACm control enzyme distribution and activity. Acylation of this enzyme results in cytoplasmic retention of this transcription factor, whilst phosphorylation of HDACm has pleiotropic effects. Phosphorylation of the putative NLS is required for nuclear import, whilst further phosphorylation of HDACm is also required for enzyme activity; dephosphorylation of the enzyme in the native complex inhibits activity.

Introduction

For many years deoxyribonucleic acid (DNA) has been known to contain the keys to development and inheritance. However, histone proteins were discovered in the nucleus of eukaryotic cells by Albrecht Kossel a long time before this [1]. As a result of the apparent biochemical simplicity of DNA and the complexity of the protein components of chromosomes it was mistakenly thought that histone proteins were the major constituents of genes [2]. Since the elucidation of its structure by Watson and Crick almost 50 years ago [3], our understanding of the structural organisation of this molecule in the nucleus has come a great distance. Improvements in methodology have resulted in the various histones being isolated and have shown that only a few types exist and that these are highly conserved in eukaryotes [4]. This information plus experiments that show that DNA alone can change the genetic characteristics of the cell [5] lead to a change in scientific opinion. It was deemed unlikely that histones were specific determinants of gene expression, they were more likely involved in the maintenance of chromosome structure. This is certainly one of the roles of histones and is achieved by DNA being complexed with histone proteins in an evolutionary conserved and rigorously controlled manner. The resulting structure is called chromatin [6,7].

The histones do more than this. In the late 1980's a number of scientists revealed that chromatin is very important with respect to the

regulation of chromatin activity, changes in nucleosomal packing have pleiotropic effects on gene activity [8]. In fact, the level of condensation of DNA (in the form of chromatin) changes throughout the cell cycle and development. Variation in the level of condensation is controlled by the extent of interaction between histone proteins and DNA, with these changes come changes in the level of gene activity. This modulation is produced by very specific post-translational modifications of the histone proteins [9], the most widespread of which are phosphorylation of the linker histone H1 and acetylation of the core histones [6]. The purpose of these modifications seem to be to relax the interaction between the nucleosome and DNA, to promote transcription factors access to the DNA and to allow nucleosome repositioning and expression of repressed genes. [10,11]. Acetylation is regulated by two sets of proteins, histone acetyl-transferases (HATs) and histone deacetylases (HDACs) [12,13,14]. We have been studying a recently cloned *Xenopus* HDAC which is novel in so far as it is synthesized from a maternal mRNA present only in oocytes and early embryo stages. This enzyme has been called HDACm ('m' for maternal).

1.1. Chromatin

Chromatin is the form in which all nuclear DNA is found in eukaryotes. The basic unit into which the chromatin is packaged is the

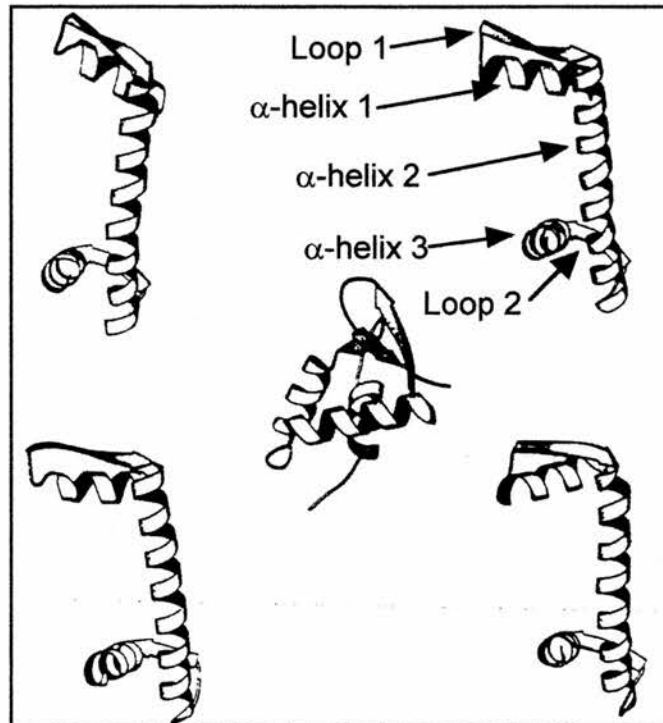


Figure 1. The histone fold. The histone fold is a globular domain common to all core histones. The histone fold, as found in histones H2A, H2B, H3 and H4, is shown (clockwise from top left) with the globular domain of histone H1 shown centrally for comparison. The histone fold consists of a long central helix (α 2), flanked on either side by a loop (L1 and L2) and a shorter helix (α 1 and α 3), these domains are indicated on histone H2B. (Figure based upon that found in Avents & Moudrianakis (1995) PNAS, 92, 11170 - 11174) [17].

nucleosome. This is of an evolutionarily conserved structure and contains the histone proteins complexed with two complete turns of DNA.

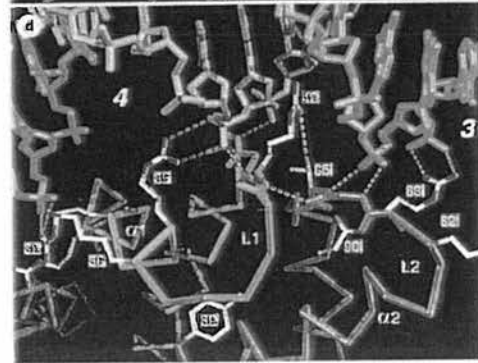
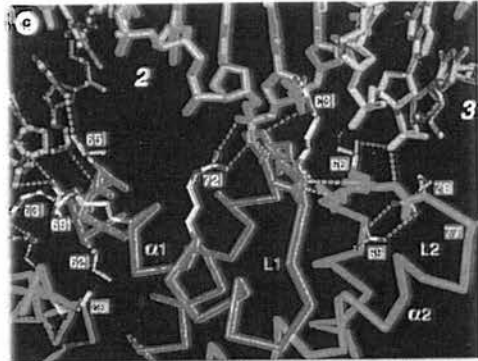
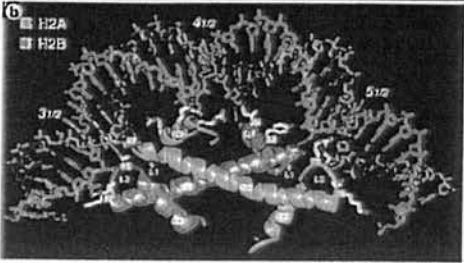
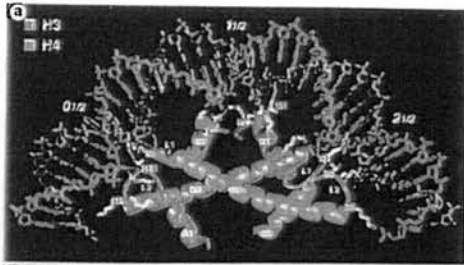
1.1.1. Histone proteins

There are two types of histone protein, core histones and linker histones. The core histone proteins are an evolutionarily conserved group of small (11-16 kD), basic proteins which compact DNA via protein-DNA and protein-protein interactions (made between themselves and other distinct chromosomal proteins) [15,16]. Each core histone contains a highly conserved globular domain consisting of a long central helix flanked on either side by a loop and shorter helix. This structure is known as the histone fold and plays an important role in organising DNA by its histone-histone interactions [15,16,17] (figure 1). Histones interact with each other in a specified order. H2A with H2B and H3 with H4 bind together in an antiparallel fashion to form crescent shaped heterodimers with a pseudo-symmetry between the two $\alpha 2$ helices [18,19] (figure 2a & 2b).

Linker histones are found outwith the central nucleosome structure. These proteins are larger than the core histones (>20 kD), and are highly basic due to their N- and C- terminal tails being enriched in lysine residues [17,20]. A number of forms of linker histone exist and

Figure 2. Representation of the molecular structure of histone proteins and their interaction with each other and the DNA backbone. **(a)** Histone-fold pair of histones H3 and H4. The α 1-L1- α 2-L2- α 3 structural elements. Side chains from these structures interact with the DNA backbone by forming hydrogen bonds or by hydrophobic association, whilst key arginine residues insert into the minor groove. **(b)** The interactions that occur between the histone-fold pair of histones H2A and H2B and DNA backbone. **(c)** Histone H3-H4 L1L2 DNA binding site. The H3 L1 and H4 L2 loops make three hydrogen bonds with each other in a parallel β -sheet. The hydrogen bond interactions between protein and DNA phosphodiester backbone involve main chain amides and side chains. **(d)** Histone H2A-H2B L1L2 DNA binding site. Interactions are the same as in (c). **(e)** Histone-Histone interaction of both molecules of histone H3 to make the core tetramer. Histone H3'-H3 four helix bundle. The histone H3-H4 histone pairs form the tetramer through the interaction of the C-terminal halves of the α 2 helices and the α 3 helices of histone H3' and H3. **(f)** Histones H2B and H4 interact to complete the octamer. The histone H2A-H2B dimers bind into the histone octamer through the interaction of histone H2B with histone H4.

Images have been adapted from those presented by Luger et al (1997) Nature, 289, 251-260 [18].



the type present in chromatin has been found to change during development [21]. The role of this protein is to stabilise the structure of the nucleosome, probably through interactions between the globular and tail domains of the linker histone and DNA, and between linker histone and histone H2A in the nucleosome core [20,22].

1.1.2. The nucleosome

DNA in the nucleus of the eukaryotic cell exists in a co-operative state with the core histone proteins (figure 3). The core histones form a complex with DNA to form a structure called the nucleosome. The nucleosome shapes DNA at the molecular and atomic level through enforced DNA bending which leads to the formation of higher order structures (eventually leading to the formation of chromosomes at metaphase). The spacing of nucleosomes is dependent on the solution conditions within which chromatin is formed, demonstrating the electrostatic nature of the interactions between DNA and the histones [18,19]. DNA sequence will also effect nucleosome deposition, showing a statistical preference for DNA where the minor groove will face the octomer at Adenine (A) and Thymine (T) rich sequences. This enforces rotational changes onto the DNA and generates tension within the helix [16].

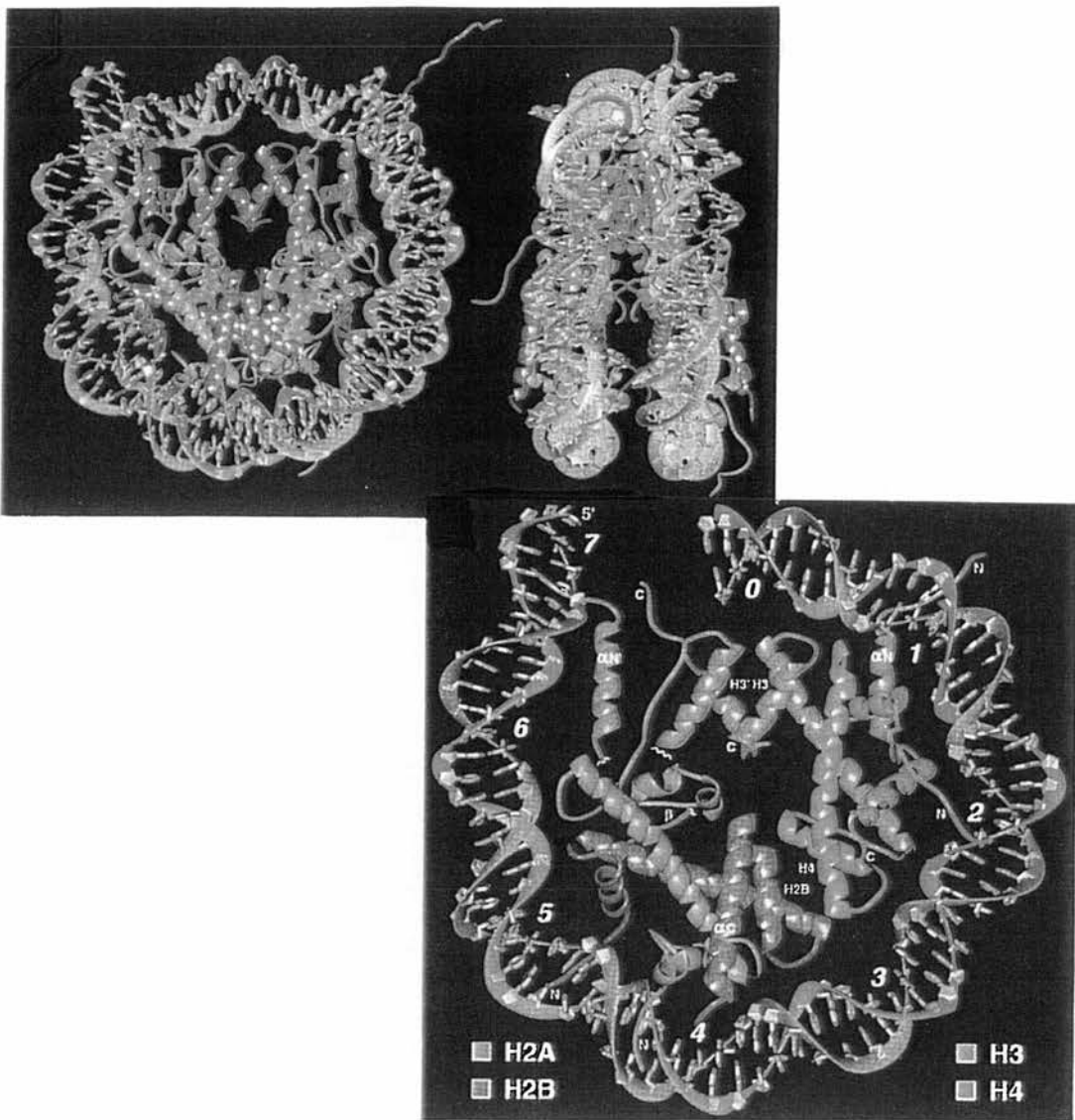


Figure 3. Nucleosome core particle; ribbon traces show the 146 bp of DNA associated with the nucleosome and eight histone protein main chains. The core histone complex has been shown, by protein crystallography, to have an obvious left handed groove in its surface into which the DNA superhelix is thought to fit in a torsionally stressed and distorted form to form a protein-DNA complex with a molecular weight of 206 kD. The views are down the DNA superhelix axis for the left hand image and perpendicular to it for the central image and show the protein-protein and protein-DNA interactions in the nucleosome. In the right hand image, the view is down the superhelix axis, but shows only one turn of the DNA superhelix. The two copies of each histone pair are distinguished as primed and unprimed copies, where the histone fold of the unprimed copy is associated with the DNA backbone in that turn of the superhelix.

Images adapted from those presented by Luger et al (1997) *Nature*, 289, 251-260 [18].

The structure of this DNA-protein complex has now been solved at 2.8 Å [18,19] (figures 3 & 4). Each core nucleosome unit consists of two copies of histones H2A, H2B, H3 and H4. This core histone complex has been shown, by protein crystallography, to have an obvious left handed groove in its surface into which the DNA superhelix is thought to fit in a torsionally stressed and distorted form. The core nucleosome associates with 145 bp -147 bp of DNA to form a complex with a molecular weight of 206 kD [17,18,19,20,22]. In addition to the core histones, a molecule of linker histone associates with the exterior of this complex and extends the amount of DNA associated with the nucleosome to 160 bp.

The core histones are actually arranged in a tripartite structure with two H2A/H2B dimers flanking a central H3/H4 tetramer (figure 4), dimer-dimer interactions occur between the carboxyl end of the $\alpha 2$ helix and all of the $\alpha 3$ helix [17,18]. The central H3/H4 pairs interact through a four helix bundle formed between H3 and H3, to form the H3/H4 tetramer. The H2A/H2B pairs then interact with the central tetramer via four helix bundles formed between H2B and H4 histone folds to turn the tetramer into the octomer, these interactions are further stabilised by hydrogen bonds between buried charged groups [18,19] (figure 2e & 2f).

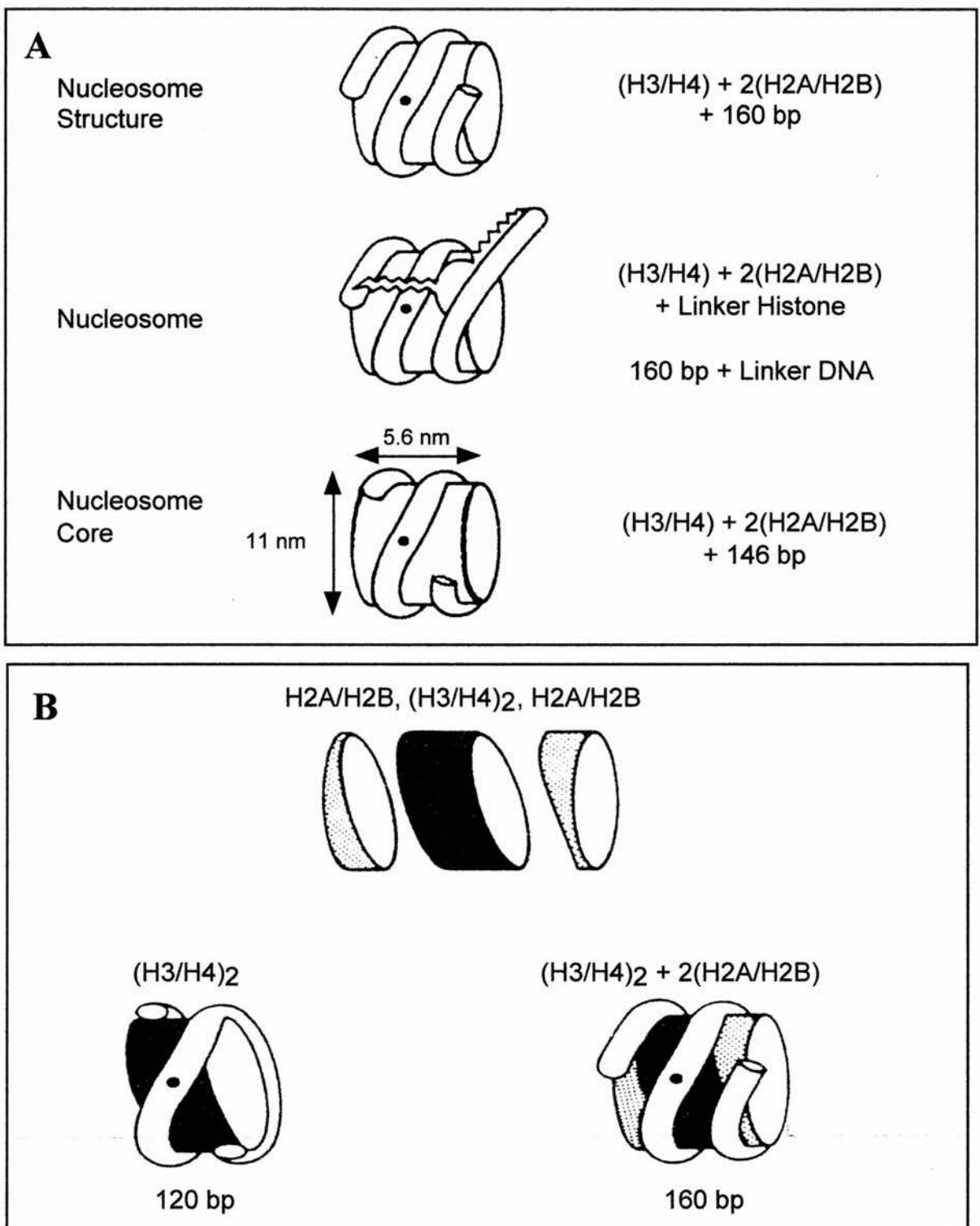


Figure 4. Tripartite organisation of the nucleosome and its interactions with histone H1 and DNA. **(A)** The three levels of interaction of DNA with the nucleosome. the dimensions of the nucleosome core are shown and the axis of dyad symmetry is indicated by the spot. **(B)** The tripartate organisation of the histone octomer. The core of the octomer (two histone H3/H4 dimers) organises the central 120 bp of DNA. The addition of the histone H2A/H2B dimers increases the amount of DNA associated with the nucleosome to 160 bp of DNA. Each histone H2A/H2B dimer adds 20 bp of DNA.

Images reproduced from Wolffe A.P. (1995) Histones and transcriptional control
In: *Eukaryotic gene transcription*. IRL Press, London. pp34-40 [16].

1.1.3. Nucleosome Formation

The assembly of regularly spaced chromatin has been studied *in vitro* using *Xenopus* egg extracts [23, 24, 25] and extracted post blastoderm *Drosophila* embryo proteins [26]. This work has revealed that the core-histone binding proteins, nucleoplasmin and N1/N2, are involved in the assembly of chromatin, but that chromatin assembled with these proteins alone does not possess regularly spaced nucleosomal arrays. Assembly of regularly spaced nucleosomes is dependent on chromatin assembly factors 1 and 4 (CAF-1, CAF-4) in addition to the histones, histone chaperone proteins, ATP and DNA. *Drosophila* CAF-1 is composed of three subunits (p48, p60, and p150) [27,28]. This factor assembles nucleosomes onto replicated DNA using newly synthesised histones H3 and H4 in the chromatin assembly complex (CAC) during S-phase of the cell cycle; CAC is composed of three molecules of CAF-1 and one each of histone H3 and histone H4. CAF-1 proteins do not contain nucleotide binding sequences, the deposition site being determined by energy favourability of non-specific interactions between DNA and acetylated histones H3 and H4 rather than being targeted to specific DNA sequences. Disruption of nucleosome position (by proteins such as SWI) involves proteins containing specific sequence recognition motifs that disrupt nucleosomes at specific loci. These proteins are not known to associate

with the CAC and do not play any part in nucleosome deposition [28,29].

1.1.4. Histone-fold/DNA interaction within the nucleosome

The central histones organise the central 120bp of DNA within the nucleosome, and it is not until this has been organised that the two H2A/H2B dimers can associate with the core through protein-protein interactions. Following the addition of these dimers, further protein-DNA interactions occur to extend the number of bases associated with the nucleosome to the full 160bp [18,19,22,31] (figure 4). Binding of DNA is by two types:

(1) L1L2 binding - core histones bind to the DNA at the edge of the DNA backbone by hydrogen bonding, utilising residues in L1 and L2 of the core histones (figures 2a and 2b).

(2) $\alpha 1\alpha 1$ binding - uses both $\alpha 1$ helices of histone dimers to bind the DNA backbone at the centre of the bound DNA stretch (figures 2c & 2d) [12].

The histone fold domains account directly for the organisation of 121bp of DNA. Each histone dimer is associated with 27-28bp with 4bp between units. The binding is primarily to the phosphodiester backbones as they face the nucleosome over 2.5 turns of DNA, each turn commits a segment of two consecutive phosphate groups to be

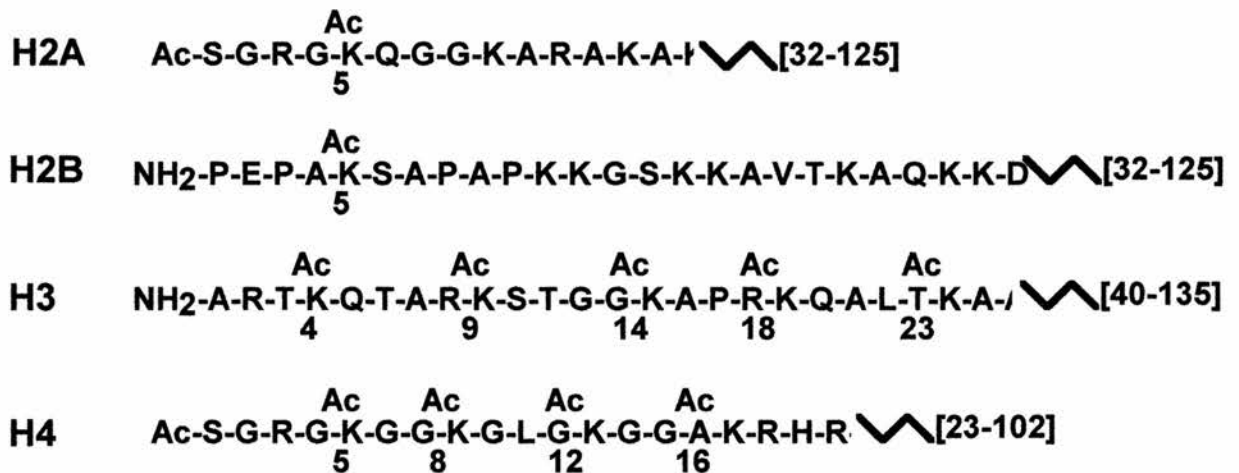
bound. The directly bound DNA is extended by an additional segment in both directions by conserved lysine residues in the L2 loops of all core histones [16,18,19,22].

1.2. Histone modification

The histone proteins are all liable to post-translational modifications. Some of the modifications are permanent, for example the acetylation of histones H1, H2A and H4 during histone synthesis which occurs to block the N-terminus; whilst many other modifications occur in a dynamic manner [6]. The core histones all contain a conserved N-terminal tail that carries a high charge density, a direct result of it being rich in lysine and arginine residues. These residues are the sites of the post-translational modifications of the histone proteins that regulate chromatin structure [17,22,31] (figure 5).

Modifications:

- Phosphorylation of linker histone on Serine (S), Threonine (T) and Tyrosine (Y) residues in the flexible N- and C- terminals during the cell cycle. This modification begins in S phase and results in the histones being hyperphosphorylated by metaphase [6,10].
- Reversible ubiquitination of histones H2A and H2B is the major cell cycle dependent modification which occurs to lysine residues located in the C-terminal tail of these histones. This modification disrupts the



Basic N-Terminal Tail



Figure 5. N-terminal tail of the core histones. All core histones have a highly conserved basic tail. Charge distribution in this tail is controlled by acetylation, which occurs at specific basic (lysine) residues in a controlled and regulated pattern. Acetylation state of the histone is controlled by the balance in activity between type A HATs and histone deacetylases. The most important substrate in this pathway is histone H4. That histone is acetylated in a specific order which is conserved between amphibians and mammals (Lys 5 is acetylated first, followed by Lys12/8 and finally Lys 16); the level of acetylation changes continually throughout the cell cycle. There would also appear to be a correlation between the site at which acetylation occurs and the function of acetylation. Acetylation at residues K5 and K12 is primarily associated with histone storage (with N1/N2) and deposition into newly replicated DNA, whilst acetylation at K8 and K16 is only associated with transcriptionally active chromatin [16, 31, 32]. Images reproduced from those presented by Wolffe A.P. (1995) Histones and transcriptional control In: *Eukaryotic gene transcription*. IRL Press, London. pp34-40 [16].

close packing of the nucleosomes opening up the chromosome and allowing the interaction of large protein complexes, such as RNA polymerase, with the DNA [6].

- Core histone acetylation is the single most studied modification, although it may not be the most important. Histone acetylation is a dynamic, metabolic modification that has been strongly correlated with transcriptional activity and histone deposition [16,32]. The acetylation process removes net positive charge from the N-terminal domain [31].

Other modifications of the histones can occur. Examples of these include methylation and ADP-ribosylation.

The amino terminal domain of histone H4 is the most studied site of influential modifications. Unfortunately, in the structural studies completed to date using recombinant proteins, the first fifth of histone H4 has not been included in the model. However the solved part of the N-terminus (residues 16-25) can be seen to make multiple hydrogen bonds and salt bridges between its basic side chains and the acidic side chains of histone H2A [18,19]. In yeast, the N-terminal domain of histone H4 is also known to bind the silencing protein SIR3, which results in the formation of heterochromatin [33,34,35]. The four acetylation sites found in histone H4 are found in this area, and successive acetylation is expected to lead to a reduction in the affinity of the acidic residues in neighbouring nucleosomes for the histone H4

tail resulting in the destabilization of higher order nucleosome structures. This may also increase the level of access to DNA for other nuclear factors, perhaps producing the generally observed increase in gene transcription associated with chromatin acetylation [18,19].

1.2.1. Acetylation of histone proteins and changes in chromatin state

The majority of chromatin remodelling is generated via the changing acetylation state of core histones, this can vary from one region of the chromatin to the next [29,32]. Nucleosome modification and the final acetylation state of the histones are the result of the balance in activity between nuclear type A HATs and histone deacetylases [36]. The most important histone substrate in this pathway is histone H4, as confirmed by genetic manipulations and biochemical studies [22,36]. This histone is acetylated in a specific order, which is conserved between amphibians and mammals (lys 5 is acetylated first followed by lys 12/8 and finally lys 16). The level of histone H4 acetylation changes continually throughout the cell cycle, peaking in S phase and reaching its minimum level in metaphase chromosomes [32,37,38]. Mutation or modification of this histone effects development and cell cycle progression to a much greater extent than for any of the other histones [22]. Within the pattern of acetylation of

these residues there would also appear to be a correlation between the sites at which acetylation occurs and the functional consequences of acetylation. Acetylation at residues K5 and K12 is primarily associated with histone storage and deposition onto newly replicated DNA, whilst acetylation of K8 and K16 is only associated with transcriptionally active chromatin [37,38].

• **Nucleosome acetylation and chromatin remodelling.**

Nucleosome acetylation status can be heterogeneous within the chromatin of a single nucleus; in general hyperacetylated histones seem to accumulate in transcriptionally active chromatin, whereas silent domains are enriched in hypoacetylated histones [30,39,40]. One possible explanation of how acetylation may bring this about has been proposed following a series of *in vitro* studies. These suggest histone acetylation may reduce the affinity of N-terminal tails for DNA and other nucleosomes and alter the extent of DNA coiling around the octomer as a result of a conformational change in the histone upon acetylation [12,36]. As a direct result, this would open up the DNA to nuclear factor binding. Studies on the level of activation of the mouse mammary tumour virus (MMTV) promoter have shown that increased acetylation of the histone core promotes higher levels of gene expression [41]. Increased histone acetylation also makes the DNA

more sensitive to DNase I activity in a manner similar to that caused by normal hormonal induction (of the MMTV promoter) [41]. Hormone induced increases in gene activity are known to be due to structural changes occurring to the nucleosome around which the MMTV promoter is stored and enable all necessary transcription factors to bind simultaneously [41]. Further studies by Vettese-Dadey *et al* on HeLa cells and the effect of inhibiting core histone deacetylation on the binding of transcription factors to chromatin have demonstrated that two common transcription factors, GAL4-AH and USF, have a higher affinity for acetylated nucleosome cores. This affinity is greater for cores hyperacetylated on H4 rather than H3 [36].

In vivo evidence to support this theory comes from studies on *Tetrahymena*, where only the transcriptionally active macronucleus contains acetylated histones [36,39]. This is also the case in male *Drosophila* larvae where the hyperactive X chromosome is more highly acetylated than the female X chromosomes or the autosomes [36,39,42]. In mammals, the nucleosomes in CpG islands surrounding active housekeeping genes are always hyperacetylated whilst silent loci are hypoacetylated [42]. This evidence applies to genes located in euchromatin. In contrast, recent inhibition assays conducted on deacetylase complexes of yeast and *Drosophila* have demonstrated a novel finding on the effect of hyperacetylation on the level of gene

expression in heterochromatin. Inhibition of the HDAC results in the silencing of gene expression in the heterochromatin, whereas normally it will promote gene expression [43]. A theoretical explanation for this has recently been proposed by Patterton and Wolffe [44]. They suggest that in the majority of instances, histone acetylation opens up the chromatin to allow transcription factor access to initiation sites and hence promotes gene expression. In the minority of cases where histone deacetylation leads to gene expression he suggests that transcription factors may be recruited to specific promoters, with the specificity of their interaction depending on a tightly constrained chromatin environment. Under these conditions the role of HDAC on transcription may be more indirect; not deacetylating large areas of chromatin, which results in chromatin condensation and inhibition of transcription directly via the formation of a higher order structure, but by packing DNA into the restricted chromatin environment required. This system may work due to the existence of extraneous/inert transcription factor binding sites being present in chromatin in the absence of histone deacetylase activity, thus allowing a large number of non-productive interactions to take place. These extra sites may be masked as a consequence of histone deacetylase activity inducing formation of the constrained chromatin conformation. This may also result in many more functional interactions between transcription factors and their cis-

activating elements which results in the gene expression seen in the heterochromatin of *Drosophila* and yeast.

• **DNA replication and development.**

The acetylation state of histones during early development has been extensively studied in *Asterina pectinifera* (starfish) and *Arbacia punctulata* (sea urchin) embryos [45,46]. These investigations have shown that histone H4 is incorporated into DNA at replication in a diacetylated form and that they stay in this form until the 64 cell stage. However, by blastulation the predominant H4 species is completely deacetylated. After this point, the acetylation state of chromatin becomes heterogeneous between regions, this is presumably due to a wave of new acetylation which is directed by some unknown mechanism to specific sites to control the expression of general and tissue specific genes. Inhibition of chromatin deacetylation using TSA can cause severe errors in development, arresting development during early gastrulation [45,46]. Incubation of *Xenopus* embryos in TSA has the same phenotypic effect. It results in the accumulation of hyperacetylated histone during gastrula and leads to a delay in the completion of gastrulation and defects in mesoderm formation [11,21]. Precise control of histone acetylation appears to be essential for correct development of the embryo with the re-initiation of gene activity.

1.3. Control of acetylation state

From the work that has been carried out on the role of chromatin in transcriptional control and development, it has become apparent that the acetylation state of core histones, especially H4, plays a very important role in these processes. The acetylation state of nuclear chromatin is controlled by the balance in activities of nuclear type A HATs and HDAC enzymes and the targeting of these enzymes to specific sites in the chromatin [13].

1.3.1. Histone acetyltransferases

Histone acetyltransferases have been studied in many species, including maize, yeast and *Tetrahymena* [47,48,49,50,51]. HATs link the acetyl moiety of acetyl-CoA to the ϵ -amino group of specific lysine residues found within the recognition sequence GXGKXG in each of the histone N-terminal tails [49]. H3 and H4 are the major substrates for these enzymes, whereas H2A and H2B represent minor substrates [47,48]. In histone H4 the lysine residues are acetylated in a specific order, K5 is most easily acetylated followed by K12 and K8, whilst K16 is the residue least frequently acetylated [30].

As mentioned previously, there are two forms of HAT: the nuclear A-type HATs and the cytoplasmic B-type HATs. The A-type

HATs have been intensely studied by Lopez-Rodas *et al* [47,48]. Their studies in yeast, *Physarum* and maize have shown that two forms of HAT-A, A1 and A2, can be found in the nucleus and are tightly associated with the chromatin, only being extracted with the use of high salt solutions. As a result of studies performed in yeast, this HAT (GCN5) is now thought to work as part of a complex containing the adapter proteins ADA2 and ADA3 [16]. This complex is then thought to interact with the SWI/SNF complex that directs the HAT to a specific site targeted for gene expression [13,51,52]. The B-type HATs have been shown to link acetylation to chromatin replication and gene activation, as they show a non-random acetylation pattern of the histone proteins [53,54]. Type B HATs show a strong affinity for free, non-chromatin bound H4 and acetylate histones at residues 5 and 12. This is the form in which these proteins are found when transported into the nucleus and later incorporated into new chromatin during DNA replication [53,54]. In yeast, the type-B HAT has been shown to be composed of two components (i) HAT1, comprising the catalytic subunit (ii) HAT2, (RbAp48) comprising a protein required for high affinity binding of the acetyltransferase to histone H4 [49,50,51]. Interestingly HAT2 has been shown to also interact with RPD3, the yeast histone deacetylase [55]; this may mean that this is a common

component of the acetylation complex that targets either enzymes to their site of activity, acting in a context dependent manner.

1.3.2. Histone deacetylases

The function of the deacetylases is to remove the acetyl group from the ϵ amino group of the lysine residues in the N-terminal tails of the histones acetylated by the HATs. Numerous histone deacetylases have now been cloned in species including humans, *Xenopus* and yeast [56,57,58,59]. These proteins all share a high degree of identity; the *Xenopus* enzyme HDACm is 58% identical to the yeast deacetylase RPD3. The *Xenopus* deacetylase shows even more sequence similarity with the human deacetylase HDAC1 (91%) [60].

The evolutionary origins of these enzymes has been investigated recently by searching the sequence data banks for similar sequences; as a result of these searches the prokaryotic gene products, acuC of *Bacillus subtilis* and atoB of *Escherichia coli* have been identified as possible evolutionary precursors of the histone deacetylases [61,62].

AcuC is an enzyme involved in converting the fermentation product acetoin to acetate via the butanediol cycle. This is a deacetylating enzyme but does not cleave an amide link but a carbon bond [61]. The second enzyme, atoB, is involved in short-chain fatty acid degradation. This enzyme works as a tetramer and deacetylates

acetoacetate (a four carbon β -keto fatty acid), a substance which can be used as a sole carbon and energy source by *E. coli* [62]. Further related prokaryotic proteins of the acetylpolyamine aminohydrolase family also show a high similarity to the histone deacetylases, in both structure and function, for this reason it is proposed that all these proteins may be derived from a common ancestral gene [63]. In all the eukaryotic histone deacetylases that have been investigated, no recognisable functional motifs have been identified. Using RPD3 as a specific example, functional studies have shown that this enzyme makes no biochemically defined interactions and does not bind DNA. This is true of all deacetylases and produces a paradox in terms of known enzyme activity [43,59]. These enzymes are known to interact with chromatin, but have differing substrate specificities, sensitivities to inhibitors and non-uniform effects on gene expression, but all display activity against histones incorporated into chromatin; but if the enzyme cannot bind DNA then how can these events take place?

In general terms the role of the histone deacetylases is to direct the equilibrium of histone acetylation towards the deacetylated state. This is usually to allow the interaction of the positively charged arms of the histone to interact with the negatively charged core of neighbouring nucleosomes and the negatively charged phosphodiester backbone of DNA so as to condense the chromatin and inhibit gene expression. The

difference in substrate specificity that is seen within some species is easily explained by the existence of multiple deacetylases within the nucleus. However this leaves us with three questions to answer on the nature of histone deacetylase:

- (i) Why do different deacetylases have different sensitivities to inhibitors?
- (ii) Where is the deacetylase found in the nucleus and how is it regulated?
- (iii) How is the deacetylase targeted to chromatin?

The answers to these questions are all based around one key fact. The histone deacetylases do not work alone but as part of a complex. The same enzyme may exist in a number of complexes within one cell type which impart different perceived properties to the deacetylase.

(i) Inhibitors of histone deacetylase

There are two families of histone deacetylase inhibiting molecules: butyric acid and its analogues, and Trichostatin A and related compounds [64,65]. These molecules inhibit histone deacetylation, resulting in the accumulation of hyperacetylated chromatin and altered gene expression. Butyric acid works by an unknown mechanism at millimolar concentrations. Its effects including

histone deacetylase inhibition but has pleiotropic side effects on cell morphology, growth rate and cellular biochemistry [64].

Trichostatin A, Tropoxin and their related compounds are much more useful in experimental situations; not only are these compounds more specific for histone deacetylases (having maximum action at nanomolar concentrations), they also have fewer side effects compared with butyric acid. As a result of their properties these chemicals are very useful as probes for the role of histone acetylation in chromatin structure and function. From acid-urea-Triton-X100 gels of histones it is apparent that acetylated histones are the target of the histone deacetylase, as there is increased histone hyperacetylation in the presence of TSA contrasted to the pattern seen in untreated samples [65]. The effect of TSA on *in vivo* systems is also much more explicable in terms of this finding; TSA inhibits cell growth at either G1 or G2 phase of cell cycle without inhibiting macromolecular synthesis [65]. Following removal of the block at G1, cell cycling resumes normally, removal of the G2 block results in the cells starting a new S phase, which in turn results in a tetraploid cell [65]. For DNA replication to take place the DNA must first be deacetylated to allow the replication machinery access. Following removal of the G1 block, the DNA is deacetylated ready for replication. Following removal of the G2 block all the DNA (original and replicated) is in the hyperacetylated

form it would be found in at the end of G1, so all is deacetylated and the cell is tricked into believing it is entering S phase [65].

Of the two compounds, Trapoxin and Trichostatin A, the latter is far more useful as its effect on the deacetylase is reversible. Treatment of cells with this chemical leads to not only differentiation of undifferentiated cells, but also inhibition of the development of embryos through gastrula, presumably by effecting the pattern of gene expression initiated at the mid-blastula transition [65]. Specific examples of altered gene expression in response to TSA treatment include reactivation of silenced, virally transduced genes and increased HbF levels by inducing γ -globin expression. In the case of γ -globin expression the change in acetylation state has been shown to increase transcription factor access to the promoter [66,67,68,69].

(ii) Sub-cellular localization

The organisation of histone deacetylases within the cell is a major method of regulation of the activity of the enzyme. The enzyme will only have activity when bound to chromatin, therefore by altering its solubility in the nucleus its time and duration of action within the cell cycle or development can be controlled. However, it is important to note that such studies are looking at the enzyme in its *in vivo* state as part of a complex rather than as a free protein. The conditions used to

study localisation of the enzyme must be strictly controlled to prevent loss of enzyme from one sub-cellular compartment to another. The importance of all this, has again, been demonstrated in yeast. Two deacetylase complexes have been identified in yeast; HDAC A and HDAC B, which are functionally distinct, showing different sensitivities to TSA and having different substrates. HDAC A is a 350 kD complex sensitive to TSA and containing the deacetylase enzymes HDAC A1 (p75) and HDAC A3 (p71) [70,71]. A great deal of varying information concerning this lower molecular weight complex exists. It has previously been reported that the complex actually has a mass of 150 kD rather than 350 kD and has been shown to be bound to the nuclear matrix in some studies [70], whilst other reports state it is only transiently associated with chromatin [71]. In addition to this, further confusion exists around the function of the enzymatic component of the complex; no *in vivo* substrate for HDAC A has been detected but it can be shown to have a high affinity for H3 *in vitro* [70]. The function of the two catalytic sub-units is also in dispute. A1 and A3 are known to immunoprecipitate each other, and removal or mutation of either has been shown to remove all enzyme activity, but the precise role of either protein cannot be discerned [71]. The reasons for the variation in findings is most likely due to the use of widely differing techniques by

the various groups concerned, with much of the earlier work lacking strict controls.

Studies of enzyme sub-cellular location have been conducted exhaustively on *Zea mays* and chicken erythrocytes. Much of the work on nuclear localization of histone deacetylases relies on the theory that the nuclear matrix does exist, and that it is a network of interconnecting protein filaments found within the nucleus that aid protein transport and lend structural support to the nucleus. The evidence for the existence of this network has been circumstantial for many years, however many recent investigations have produced stronger, more direct evidence for the existence of the nuclear matrix [72]. For this reason information on the association of the deacetylases with the nuclear matrix can now be considered with a greater level of confidence. The deacetylases studied to date all show a very low level of association with the nuclear matrix, the nuclear matrix being the residual structure that remains after high salt extraction of nuclease-digested nuclei. This finding has been replicated in plants, yeast, *Physarum* and rat liver independently of the method used to prepare the matrix [47]. This finding is again in conflict with previous reports [48], but lack of reasonable experimental control can explain this. In the earlier investigations, activity of total homogenate was not measured, thus it is impossible to know how much activity was lost through isolation of nuclei.

The investigations have made it apparent that the HATs and the HDACs do associate with chromatin and the nuclear matrix, but differ in their affinity for these sites. Nuclear HATs bind chromatin tighter than the deacetylases in general, but deacetylases fluctuate in their ability to bind chromatin during the cell cycle [48]. This may well suggest that by controlling HDAC solubility, the cell may modulate the activity of a deacetylase in different nuclear processes. When this idea is joined with that of site-specific acetylation, it is apparent that by controlling the solubility of both the nuclear HATs and the HDACs a pattern of acetylation may be established, especially as it is now evident that the HDACs may also be targeted to specific sites in the chromatin. Further evidence for control of deacetylase substrate specificity has emerged with the discovery that the specificity of HDAC-1A in *Zea mays* is regulated by reversible phosphorylation [73]. In the maize embryo three distinct enzymes are present, HDAC-1A, HDAC-1B and HDAC-2, all of which differ in their substrate specificity and follow distinct activity patterns during embryo germination [47,48,74]. HDAC-1 activity is at a constant level through most of germination but peaks around 40 hours post germination. By comparison, HDAC-2 is active in the dry embryo and during initial germination where its major activity is thought to be as part of DNA repair due to the damage accumulated during seed storage [47,48]. In the normal state HDAC-1A

uses H2A/H2B and H3 as its main substrates. Following phosphorylation, selectivity for H2A is increased dramatically whilst that for H3 drops by 40 % [48,73]. The increased deacetylation of the H2A/H2B dimer may result in the dimer being displaced, which may be important for remodelling chromatin and allowing transcription to occur. Experimentally it has been seen that nucleosomes of transcriptionally active chromatin are transiently deficient in at least one H2A/H2B dimer [73].

Studies on the chicken erythrocyte have shown that 90% of the histone deacetylase activity is nuclear, and that within the cell the histone deacetylase is found in three forms. These are HDAC1 (55 kD), HDAC2 (220 kD), which can be broken down to 4[55 kD/HDAC-1] subunits under high salt conditions). The third form is internal nuclear matrix associated, has a molecular weight of 400 kD that is stable under high salt conditions but which can be disrupted and shown to contain the 55 kD protein HDAC-1 [75,76]. The three complexes have different properties and histone specificities but seem to contain the same enzymatic subunit [76]. The deacetylase in erythrocyte nuclei has been shown to be associated with two locations: active gene containing regions of chromatin and the internal matrix [77]. This raises interesting questions as not only does the enzyme have a role in modulating the level of acetylated histones in active chromatin, but it may also have a

secondary role, similar to that of topoisomerase II, in organising the three dimensional structure of the nuclear matrix.

(iii) Histone deacetylase complexes, co-proteins and DNA interactions

(A) Euchromatin and heterochromatin: histone proteins, deacetylation, silencing proteins and their roles in the transition between chromatin states and general suppression of gene expression.

The majority of studies on gene silencing have been conducted in yeast (*Saccharomyces cerevisiae*) and these studies are discussed here first. A great deal is known about the structural organization of chromatin and the mechanisms by which transition occurs between the two major states: euchromatin and heterochromatin. Euchromatin is the less condensed form of chromatin that is found in the “beads on a string” form, the DNA being replicated early in S phase of the cell cycle. The core histones in this chromatin are hyperacetylated, the DNA is accessible to nucleases and the majority of genes in these regions of DNA are in a potentially active state. Conversely, heterochromatin is found at specific sites in DNA, such as telomeres, centromeres and the silent mating type loci HML and HMR. Chromatin structure may be linked to the histone acetylation state, euchromatin contains histone H4 which is at least diacetylated, whilst histone H4 in heterochromatin is

only acetylated at lysine residue 12. Heterochromatin is thought to repress genes in its periphery in an epigenetic manner that is inherited between successive generations. It regulates the gene locus and is a template for its own reformation during each cell division [77].

Remodelling of chromatin from the active to silent state is thought to involve a number of cis-elements and trans-acting factors, including histone deacetylase. In *S. cerevisiae* the best model of this is regulation of mating type. The MAT locus contains the expressed mating type. HML and HMR sites contain the possible mating types. These sites are found on the same chromosome and are not expressed despite containing the correct signals [77]. The silencing of these sites is due to the cis-acting flanking elements E and I, and a group of trans-acting factors. The identified silencers are the SIR family of proteins SIR1, SIR2, SIR3 and SIR4 plus RAP1 and the origin of replication complex (ORC) [77]. Both elements (silencer DNA and proteins) must be present for silencing to occur (figure 6). In addition, it can be shown that the silencers are not required for maintenance of the repressive structure at the HML locus, repression in G1 arrested cells is unaffected by deletion of E and I sequences. However silencers are required for the inheritance of the repressed site in cycling cells, as in the absence of silencers the repression is abolished within one generation in cycling cells [77]. A recently identified protein with a role in silencing is CAF-

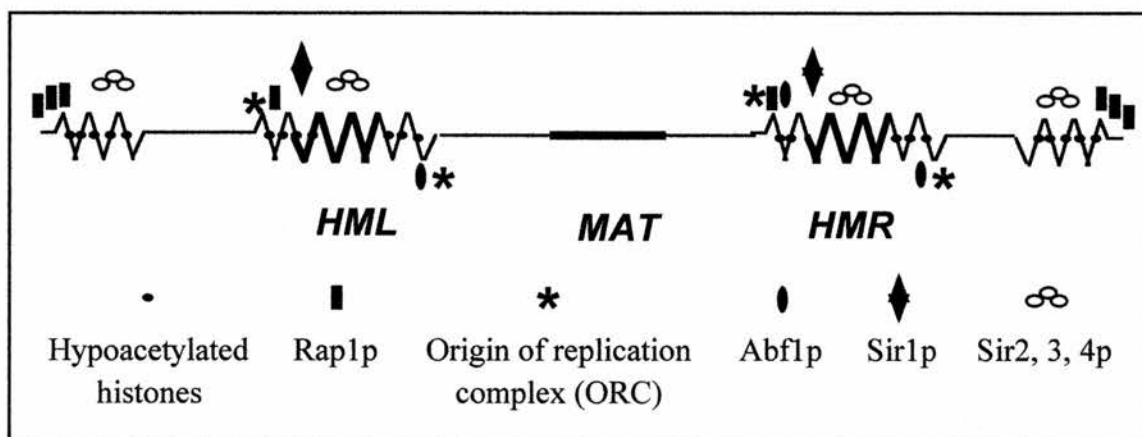


Figure 6. Model of the protein-DNA interactions and the protein-protein interactions which take place in repression of the silent mating-type loci in yeast. None of these repressing proteins interact with the MAT locus. As a result of the interaction of these proteins with the DNA in the silent mating-type loci, DNA at this location is found in the form of heterochromatin. As a comparison, the interactions which take place at the MAT locus (transcriptionally active site) are shown.

Formation of heterochromatin also requires specific residues in the N-terminal tails of histones H3 and H4. In the case of histone H4, these residues (residues 16-29) interact with SIR3/SIR4 and are required for interaction with the external surface of the histones H2A/H2B dimer on the neighbouring nucleosome.

This figure has been produced based upon a diagram in Stone, E.M. & Pillus, L. (1998) *BioEssays*. 20, 30-40 [79].

1. Mutations in the CAF-1 sub-unit of the chromatin assembly complex (CAC) result in loss of repression at the *HM* loci (figure 7). The role of CAF-1 in the assembly of silent chromatin is thought to be two fold, (i) CAF-1 ensures that replication coupled nucleosome assembly occurs as soon as possible after the replication fork has passed through the heterochromatin. (ii) CAF-1 ensures that the nucleosomes are assembled from the appropriately acetylated histones. This gives a solid base upon which the Sir complex can be built [78].

Heterochromatin formation in metazoans is controlled by a different mechanism. The most common effect of heterochromatin formation is the repression of transcription in the heterochromatin itself and adjacent regions. The variability in gene expression at the junction between heterochromatin and euchromatin is known as position effect variegation (PEV). The most popular approach by which to study the molecular basis of this heterochromatin formation has been to look for mutations in *Drosophila* that enhance or suppress PEV. Such proteins are called “modifiers of PEV”. This group includes chromosomal proteins involved in forming heterochromatin. A protein that has been identified by this approach as being involved in heterochromatin formation is heterochromatin protein 1 (HP1) [80]. This protein preferentially associates with the heterochromatin regions of polytene chromosomes and mutation of the gene encoding this protein reduces

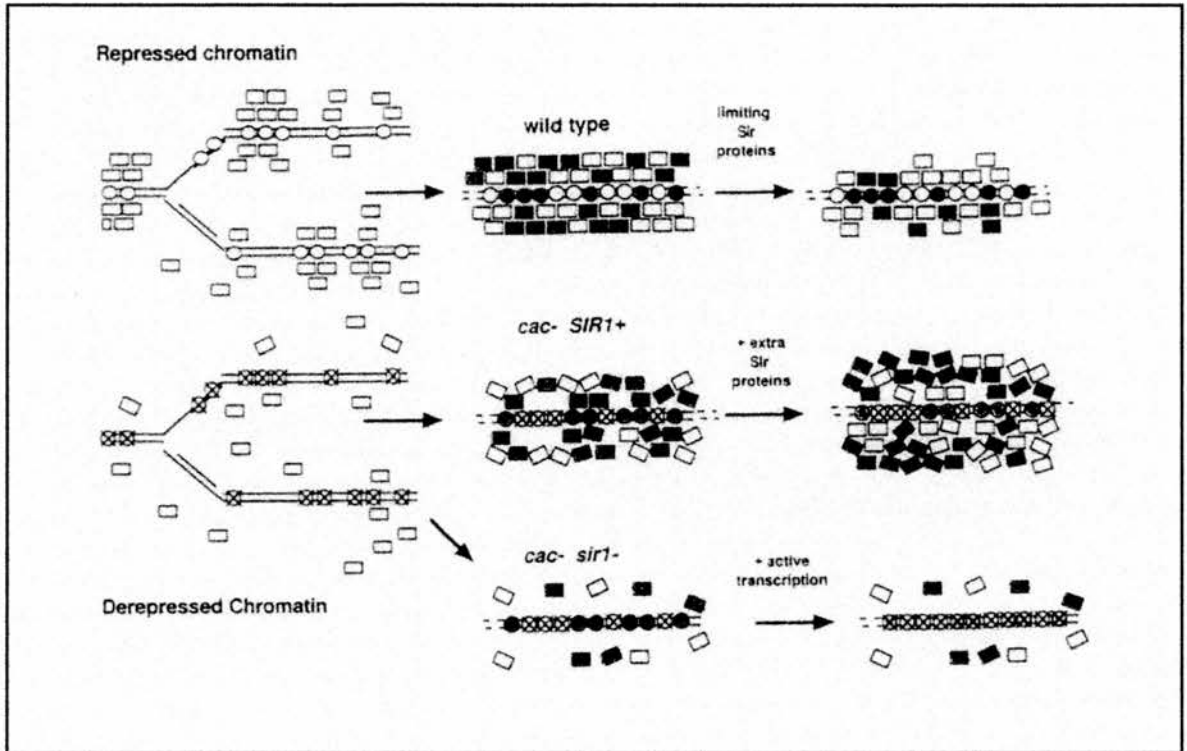


Figure 7. Model of the mechanism by which CAF-1 contributes to formation of stable heterochromatin. Heterochromatin is represented as a “wall” of Sir protein complexes built on a foundation of nucleosomes composed of appropriately acetylated histones. After replication, existing nucleosomes (white circles) are randomly distributed between daughter strands of DNA. CAF-1 assembles newly synthesised nucleosomes (black circles) into chromatin. Existing Sir protein complexes (white rectangles), as well as newly complexed Sir proteins (black rectangles), associate with the nucleosomes to form a wall of proteins that restrict accessibility to the DNA. By altering the function of either CAF-1 complex or the Sir protein complex the chromatin becomes disrupted and eventually derepressed. This figure was reproduced from Enomoto & Berman (1998) *Genes & Development*, 12, 219-232 [78].

PEV [81]. A number of proteins homologous to HP1 have now been identified in *Drosophila* and mammals. One of the best known *Drosophila* homologues is Polycomb, this protein is known to influence the expression of many genes in euchromatin [82]. These proteins share a common amino acid sequence called the chromodomain. This domain is highly conserved and generally found in proteins associated with heterochromatin [83]. In *Drosophila* an entire family of Polycomb proteins have now been identified. They are known as the Polycomb-group (PcG) proteins and they are very important in regulating the expression of homeotic genes that control the segmental identity of the insect body in development. Mutation of the genes encoding these proteins leads to the aberrant activation of the normal target genes [84].

In general, studies that have examined how “modifiers” work have shown a strong correlation between the number of copies of the gene within the nucleus and the extent of heterochromatin formation [85]. This has led to the theory that these modifiers work by mass action i.e. the more “modifier” present, the more heterochromatin assembled. It also appears that chromodomain proteins may cooperate to assemble multimeric complexes that can alter the structure of long stretches of chromatin [84]. An example of this is the effect of Polycomb on the area of chromatin that contains the three homeotic genes that make up the bithorax complex, Polycomb protein is

associated with transcriptionally inactive chromatin over more than 200 kb of DNA that covers this group of genes [86]. Histone proteins have also been identified as proteins “modifiers of PEV” [87]. These proteins do not contain a chromodomain and their role in PEV is probably related to chromatin condensation. However, this result may indirectly indicate the importance of histone deacetylation in heterochromatin formation. There is evidence to support this idea too, maintenance of histones in a hyperacetylated state suppresses PEV [88].

(B) Histone deacetylase and transient inhibition of transcription

The influence of histone deacetylase action on chromatin in higher eukaryotes can be transient or maintained through cell division and involves a vast number of associated proteins. Developmentally relevant examples of both methods of transcription repression are described below. It in no way contains the names of all identified partner proteins but describes the two major mechanisms by which histone deacetylases of higher eukaryotes repress transcription.

The rate of transcription is governed by both positive and negative regulatory proteins that interact with specific DNA sequences (promoters or enhancers) upstream of the gene in question. In many cases the negative regulation involves recruitment of histone deacetylase to the promoter, changing the degree of chromatin packing

[89]. However, HDACs do not contain DNA binding sequences and must rely on other factors to target them either generally or to specific sites in the DNA where their action is required.

Transcriptional control can be mediated through proteins of the Mad/Max family of bHLH-zip proteins that bind DNA at E box sequences [90]. These transcription factors are known to play key roles in cell differentiation and, with the third protein of the family, Myc, can both up or down regulate gene expression. These three proteins form heterodimers, Max being the common component of dimers. Myc-Max dimers normally result in activation of genes containing E box sequences. Competition for Max is present from Mad, formation of Mad-Max dimers results in repression of target genes and usually a transition of the cells effected from proliferation to the differentiated state. The action of Mad-Max dimers in producing this switch is thought to involve histone deacetylase action (figure 8a). Unfortunately, histone deacetylase activity cannot be co-precipitated with Mad [90,91,92]. Further studies have shown that Mad can precipitate the global transcription factors mSin3a/3b, and that it is through this interaction that Mad represses transcription by mSin3, acting as the scaffold on which a higher order repressive complex can be formed [90].

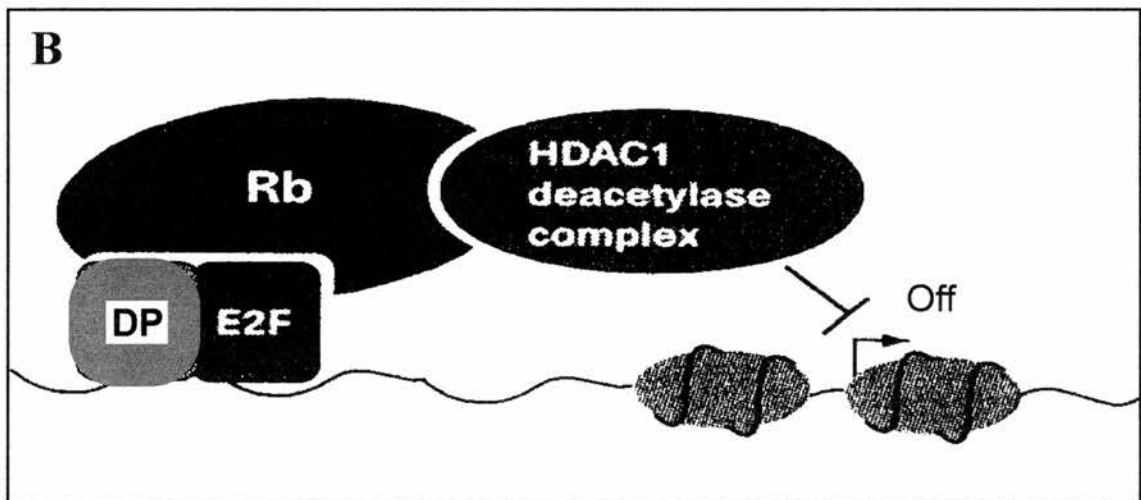
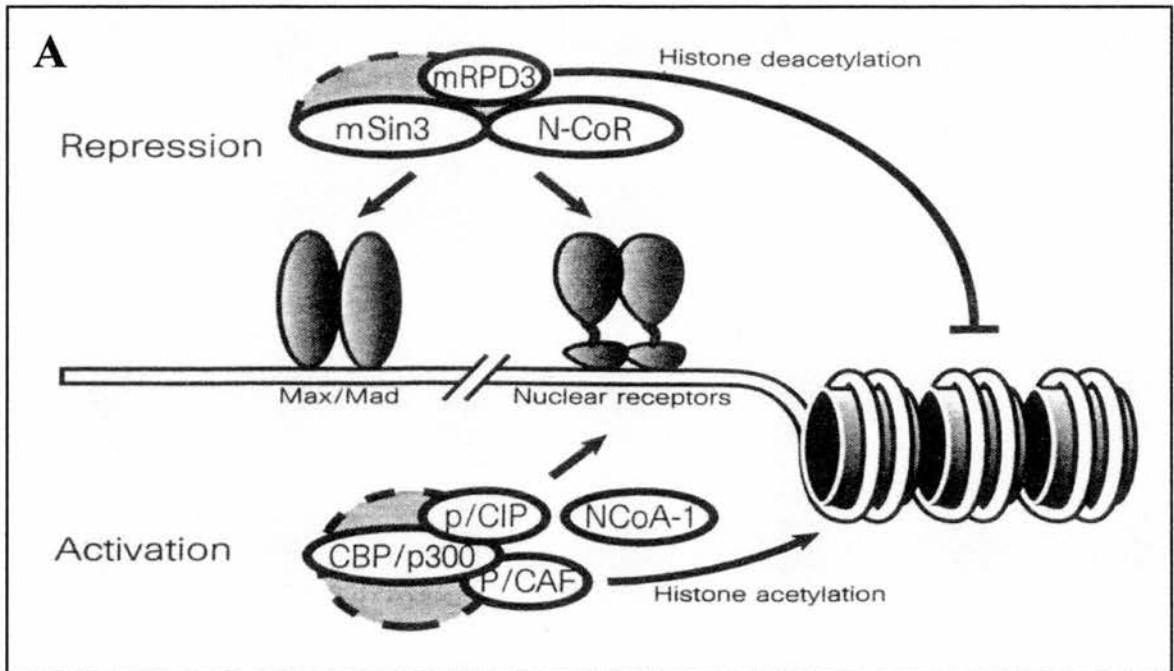


Figure 8. Histone deacetylase can be found in complexes of differing composition. **(A)** Model of the protein complex required to inhibit gene expression from promoters under the control of MAD/MAX transcription factors. Transcription repression requires a complex containing N-CoR, mSin3 and a histone deacetylase (mRPD3). Upon binding of activating ligand, the co-repressor complex dissociates and is replaced by an activating complex. This acetylates histones and facilitates the entry of core transcription factors. Figure taken from Heinzek *et al* (1997) *Nature*, 387, 43-48 [95]. **(B)** Representation of the complex of proteins required for repression of gene expression by the retinoblastoma protein (Rb). Repression of E2F by Rb involves deacetylase activity. Rb can bind simultaneously to E2F and HDAC1, and uses deacetylase activity to silence the promoter, the mechanism of this binding is known to be via the retinoblastoma associated protein p48 (RbAp48). Figure taken from Brehm *et al* (1998) *Nature*, 391, 597-601 [101].

In yeast, mating type switching is controlled by the endonuclease encoding gene HO. Expression of HO is controlled by six proteins, Swi1-6. Of these, 1-3 are general transcription factors, 4/6 are involved in regulation of HO expression during the cell cycle. Swi 5 is a Zinc finger DNA-binding protein. Expression of HO is regulated in two ways; (i) the gene is only transcribed during G2 of the cell cycle, (ii) nuclear localization of Swi 4/6 proteins are regulated during the cell cycle. Mutation of the genes encoding the Swi proteins results in loss of ability to switch mating type. The existence of Sin3 was discovered because it was found to be a member of a second family of proteins that could suppress the effect of mutations in swi1/2/3/5, if they themselves were mutated [93].

Sin3 is a 175 kD protein which generally acts as a negative regulator of gene expression. Although it has no DNA binding ability itself it can interact with many DNA binding proteins/transcription factors and repress transcription. In yeast it has been demonstrated that this protein can also bind the yeast histone deacetylase RPD3 [89,94,95]. The mammalian form of Sin3 is also a co-repressor for the Mad-Max complex, interacting with the Mad protein as part of the heterodimer, and other proteins via specific protein-protein interactions involving the four paired amphipathic helices (PAH1-4) it contains. PAH-2 controls the Mad-mSin3 interaction with the Sin3 interaction

domain (SID) in the NT of Mad, whilst PAH-3/4 control interactions with deacetylase. HDAC 1 & 2 will precipitate with mSin3. Mad, mSin3 and HDAC2 may be components of a complex with histone deacetylase activity that inhibits transcription at specific target sites. To complete this story, further experiments have been conducted to confirm the implications of these findings. It is now known that in colony formation assays, formation of an mSin3/mRPD3 complex on Mad-Max heterodimers results in deacetylase activity and inhibits colony formation at S-phase. Sommer *et al* [91] transiently transfected Saos-2 cells with a neomycin resistance plasmid plus expression vectors containing the cDNA for Mad1, Max, Sin3B and HD1. On growing these transfected cells in medium containing neomycin they found fewer cell clusters compared to the control. The transfected cells were stopped from entering S-phase because the Mad/Max-HDAC complex prevents expression of the necessary genes. This block could be overcome by incubating cells in TSA. Expression of these Myc-Max controlled genes can be inhibited by histone deacetylation that results in chromatin remodelling [93,94,95].

A further component of Sin3 containing deacetylase complexes has been elucidated by Heinzl *et al* [95]. They have demonstrated that histone deacetylase complexes may play an important role in regulating expression of genes under the control of the thyroid hormone receptor.

In this complex N-CoR or its related protein SMRT plays an important role [95,96]. These are co-repressors recruited to DNA by unliganded nuclear hormone receptors, such as the RAR-RX hormone heterodimer. These proteins can be shown to interact directly with mSin3 via PAH1. The interaction of the complex thus involves the nuclear receptors and the Mad-Max heterodimer. Additionally, a number of other proteins, such as Ski, may be required for transcriptional repression by Mad and thyroid hormone receptor [97]. Upon receptor binding hormone the complex is destabilised and dissociates from the nuclear receptors, thus allowing the repressor complex to be replaced by a co-activator complex containing CBP and P/CAF, which confer HAT activity on the complex and reinitiate gene expression [96,97,98] (figure 8a).

However the overall situation is much more complex than this. MBP-1, the c-myc promoter binding protein has been shown to recruit a histone deacetylase complex to the Myc-Max bound promoter, this promotes the transcriptional repression of cellular genes [99]. SMRT may also be able to repress transcription by a second mechanism not involving histone deacetylase activity. By binding TFIIB into the repressor complex SMRT reduces the level of free TFIIB in the nucleus so that the transcription complex cannot form [100].

(C) Histone deacetylase and stable inheritance of transcription repression

The corepressors mentioned in section B are not the only possible partners for histone deacetylase, as recent reports have shown [101,102,103]. The action of retinoblastoma protein (Rb) is known to be mediated through its binding with histone deacetylase. Rb can repress transcription of cell cycle genes containing E2F sites through the action of associated histone deacetylase [104]. The interaction of Rb with HDAC1 has recently been confirmed by Brehm *et al* and Magnaghi-jaulin *et al* [101,102]. It has been shown that Rb associates with HDAC1 through the Rb pocket domain, using residues distinct from the E2F-binding site, this indirectly recruits histone deacetylase to E2F and allows repression of E2F-regulated promoters. There is no evidence of a direct link between HDAC1 and Rb. Reports from other groups record the co-immunoprecipitation of retinoblastoma associated protein 48 (RbAp48) with HDAC1, indicating that this may play a role similar to that of Sin3 of co-ordinating the different parts of the complex and targeting this to chromatin (figure 8b). Vermaak and Wolffe [103] have produced the evidence for the role of RbAp48 in targeting histone deacetylases to chromatin. By studying the *Xenopus* homologue of RPD3 (xRPD3) they have discovered that when RbAp48 is injected

into oocytes, it is incorporated into a high molecular weight complex containing xRPD3.

The role of a RbAp48-like protein in targeted deacetylation of newly assembled chromatin has also been demonstrated recently. p55 is a homologue of RbAp48 and is an integral part of the CAF-1 complex in *Drosophila*. This protein co-immunoprecipitates HDAC1 activity, furthermore a fraction of the p55 protein becomes associated with newly synthesised chromatin following replication. These findings suggest that p55 may act as a link between DNA replication-coupled chromatin assembly and histone deacetylation [27].

There is also a deacetylase complex containing both RbAp48 and Sin3. This complex contains a further complex targeting protein, methyl-CpG-binding protein 2 (MeCP2) and has been studied in both mammalian cells [105] and *Xenopus* oocytes [106]. In mammalian cells MeCP2 contains a transcription repression domain that binds a co-repressor complex containing RbAp48, mSin3 and histone deacetylases [105]. In oocytes, methylated DNA assembled into chromatin binds the transcription repressor MeCP2, which isolates with Sin3, RbAp48 and histone deacetylases. The silencing imposed by MeCP2 and methylated DNA can be relieved by inhibiting the deacetylase with TSA [106].

This method of repression establishes an epigenetic imprint on the chromatin that is maintained through cell division. Maintenance

methylases continue the pattern of CpG methylation between cell generations and MeCP2 containing deacetylase complexes continue to bind and repress these sites from generation to generation [107]. In the development of complex organisms that contain a large number of tissue specific genes DNA methylation provides a mechanism for permanently inactivating genes whose activity is not required in a particular cell type i.e. site-specific gene inactivation [108]. This stable silencing of a large part of the genome means the transcriptional machinery only has to transcribe the genes necessary for establishing and maintaining the differentiated phenotype. The importance of this is seen when you inhibit DNA methyltransferase activity. This treatment leads to the activation of repressed genes [109].

1.4. Synthesis and incorporation of histone isoforms during early *Xenopus* development

Development of the oocyte and early embryo is through an RNA-only environment. Every protein produced is from mRNA pre-stored in the oocyte before maturation. In the oocyte these messages are used to create a store of proteins vital for early development [110].

Histone proteins are one of the most important products of the mRNA pool found in the oocyte. Histones are essential for the replication of chromatin during the rapid cleavage divisions. The core

histones and histone H1 are synthesised at a low rate during oogenesis. For the core histones this rate is increased 50 fold upon progesterone-induced maturation and results in the production of a large store of histone proteins. The storage of these histones once synthesised has been best studied with histone H4 [110]. Once made, the protein is diacetylated by type B cytoplasmic HATs before being transported into the nucleus and stored in complex with nuclear proteins N1 and N2 [11]. These chaperones aid nuclear import, are essential for incorporating H4 into nascent chromatin, and may also protect the stored histones from deacetylase action. The store is large enough to provide for chromatin replication until MBT. [11,21,111].

This situation can be further complicated by variation in the histone proteins synthesised at different stages in development and the susceptibility of these isoforms to post-translational modifications. In sea urchins, pools of maternal cleavage stage histones replace the sperm histones post fertilization, before being replaced themselves by somatic histones after the 16 cell stage [39]. In *Xenopus* these changes in core histones are more modest. The core histones are constitutively active in the oocyte and in the developing embryo following MBT. The only core histone variant is H2A.X. This is produced in the oocyte and accumulates in the early embryonic chromatin but is diluted rapidly with proceeding cell division [39].

The rate of synthesis and the degree of variability in the number of isoforms expressed is very different for histone H1. Its rate of synthesis is not stepped up at maturation but remains low until MBT [110]. This step up in synthesis rate coincides strongly with the resumption of gene expression and the deacetylation of histone H4. The presence of diacetylated histone H4 seems to reduce histone H1 deposition. At MBT most of the chromatin is deacetylated and only then is histone H1 incorporated into chromatin, concomitant with the resumption of gene transcription [21,111]. However, throughout the early stages of *Xenopus* development there are significant variations in linker histone; the various forms are thought to have selective functions in transcriptional regulation. In post-MBT somatic cells histone H1 exists in three isoforms; H1A, H1B and H1C. H1A is the most common of these isoforms making up 95% of post-MBT chromatin associated linker histone, H1B and H1C make up the remaining 5% in roughly equal amounts [112,113,114]. Histone H1 is not detectable in the oocyte (or in sperm), it is only detected post-MBT. The linker role prior to this point is performed by HMG-1, (a linker histone like protein) and by the linker histone B4 (H1m). Histone B4 shows 30% similarity to somatic H1 but is much less basic. This protein competes with HMG-1 and the two can influence chromatin structure and gene expression in a manner similar to that following incorporation of H1 into nucleosomes,

though their affinity for DNA is much less than that of H1. These two proteins are made and stored in the oocyte and are the common forms until MBT; by MBT B4 and H1 are present in equal amounts and HMG-1 is almost completely displaced. After this point the level of B4 drops off rapidly and H1 becomes the only type of linker histone [21,39,114].

Following MBT, B4 is progressively replaced by the three somatic histone isoforms, this replacement is complete by early neurula and accumulation of H1A specifically is strongly associated with the loss of mesodermal competence, showing its transcriptional regulation function [112,113]. The reason for the use of histone B4 and HMG-1 before MBT and histone H1 after MBT is not known. Theory predicts that it is probably because these proteins confer different qualitative properties to chromatin compared to H1A containing chromatin, and that the B4 chromatin is better suited to the needs of oocyte and early embryos with respect to chromatin remodelling.

It has been questioned whether or not histone H1 is necessary for *Xenopus* development. Premature expression of histone H1 causes oocyte specific 5S RNA genes to become transcriptionally repressed, whilst inhibition of H1 synthesis sustains their expression [115]. This is the only direct effect of H1 in development on gene expression. However, as accumulation of histone H1 in *Xenopus* chromatin

correlates with the restriction in cell lineage specific gene expression through gastrulation it is possible that somatic linker histones may have a role as repressors of alternative programs of transcription and in maintaining stable states of gene activity.

1.5. *Xenopus* histone deacetylase, HDACm

In 1994, Dr. J. Sommerville and co-workers isolated, cloned and sequenced a unique *Xenopus* protein (accession number X78454, appendix A). The mRNA for this protein is a maternal message that accumulates during oogenesis and encodes an enzyme that demonstrates histone deacetylase activity *in vitro*, because of its maternal origins this enzyme has been called HDACm. The mRNA encoding HDACm remains at a constant level through early development before disappearing at neurula. The HDACm protein has a molecular weight of 57 kD and accumulates in the oocyte during oogenesis, reaching maximum levels in stage VI oocyte. Following fertilisation the amount of HDACm in the embryo decreases continually, reaching an undetectable level by neurula. The protein sequence contains several recognisable motifs, the majority of which are concentrated in the carboxy-terminal of the protein. These motifs consist of potential phosphorylation sites [116] and a putative nuclear

localisation signal, similar to that of N1 that may be regulated by phosphorylation [117,118,119].

1.5.1. Aims of the project

The aim of this project is to further our understanding of the role played by HDACm in early development. Specifically, it addresses three questions;

(1) What is the sub-cellular location of HDACm throughout early development, and how may the enzyme be held in distinct compartments?

(2) How does the enzyme function *in vivo*? Which proteins does it associate with and when does it become active?

(3) How is this protein regulated and what role do the recognised structural motifs play? Within the amino acid sequence of HDACm there is a putative NLS and a number of potential protein kinase CK2 phosphorylation sites [116,117]. The phosphorylation state could be a regulatory mechanism controlling nuclear import of HDACm, complex formation, activity and substrate specificity.

Answering these questions could prove vital, as initial theories would indicate that mutation of an enzyme of this nature may lead to inhibited development and premature death.

Materials & Methods

2.1. *Xenopus laevis*, bacteria , plasmids and fusion proteins

2.1.1. *Xenopus laevis*

The South African clawed toad (*Xenopus laevis*) has been studied as a developmental system because its oocytes are large, and easy to collect and manipulate. Mature *Xenopus laevis* were purchased from Blades Biological, Edenbridge, Kent.

Oogenesis in *Xenopus* is special among animals used in laboratory work, as the process is continuous and asynchronous. Oocytes of all developmental stages are present in a sexually mature ovary [120]. In addition to this, sexually mature *Xenopus* females can be readily induced into a new reproductive cycle during any season by the administration of chorionic gonadotrophin (CG); this induces ovulation and ovipositioning as well as further physiological events, culminating in the formation of a new group of matured oocytes [121].

2.1.1.1. Oogenesis

Xenopus oocytes can be classified into six stages, numbered I to VI. This covers the progression from previtellogenic to postvitellogenic oocyte to full-grown oocyte (figure 9) [120]. This system of notation follows the

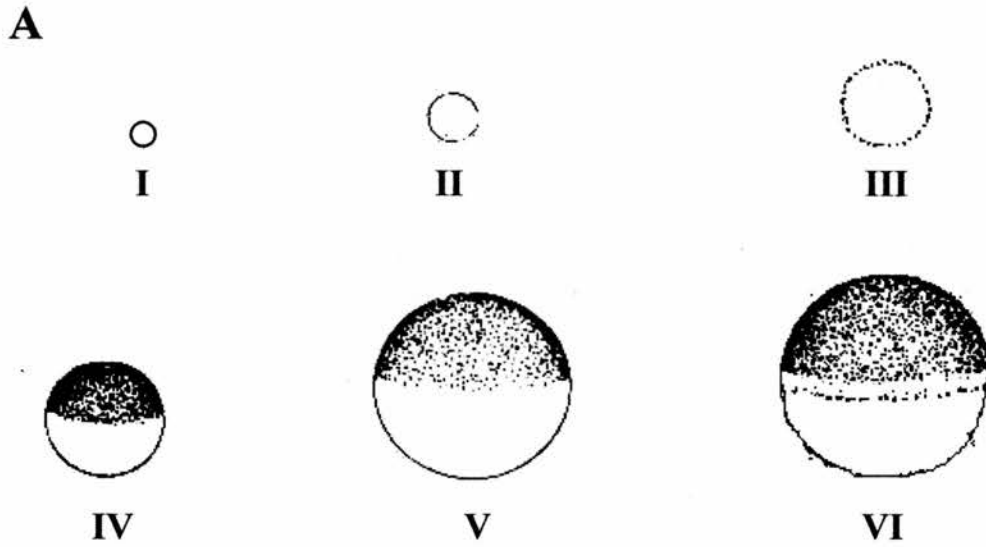


Figure 9. *Xenopus* oocyte stages and summary of key features of each stage. **(A)** Representation of the typical appearance of *Xenopus* oocytes at each stage in oogenesis from stage I to stage VI, courtesy of J. Sommerville. **(B)** Summary of the key histological features and physiological changes occurring in oocytes through oogenesis. The changes in appearance allows us to differentiate between oocytes at different points in oogenesis.

B

| Oocyte Stage | Size (µm) | General Appearance | Cortical Granules | Yolk | Nucleus | Chromosomes |
|--------------|-----------|---|---|---|--|--|
| I | 50-300 | Transparent cytoplasm; nucleus clearly visible. | None | None | Centrally located | Diplojene and early lampbrush |
| II | 300-450 | Cytoplasm translucent, turning to white and opaque by end of stage; nucleus still visible in early stage II | Formation begins; granules scattered throughout oocyte | Small platelets and lipid in periphery | Membrane attached | Zygotene and very early diplotene |
| III | 450-600 | Pigment formation begins. Stage III oocytes change from light brown at the beginning of stage to uniformly dark brown/black at the end of stage | Increase in number and size; movement towards surface of oocyte | Loosely packed platelets surrounded by lipid filled cytoplasm by end of stage | | Mid-diplojene; maximum lampbrush |
| IV | 600-1000 | Animal and vegetal hemispheres become differentiated by changes in pigment distribution | | Progressive accumulation - rapid in stage IV, decreasing in stage V; larger platelets in vegetal hemisphere | Located near animal pole | Late diplotene; chromosomes retract |
| V | 1000-1200 | Hemispheres clearly delimited at mid-line; animal hemisphere appears light brown and vegetal creamy | | | Located at animal pole; membrane is smooth facing animal pole but infolded toward vegetal pole | Chromosomes condense; become massed in centre of nucleus |
| VI | 1200-1300 | Unpigmented band forms at equator. Animal hemisphere remains light brown and vegetal creamy | Aligned in a single row beneath the oolemma | Cytoplasm packed with platelets and lipid | | |

oocyte as far as arrest at meiosis I. Further development involves a complex series of signals, second messengers and signal transduction pathways that induce and a range of changes in cell structure and function. Progesterone is the stimulus that induces the resumption of meiosis I by the MEK/MAPK signal transduction pathway [122], before arresting for a second time during meiosis II. Meiosis II is completed and the egg reactivated when the sperm crosses the vitelline membrane and fertilizes the egg. Activation is accompanied by a further series of intracellular signals and changes (figure 10) [122].

2.1.1.2. Embryogenesis

Following fertilization the embryo goes through twelve rapid cleavage divisions which lack G1 and G2 phases of the cell cycle and rely on internal stores of key mRNAs and proteins made during oogenesis to allow this process to be completed [121]. This regime persists until blastula; by blastula most of the intracellular stores are used up and the rate of production from stored mRNA is not fast enough to cope with demand [110]. A change occurs in the nuclei of these cells midway through blastula (mid-blastula transition - MBT), and gene transcription is turned on.

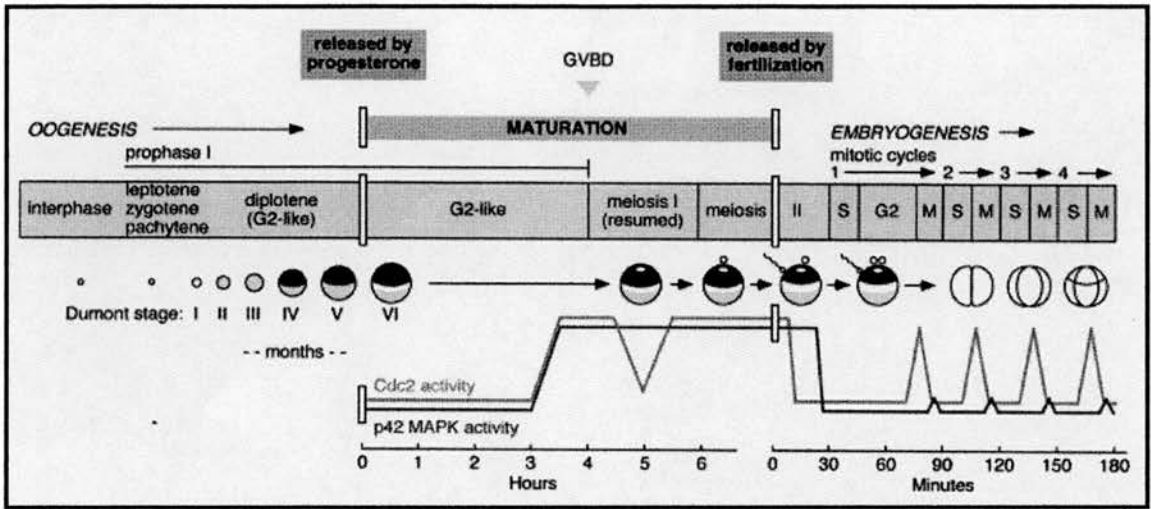


Figure 10. Sequence of intracellular signals that accompany resumption of meiosis and egg activation in *Xenopus* ovary. Progesterone and fertilisation are specific signaling events which cause cellular reorganisation by signal transduction. Oocyte maturation is initiated by ligand binding by a plasma membrane based progesterone receptor, progesterone binding is the signal for break down of the germinal vesicle (nucleus) and brings about the completion of meiosis I by activating the M phase trigger Cdc2/cyclin B. Cdc2/cyclin B activation is the end point of the Mos signalling pathway. Meiosis is arrested a second time during meiosis II and the egg is only reactivated when the sperm crosses the vitelline membrane and fertilizes the. Egg activation is accompanied by a further series of intracellular signals and changes that prepare the fertilized egg for the stress of the rapid cleavage divisions. Figure reproduced from Ferrell, J.E. Jr. (1999). *BioEssays*. 21, 833-842 [122].

After this point G1 and G2 are restored to the cell cycle, the rate of cell division slows, cells begin to commit to specific lines and morphological changes occur within the embryo as cell migration is initiated [21,111,121]. The gut begins to form (gastrulation), followed by the neural tube (neurula) and later specific anatomical features become obvious (tail bud) (figure 11).

2.1.2. Bacteria

Untransformed *Escherichia coli* (*E. coli*) super competent cells of the strains B121 (DE3) and NovaBlue (DE3) were purchased from Novagen. Bacterial cells were transformed with plasmids conferring ampicillin resistance and were grown on ampicillin treated agar plates to select for successfully transformed bacteria.

Luria broth (LB) per litre distilled water (dH₂O)

| | |
|------------------------------|------|
| Tryptone (Merck) | 10 g |
| Bacto® Yeast extract (Difco) | 5 g |
| NaCl | 10 g |

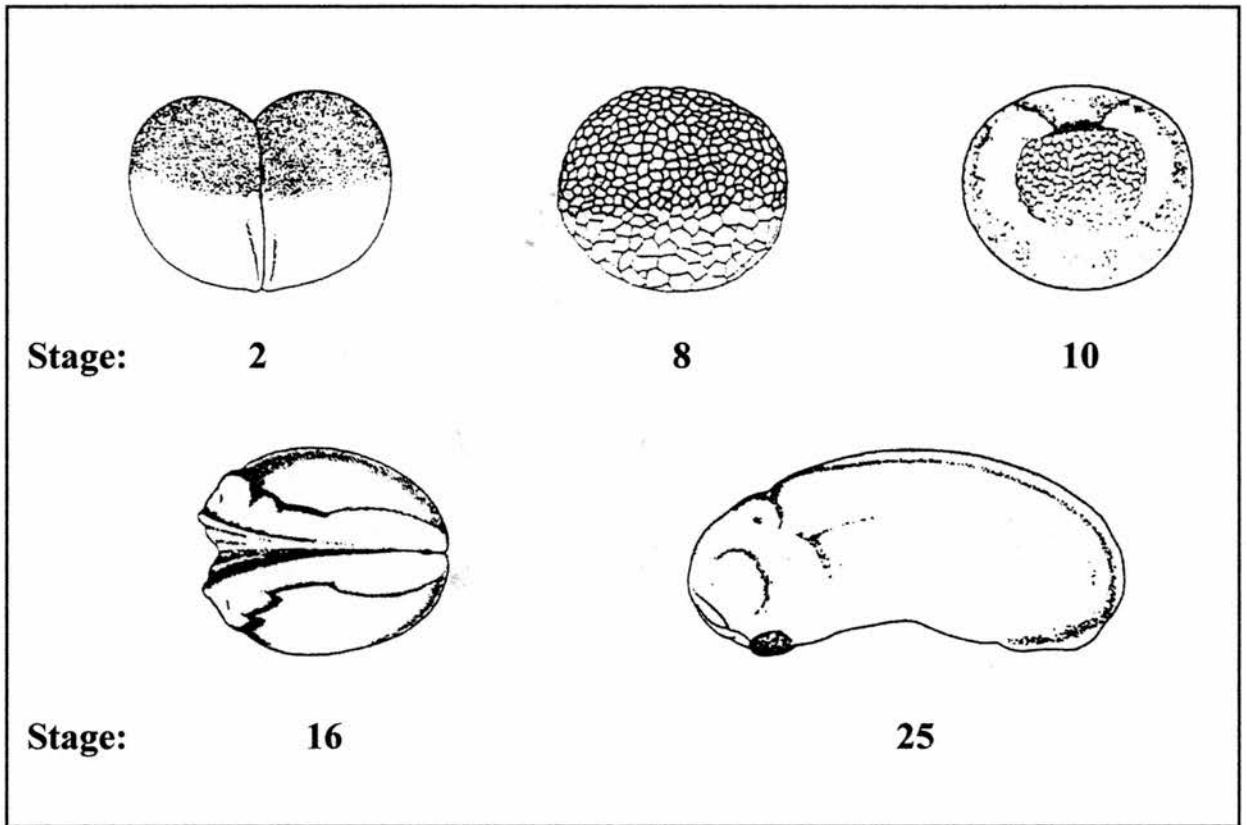


Figure 11. The main histological stages in early *Xenopus* embryogenesis. Embryogenesis starts with the rapid cleavage divisions (2) of the newly fertilised egg during which cell numbers increase rapidly. Blastula follows this initial stage. The embryo enters early blastula (7-9) when the cell number reaches 1024. After this point the rate of division slows as G1 and G2 phases of the cell cycle are introduced. During mid-blastula (8) a transition occurs (MBT) in activity and gene activity is turned on. As development progresses further, through gastrula (10), neurula (16) and tailbud (25), the cells of the embryo commit to different fates and then differentiate. Figure reproduced from Nieuwkoop, P.D. & Faber, J.(1956). *A systematical and chronological survey of the development from the fertilized egg till the end of metamorphosis*. North-Holland Publishing Company [123].

LB-agar plates.

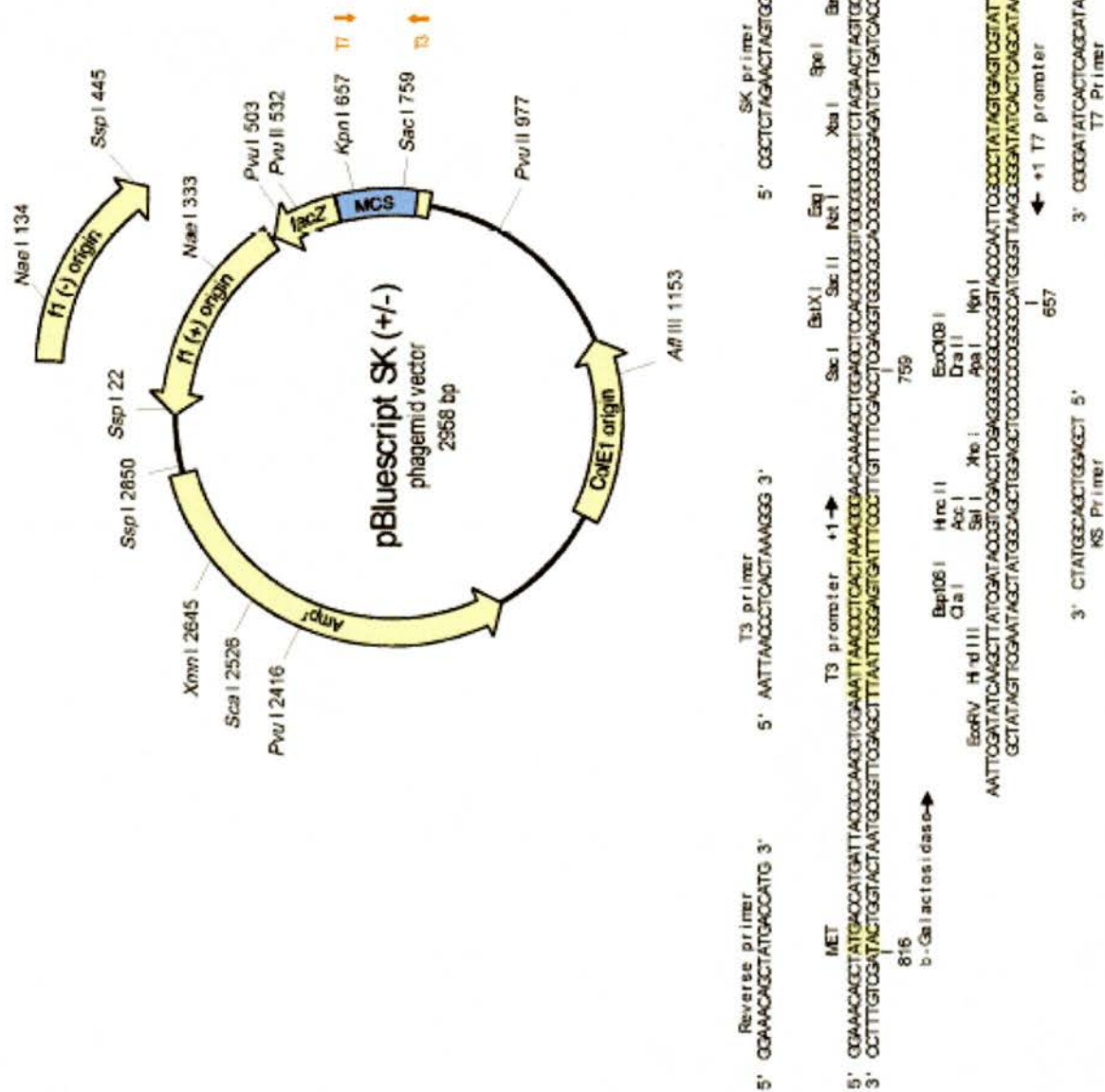
15 g of bacteriological agar (Gibco BRL) was added to 1 litre of LB and autoclaved. The agar was cooled to 45°C, the required antibiotic was added at 100 µg/ml and the plates were poured.

2.1.3. Plasmid vectors and fusion proteins

pBLUESCRIPT®

The cDNA of the HDACm gene (AB21) was screened for and selected from a Unizap II® λ phage cDNA expression library prepared by Dr. Sommerville and screened by Dr. Ladomery. The identified AB21 cDNA was recovered in the pBluescript® vector (Stratagene). This vector is a 2.96-kb, colony producing plasmid that carries ampicillin resistance (β-lactamase gene) and contains 21 unique restriction sites in the polylinker region (figure 12). The insert was directionally cloned between the EcoRI and XhoI sites. *In vitro* production of RNA transcripts is possible using the T3 and T7 bacteriophage RNA polymerase promoters.

Figure 12. Composition of pBLUESCRIPT® (SK) plasmid. This is a 2.96 kb vector derived from pUC19, the SK designation indicates the polylinker is orientated such that *lacZ* transcription proceeds from *SacI* to *KpnI*. The *lacZ* gene provides a-complementation for blue/white selection of recombinant plasmids. An inducible *lac* promoter upstream from the *lacZ* gene permits fusion protein expression with the β -galactosidase gene product. Plasmid also contains a multiple cloning site (polylinker) flanked by T3 and T7 RNA promoters and the ampicillin resistance gene for antibiotic selection of vector containing bacteria.



pGEX[®]

GST fusion vectors are part of an integrated system for the expression, purification and detection of fusion proteins. The plasmids are designed for inducible, high level intracellular expression of genes or gene fragments as a fusion with *Schistoma japonicum* glutathione-S-transferase (GST). As a result of this “tag”, fusion proteins are easily purified by the use of glutathione coated Sephadex beads.

Sub-clones of the AB21 cDNA were inserted into the polylinker region of pGEX 4T plasmids (figure 13) using an appropriate open reading frame. The polylinker region is found down stream of the GST gene. The polylinker region contains multiple unique restriction sites and encodes a thrombin cleavage site so that once expressed, the carrier protein can be cleaved from the fusion protein. The cDNA of AB21 contains several useful restriction sites. These were used to construct three sub-clones of AB21; ΔR , ΔV and $\Delta R/\Delta H$. The most widely used of these sub-clones was ΔV ; this protein encodes the final 174 residues of the protein. A number of important motifs are apparent in this fusion protein, including a putative nuclear localisation signal (NLS) as well as six putative protein kinase CK2 and up to four receptor tyrosine kinase phosphorylation sites.

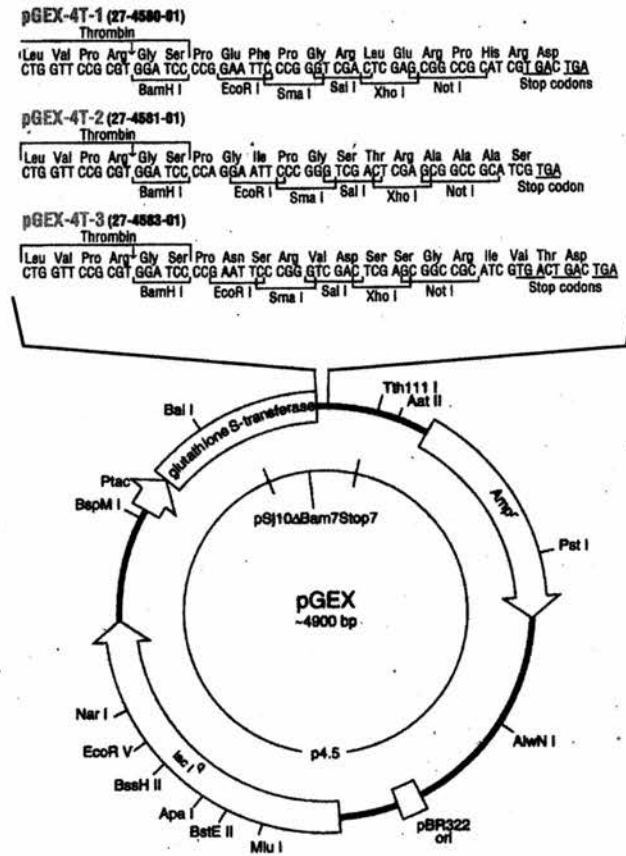


Figure 13. Composition of pGEX 4T[®] plasmid series. This series contains three plasmids, each of approximately 4.9 kb in size. These plasmids offer all three translational reading frames beginning with the EcoRI restriction site. These inserts are ligated downstream of the GST gene into the polylinker region which facilitates unidirectional cloning of cDNA inserts; that region also contains a number of unique restriction sites and encodes a thrombin cleavage site to allow removal of the fusion protein from the carrier protein once purified. Expression of the insert is under the control of an IPTG inducible *tac* promoter. The plasmid also contains an internal *lac Iq* gene to allow use in any *E. coli* host.

GFP[®] plasmids

Sub-clones of AB21 were inserted into GFP plasmids to produce green fluorescent protein (*Aequorea victoria*) tagged products. To produce a C-terminal tagged fusion protein inserts can be introduced between the 6 myc-tag sequence and the GFP of pCS2*mt-SGP by use of limited restriction sites (figure 14). To produce an N-terminal tagged fusion limited restriction sites between the myc-tag and GFP sequence of pCS2*mycGFP-NOTB4-Tail were used. These vectors were kindly supplied by Dr. M. Klymkowsky, University of Colorado.

pCGT7 plasmid

The pCG plasmid is derived from pSTC [124]. To create pCG, an M13 origin of replication was inserted, a unique Xba I site created and a polylinker inserted after removal of glucocorticoid receptor gene sequences [125]. To create pCGTVP16 Δ C (pCGT7) a sequence encoding the T-epitope residues 1-11 of T7 gene 10 was inserted into the polylinker. This form of the vector was kindly supplied by Dr. J.F. Caceres, MRC Human Genetics Unit, Edinburgh. The pCGT7 vector can accept inserts between the Xba I site downstream of the T7 epitope sequence and the BamHI site.

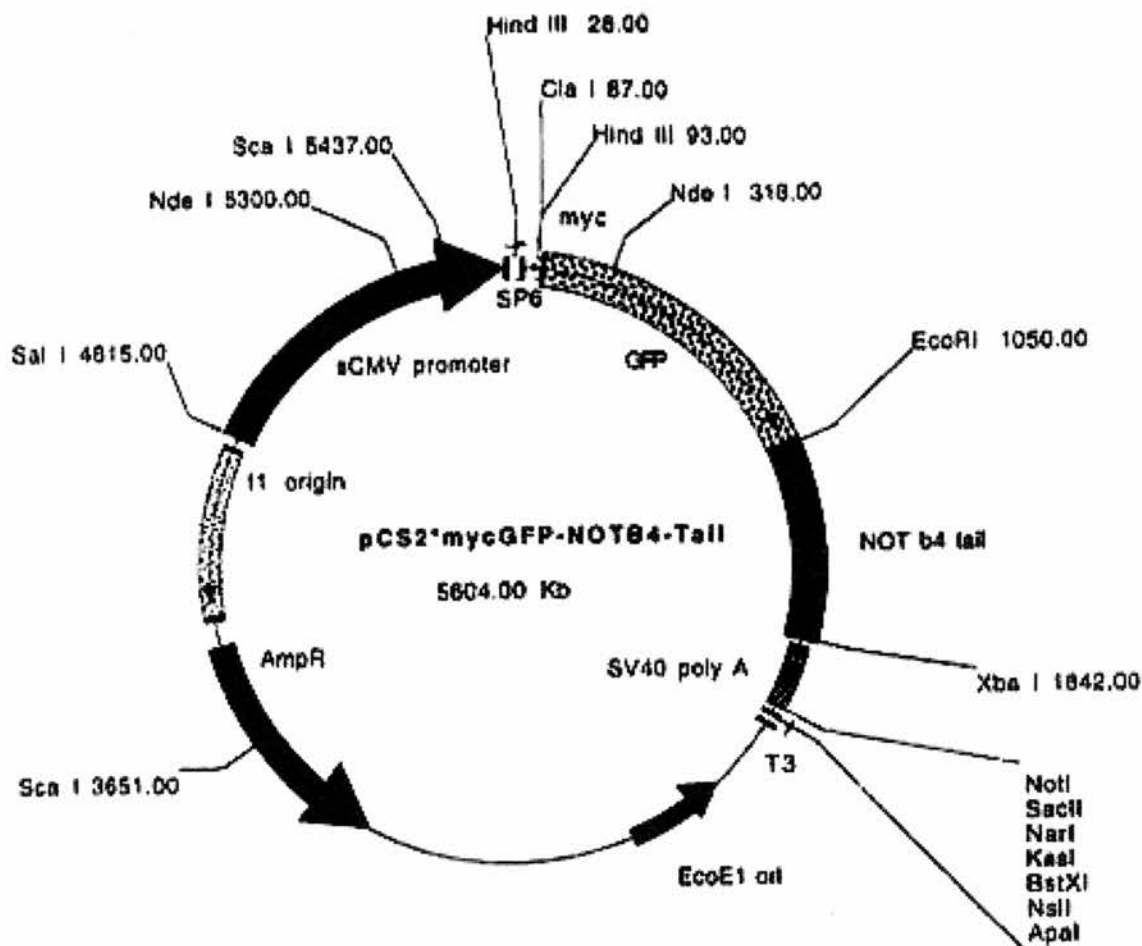
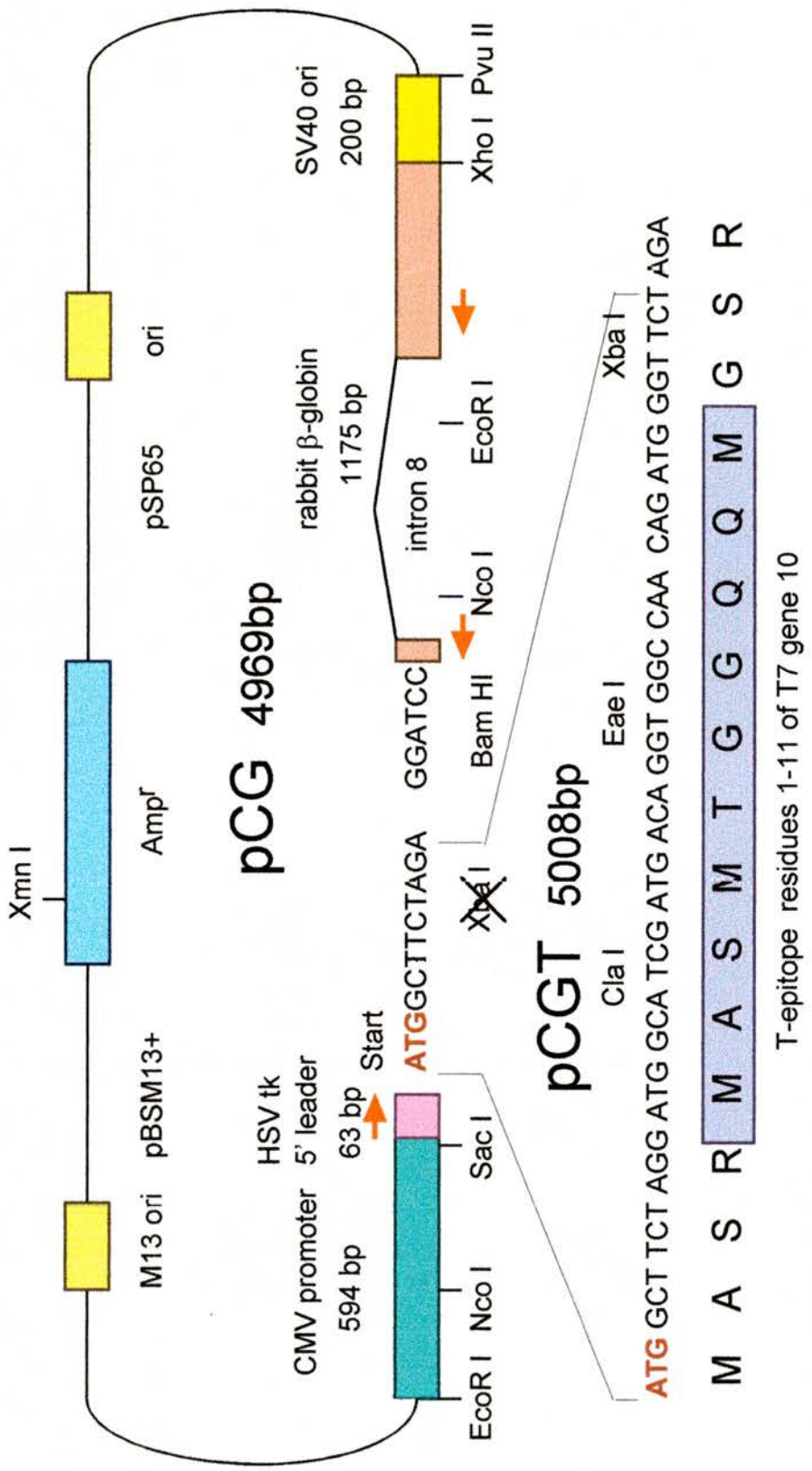


Figure 14. Composition of the GFP[®] plasmid pCS2*mycGFP-NOTb4-tail. The GFP plasmid has a size of 5604 kb. The vector is based on the pCS2-mt plasmid. The plasmid contains an SP6 promoter to allow synthesis of strand specific RNA *in vitro*, and a CMV promoter which allows eukaryotic expression of the insert. The unique EcoRI and XbaI restriction sites allow insertion of the DNA fragment such that a chimeric N-terminal tagged polypeptide is produced.

Figure 15. Composition and derivation of pCGT plasmid. This vector was kindly supplied by Javier Cacaes. pCG was derived from pSTC; an M13 origin of replication was inserted, an unique XbaI site created and a polylinker inserted after removal of glucocorticoid receptor gene sequences. Bacterial plasmid vector sequences are derived from pBSM13⁺ between the non-polylinker EcoRI site shown in pCG and the XmnI site within the β -lactamase gene (Amp^r) and the remainder are derived from pSP65, between the XmnI site and the unique pSP65 PvuII site, the latter forming the junction with the SV40 ori sequence. Plasmid also contains the CMV promoter fragment, rabbit β -globin 3'UTR containing intron 8 and the polyadenylation motif and the SV40 ori fragment. pCGTVP16 Δ C was created by insertion of the sequence encoding the T-epitope residues 1-11 of T7 gene 10. Vector can accept inserts between the unique XbaI site immediately downstream of the T-epitope sequence and the BamHI in the polylinker



T7 promoter / tk primer: TAATACGACTCACTATA G GGAGGTGGCGTGAAACTCCCGCAC

β-globin 5' reverse primer: GGAGGGGCAAGTTTTCAGGGTG CCTCCCCCGTTTCAAAAGTCCAC

The vector could be injected into oocyte nuclei or transfected into mammalian cells or mRNA could be made as shown in figure 15 and injected. The T7 epitope tag on the N-terminus of the expressed protein was detected using a monoclonal antibody directed against the T7 epitope (Novagen).

2.2. Plasmid DNA extraction, purification and insertion of foreign DNA. Use of plasmid DNA to transform bacteria cells and *in vitro* transcription of inserted DNA

2.2.1. Preparation of plasmid DNA by alkaline lysis [126]

One colony of bacteria was inoculated into 5 ml of Terrific Broth (TB) containing ampicillin (100 µg/ml) and grown to confluence at 37°C with aeration. 1.6 ml of the culture was spun in a microcentrifuge to pellet bacteria, the supernatant was removed by pipette and a further 1.6 ml of culture was added and spun to increase the size of the bacteria pellet. The supernatant was again removed and the tube was drained of residual supernatant.

The pellet was raised in 180 μl GTE solution before the serial addition of 360 μl of fresh 0.2 M NaOH/1% SDS solution and 270 μl 3 M potassium acetate (pH 4.8). The solutions were then mixed by inversion and the sample was spun at high speed for 10 minutes in a microcentrifuge. The supernatant was removed and respun under the same conditions for a further 5 minutes to remove any remaining precipitate.

The supernatant was again transferred and mixed rigorously with 600 μl of phenol in chloroform (50% v/v phenol and 24:1 chloroform/isoamyl alcohol, plus 1/10 volume of 1 M Tris-HCl pH 8.0) before being spun in a microcentrifuge at high speed for 5 minutes. After this time the top phase was removed, mixed with 600 μl of chloroform and spun for another 5 minutes. The top phase was again removed and to this an equal volume of absolute ethanol was added before being left at -20°C for at least 1 hour to precipitate the plasmid DNA. After this time the sample was spun at high speed in a microcentrifuge for 10 minutes, the pellet was then drained of supernatant and dried in a vacuum pump before being raised in 20 μl of sterile dH_2O .

GTE Solution

| | |
|-------------------|-------|
| Tris-HCl (pH 8.0) | 25 mM |
| EDTA | 10 mM |
| glucose | 50 mM |

Terrific Broth 1 litre

| | |
|---------------------------------|---------|
| Tryptone | 12 g |
| Yeast Extract | 24 g |
| Glycerol | 4 ml |
| KH ₂ PO ₄ | 2.31 g |
| K ₂ HPO ₄ | 12.54 g |

2.2.2. Preparation of Plasmid DNA with the Wizard[®] Plus DNA purification system

One colony of bacteria was inoculated into 5 ml of TB containing ampicillin (50 mg/ml) and grown to confluence at 37°C with aeration. 1.6 ml of the culture was spun in a microcentrifuge to pellet bacteria, the supernatant was removed by pipette and a further 1.6 ml of culture was

added and spun to increase the size of the bacteria pellet. The supernatant was again removed and the tube was drained of residual supernatant.

This pellet was raised in 300 μ l of resuspension solution (50 mM Tris-HCl pH 7.5, 10 mM EDTA, 100 μ g/ml RNase A), lysed with 300 μ l of lysis solution (0.2 M NaOH, 1% SDS) which was neutralised by the addition of 300 μ l neutralisation solution (1.32 M KAc). The resulting mixture was centrifuged at 13 000 rpm for 20 minutes in a bench top centrifuge and the supernatant was removed. The supernatant was mixed with 1 ml of Wizard Miniprep[®] DNA purification resin and passed through a mini-prep column. The column was washed with 2 volumes of wash solution (80 mM KAc, 8.3 mM Tris-HCl pH 7.5, 40 μ M EDTA, 55% ethanol v/v), centrifuged for 30 seconds in a bench top centrifuge at 13 000 rpm to remove residual wash solution. To elute the DNA from the silica matrix, the column was soaked in 50 μ l of sterile dH₂O for 2 minutes before again being centrifuged at 13 000 rpm in a bench top centrifuge and the eluate was collected and saved.

2.2.3a. Polymerase Chain reaction (PCR)

PCR was performed by the recommended protocol [127] using Ready-To-Go PCR beads (Pharmacia Biotech) dissolved in a final volume of 25 μ l. The beads contained 1.5 units Taq polymerase, and enough buffer, salts and stabilisers to keep the final reaction mixture at the correct salt level and pH 9.0; the beads also contained enough dNTP to give a final concentration of 200 μ M each. 50 pg of plasmid template DNA in 1 μ l dH₂O was added to the bead before forward and reverse primers, synthesised to sequence required by PE-Applied Biosystems UK, were added to the beads to give a final concentration of 0.2 mM (approximately 1 μ l). A layer of light mineral oil was added to the top of the mixture.

The PCR amplification reaction was carried out in a Minicycler™ thermocycling unit (M J Research, Inc). The amplification of DNA fragments was conducted over 30 cycles. Following initial denaturation of all DNA at 95°C the temperature was reduced to the annealing temperature where primers and template were allowed to meld. The annealing temperature is reaction dependent and was set at a temperature 2°C below

the melting temperature (T_m) of primers used. The temperature was then raised to 72°C to allow the elongation of the PCR product.

2.2.3b. Site-Directed mutagenesis by PCR

Site directed mutagenesis was conducted using high melting temperature oligonucleotide primers containing the point mutation to be produced (PE-Applied Biosystems) and the QuikChange™ Mutagenesis Kit (Stratagene). This system uses the Pfu Turbo DNA polymerase, which replicates both DNA strands of plasmid with high fidelity and without displacing the oligonucleotide primers.

The protocol followed was that which is stated in the Stratagene instructions. The reaction was set up as recommended: 5 µl of 10x reaction buffer (100 mM KCl, 100 mM (NH₄)₂SO₄, 200 mM Tris-HCl pH 8.8, 20 mM MgSO₄, 1% Triton X-100 and 1 mg/ml nuclease free bovine serum albumin), dsDNA template to a final concentration of 50 ng, oligonucleotide primers to a final concentration of 125 ng each, 1 µl dNTP mix and sterile dH₂O to 50 µl. 1 µl of Pfu Turbo DNA polymerase was then added to the reaction mix.

Once set up the reaction mix was cycled through the following parameters. The DNA was melted at 95°C for 30 seconds before being cooled to 55°C for 1 minute to allow the annealing of primers and template. Elongation was performed at 68°C for 2 minutes/kb of plasmid length. This cycle was repeated 18 times. At the end of the reaction 1 µl of Dpn I restriction enzyme was added to the reaction mix and allowed to digest the parental (methylated) dsDNA (37°C for 1 hour). Super competent XL-1 blue cells were then transformed with 1 µl of the final reaction mix by the method described in section 2.2.8.

2.2.4. Restriction Digest of DNA

Samples of DNA were digested for 1 hour in a 20 µl volume containing the required restriction endonuclease and restriction buffer. When required RNase A was added to a final concentration of 50 µg/ml. If a double digest of DNA was required, the digests were performed sequentially unless both restriction endonucleases worked in the same restriction buffer. If dephosphorylation of DNA was required, 1.5 µl of calf intestinal phosphatase (1400 U/ml) was added to the digest for its final 20 minutes.

2.2.5. Agarose gel electrophoresis

1% agarose mini gels were used to analyse PCR and restriction digest products. Agarose (Bio-Rad) was dissolved in 50 ml of TAE by boiling before cooling to 45°C. Ethidium bromide was then added to a final concentration of 0.5 µg/ml before allowing the gel to set. The gel was covered in TAE buffer and DNA samples, with loading buffer added to 1/10 volume, were loaded into the gel wells. Samples were run at 100 V and the DNA bands were visualised using a 300 nm UV-light transilluminator.

Tris-Acetate buffer (TAE)

50 x stock per litre:

| | |
|---------------------|---------|
| Tris base | 242 g |
| Glacial acetic acid | 57.1 ml |
| 0.5 M EDTA (pH 8.0) | 100 ml |

1 x running buffer:

| | |
|--------------|---------|
| Tris-acetate | 0.04 M |
| EDTA | 0.001 M |

10 x TAE DNA gel loading buffer

| | |
|------------------|-----------|
| Glycerol | 50% v/v |
| Bromophenol blue | 0.42% w/v |
| Xylene cyanol FF | 0.42% w/v |

2.2.6. Purification of DNA excised from DNA gels

The required DNA band was excised from the agarose gel using a clean razor blade. Bands were visualised as described in section 2.2.5 and extracted by the recommended protocol [128,129]. The first step of the extraction involved melting the agarose in three volumes of 5M NaI at 50-55°C. Secondly, glass milk suspension was added at 2 µl for every 1 µg of DNA and vortexed to mix thoroughly. The sample was then incubated on ice for 5 minutes with occasional mixing to keep the glass milk in suspension before the DNA/glass milk complex was pelleted by spinning in a microcentrifuge for 5 seconds. The supernatant was removed and the pellet was washed three times in wash buffer. Each time the pellet was washed it was first resuspended in 0.5 ml of wash buffer before being

pellet by centrifugation, the wash buffer was then removed and the pellet was washed in 0.5 ml of fresh wash buffer. After the final wash care was taken to ensure all wash buffer was removed. The DNA was eluted from the glass milk by resuspending in at least an equal volume of dH₂O, incubating at 50-55°C for 3 minutes, centrifuging at high speed for 30 seconds and collecting the supernatant.

Glass milk [129]

| | |
|----------------------|-----------|
| NaI | 3 M |
| Silica resin (Sigma) | 100 mg/ml |

Wash solution [129]

| | |
|-------------------|----------|
| NaCl | 50 mM |
| Tris-HCl (pH 7.5) | 10 mM |
| EDTA | 2.5 mM |
| Ethanol | 50 % v/v |

2.2.7. Ligation of DNA fragments

Insert DNA was mixed with dephosphorylated, linearized plasmid in a 5:1 ratio. The total reaction volume was 20 μ l. The reaction was conducted by the recommended protocol [130] using Ready-To-Go™ T4 DNA ligase reaction tubes (Pharmacia Biotech). These contained a buffered salt mix (pH 7.6), 6 Weiss units FPLCpure® T4 DNA ligase, stabilisers and once made up to 20 μ l; 0.1 mM ATP, 0.1 mM spermidine and 10 mM Dithiothreitol (DTT). The ligation was performed overnight by heating the mix to 16°C. The reaction was stopped by denaturing the ligase by heating to 65°C for 10 minutes.

2.2.8. Transformation of competent cells

Transformations were performed using competent Novagen NovaBlue (DE3) cells. These cells contain bacteriophage λ DNA in their genome as a stabilised lysogen; this phage DNA encodes the T7 bacterial RNA polymerase under the control of the *lacUV5* promoter. In addition to this the bacteria have had the gene encoding endonuclease A1 removed, are *recA1*⁺ (which leads to increased plasmid stability), encode *lacIq* which represses basal T7 RNA polymerase expression from the *lacUV5* promoter

and are tetracyclin resistant. These cells have a very high transformation efficiency (1×10^8 transformants/ μg test plasmid).

The transformation process was conducted as recommended by Novagen [131]. 20 μl of cells were thawed on ice and mixed gently to ensure they were properly suspended, before 5 μl of diluted ligation product (1 μl ligation reaction: 4 μl dH_2O) were added. The cells were left on ice for 5 minutes before being incubated at 42°C for 30 seconds and then left on ice for a further 2 minutes. 80 μl of SOC medium was added to the cells, mixed and the cells were then left to grow at 37°C for 30 minutes before plating on ampicillin plates and grown over night at 37°C . Ampicillin plates were made with ampicillin at a final concentration of 50 $\mu\text{l}/\text{ml}$, compared to 100 $\mu\text{l}/\text{ml}$ final concentration that was normally used.

2.2.9. Synthesis of capped mRNA from plasmid DNA

A “mini-prep” of plasmid DNA was prepared by alkaline lysis (1.2.1), linearised and raised to a concentration of 1 mg/ml , message was produced by the mMessage mMachine™ protocol [132]. The transcription reaction was set up using this freshly prepared material; to 1 μl of template were added 10 μl of “2x ribonuclease mix”, 2 μl “10x transcription buffer”

and 2 μl "10x enzyme mix". If radiolabelling of the message was required, this could be achieved by the addition of γ -CTP to the reaction. The volume was made up to 20 μl with RNase free dH_2O and mixed by pipette action before being incubated at 37°C for 1 hour. Template DNA was removed by the addition of 1 μl RNase-free DNase 1 (2U/ μl) and incubation at 37°C for 15 minutes, the transcription reaction was stopped addition of 115 μl nuclease free dH_2O and 15 μl ammonium acetate stop solution. RNA was then collected by phenol/chloroform extraction and alcohol precipitation (2.2.1).

Ammonium acetate stop solution

| | |
|------------------|--------|
| Ammonium acetate | 5 M |
| EDTA | 100 mM |

2.2.10. Denaturing RNA gel

RNA could be analysed by electrophoresing under denaturing conditions. A denaturing formaldehyde gel was prepared by dissolving 0.9 g of agarose in 35 ml of dH_2O . Once the mix had cooled to 50°C, 12 ml of 5x 3-[N-morpholino]propanesulfonic acid (MOPS) buffer was added (41.9

g MOPS, 4.1 g sodium acetate, 3.1 g EDTA.Na₂ dissolved in 1 litre dH₂O, pH 7.0), followed by the addition of 13 ml of formaldehyde prior to pouring the gel. This procedure was performed in a fume cupboard. The RNA sample was prepared as follows:

| | |
|---------------------|--------|
| RNA | 5 µl |
| 5x MOPS | 2 µl |
| Formaldehyde | 3.5 µl |
| Deionised formamide | 10 µl |

Denaturing RNA gel.

| | |
|-------------------|-------|
| Agarose | 0.9 g |
| dH ₂ O | 35 ml |
| 5x MOPS | 12 ml |
| Formaldehyde | 13 ml |

This mixture was then heated to 65 for 15 minutes, 4 µl of sample buffer (50% glycerol, 1 mM EDTA, 0.4% xylene cyanol, 0.4% bromophenol blue)

were added to the sample just before loading. The gel was run at 15 v for 16 hours in 1x MOPS.

2.3. Protein sources, treatments, separation and detection techniques

2.3.1. Bacterial expression and purification of fusion proteins [133]

A 5 ml culture of bacteria transformed with the pGEX plasmid containing the GST-subclone insert was grown up overnight. This starting culture was then added to 200ml of LB containing ampicillin (100 µg/ml) and grown to mid-log phase ($OD_{600} = 0.5$) at 37°C with aeration. IPTG was then added to a final concentration of 0.1 mM and the culture was grown for a further 3 hours at 25°C with aeration.

To harvest and lyse the cells, the induced culture was first cooled on ice for 10 minutes before being centrifuged at 3000 rpm for 10 minutes at 4°C to pellet the cells. The pellet was then raised in a lysis buffer containing proteinase inhibitors and frozen, the suspension was thawed and sonicated to disrupt the cell membranes. Triton-X 100 (Sigma) was added

to 1% v/v to solubilise protein products and the lysate was centrifuged at 10 000 rpm for 15 minutes at 4°C and the supernatant was collected.

The fusion protein was extracted from the supernatant by the addition of 2 ml of 50% glutathione Sephadex beads solution (Pharmacia) and incubating to allow binding of the GST tagged protein to the beads. Beads were collected by centrifugation at 500 rpm for 10 seconds and washed repeatedly in ice cold tris (tris(hydroxymethyl)aminomethane) buffered saline (TBS). GST-fusion protein was thrombin cleaved on the beads; the beads were raised in 2 ml of digestion buffer containing thrombin at 100 U/ml for 3 hours at room temperature. To harvest the cleaved product the supernatant from the beads was removed and dialysed, the product was then stored at -20°C until required [133].

Tris buffered saline pH 7.5

| | |
|------|--------|
| NaCl | 40 g/l |
| KCl | 1 g/l |
| Tris | 15 g/l |

Lysis buffer in TBS

| | |
|-----------|-----------|
| EDTA | 10 mM |
| PMSF | 1 mM |
| Lysozyme | 0.5 mg/ml |
| Leupeptin | 2 mg/ml |
| Pepstatin | 2 mg/ml |
| Aprotinin | 4 mg/ml |

Cleavage buffer

| | |
|-------------------|--------|
| Tris-HCl (pH 8.0) | 50 mM |
| NaCl | 150 mM |
| CaCl ₂ | 2.5 mM |

GST elution buffer

| | |
|---------------------|-------|
| Reduced glutathione | 10 mM |
| Tris-HCl (pH 8.0) | 50 mM |

2.3.2. Expression of mRNA in the rabbit reticulocyte lysate system

The mRNA produced by the mMessage mMachine system could be expressed *in vitro* by the use of a rabbit reticulocyte lysate. 1 μ l of RNA was added to 17.5 μ l of reticulocyte lysate and incubated at 30°C for 2 hours. To allow translation of the message in this system the reticulocyte lysate was modified by the addition of amino acids and RNase inhibitors. If a labelled product was required 1 μ l of 0.6 mCi/ml of ³⁵S-methionine (1000 Ci/mmol, Amersham) was added to the reaction. The resulting protein could be analysed by SDS-PAGE or used directly in microinjection studies.

Rabbit Reticulocyte Lysate translation

| | |
|--------------------------------------|---------------|
| RNA | 1 μ l |
| Reticulocyte lysate | 17.5 μ l |
| Amino acid mix | 0.5 μ l |
| RNase inhibitors | 0.5 μ l |
| ³⁵ S-methionine(optional) | 1 μ l |
| Nuclease free H ₂ O | to 25 μ l |

2.3.3. Oocytes

Sexually mature *Xenopus* females were used to obtain ovarian tissue containing all oocyte stages. Material was obtained by anaesthetising the animal in MS222 (0.2% in water) before destruction of the brain and surgically removing the ovarian tissue [134]. Connective tissue around the oocytes was digested away by continual mixing with 0.2% type I collagenase (Sigma) in Calcium free OR2 medium at room temperature until all oocytes had separated. The oocytes were then washed three times in 20 ml fresh Calcium free OR2 medium followed by three 20 ml washes in 1x Modified Barths' solution. Oocytes were then stored in this medium before being separated by developmental stage according to the classification of Dumont [120] and either used immediately or stored at -20°C in the minimum volume of 1x Modified Barths' solution until required.

Modified Barths' solution

| | |
|----------------------------------|-------|
| 2x modified Barths' solution | 50 ml |
| sterile dH ₂ O | 50 ml |
| Antibiotic & Antimycotic (Sigma) | 1 ml |

Concentrated (2x) stock solution:

| | |
|-----------------------------------|---------|
| NaCl | 88 mM |
| HEPES (pH 7.4) | 10 mM |
| NaHCO ₃ | 2.4 mM |
| KCl | 1 mM |
| MgSO ₄ | 0.82 mM |
| CaCl ₂ | 0.41 mM |
| Ca(NO ₃) ₂ | 0.33 mM |
| Phenol red | Trace |

Calcium free OR2 medium

| | |
|----------------------------------|---------|
| NaCl | 82.5 mM |
| HEPES (pH 7.4) | 5 mM |
| KCl | 2.5 mM |
| MgCl ₂ | 1 mM |
| Na ₂ HPO ₄ | 1 mM |
| PVP | 0.5 g/l |
| Phenol red | Trace |

2.3.4. Collection of embryos

A sexually mature male and a sexually mature female *Xenopus* were injected with chorionic gonadotrophin (Sigma) four hours before being introduced to each other in a darkened tank of chlorine free water and allowed to mate overnight [122]. The fertilised eggs were collected from the mating tank and selected at different stages in their development according to the staging criteria of Nieuwkoop [123]. Embryos at stages 2 (cleavage), 7 (early blastula), 8 (mid blastula), 9 (late blastula), 12 (gastrula), 16 (neurula) and 25 (tail bud) were collected. The outer jelly coat was removed by digestion in 2% (Sigma) pH 7.9 for 5 minutes. The inner coat was then removed by mechanical manipulation using two pairs of watchmakers' forceps to pull the coat off. The embryos were then used immediately (microinjection) or frozen in the minimum volume of 1x Modified Barths' solution until required.

2.3.5. Fractionation of oocytes

(I). *Nucleus isolation.* Nuclei from stage III to stage VI oocytes were isolated under light paraffin oil (BDH) by a modified method of that first reported by Paine *et al* [135]. Oocytes of required stage were collected and placed animal pole upward onto a 3MM paper lined 25 mm culture

dish. The oocytes were covered in a layer of light paraffin oil and pierced at the animal pole with a fine pointed needle, taking care to control the angle and depth of the puncture so as not to damage the nucleus. Following the puncture, the nucleus alone will make its way out of the oocyte and can be collected. Collected nuclei were stored at -20°C in a minimum of modified Barths' solution ($0.5\ \mu\text{l}/\text{nucleus}$).

(II). Cytoplasm collection. Once the nuclei had been removed from the oocytes, cytoplasm was collected and stored in a minimum of modified Barths' solution ($5\ \mu\text{l}/\text{cytoplasm}$). Isolation of nuclei and cytoplasm occurred in oil. To remove the fractions from oil to modified Barths' solution oil containing fractions were placed on a cushion of modified Barths' solution and pelleted into the Barths' solution by microcentrifugation at high speed for 5 minutes and then frozen. Once frozen, the oil could be taken off the top of the aqueous phase.

(III). Fractionation of whole ovary into vesicle and soluble fractions [136]. Ovarian tissue was removed from a mature female animal and the tissue was homogenised in homogenisation buffer by sonicating. The homogenate was spun at 500 rpm for 2 minutes and free lipid was removed. The rest of the homogenate was layered onto a 20% sucrose in

homogenisation buffer solution and centrifuged in a swing out rotor of 30 cm diameter at 10 000 rpm at 4°C for 30 minutes. The resulting supernatant was removed; this was the soluble fraction.

The pellet formed in the previous stage was raised in Tris buffered saline (pH 7.5) and centrifuged under the same conditions as before for a further 10 minutes. The resulting supernatant was removed. This was the vesicle or membrane fraction.

(IV). Fractionation of whole ovary in to aqueous and detergent fractions

[137]. Whole ovary was homogenised by mechanical shearing in 1% Triton X-114 in TBS (pH 7.5). After incubating at 0°C for 10 minutes with occasional mixing the insoluble material was removed by centrifuging at 10 000 rpm for ten minutes at 4°C. The resulting supernatant was removed and warmed to 37°C for 2 minutes. This solution was then centrifuged at room temperature in a microcentrifuge at 10 000 rpm for 2 minutes. The upper phase was the aqueous phase (detergent depleted) and the lower the detergent-enriched.

Homogenisation buffer

| | |
|-------------------|--------|
| KCl | 100 mM |
| Tris-HCl (pH 7.5) | 20 mM |
| MgCl ₂ | 2 mM |

2.3.6. Freon extraction of yolk protein and lipid from oocytes and fractions [139]

After homogenisation of whole oocytes in an equal volume of homogenisation buffer, or production of oocyte fractions containing yolk proteins and lipid, the yolk and lipid was removed by Freon extraction. Upon production of oocyte homogenates, an equal volume of Freon (1,1,2-Trichlorotrifluoroethane, Sigma) was added and mixed vigorously before centrifuging for 10 minutes at 10 000 rpm and 4°C. The resulting clear phase of the supernatant was removed, leaving the yolk and lipid trapped in the lower Freon phase.

An SN100 for use in pull down assays could be made from the Freon extracted whole oocyte extract. The clarified supernatant produced from the Freon extraction was transferred to a Beckmann 5 ml centrifuge tube, paraffin oil was layered on top of the extract to protect it. The extract was

then centrifuged at 36 000 rpm for 2 hours at 0°C in a Beckmann SW55Ti swing-out rotor, this produced a supernatant lacking mRNP particles and other very large multimolecular complexes, such as chromatin. The clarified supernatant was collected from under the oil, aliquotted and stored at -70°C until needed.

2.3.7. Progesterone induction of oocyte maturation

Stage VI oocytes were isolated after collagenase treatment and then placed in modified Barths' solution containing progesterone (Sigma) to a concentration of 2 nM. The oocytes were left in this solution to mature. During this process nuclei and cytoplasms were collected at 1 hour intervals until the nuclei broke down (GVBD) at meiosis I.

2.3.8. Dephosphorylation of oocyte material

Stage VI oocytes were isolated from collagenased ovary and nuclei and cytoplasms were isolated from half of the sample. These fractions and whole oocytes were then mechanically disrupted before being incubated with calf intestinal alkaline phosphatase for 30 minutes at room temperature. Nuclei were incubated with 1 µl phosphatase; whole oocytes

and cytoplasm were incubated with 5 μ l phosphatase. The material was then Freon extracted.

2.3.9. Extracting histones from oocytes and embryos

Material was homogenised in homogenisation buffer and Freon extracted as normal, the aqueous layer of the Freon extracted material was then raised in 10 volumes of 0.22 M HCl and left over night at 4°C to extract the histones [32].

2.3.10. Characterisation of HDACm, its activity, post-translational modifications & partner proteins

(I). Oocyte microinjection. Oocytes for injection (stages V or VI) were isolated from collagenased ovary and put onto 700 nm Nitex mesh in a 25 mm diameter petri dish, animal pole up. The oocytes were then centrifuged in a swing out rotor at room temperature and 650 g for 10 minutes to fix the oocytes into place on the grid and to bring the germinal vesicles to the oocyte surface.

To inject the material, whether DNA, RNA or protein, it was first raised in injection buffer and drawn into a micropipette needle having a

diameter of 20-30 μl connected to a microsyringe and a micrometer; the needle was under the control of a micromanipulator. The petri dish was mounted under a binocular microscope and moved so that it was near the needle, the micromanipulator was then adjusted so that the needle just pierced the surface of oocyte (protein, RNA) or so that it just pierced the nucleus (DNA). Volumes injected ranged from 5 nl of DNA to 30 nl for protein. Once injected the oocytes were washed out of the grid and transferred into fresh modified Barths' solution to recover [139].

(II). *Hydroxylamine treatment* [140]. Hydroxylamine (pH7.5) was added to Freon extracted vesicle fractions to final concentrations varying from 0.1 M to 2 M and incubated at 37°C for 1 hour.

Hydroxylamine stock solution (Tris to pH 7.5)

| | |
|---------------|-----|
| Hydroxylamine | 3 M |
|---------------|-----|

(III). *Protein digestion* [141]. Partial protein digests were performed on oocyte material using V8 protease (Sigma) or Trypsin (Sigma), digests were performed on acetone precipitated material. The conditions of digest for V8 protease required raising the acetone precipitated material in 5 M urea and 0.1% SDS, the protease was added to final concentrations of 10

ng/ml to 1 μ g/ml and incubated at 37°C for 1 hour. The conditions for Trypsin digest required raising the material in 4 M urea and 0.05% SDS; trypsin was added to a final concentration of 10 μ g/ml and incubated at 37°C for 5 hours.

(IV). *Gradient centrifugation.* 5 ml gradients containing 10%-30% glycerol were prepared in homogenisation buffer (without protease inhibitors) plus 0.1% Nonidet P-40 (NP-40, Sigma). Samples containing oocytes, cytoplasm or nuclei homogenised in homogenisation buffer were loaded to the top of the gradients before the gradients were centrifuged at 30 000 rpm for 18 hours at 0°C in an SW55 Ti rotor in a Beckman L-7 ultracentrifuge. Marker proteins were run on the gradient, marker proteins were haemoglobin (67 kD), IgG (160 kD), apoferritin (443 kD) and catalase (250 kD). 300 μ l samples were collected by careful pipetting from the top of the gradient. Protein was extracted from the fractions by precipitation with 3 volumes of ice cold acetone, the pellet was raised in saturated urea.

(V). *Micrococcal nuclease digestion of chromatin.* A chromatin enriched pellet of insoluble material was collected from oocyte nuclei or embryo extracts by gradient centrifugation. This material was incubated with one

unit micrococcal nuclease at 37°C for 1 hour in the presence of 0.0015 M CaCl₂ and 0.03 M borate buffer (pH 8.8) to release the nucleosomes from the chromatin.

(VI). *Immunoprecipitation* [105]. 5 µl of protein A Sephadex beads (Pharmacia) were washed in borate buffer and pre-incubated with 5 µl of serum and incubated with occasional mixing for 2 hours at room temperature. The beads were then washed in borate buffer before the adsorbed IgG was cross-linked to the beads using 20 mM dimethyl pimelimidate in borate buffer. Following cross-linking the beads were washed in 0.2 M ethanolamine, followed by elution buffer and then TBS containing 0.1% Tween 20 (TBST). 50 µl of nuclei, raised in 300 µl TBST containing bovine serum albumin (BSA) to a final concentration of 1 µg/µl, were incubated with the beads for 1.5 hours at room temperature. To elute precipitated protein from the beads, the beads were first washed thoroughly in TBST before protein was eluted in 4 x 50 ml aliquots of elution buffer.

0.1 M Borate buffer pH 9.0

| | |
|------------|---------|
| Boric acid | 6.2 g/l |
| NaCl | 8.8 g/l |

Elution buffer

| | |
|------------------|-------|
| Glycine (pH 3.0) | 0.1 M |
|------------------|-------|

(VII) *micromanipulation of isolated nuclei.* Nuclei isolated under oil [1.3.6] were transferred to a small petri dish containing light paraffin oil; a small vesicle (generally one half of the nuclear diameter) of intracellular medium containing the substance to be studied was then placed in the petri dish with a micromanipulator and fused with the nucleus. As the isolated nucleus retains normal *in vivo* composition for 24 hours under these conditions [135], uptake and incorporation kinetics could be studied.

Intracellular medium pH 7.2

| | |
|---------------------------------|--------|
| NaCl | 10 mM |
| KCl | 125 mM |
| KH ₂ PO ₄ | 1 mM |
| NaHCO ₃ | 2 mM |

(VIII) *Histone acetylation by a HAT B extract* [53]. A cytoplasmic extract enriched in oocyte HAT B was made by homogenising 100 µl of oocyte

cytoplasms collected under oil [1.3.6] in 100 μ l of cytoplasm homogenisation buffer and Freon extracting [1.3.7]. The aqueous layer was removed and centrifuged for a further 30 minutes at 10 000g and the clarified supernatant containing HAT B was collected.

Typically, 1 μ g of purified histone H4 from calf thymus (Boeringer Mannheim) was added to 10 nmol of [3 H]acetyl Co-A (4.2 Ci/mmol; Amersham) and 1 μ l HAT B extract in the presence of 1x TENDS buffer; the reaction was conducted in a volume of 25 μ l. The mixture was incubated at 25°C for 45 minutes (longer incubation times do not increase the level of histone labelling), the reaction was terminated by the addition of 10 volumes of 0.22 M HCl. The histones were then acetone precipitated on ice, pelleted, washed in acetone and dried under vacuum. Acetylated histones were raised in dH₂O ready for oocyte/embryo injection or for use in an *in vitro* histone deacetylation assay. The addition of TSA to the reaction does not increase the level of labelling of histone H4, indicating that the HAT preparation contains no HDAC activity.

The advantage of labelling histone H4 by this method is that the histone is only acetylated at the sites in the N-terminus at which the histone is normally acetylated *in vivo*.

(IX) *Histone deacetylation assays.* The *in vitro* deacetylation assay was conducted in the presence of 25 mM sodium phosphate/citric acid pH 7.0. 1 µg acetylated histones raised in dH₂O, and either a crude homogenate of nuclei or gradient fraction material were mixed and the volume adjusted to 100 µl with buffer. The mixture was then incubated at room temperature for 1 hour. The reaction was terminated by precipitating onto glass fibre disks (Whatman) in 20% TCA before washing in acetone, drying and counting the filters in scintillation fluid (Packard).

An *in vivo* histone deacetylation assay was conducted by injecting oocytes or embryos with [³H]acetyl labelled histone H4. Post injection, the oocytes or embryos could be isolated, homogenised and Freon extracted. The remaining [³H]acetyl histone H4 in these extracts was then measured by scintillation counting as described above. Similarly, nuclei could be isolated from oocytes post injection, and the remaining [³H]acetyl histone H4 measured by scintillation counting as described above

TENDS buffer pH 8.0

| | |
|----------|-------|
| Tris-HCl | 20 mM |
| EDTA | 1 mM |
| NaCl | 50 mM |
| DTT | 1 mM |

HAT B homogenisation buffer pH 7.5

| | |
|-------------------|--------|
| Sucrose | 0.25 M |
| Tris-HCl | 20 mM |
| CaCl ₂ | 1 mM |
| EDTA | 2 mM |
| NaCl | 100 mM |

(X) Purification of protein kinase CK2 and phosphorylation of fusion proteins. Fusion proteins were made as described previously (1.3.1). This material may be phosphorylated by protein kinase CK2 extracted from nuclear and cytoplasmic homogenates. To extract protein kinase CK2, nuclei and cytoplasm were isolated as described previously (1.3.5) and homogenised in 1 x kinase buffer. Protein kinase CK2 was typically extracted from homogenates made from either 200 nuclei or 200

cytoplasms. 50 μ l of heparin Sephadex beads (Pharmacia) pre-swelled in TBS were added to the homogenates and the volume was made up to 1.5 ml with 0.1 M KCl and incubated on ice for 1 hour with occasional mixing. The beads were then washed four times in ice cold TBS before eluting protein kinase CK2 with 200 μ l 1.0 M KCl. The eluate was supplemented with glycerol to 50% v/v and stored at -20°C .

In vitro phosphorylation of the fusion protein was conducted as follows. To the fusion protein was added 1 μ l 10 x kinase buffer (minus KCl), 1 μ l kinase extract and 0.1 μ l ^{32}P -ATP, the volume was made up to 10 μ l with dH₂O. This mix was incubated at room temperature for 30 minutes to permit phosphorylation. The reaction was stopped by freezing or denaturing the sample by boiling with an equal volume of page buffer (1.3.11).

10x kinase buffer

| | |
|-------------------|--------|
| Tris-HCl (pH 7.4) | 200 mM |
| KCl | 200 mM |
| MgCl ₂ | 100 mM |
| DTT | 10 mM |

This was made up to 1x kinase buffer in 50% glycerol if being used to isolate the nuclei/cytoplasms for preparation of the crude nuclear homogenate or kinase extracts.

2.3.11. SDS PAGE [142]

Proteins were analysed by SDS-polyacrylamide gel electrophoresis (SDS-PAGE) separation in a Tris-SO₄²⁻ glycine running buffer using the Hoefer mighty Small™ system. The final concentration of polyacrylamide in the separating gel could be varied to give better separation of higher (above 40 kD) and lower (below 40 kD) molecular weight proteins. Generally, 12% gels were used to study higher molecular weight proteins and 15% gels for lower molecular weight proteins. The separating gel was poured and a layer of dH₂O was layered over the setting gel to give a level surface to the gel, once polymerised the dH₂O was removed and the stacking gel was poured on top. Samples were prepared by mixing with an equal volume of sample buffer and boiling for 2-3 minutes. Molecular weight markers were obtained from Bio-Rad and were pre-stained SDS-PAGE standard molecular weight markers. Samples were loaded onto the SDS-PAGE gel at a maximum of 20 µl/well and run at 300 V for 1 hour.

| SDS-PAGE gels | <u>12% gel</u> | <u>15% gel</u> | <u>Stacking gel</u> |
|---|----------------|----------------|---------------------|
| 30% (w/v) acrylamide solution | 1.6 ml | 2.0 ml | 200 μ l |
| 1M Tris- SO_4^{2-} (pH 8.3) | 0.5 ml | 0.5 ml | - |
| 0.5 M Tris- SO_4^{2-} (pH 6.9) | - | - | 125 μ l |
| dH ₂ O | 1.3 ml | 0.9 ml | 670 μ l |
| Glycerol | 0.57 ml | 0.57 ml | - |
| 10% SDS | 60 μ l | 60 μ l | 15 μ l |
| 25% AMPS | 8 μ l | 8 μ l | 5 μ l |
| TEMED | 8 μ l | 8 μ l | 5 μ l |

2x SDS-PAGE sample buffer

| | |
|-------------------|---------|
| Tris-HCl | 0.125 M |
| SDS | 6% |
| Glycerol | 20% |
| 2-mercaptoethanol | 5% |
| Bromophenol blue | 0.1% |

SDS-PAGE running buffer

| | |
|---------|----------|
| Tris | 3 g/l |
| glycine | 14.4 g/l |
| 10% SDS | 10 ml/l |

2.3.12a. Visualisation of proteins by coomassie staining [143]

Proteins were separated by SDS-PAGE and detected by staining with coomassie brilliant blue. The gel was immersed in coomassie brilliant blue solution for 1 hour with gentle agitation. The stain was then washed away and background colour was destained using several changes of destaining solution until the individual protein bands could be seen.

Coomassie brilliant blue stain

| | |
|--------------------------|--------|
| coomassie brilliant blue | 1 g |
| 96% ethanol | 250 ml |
| Glacial acetic acid | 50 ml |
| dH ₂ O | 200 ml |

Coomassie destain

| | |
|---------------------|--------|
| 96% ethanol | 250 ml |
| Glacial acetic acid | 100 ml |
| dH ₂ O | 650 ml |

2.3.12b. Visualisations of proteins by silver staining

Proteins were separated by SDS-PAGE and detected by silver staining. The gel was fixed for 30 minutes in a solution of 50 % methanol and 10% acetic acid and washed in distilled water. The gel was then immersed in the silver staining plus (Sigma) solution and mixed gently until the protein bands were visible. The reaction was stopped by washing the gel in 10% acetic acid.

2.3.13. Western blotting

Once proteins had been separated by SDS-PAGE they were electrophoretically transferred to a nitrocellulose membrane. The gel was removed from the gel frame and soaked in transfer buffer for fifteen minutes, a piece of nitrocellulose paper and 4 pieces of 3M blotting paper cut to the same dimensions as the gel were also soaked in the buffer. The gel was laid exactly on top of the nitrocellulose and sandwiched between 2x

two sets of blotting papers. The stack was rolled flat to remove any bubbles and placed between Hoefer SemiPhor™ plates with the protein gel at the cathode and a current of 35 mA was applied for 2.5 hours. The membrane was carefully removed and incubated in blocking solution over night.

Transfer buffer

| | |
|----------|-----------|
| Tris | 3 g/l |
| Glycine | 11 g/l |
| Methanol | 20% (v/v) |

Blocking solution

5 % (w/v) powdered skimmed milk in TBS containing 0.1% Tween-20 (TBST).

Specific proteins were located by their individual reactivity with antisera raised against purified protein or fusion proteins. Primary antisera was added to the nitrocellulose paper at a 1/2 000 dilution in TBST and incubated at room temperature for 1 hour. The membrane was washed for one hour in TBST to remove unbound antibody before horseradish peroxidase conjugated secondary antibody was incubated with the

nitrocellulose membrane at a 1/10 000 dilution in TBST. The membrane was again washed in TBST for 1 hour before being washed in TBS to prepare the membrane for visualisation of targeted protein by the DAB (diaminobenzidine) reaction or the chemiluminescent ECL™ western blotting analysis system (Amersham) [144].

DAB detection. 100 µl of 60% w/v DAB solution and 15 µl of 30% hydrogen peroxide were added to 12 ml of TBS and mixed. This solution was then washed over the filter for 1-2 minutes until a strong colour reaction had occurred at the location of immunoreactive protein bands. The reaction was stopped by washing the filter in copious volumes of dH₂O.

ECL chemiluminescence. ECL reagents 1 and 2 were added to the nitrocellulose membrane in a 1:1 ratio and allowed to wash over the membrane for 1 minute before excess fluid was drained from the membrane. The membrane was then wrapped in clingfilm before a photosensitive film was exposed to the nitrocellulose membrane for 10 minutes. The film was developed in Kodak x-ray developer and fix to give a stable, hard copy of the position of reactive bands on the membrane.

The membrane could then be stripped of antibody by incubating in stripping solution for 30 minutes at 50°C and the blocking a probing

process could be repeated on the same membrane to detect other proteins by repeating the above procedure.

Stripping solution

| | |
|-------------------|---------|
| SDS | 2% |
| 2-mercaptoethanol | 100 mM |
| Tris-HCl (pH 6.7) | 62.5 mM |

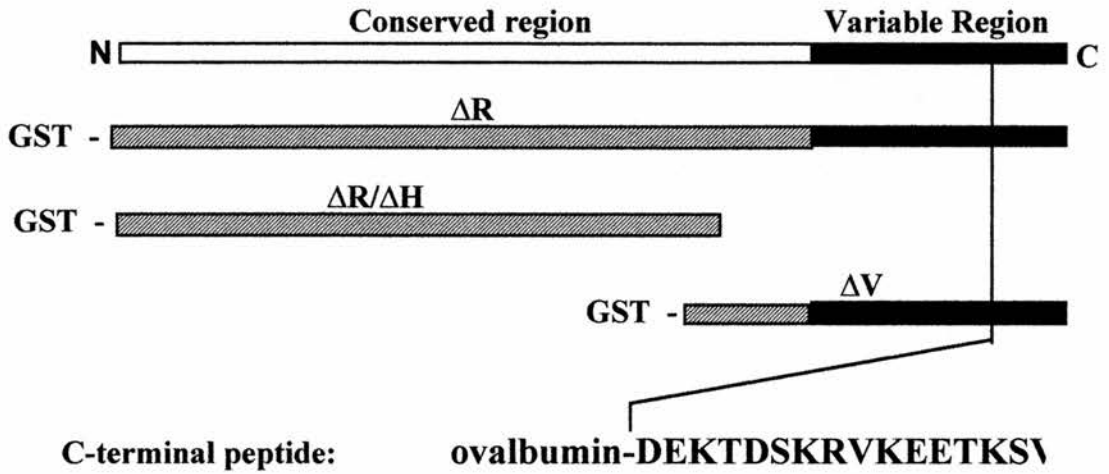
2.3.14. Antibodies

Four different antisera were available for use in detecting the deacetylase enzyme. Three of these antisera were raised in rabbits against the fusion proteins ΔR , $\Delta R/H$ and ΔV by Dr. Sommerville. The fourth antibody was produced against the seventeen carboxy-terminal residues of the HDACm enzyme (figure 16) by Dr. Brian Turner.

Antibodies raised against possible partner proteins were either donated by Dr. B. Turner (anti-RpAp48, anti-K5 acetylated histone H4, anti-K8 acetylated histone H4, non-acetylated histone H4) or Dr. Adrian Bird (anti-MeCP2); these polyclonal anti-sera were raised in rabbits. Other antibodies used were obtained from commercial sources and were supplied as monoclonal IgG's that had been raised in mice.

A

HDACm



B

RbAp48

C-terminal peptide: ovalbumin-CENIYNDEDPEGSVDPEGQGS

C

Histone H4

H4Ac0 N-SGRGKGGKGLGKGGAKRHYC-ovalbumin

H4Ac5 N-SGRG^{*}KGGKGLYC-ovalbumin

H4Ac12 N-GKGL^{*}GKGGAKRHYC-ovalbumin

Figure 16. Peptides used to produce polyclonal antisera. (A) Representation of the HDACm protein. The parts of the protein used to raise the antibodies anti-ΔR, anti-ΔR/ΔH, anti-ΔV and anti-Cpep. (B) The C-terminal peptide of *Xenopus* RbAp48 used to raise the anti-RbAp48 serum. (C) The ovalbumin tagged synthetic polypeptides used to create the anti histone H4 antibodies. * indicates the site of acetylation in the peptide sequence

2.3.15. Extracting IgG from serum

IgG was extracted from 500 μ l aliquots of serum. 50 μ l of Protein A coated Sephadex beads (Pharmacia) were first washed five times in 10 volumes of elution buffer (0.1 M glycine, pH 3.0) before being washed 5 times in 10 volumes of binding buffer (0.1 M Tris pH 8.0). Once these initial washing stages had been completed the serum plus 1/10 volume of 0.1 M Tris (pH 8.0) was added to the beads and the mixture was mixed continually for 2 hours at room temperature. At the end of this period the serum was removed and the beads were washed in 10 volumes of 0.1 M Tris (pH 8.0) a further five times. The IgG was then eluted from the beads by mixing the beads with 250 ml of elution buffer for 5 seconds. The eluate was mixed with 1/10 volume of 1.0 M Tris (pH 8.0) and an equal volume of glycerol and stored at -20°C .

2.3.16. Immunostaining of ovarian and embryo sections

Tissue to be immunostained was placed in a solution of 3% paraformaldehyde, 0.25% gluteraldehyde in 0.1 M phosphate buffer (pH 7.4) for 1 hour at room temperature to fix. Fixed tissue was then washed overnight in 0.1 M phosphate buffer containing 0.1% sucrose at 4°C and then in 70% ethanol at 4°C before embedding. To embed, the sample was

rehydrated and placed in a mould, molten wax was added to the mould and the block was left to cool. Once cooled the block was trimmed and placed in a cryostat machine where 7 μm sections were cut, once cut the sections were floated on a water bath at 23°C and then drawn onto albumin coated slides and then dried on a hot plate before desiccating over night.

To immunostain, the section were firstly dewaxed in xylene substitute (Shandon) before being rehydrated by taking the sections through decreasing concentrations of alcohol from 100% ethanol to 70% ethanol, from there the sections were washed in TBST to complete the rehydration process and prepare the sections for immunostaining. The sections were blocked with 10% foetal calf serum (FCS) in TBST for 1 hour, washed thoroughly in TBST, and then incubated with primary antibody diluted 1/50 in 10% FCS in TBST. The sections were washed again before being incubated in the dark with fluorescein isothiocyanate (FITC) conjugated secondary antibody (Chemicon) diluted 1/100 in 10% FCS in TBST for 1 hour. The slides were washed for a final time in TBST containing 0.1% w/v ereochrome black (Aldrich) before being mounted in DAPI mounting solution and viewed under a Leitz ortholux II microscope and a 25 x water

immersion lens. Photographs of fluorescent and DAPI staining as well as phase contrast pictures were taken using Kodak TMAX p3200 film.

Mounting solution

| | |
|-------------------|------------|
| Tris-HCl (pH 8.0) | 50 mM |
| n-propyl gallate | 1.5 mg/ml |
| Glycerol | 50 % (v/v) |
| DAPI | 20 µg/ml |

2.3.17. Whole mount immunostaining of oocytes and nuclei

Oocyte and nuclei whole mounts were immunostained in the same manner [145,146]. Oocytes of all stages were isolated and fixed overnight in Dent's fix (1 part dimethylsulphoxide (DMSO): 4 parts methanol) in siliconised watch glasses. Nuclei were isolated by manual dissection from oocytes under fixative saturated oil before being transferred to a siliconised watch glass and fixed over night. Material which was highly pigmented i.e. stage IV to VI oocytes, were bleached in 10% hydrogen peroxide in Dent's fix before continuing with the immunostaining process. To immunostain, fixed material was first washed in TBS before being incubated in primary antiserum diluted 1/25 in 95% FCS, 5% DMSO for 24 hours. The material

was then washed for 5 hours in TBS before being incubated with FITC conjugated secondary antibody, diluted 1/50 in 95% FCS, 5% DMSO for 24 hours. At the end of these 24 hours the material was again washed in TBS before dehydrating for 1.5 hours in methanol before placing the material in to benzyl alcohol/benzyl benzoate (1:2) to clear. Whole mounts were viewed using a Bio-rad MRC 600 series scanning confocal imaging system.

2.3.18. Immunostaining lampbrush chromosomes [32]

Having removed the ovary from an anaesthetised animal and collagenased this ovary as described previously, individual oocytes were placed in OR2 over night before attempting the isolation of lampbrush chromosomes.

To start the isolation process, individual oocytes were transferred to a black watch glass containing isolation medium. This medium has two purposes; (1) it maintains the morphology of the nuclear contents, (2) it maintains the contents of the nucleus as a gel during the initial manipulation but allows subsequent dispersal. Once in this medium the nucleus was removed from an oocyte by piercing a whole in the animal pole of the oocyte and easing the nucleus out by gently squeezing the

oocyte with a pair of forceps. Once free of the oocyte, the nucleus was transferred to a bored glass isolation chamber containing $\frac{1}{4}$ strength isolation medium + 0.5 mM Mg^{2+} + 0.1% w/v (dispersal medium) with a fine bored glass pipette. The membrane was then removed; grasping the nucleus with a pair of fine forceps the nucleus was forced to the bottom of the chamber, a fine tungsten needle was then used to tear open the nuclear envelope. The nuclear contents were then allowed to fall out of the envelope and spread on the base of the chamber. Up to 5 spread nuclei were prepared in each dispersal chamber before it was sealed and the contents allowed to continue spreading for 1 hour.

At the end of this time period the chambers were centrifuged at 5000g for 45 minutes in a Sorval HS-4 rotor using special holders designed for this purpose. At the end of this spin the cover slip was removed from the chambers and they were flooded with 70% ethanol to ensure the sample was fixed. The spread preparations could be stored overnight in a dish of 70% ethanol. To immunostain the chromosomes the ethanol was removed and the chamber washed in excess 0.1% TBST for 30 minutes to rehydrate the material before immunostaining the section as described in section 2.3.16.

2.3.19. Immunostaining of karyomeres

Embryos were produced as described previously (2.1.) and G2/prophase-synchronised embryos were obtained by 1 hour incubation in 0.1x Barths' solution containing 50 µg/ml cyclohexamide prior to homogenisation. Embryos were dejellied at the 4 to 8 cell (see section 2.3.4) and collected at all stages of embryogenesis between the 64 cell stage and stage 42. After washing the embryos in copious amounts of 0.1x Barths' medium the embryos were homogenised through a 1 ml Gilson pipette tip and centrifuged at 4°C for 10 minutes at 15 000 rpm, the supernatant was collected avoiding the fatty surface layer, this homogenate contained the karyomeres. This nuclei containing extract was diluted 10-fold with fixation buffer and incubate at room temperature for 30 minutes. At the end of this period of time the homogenate was overlaid on a 0.6 M sucrose cushion and particulates were centrifuged down onto a glass cover slip (30 minutes, 4 C, 10 000 rpm in swing-out rotor) [147]. Samples were post-fixed on the cover slips in 70% ethanol before being rehydrated in TBST and blocked over night in 10% foetal calf serum before immunostaining.

Fixation buffer. pH 7.6

| | |
|-------------------|--------|
| KCl | 50 mM |
| HEPES | 20 mM |
| MgCl ₂ | 5 mM |
| EDTA | 0.5 mM |
| Formaldehyde | 4% |
| Sucrose | 2% |

Results

3.1 HDACm and oocytes.

The HDACm clone was isolated from a cDNA library constructed using mRNA expressed in pre-vitellogenic oocytes. It was selected by a fortuitous cross-reaction whilst immunoscreening the library with antibodies raised against a subset of mRNA-associated proteins. The nature of this cross-reaction with HDACm is still unknown. This preliminary identification was conducted by Scott Lyons in 1994 whilst working in the laboratory of John Sommerville.

The initial clone was catalogued as Ab21 (accession number: X78454). The cDNA was sequenced and found to be of 2305 bp in length, with an open reading frame of 1440 nucleotides. The Ab21 cDNA carries several unusual features. The 3' UTR is U-rich and contains several mRNA instability elements, whilst near the 3' end there is a cytoplasmic polyadenylation element (CPE). This CPE is a feature common to maternal mRNAs and its length and location may determine the timing and extent of cytoplasmic polyadenylation and translation (figure 17). Theory predicted the translated protein would have a molecular mass of 54.7 kD and a pI of 5.6. This sequence is 58 % identical to the histone deacetylase found in *S. cerevisiae*, called RPD3, and 91 % identical to the human histone deacetylase HD1 [60]. Sequence comparison of HDACm with these other proteins indicates that all these histone deacetylases contain a conserved core, that is

thought to contain the active site, plus an additional, more variable carboxyl terminus.

3.1.1. Sequence, size and levels of HDACm protein.

The initial experimental work involved investigating the levels of HDACm in oocytes and embryos and how these levels change throughout early development. This work was conducted by Western blot analysis using the range of anti-HDACm antibodies described in section 2.3.14 (figure 16). Native HDACm migrates with an apparent molecular mass of 57 kD, a value similar to the predicted molecular mass of Ab21 cDNA. The experimental value was obtained by immunoblotting an oocyte nuclear extract with anti-Cpep, and comparing the distance migrated by the detected protein with known standards (figure 17).

Northern blot analysis shows the presence of a transcript of approximately 2.5 kB which accumulates in pre-vitellogenic oocytes and is maintained at a constant level throughout oogenesis and into early embryogenesis. The transcript level declines from being abundant to undetectable between neurula and tailbud. Western blot analysis of oocyte and embryo extracts with anti-Cpep antiserum shows the existence of a protein with apparent mass of 57 kD. In oocytes this protein reaches detectable levels in stage II oocytes and increases

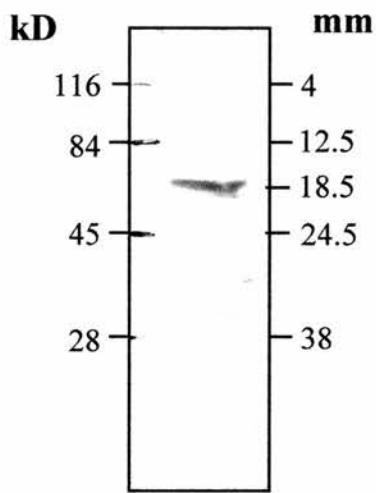
A

Number of amino acids: 480
Predicted molecular mass: 55 kD

```

p88 EcoRI      G AAT TCG GCA CGA GGC GGA AGG AAA -1
ATGGCCCTGACTTAGGAACAAAGAAAGTGTCTACTACTATGATGGTATGTTGGA
60  M A L T G G F K K K F C Y Y D G D V G
EcoRI      AATATTATTATGGTCAAGGCTATCCCATGAACCTCATAGAAATTCGATGACACACAC
120  N Y Y G G G G H P H K P H R I R M T H H
CTGCTGCTCAACTATGGACTTTACCGAAAATGGAAATCTTAGGCCCCCAAGCCAGC
180  L L L N Y G L Y R K M E F K F H K A E
OCCGAGGATATGACAAAGTACACAGTATGATTATATAAATTCCTGGCCCTCCTACGA
240  A D M C K I H S S D D Y K F L R S I R
CCAGCACATATGTCGAAATACGTAACAGAGTGGAGAGATTTAATGTTGGAGGAGTGT
300  P D N M S E Y S K Q M Q R F N V G E D C
PstI      CCTGTGTTTGTATGGCTATTTGAGTCTCCAGCTCTCTGCAAGGGGTTCTGTAGCAAGT
360  F F D D L F F F C Q L S A G D H V A S
GCTGTATAACTAAACAACAGCAGCTGACATTTCACTGCACTGGTCTGGTGGCCCTCAT
420  A K L R K Q Q T D I S N W S G G L H
CATGCAAGAAATCTGGGCTATCGTTTTTGTATGTCAGATATATGCTCTGCCATC
480  H A K K S E A S G F C Y V N D I V L A I
CTGGAACCTAAAGTATCACAGAGAGTGTGTATATTGATATAGACATCACACCGGT
540  L E L L K Y H Q R V V Y I D I D T H S G
GATGGTGTGAGGAGGCAITTTACACACCGATAGGTTATGACTGTGCTCCCTCCATAAG
600  D G V E E A F Y T T D R V M T V S F H K
Bgl II     TATGGAGATATTTTCTGGAACTGGAGTCTGAGAGATTTGTGCAAGGAGAGCAAA
660  Y G E Y F F G T G D L R D I G A G K K K
TACTATGCTGAAATTTGCTTACGGGATGGATTGACGATGAGTCTATGAGCAAT
720  Y A V A Y A L R D G I D D E S Y E A I
TTTAAACCAATATGTCAAAGTTATGGAAATGTTTCAGCCAGTGCAGTGTCTTACAG
780  F E L H I S F S H V W Q N Y H E T L E
CAGTCTGAGTATCATTTCTGGGATGAGCTGGATGCTCATTTGACCATTAAGGGA
840  C G A D S L S G D R L G C F N L T I K G
CATGCAAGTGTGGAGTATTATAAAGACCTTTAAGTGGCACTGTTGATGTTAGAGGT
900  W A R S I R S S D K E I A C D E E F
FvuII     GGAGGTTACACTATCCGGAATGGGCTGCTGGACATATGAAACAGCTGTGGCTCTG
960  G S Y T R N V A R C N Y E T A V A L
GACTCTGAGTATCCCAATGAGCTCCATATATGATTTATTTGATATTTGCTCCGAC
1020  D S E I P N K L F T N D Y F E Y F G P D
HindIII   TCAAGCTTCACTACAGCCATCCAACTGCTAATGAGACACTAATGAATATCTGGAG
1080  F E L H I S F S H V W Q N Y H E T L E
AAAATTAAGCAGCCCTCTTGAAGACTTGCCTATGCTCCCCATGCTCTCGGAGTTCAG
1140  K N Q L F E N L R M L F N A F Q V Q
ATGCAAGCCTTCCAGAGGCTCCATACACGATGACAGTGTGAGAGAAATGAGATGAT
1200  M Q A V A E D S I H D D S G E E D E D D
CCGACAGGCTATTTCAATTCGGTCACTGATGATGAGGATGCTGTGATGAGGAGTTC
1260  F D A R S I R S S D K E I A C D E E F
EaeI      TCAGATTCGAGGATGAGGGGAGGAGGTCGCAAAAAGTGGCCAATTCAAAAGTA
1320  S D S E E G E G R K N V A N F K K V
AAACGGGTTAAACTGAGAGGAAAGGAGAGGACAGAAAGATGTTAAGAAAG
1380  K R V K T E E E K E G E D K K D V K E E
GAGAAAGCTAAGATGAGAAAGCGGATGACAAAGGTTAAAGAGAGACCAATCACTC
1440  E R A X D E K T D E K R V E E T K S V
TGATCCTCAACTATGGGAGAAAATCCGAAAGCCAAACTAATCTCATGGTATTATATT
1500  TFGTATAGCCCTGACAGAGCCCTACTATGAAATATAGTCCACACATTCATAATATT
1560  HIIITCTGCCCAGCTGGTGGAGGGGGTGAAGTGTGCTGATGATGATGATGATGATGAT
1620  GTTACCTTTTTTAAAGATTCACATCTGTACCTTTTACAGATGTTCCAGCTCTTTGG
1680  CTTTTTTTTTTTTTACCAAAACITTCATGTTTTCTGCTCTGTATATCTTCGG
1740  TGGTGCATATTTTTACGATTTATTTCTGCTCTCTTATACACACTTTTGTGTGAGA
1800  CTACAGACTTTTGTACAGTACATGAAATGTACACTATGCTCAGGATCAGGATATG
1860  TACACTATGCTCAGGATCAGGCACTGAGAGGAGGAGGTTCCAGCTGTCTCCAAATG
1920  AATTTGAGAGGTTTACTTGGAGGATGAGAGGAGGAGGAGGAGGAGGAGGAGGAGGAGG
1980  CTATTCAGGATTCCTGTTCACTTAATGCTGCTAACCTCCAGATTAATGATGATGAA
2040  GCAGATTTTATGATGATGAGAACTGCTCCAGATTAATGATGAGGAGGATGAGGAGG
2100  ATTTGCAATTTGGTTCTGCTTTAATGATGAGGAGGAGGAGGAGGAGGAGGAGGAGG
2160  AGTGAAGAAATGGAGAAATTTTATGCTAATTTTGTGATGAGGAAATTTCTTTTTTT
2220  HIIITTTTTTATGTTGAGTGTAGAAAGCTTTGATATAATGCTGACTTATACAAAAAAA
2286  AAAAAAAAAAAGCTCGAG
p88 SbcI
  
```

B



C

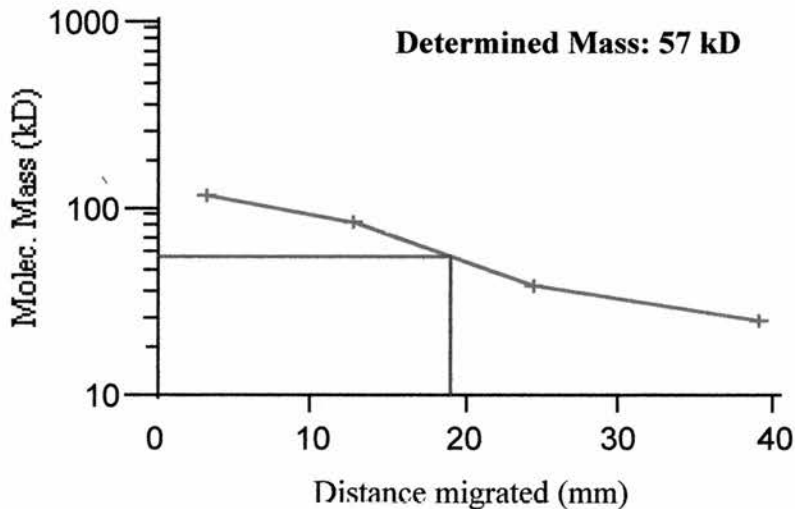


Figure 17. Sequence and size of HDACm protein. (A) cDNA sequence and corresponding amino acid sequence of HDACm. The number of amino acids and the predicted molecular mass are given (See also Appendix A). (B) Immunoblot, using anti-Cpep, of nuclear proteins from stage VI oocytes. Track contains the protein equivalent of ten nuclei. Distance migrated by HDACm and the molecular markers are shown. (C) Molecular mass of detected HDACm.

throughout oogenesis and through stage VI oocytes to peak in fertilization-competent, progesterone-induced eggs (figure 18A). Post-fertilization, these high levels are maintained through the rapid cleavage divisions and into the blastula stage embryo. Post-blastula, the level of endogenous HDACm declines through gastrula and neurula. The protein is undetectable by the end of tailbud (figure 18B). This pattern of expression follows very closely that of the message described by Ladomery *et al* [60]. The enzyme is disappearing from the embryo by the time cells commit to specific fates.

3.1.2. Sub-cellular location of HDACm protein in oocytes.

On closer analysis of oocyte extracts and fractionation of the oocyte into nuclear and cytoplasmic portions, it becomes apparent that HDACm is stored at specific locations within the oocyte, and that the specific location of the HDACm changes throughout oogenesis. To aid the study of this sub-cellular distribution it was necessary to develop a number of anti-HDACm antibodies. These antibodies were raised against GST fusion proteins containing the conserved region of HDACm ($\Delta R/\Delta H$) and the charged tail domain (ΔV), and an ovalbumin-conjugated peptide representing the carboxy-terminal 17 residues of HDACm (Cpep), these antibodies are described more completely in figure 16. All three antibodies recognise a protein of 57

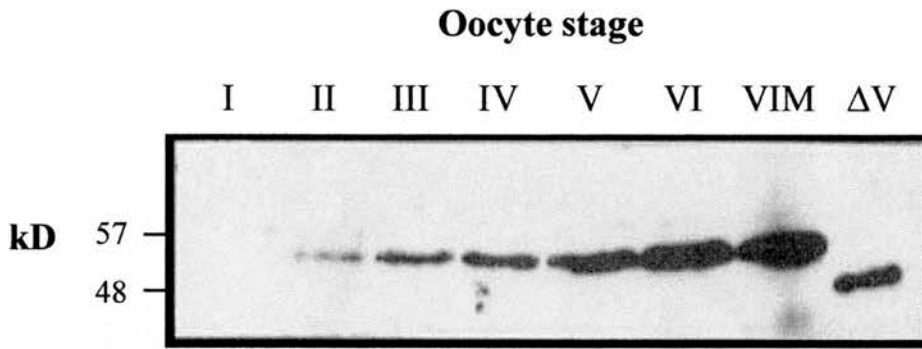
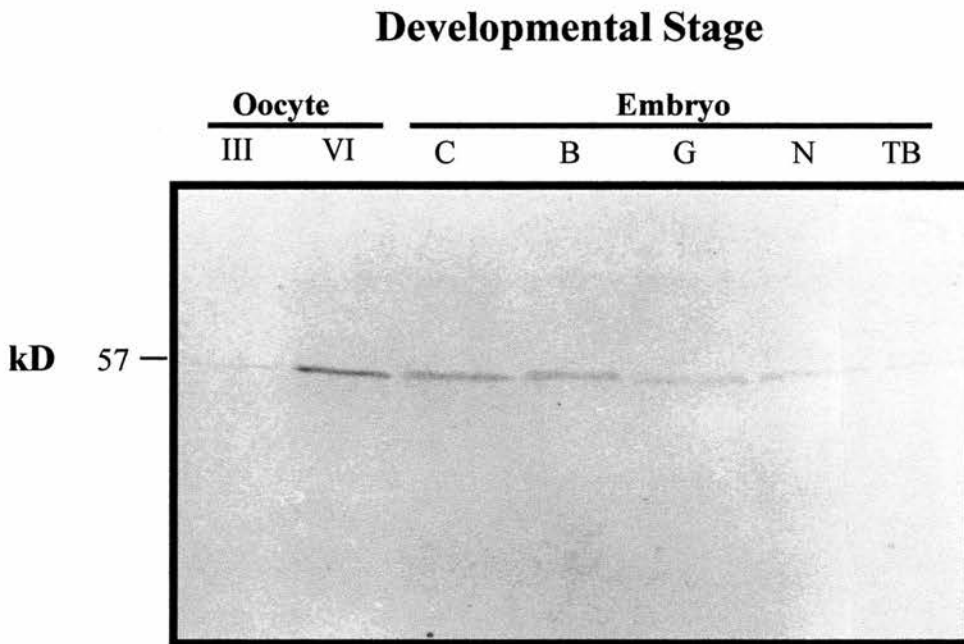
A**B**

Figure 18. Levels of HDACm protein at different stages of development. **(A)** Immunoblot of extracts of different stage oocytes. Each track contains the protein equivalent of two oocytes. Stages are from I to VI plus stage VI oocytes matured (VIM) by treatment with progesterone for 16 hours. GST-ΔV fusion protein (0.1 μg) is used as a positive control. **(B)** Immunoblot, using anti-ΔV, of extracts from different developmental stages of oocytes and embryos (C, 16 cell; B, mid-blastula; G, gastrula; N, neurala; TB, tailbud). Each track contains the protein equivalent of 2 oocytes/embryos. Western blot was immunostained using anti-Cpep as the primary antibody and the Horseradish peroxidase method to visualize the bands.

kD in extracts from stage VI oocytes separated by SDS-PAGE (figure 19).

Quantitative analysis of the relative amounts of HDACm in the nucleus and cytoplasm of oocytes at various stages of development has been made possible by the development of the technique first described by Paine *et al* [135]. By isolating oocyte nuclei under oil, an hermetically sealed nucleus is obtained that allows accurate investigation of the nuclear level of protein as soluble material cannot leech out. Immunoblots, comparing the amounts of HDACm in the nucleus and cytoplasm of oocytes from stage III to stage VI show that HDACm is present at much higher concentrations in the nucleus (figure 20A). As a standard procedure similar total amounts of protein are loaded/track. In such immunoblots this equates to the protein equivalent of 10 nuclei/track or 2 cytoplasm/track. Despite the 5:1 number ratio, it is evident that HDACm is present at much higher concentrations in the nucleus than the cytoplasm. This implies that the 57 kD protein undergoes an immediate post-translational translocation from the cytoplasm to the nucleus.

The amount of enzyme stored in the oocyte must be great enough to deacetylate the core histones incorporated into the chromatin of the blastula embryo. It would be inconvenient from the standpoint of regulation if this enzyme was stored near the histone store or the

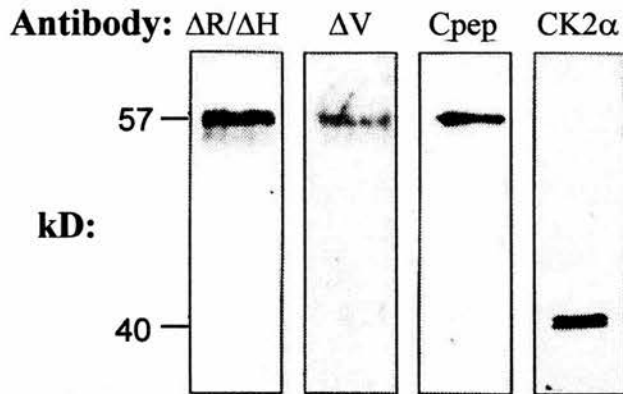
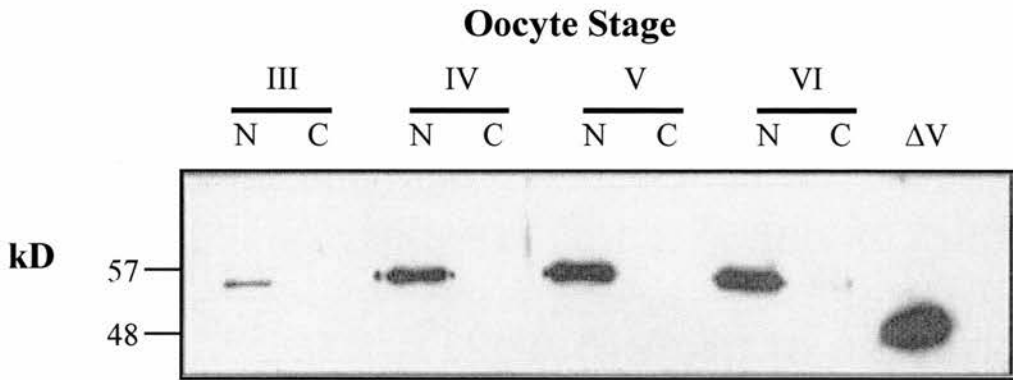
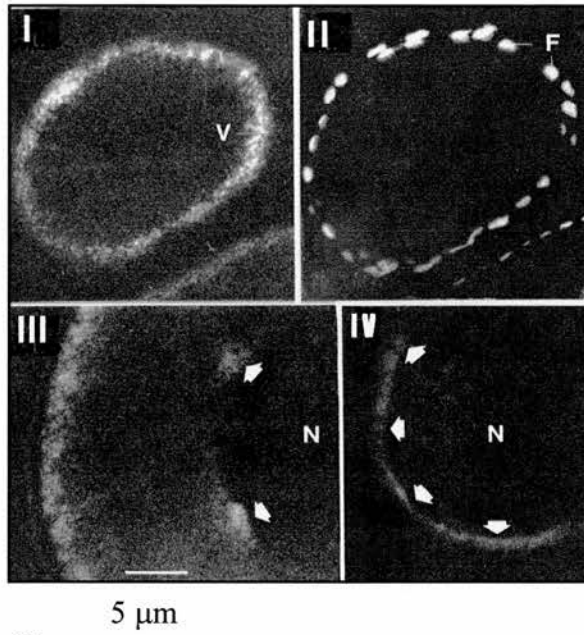
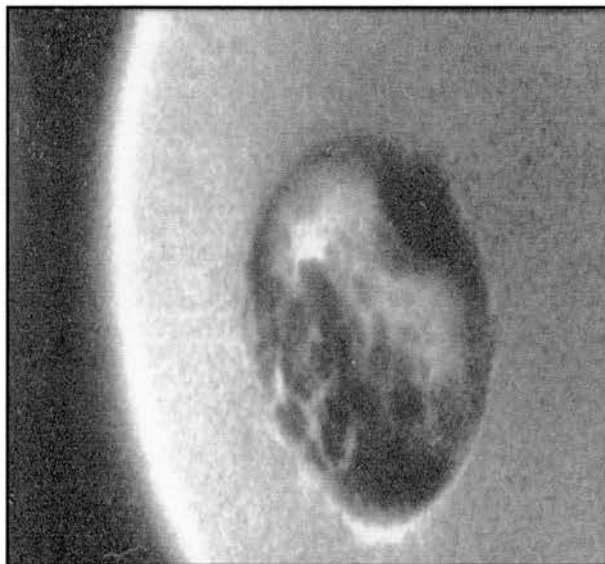


Figure 19. Analysis of antibody specificity. Immunoblots of soluble extracts from the equivalent of two stage VI oocytes, using anti- $\Delta R/\Delta H$, anti- ΔV and anti-Cpep IgG. The same extract is blotted with antibodies raised against the α -subunit of casein kinase II (CK2- α) as a control.

chromatin. If the active enzyme could access the histone store, histones might not be incorporated efficiently into new chromatin. Likewise, premature deacetylation of newly synthesised chromatin could have disastrous effects on oocyte maturation or the cleavage divisions of the newly fertilised embryo.

Immunostaining sections of pre-vitellogenic ovary, and wholemount immunostaining of larger oocytes provides confirmation of the intracellular distribution of HDACm demonstrated by immunoblotting. They also allow analysis of the level of protein expression in the nucleus and cytoplasm of small oocytes (stage I/II) that are difficult to isolate under oil. In stage I/II oocytes HDACm is mainly cytoplasmic. The enzyme is located immediately beneath the follicle cell layer and appears to be associated with the oolemma. By stage III, HDACm is still present in a thickening, but less intensely staining, ring inside the oolemma. The enzyme has also begun to accumulate in the nucleus. Specifically the enzyme is accumulating in the nucleus around the nuclear periphery (figure 20B). Immunostaining of mature ovary sections is difficult to resolve, the fluorescence of all fluorochromes is swamped by the autofluorescence of the yolk platelets. This problem can be partially relieved by washing the immunostained section in eriochrome black [148], however the background fluorescence is not completely quenched. For this reason,

Figure 20. Characterisation of sub-cellular localisation of HDACm proteins in oocytes **(A)** Immunoblot using anti-Cpep, of nuclear and cytoplasmic extracts from stage III to stage VI oocytes. Each track contains the protein equivalent of either two cytoplasms (C) or ten nuclei (N). GST- ΔV fusion protein (0.1 μg) was used as a positive control. **(B)** Immunostaining of sections of pre-vitellogenic ovary using anti-Cpep. The fluorescent image is provided by fluorescein-conjugated anti-rabbit IgG used as the secondary antibody. (I and II) Fluorescence and DAPI images of the same stage I oocyte. The “v” indicates the position of the cortical vesicles in the immunostained image (I), whilst the “F” indicates the position of the nuclei of the follicle cells surrounding the oocyte. HDACm is never detected in these cells. (III) Fluorescence image of stage III oocyte. The “N” indicates the position of immunostaining around the periphery of the nucleus. (IV) Fluorescent image of ovary section through nucleus of stage III oocyte. “N” indicates staining around the nuclear envelope. **(C)** Immunostaining of whole stage VI oocyte using anti-Cpep. The fluorescent image is again provided by fluorescein-conjugated anti-rabbit IgG used as the secondary antibody. The image has been obtained by taking an optical section through the whole oocyte by confocal microscopy. The cytoplasmic signal is due to autofluorescence of yolk platelets.

A**B****C**

immunostained wholemount oocytes were studied by confocal laser microscopy. Optical sectioning of large, post-vitellogenic oocytes shows that HDACm has reached much higher levels in the nucleus at this stage in development and is still restricted to the nuclear periphery (figure 20C). This method does not remove the problem posed by autofluorescence, it is difficult to estimate how much of the cytoplasmic signal is due to the fluorochrome and how much is due to the yolk. However, it does allow insight to the situation in the nucleus.

3.1.3. HDACm is a component of a multimolecular complex.

To date, all identified histone deacetylases are associated with protein complexes. Yeast HDAC-A is in a complex of molecular mass 350 kD, HDAC-B is in a complex of molecular mass 600 kD [71]. In vertebrates, histone deacetylases can be found in complexes of molecular mass ranging from 220 kD in chicken erythrocytes [75,76] to 1.5 MD in *Xenopus* [149].

To examine the size of HDACm-containing complexes when located in the nucleus, extracts were separated under near-physiological conditions by rate-zonal centrifugation. Clarified supernatants were layered on linear 10%-30% glycerol gradients that were centrifuged until a 960 kD (IgM \equiv 19S) marker approached the bottom of the tube. The gradients were then fractionated and analysed for HDACm content

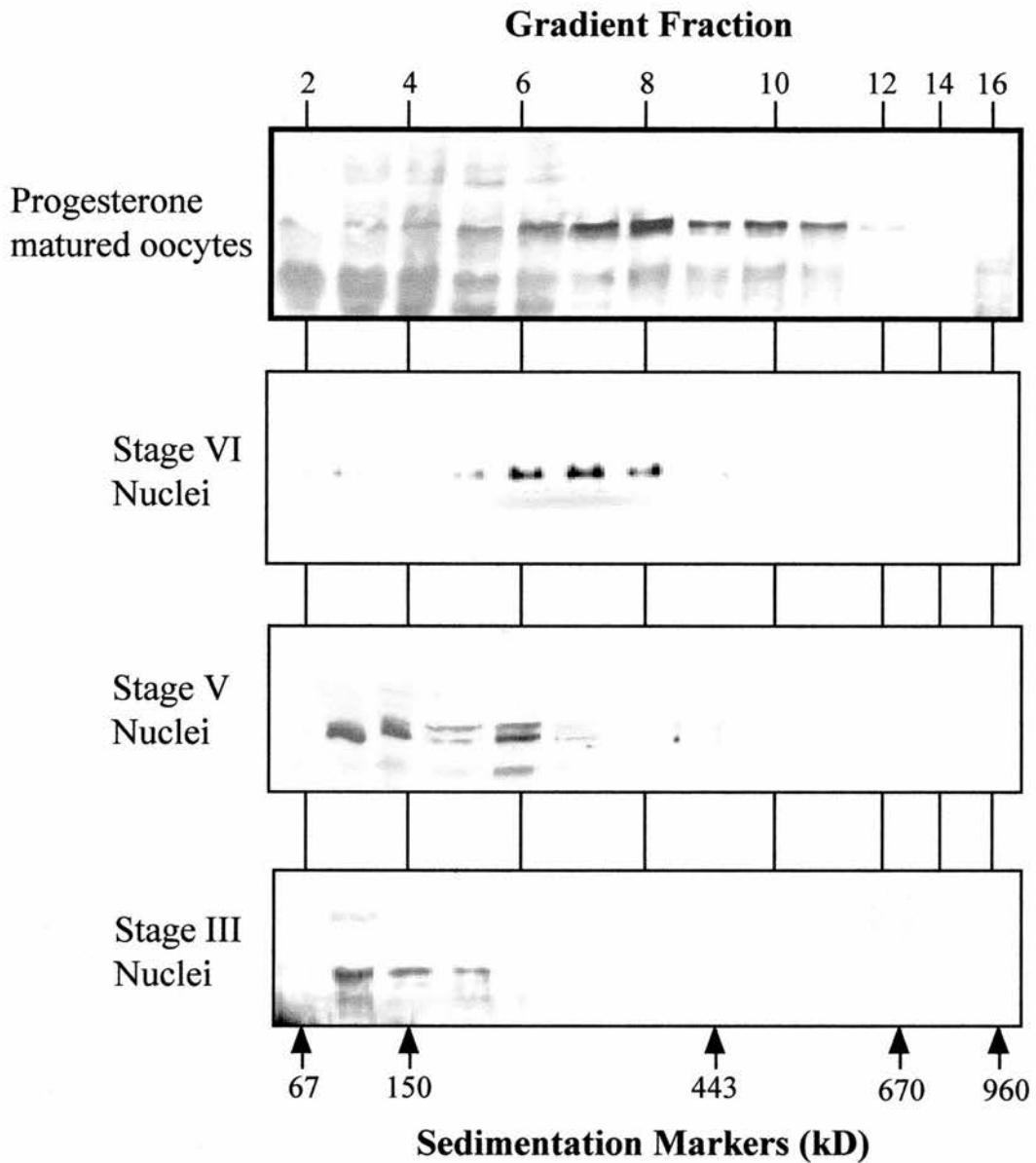
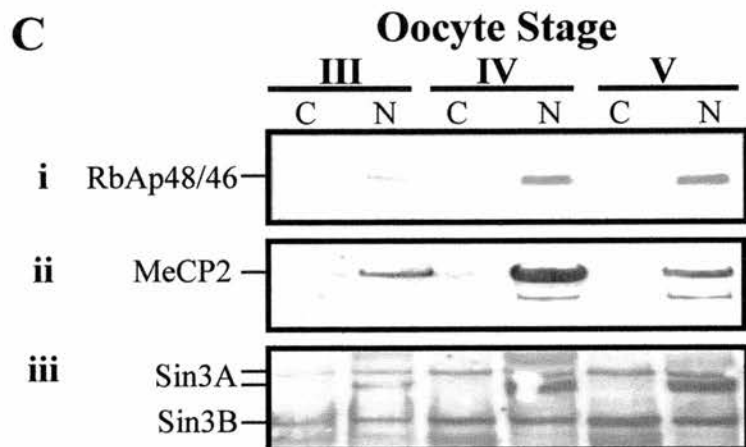
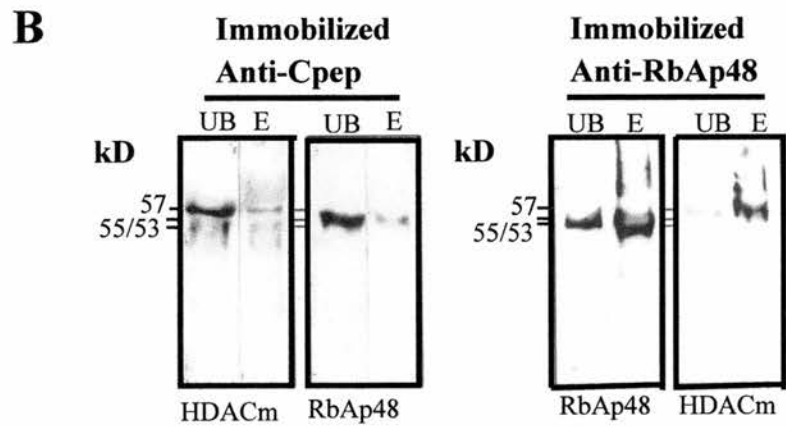
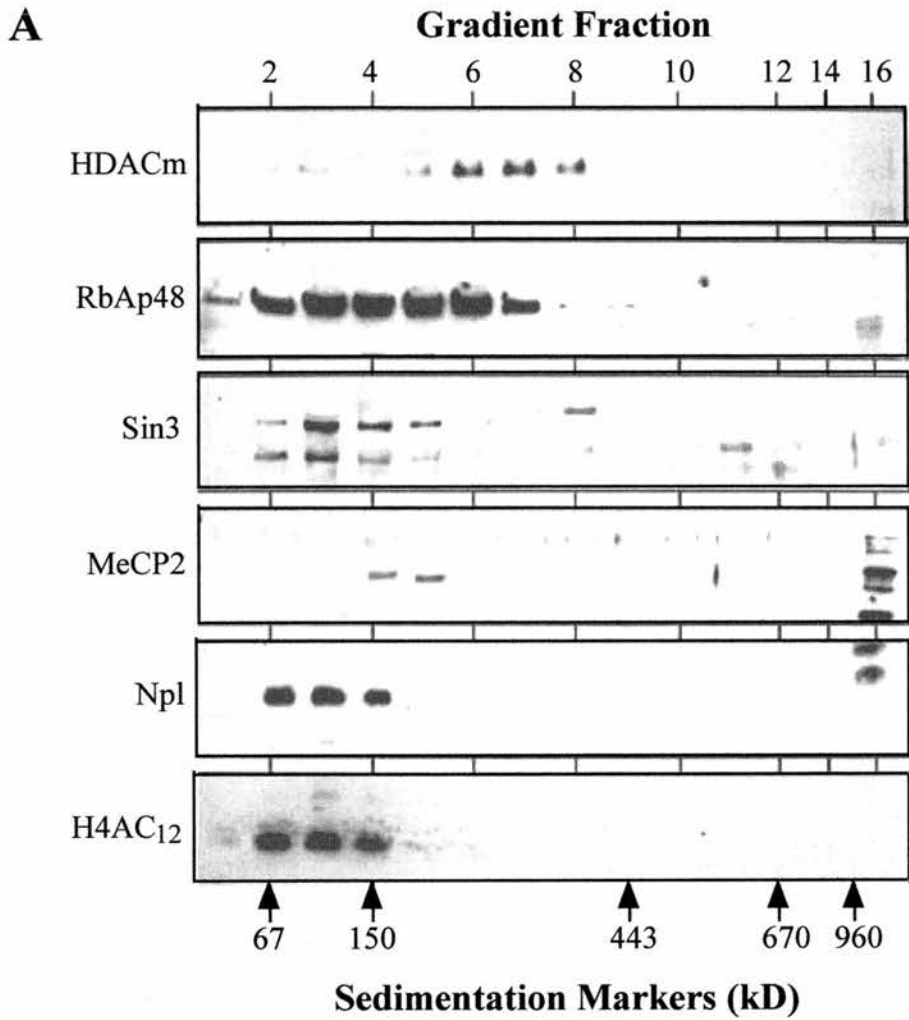


Figure 21. HDACm is found in complexes of increasing size as oocytes mature. Detection of HDACm in extracts (from stage III nuclei, Stage V nuclei, stage VI nuclei and progesterone matured oocytes) separated by rate-zonal sedimentation. The gradient fractions were immunoblotted with anti-Cpep. The position of protein sedimentation markers are indicated (kD). Each gradient contained the protein equivalent of 50 nuclei.

by immunoblotting. A clarified supernatant of oocytes matured by incubation in progesterone for 10 hours sedimented over a very broad range, with a peak at approximately 400-450 kD. Supernatants from stage VI nuclei show HDACm sedimenting with a peak at approximately 300 kD. The extract from stage V nuclei is slightly slower sedimenting, peaking between 200kD and 250kD, whilst a nuclear extract from stage III nuclei sediments with a peak at approximately 100 kD (figure 21).

The changing sedimentation rate indicates that HDACm is found in complexes of increasing size as oocytes grow. In stage III oocytes, nuclear uptake of HDACm begins and the enzyme is incorporated into small complexes. As oogenesis continues more deacetylase is imported and is incorporated into larger complexes. By stage VI, nuclear levels of HDACm are at maximum and the complex size increases to approximately 300 kD. The complex appears to become further enlarged upon progesterone induced maturation, prior to the resumption of meiosis. The relevance of this change is not known. It cannot be to target HDACm to the chromatin at the resumption of meiosis, as chromatin is hyperacetylated in the egg. Presumably it is related to the assembly of a competent complex with *in vivo* activity that can be targeted to the necessary sites when required. Nuclear breakdown will expose the previously nuclear HDACm to cytoplasmic components it



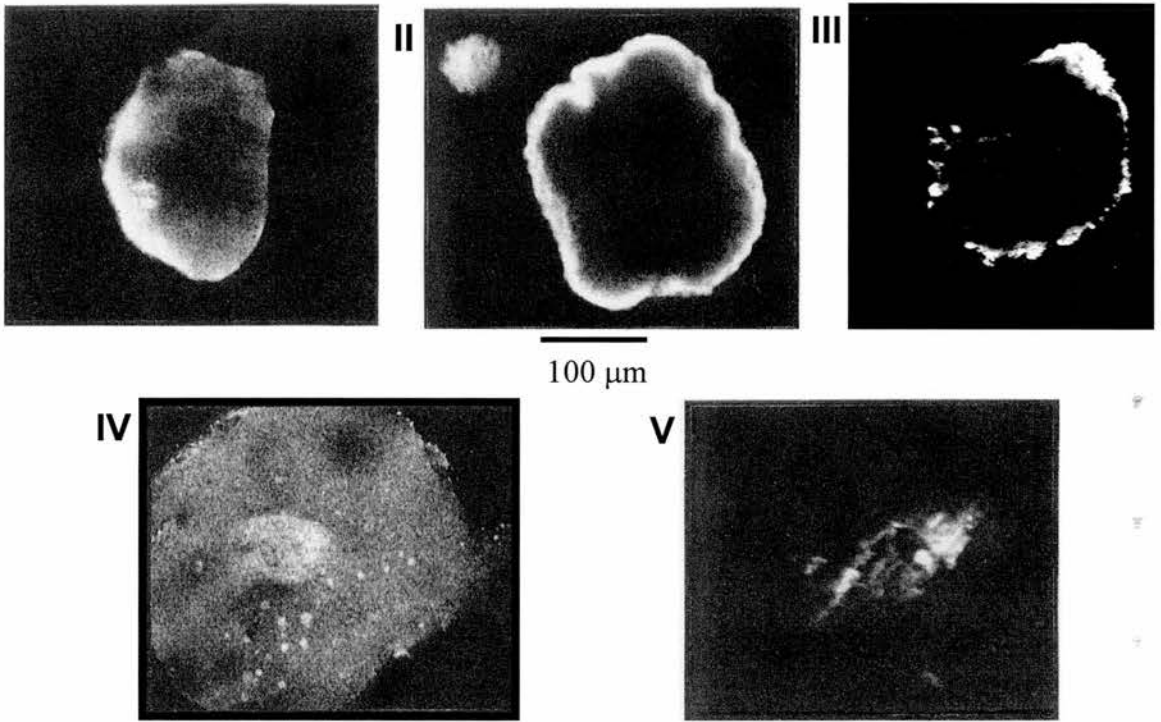
D

Figure 22. Investigation of the interactions of HDACm with previously identified HDAC partners. **(A)** Detection of various proteins in an oocyte nuclear extract, equivalent to 50 stage VI nuclei, separated by rate sedimentation. The same gradient fractions were immunoblotted with anti-Cpep and a panel of other antibodies raised against possible partners to HDACm. These other antibodies included; antibodies raised against a C-terminal peptide corresponding to RbAp48; antibodies to mammalian Sin3, antibodies raised against mouse MeCP2; antibodies detecting *Xenopus* nucleoplasmin (Npl); antibodies specific for acetylated lysine 12 of histone H4 (H4AC₁₂). The position of sedimentation markers are also indicated (kD). **(B)** Co-precipitation of HDACm and RbAp48 with antibodies to HDACm and RbAp48. Nuclear extracts from the equivalent of 50 stage VI oocytes were incubated with anti-Cpep or anti-RbAp48 immobilized on protein A beads. Unbound (UB) and eluted (E) fractions were immunoblotted with anti-Cpep and anti-RbAp48. **(C)** Immunoblot, using (i) anti-RbAp48 (ii) anti-MeCP2 (iii) anti-sin3, of cytoplasmic (C) and nuclear (N) proteins from stage III to stage V oocytes. Each track contains the protein equivalent of ten nuclei or two cytolasms. **(D)** Immunostaining of intact, hand isolated stage VI oocyte nuclei using: (I) anti-Cpep; (II) anti-RbAp48; (III) anti-lamin B; (IV) anti-H4AC₁₂; (V) propidium iodide. Fluorescent image is provided by fluorescein conjugated anti-rabbit IgG used as the secondary antibody. Material was viewed by confocal microscopy, images shown are representative of several images seen through the approximate centre of the nucleus.

was isolated from, possibly allowing the construction of a larger complex.

3.1.4. Examination of the interactions of HDACm with previously identified deacetylase partners.

It has previously been demonstrated that HDACm cannot bind chromatin as the enzyme itself contains no DNA binding motif [60,150]. It is also unlikely that the deacetylase sedimenting at a rate indicating a particle mass of 300 kD consists simply of a multimer of HDACm, therefore the enzyme must be active as part of a complex. From work by numerous other groups [94,95,96,97,99,100,101,105,106,149], it has been possible to identify a number of possible proteins that may be present in the complex with the deacetylase. These potential partners include retinoblastoma associated protein 48 (RbAp48, appendix B), the methylated DNA binding protein MeCP2 (appendix C) and the transcriptional co-repressor Sin3 (appendix D).

In order to check if these and other candidate partners are present in the oocyte nuclear particles, glycerol gradient fractions were immunoblotted with a range of antibodies (figure 22A), the sedimentation rate of the potential substrate of HDACm was checked by immunoblotting. The sedimentation rate of nucleoplasmin (the

chaperone of histone H2A/H2B) was also checked by immunoblotting, its location in the gradient acting as an internal marker of sedimentation rate as it is known to be in a complex of 130-170 kD [24,151]. Similarly, the location of the 120 kD complex containing the phosphoproteins N1/N2 was detected by phospholabelling a nuclear extract with ^{32}P -ATP (not shown). These proteins chaperone import of histone H3/H4 into the nucleus and remain complexed with these histones until they are incorporated into newly synthesised chromatin [32]. On comparing the various immunoblots, it can be seen that the only substantial overlap in distribution is between HDACm and RbAp48. This means it is possible that most HDACm particles also contain RbAp48. It would appear that the distribution of Sin3 and MeCP2 overlaps only slightly with that of HDACm, only minor amounts of HDACm can be present in particles containing Sin3 and MeCP2. Complexes containing Sin3, MeCP2 and HDAC in *Xenopus* oocytes have been described previously [105,106]. However, these complexes have been isolated from whole tissue homogenates that have gone through a number of chromatography steps, including ion-exchange. The limitations of these procedures are that the chance of spurious interactions between proteins is increased during shifts in ionic conditions, and select for only a subclass of complex. These techniques may give an idea of the proteins that can interact with the target under

certain conditions or at other times in development but do not necessarily reflect the situation *in vivo*. For this is the reason I have limited my investigation to rate-zonal sedimentation of nuclei hand isolated under oil and have kept ionic conditions to near physiological. Nucleoplasmin and diacetylated histone H4 both sediment in small complexes (approximately 150 kD), phospholabelled N1/N2 sediments at a similar rate as it is presumably still bound to stored, diacetylated histone H4 at this stage in development. N1/N2 and histone H4 are in a particle not associated with the deacetylase.

The association of RbAp48 with HDACm was further investigated by immunoprecipitation. Anti-Cpep was chemically cross-linked to protein A coated glass beads. The anti-Cpep beads were incubated with a nuclear homogenate of hand isolated nuclei before being thoroughly washed to remove loosely associated protein. Immuno-bound protein was then eluted with 0.1M glycine (pH 3.0) and immunoblotted for RbAp48. HDACm was eluted from this mix by anti-C-pep beads, but most of the protein was not released from beads using glycine (figure 22B). Residual protein has since been recovered by boiling the beads in SDS-PAGE sample buffer (not shown). The reciprocal immunoprecipitation was also performed. HDACm is eluted from a nuclear homogenate along with RbAp48 after incubating the extract with anti-RbAp48 beads. These results indicate that HDACm

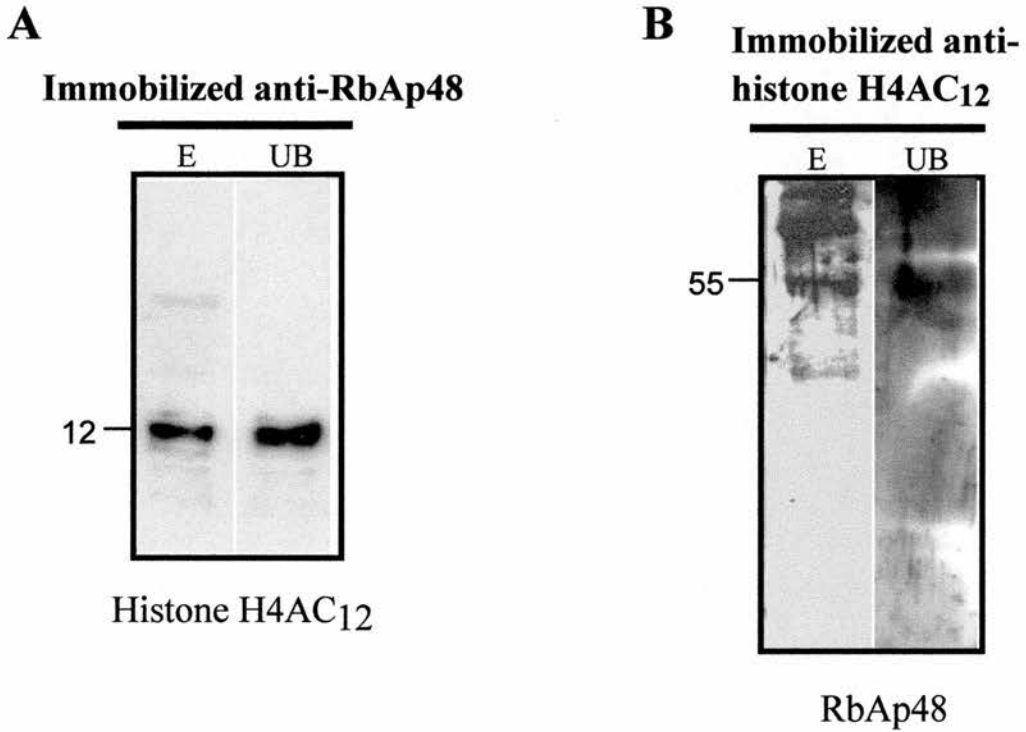


Figure 23. RbAp48 interacts with diacetylated histone H4 in the oocyte nucleus. **(A)** Co-precipitation of Histone H4AC₁₂ with antibodies to RbAp48. **(B)** Co-precipitation of RbAp48 with antibodies to Histone H4AC₁₂. Nuclear extracts of stage VI oocytes were incubated with anti-Cpep or anti-RbAp48 immobilized on protein A beads. Unbound (UB) and eluted (E) fractions were immunoblotted with anti-Cpep and anti-RbAp48. Immunoprecipitations were conducted with an equivalent to 50 nuclei isolated from stage VI oocytes.

and RbAp48 are components of a common particle present in the nuclei of large oocytes. Since less than 20% of the total RbAp48 was bound by anti-Cpep beads and almost 80% of HDACm was bound by anti-RbAp48 beads it would seem that most HDACm present in the nucleus is associated with RbAp48. The reciprocal is not true; the majority of RbAp48 in the oocyte nucleus might not be associated with HDACm. This may be because the deacetylase is itself the limiting factor in forming the complex or that RbAp48 is found in particles without the deacetylase. The latter explanation is likely because it is already known that RbAp48 is a sub-component of the chromatin assembly factor (CAF-1) complex [25]. Further immunoprecipitations using anti-RbAp48 beads have provided supporting evidence for the presence of RbAp48 in particles not containing HDACm. Anti-RbAp48 beads can pull down diacetylated histone H4 and anti-H4Ac₁₂ beads can pull down RbAp48, an interaction that cannot be demonstrated using anti-C-pep beads (figure 23). This confirms the existence of RbAp48 in at least two distinct particles. Immunoprecipitation of nuclear extracts with anti-C-pep gave no signal on blotting with anti-Sin3 and anti-MeCP2 (not shown). Since complexes containing Sin3, MeCP2 and HDACm have been isolated from whole ovarian tissue as described earlier, I can only conclude this is either proof of the limitations of these chromatographic methods [152] or a limitation of the anti-C-pep

antibody. From the information I have generated it is only possible to conclude that an HDACm complex containing MeCP2 and Sin3 appears to be much less common than the HDACm/RbAp48 complex.

Immunoblotting of nuclear and cytoplasmic extracts with anti-RbAp48, anti-MeCP2 and anti-Sin3 shows that RbAp48 accumulates in oocyte nuclei through oogenesis in much the same way as HDACm, with a major increase in amount between stages III and IV (figure 22C). Immunoblotting the same extracts for MeCP2 shows that although this protein accumulates in the nucleus through oogenesis, MeCP2 reaches its peak nuclear concentration by stage IV and then begins to decline. Sin3 shows an even greater variance in nuclear/cytoplasmic distribution compared to HDACm and RbAp48. The major form of Sin3A accumulates in the oocyte nucleus, and like MeCP2, levels peak by stage IV, but unlike MeCP2 it remains at this level into stage V. The level of Sin3B increases in concentration in the nucleus and cytoplasm throughout oogenesis. All three of these proteins demonstrate a significant difference in their accumulation in the oocyte compared to HDACm and RbAp48, indicating that their production is not coordinated with the formation of HDACm particles.

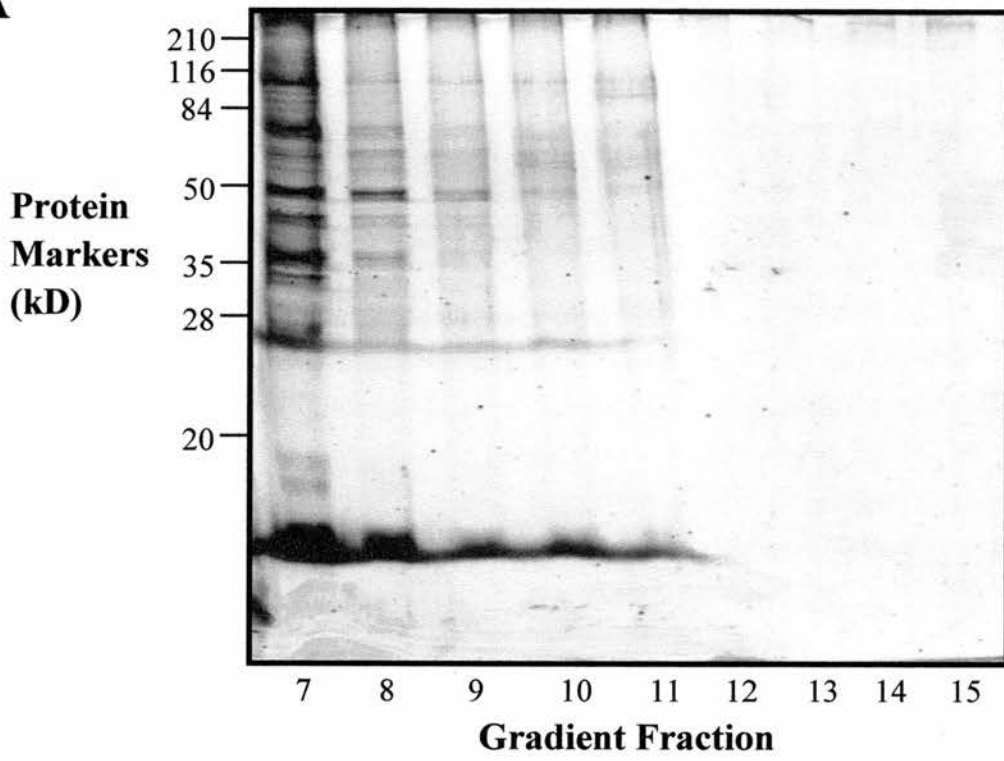
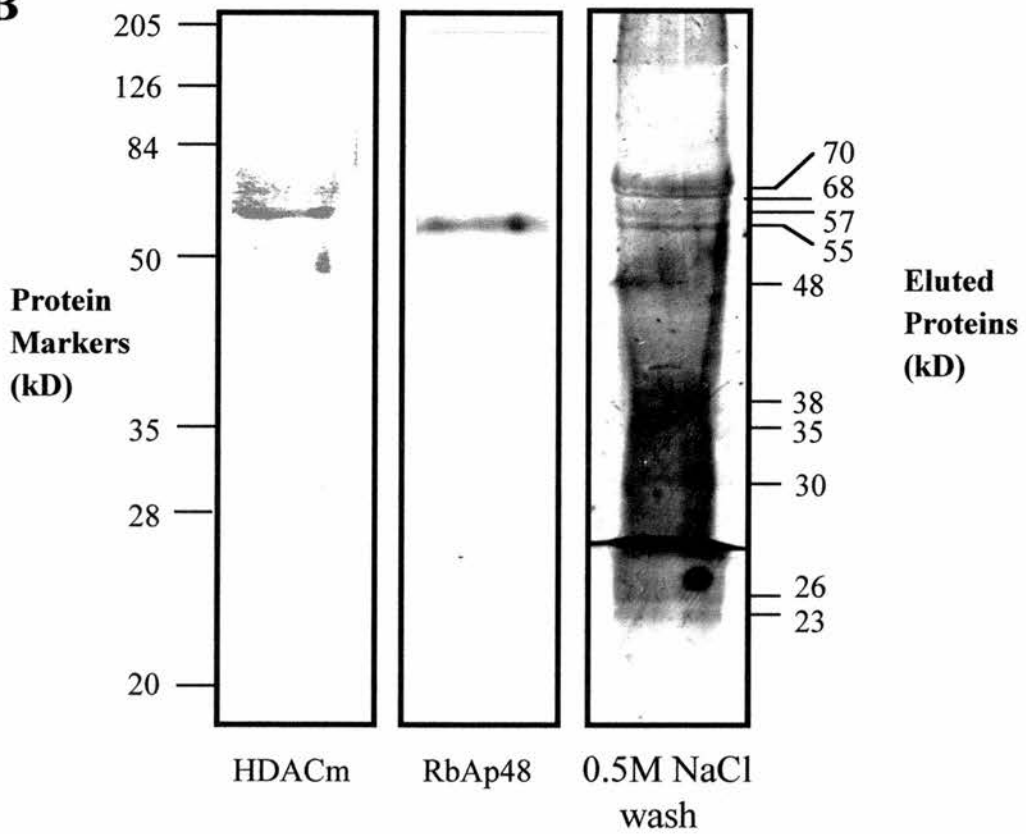
Immunostaining of whole-mount oocytes (not shown) and hand-isolated nuclei (figure 22D), shows that HDACm and RbAp48 are located mainly around the internal margins of the nucleus with similar,

but not identical distributions. HDACm has an asymmetric distribution around this margin, an observation it was not obvious whilst looking at sections of pre-vitellogenic ovary or whole-mount oocytes (section 3.1.2, figure 20), RbAp48 appears to form a continuous border. Neither protein could be detected on the active chromatin that constitutes the lampbrush chromosomes in stage IV oocytes but lie internally in the nucleoplasm close to the lamin layer. The considerable overlap seen in the location of HDACm and RbAp48 is consistent with the information gained from the rate-zonal sedimentation analysis and the immunoprecipitations. This contrasts with the distribution of acetylated histone H4, which occurs throughout the nucleoplasm in a largely punctate fashion and on the chromatin, which is located towards the centre of the nucleus as detected by DNA staining. These results indicate that most of the HDACm-containing particles are located away from the chromatin, and show no association with particles containing stored, acetylated histone H4.

In an attempt to identify additional proteins found in the major HDACm particle of stage VI oocytes, further immunoprecipitations have been attempted from the fraction of the glycerol gradient that contains the highest amount of HDACm protein. Silver staining of proteins contained in the fractions containing peak levels of HDACm indicates that there are a large number of proteins in this fraction in

addition to HDACm and RbAp48 (figure 24A). Not all of these proteins will be members of this particles, in fact many different particles of approximately 300 kD may sediment at this rate. To aid with identification of other proteins in the HDACm/RbAp48 particle I have attempted to immunoprecipitate these proteins from fraction 8 of the gradient using anti-Cpep beads. The eluted protein was immunoblotted with anti-Cpep or anti-RbAp48 to check the precipitation of known components and efficiency of the precipitation from a glycerol rich fraction and silver stained (figure 24B). The two previously identified components of the particle can be immunoprecipitated from fraction 8 of the glycerol gradient. For silver staining, to ensure the core deacetylase complex only was eluted, the beads were washed in a high salt solution (containing 0.5 M NaCl) to remove any weakly bound proteins prior to elution and staining. The silver stained proteins immunoprecipitated from this fraction are numerous and range in size from 70 kD to 23 kD. The precipitated proteins of sizes 57 kD and 55 kD are likely to be HDACm and RbAp48 respectively. There is also a strong possibility that the eluted proteins of 48 kD and 26 kD are the heavy and light chains of anti-Cpep, which have been eluted from the beads along with the particle. This leaves us with a total of six unidentified proteins that immunoprecipitate with HDACm and RbAp48 in stage VI oocytes. These proteins are not necessarily an

Figure 24. Components of the HDACm complex found in the nucleus of Stage VI oocytes. **(A)** Silver stained gel of soluble proteins extracted from 50 stage VI oocyte nuclei separated by rate sedimentation. Fractions shown are those from the HDACm rich region of the gradient. **(B)** Immunoprecipitation of proteins from fraction 7 of sedimentated material with anti-Cpep immobilized on protein A beads. Beads were either washed in 0.1% TBST before eluting for Western blotting with anti-Cpep or anti-RbAp48, or 0.5M NaCl before elution for silver staining. Silver stained proteins eluted include HDACm and RbAp48, however IgG heavy (48 kD) and light chains (26 kD) have also been eluted.

A**B**

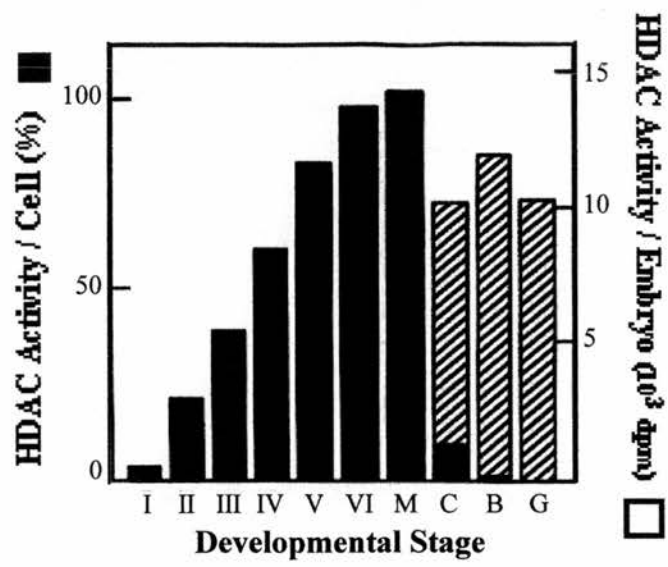
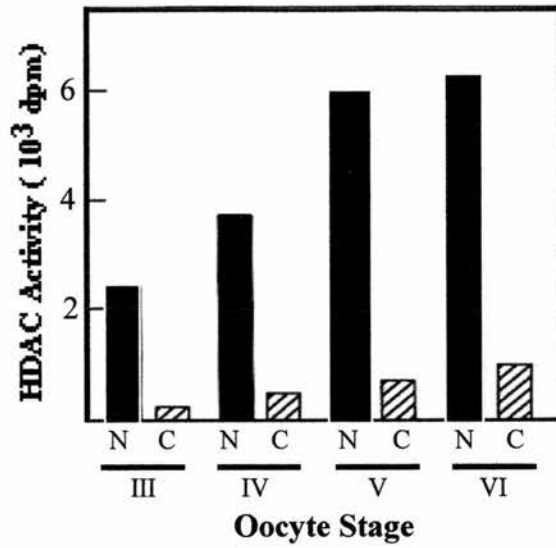
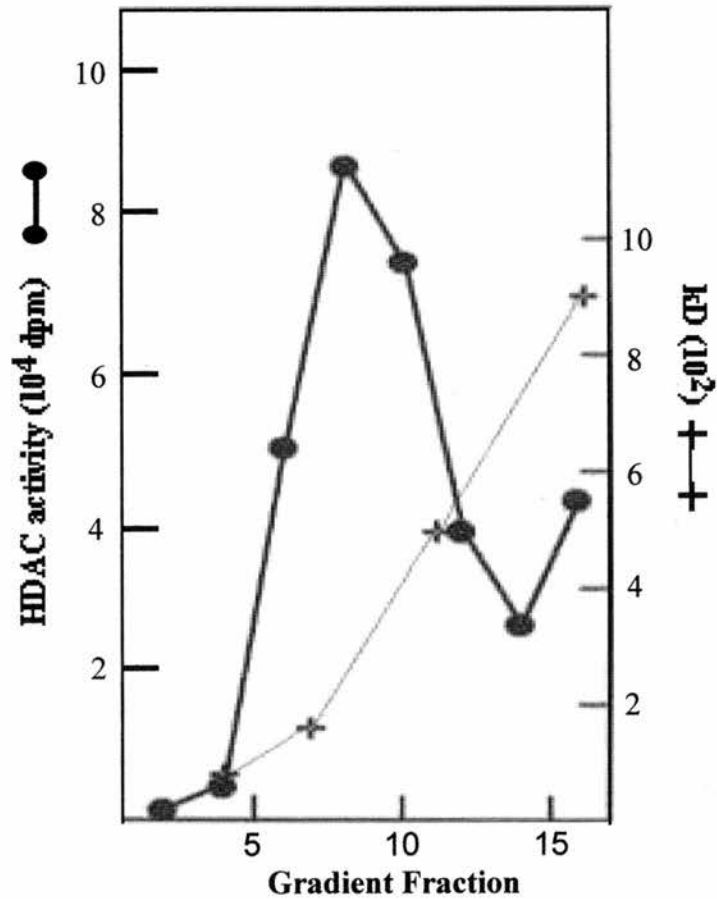
exhaustive list of HDACm associated proteins either, silver staining is very sensitive but notoriously selective with respect to the proteins it reacts with, other proteins may have been eluted that do not react with the silver staining reagents. To date, I have been unable to identify any of these proteins. To achieve this end it would be necessary to purify the immunoprecipitated proteins from a silver stained gel and proceed with protein sequencing, a technique we were not in a position to perform at this time.

3.1.5. Histone deacetylase activity in the *Xenopus* oocyte nucleus.

The Birmingham laboratory of Dr. Brian Turner performed initial assessment of histone deacetylase activity on samples provided to them. *In vitro* activity assays were performed on extracts from whole oocytes and embryos, as well as nuclear and cytoplasmic extracts from stage III to stage VI oocytes (figure 25). These assays accompany the corresponding immunoblots of oocyte and embryos for HDACm (figure 18, figure 20A and figure 22). The assays monitored the level of HDAC activity in the various extracts and fractions and although free histones were used as the substrate, recent assays using nucleosomal histones have shown no substantial difference in HDAC specificity for single nucleosomes, as opposed to free, histones [153]. To confirm that the HDACm protein itself is associated with the HDAC activity detected in

these extracts immunoprecipitation experiments were carried out using anti-Cpep beads. Of the total amount of enzyme activity incubated with affinity-selected IgG, over 50% was recovered bound to the beads after washing. This compares to 0.6% of the activity bound to the beads in the presence of non-specific IgG (not shown).

HDAC activity also mirrors the level of HDACm expression. As can be seen (figure 25A), the amount of activity increases steadily through oogenesis to reach a peak in full-grown oocytes (stage VI). It remain at this elevated level through to cleavage before declining after blastula, this is very similar to the profile of enzyme activity over the same time course (figure 18). However, although the total amount of enzyme and therefore activity, remains at the same level in stage VI oocytes and early embryos, the value represents approximately a 400-fold higher level of activity in oocytes compared to a late blastula embryo on a per cell basis. Analysis of nuclear and cytoplasmic enzyme activity, normalised to a per nucleus or per cytoplasm, is portrayed in figure 25B. Activity is much greater in a single nucleus than in a single cytoplasm, with the same increase in activity between oogenic stages as predicted from studying the level of HDACm expression. In terms of concentration of both HDACm protein and activity, the relative values for nuclei would be even higher, due to the 50:1 ratio of available cytoplasmic: nuclear volumes. In stage VI oocytes it is estimated that

A**B****C**

D

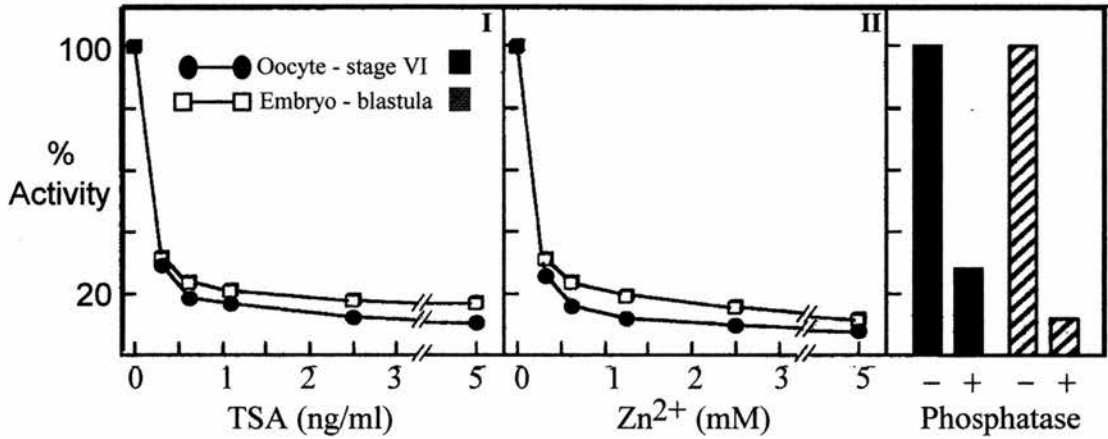


Figure 25. Characterisation of HDACm enzyme activity in oocytes and embryos (assays performed by Dr. B. Turner. **(A)** HDAC activity assayed in extracts from oocytes (stages I, II, III, IV, V, VI and mature) or embryos (C, 8-cell stage; B, mid-blastula; G, gastrula). Activity is expressed as dpm of [³H]acetate released from extracts equivalent to a single cell (oocyte or embryo cell-black columns). The activity/whole embryo is also indicated (striped columns). **(B)** Histone deacetylase activity assayed in extracts from nuclei and cytoplasms. Activity is given as a value per nucleus or cytoplasm. **(C)** Activity profile of soluble extracts from 100 nuclei isolated from stage VI oocytes, HDAC activity peaks over the same fractions as HDACm protein. Positions of protein sedimentation markers (kD) are also shown **(D)** Sensitivity of HDAC activity in stage VI oocytes and blastula embryos to (I) TSA (II) zinc ions (III) alkaline phosphatase (2 i.u./ μ l of extract). I thank Darren White and Bryan Turner (University of Birmingham) for carrying out the deacetylation assays shown here.

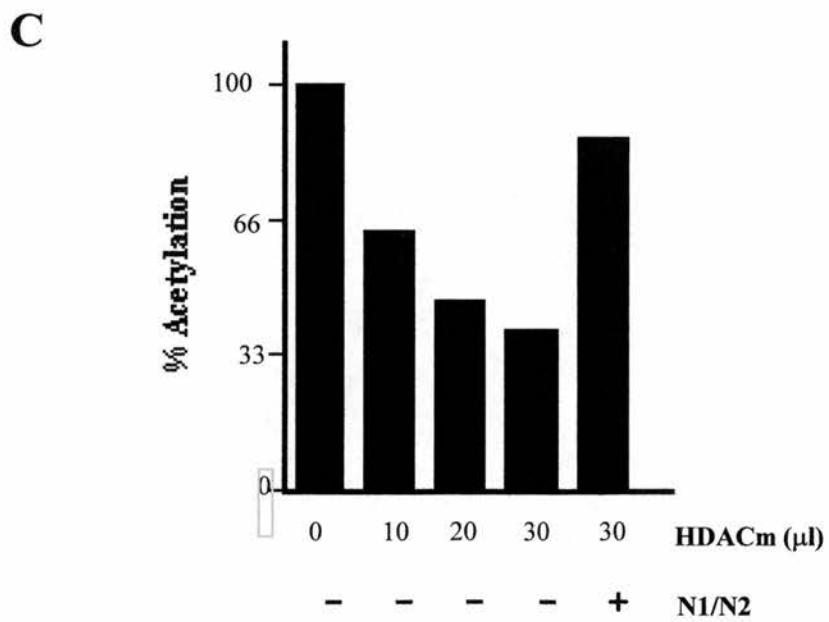
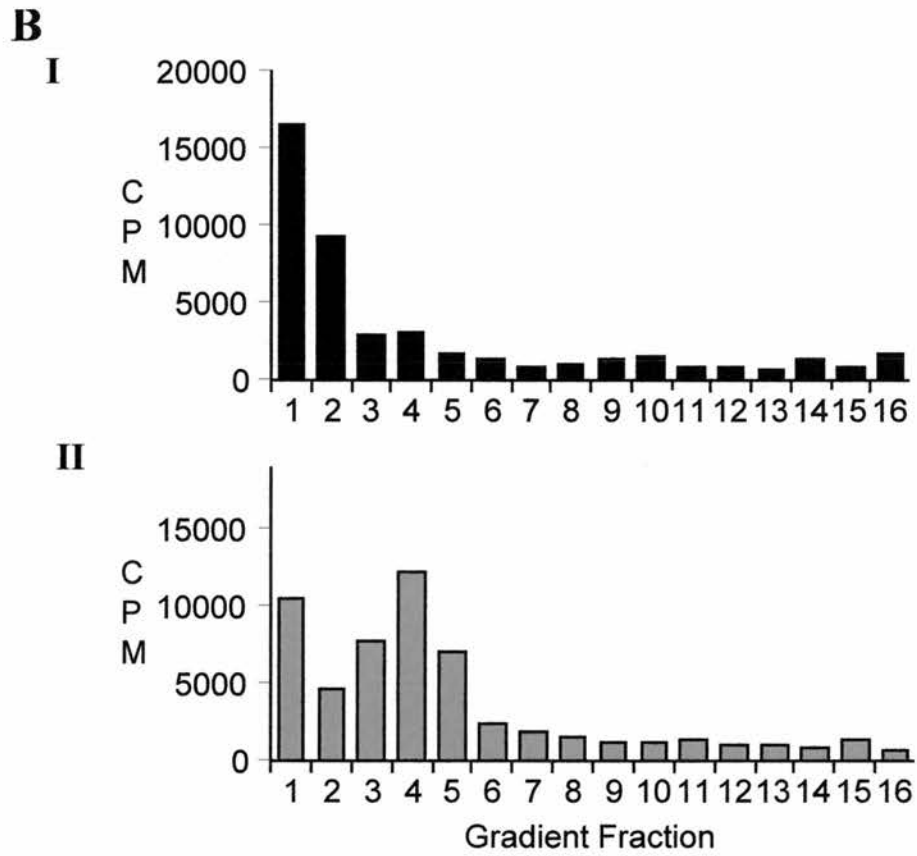
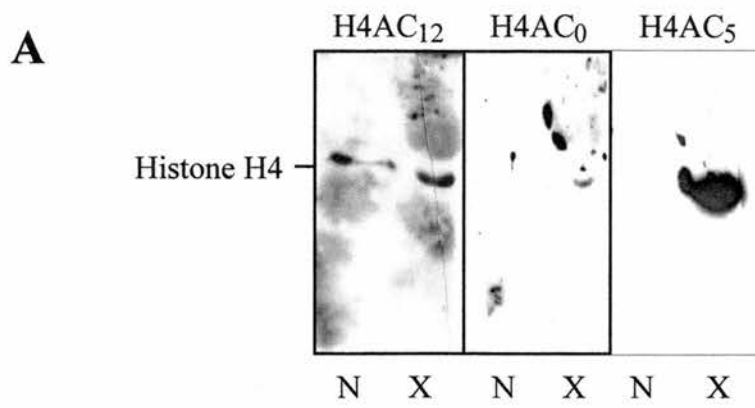
the concentration of HDAC activity is at least 400 times higher in the nucleus than in the cytoplasm. On analysis of HDAC activity in a nuclear extract separated by rate-zonal sedimentation, activity can be seen to peak in the same gradient fraction as HDACm protein (figure 25C). The activity appears to be associated with the HDACm/RbAp48 particle.

HDAC activity has previously been classified into types, based upon sensitivity to TSA [71]. HDAC-A is inhibited by 80% in the presence of 10 nM TSA, HDAC-B is inhibited by less than 20% under the same conditions. On titrating HDACm activity with increasing concentration of TSA, extracts from oocytes and embryos show a single transition of sensitivity, developing approximately 80% inhibition at 0.5 ng/ml (approx. 2nM) TSA. Activity in *Xenopus* oocytes and early embryos would appear to be of the HDAC-A type. This is equivalent to vertebrate class HDAC1. The *Xenopus* HDAC also shows sensitivity to Zn^{2+} ions, both oocytes and embryos being 80% inhibited by 1 mM $ZnCl_2$, Mg^{2+} has no effect on activity, indicating Zn^{2+} may be specifically disrupting the structure of HDACm. Sensitivity to Zn^{2+} ions has previously been demonstrated with yeast HDAC [71]. HDAC substrate specificity may also be influenced by treatment with alkaline phosphatase [73]. Treatment of oocyte and embryo extracts with 50 units/ml alkaline phosphatase at 22°C for 1 hour results in the loss of

60-90% of the HDAC activity in the *in vitro* assay (figure 25D). This result is has precedent, experiments in *Zea mays* have demonstrated the dependence of histone deacetylase activity and specificity upon phosphorylation [73].

If the oocyte contains so much active enzyme, it must be under a great deal of control. The transcriptionally active lampbrush chromosomes maintain acetylated forms of histone H4 [32], whilst histone H4 is being accumulated in a diacetylated state. Is the diacetylated histone H4 store protected from HDAC activity? In the fully developed oocyte the vast majority of histone H4 is maintained in the diacetylated state (figure 26A), it is already known that in the nucleus this histone is stored in a complex with N1/N2 [24,25,151]. To analyse the stability of this complex, a sample of ³H-acetylated histone was incubated with an N1/N2 rich gradient fraction (section 3.1.4). After one hour of incubation this material was run on a 10%-30% glycerol gradient under conditions identical to those used in the rate-zonal sedimentation experiments in section 3.1.4. Whereas some radioactivity remained unincorporated at the top of the gradient, the majority of the labelled histone sedimented to the fractions in which diacetylated histone H4 and N1/N2 have previously been detected (figure 26B). All ³H-acetylated histone H4 that has not been pre-incubated with N1/N2 enrich material prior to rate-zonal sedimentation

Figure 26. Histone H4 acetylation and protection from histone deacetylase activity in the oocyte nucleus. **(A)** Immunoblot, using antibodies raised against specific acetylation sites in histone H4. Each track contains the protein equivalent of ten nuclei (N) or 1 μ g commercial histone (X). **(B)** Rate sedimentation of 30 μ g 3 H-acetylated histone H4 on a 10%-30% glycerol gradient for 18 hours at 30 000 rpm, with and without pre-incubation in an N1/N2 enriched nuclear extract. **(I)** In the absence of pre-incubation with N1/N2, and **(II)** upon pre-incubation of the 3 H-acetylated histone H4 with an N1/N2 enriched nuclear extract for 30 minutes at room temperature **(C)** Assayed histone deacetylase activity in the gradient fraction containing the greatest amount of histone deacetylase. The effect of pre-incubation of 3 H-acetylated histones with a nuclear extract enriched in N1/N2 on the extent of histone deacetylation is also demonstrated.



is retained in the top fractions of a gradient (figure 26B). The faster sedimentation of the histone material incubated with the N1/N2 rich solution prior to centrifugation is presumed to be due to association with N1/N2, suggesting that ^3H -acetylated histone H4 can replace “cold” histone H4 in the N1/N2-histone complex. To confirm this the ability of specific N1/N2 antibodies to immunoprecipitate labelled histone H4 incubated with N1/N2 would need to be demonstrated, however this experiment is not possible at present because no specific N1/N2 antibodies are available.

To investigate the possibility of N1/N2 protecting stored acetylated histone H4 a further series of experiments was performed. Using rate-zonal sedimentation as a fast and reliable method for collecting a concentrated sample of active HDACm, the gradient fraction containing peak HDAC activity was used to assay the sensitivity of acetylated histone H4 to enzyme activity. 30 μg of ^3H -acetylated histone H4 was incubated with an aliquot of HDACm for 1 hour at room temperature, the aliquots increasing in size from 10 μl to 30 μl (10 μl contains the enzyme equivalent of 1.5 nuclei). This treatment resulted in deacetylation of the histones (figure 26C) the level of deacetylation was proportional to the amount of enzyme added. Deacetylation could be inhibited if ^3H -acetylated histone H4 was pre-

incubated with 30 μ l of a gradient fraction containing N1/N2. Storage of diacetylated histone H4 in complex with its chaperone protein N1/N2 appears to offer the diacetylated histone protection from deacetylation.

Since HDACm-containing fractions always have enzyme activity, restricting its distribution to the nuclear margins in large oocytes may be one method of controlling its activity. The results from the mixing experiments suggest that a second level of control is implemented when HDACm is released from its peripheral location prematurely. N1/N2 might further protect diacetylated histone H4 in the nuclear store from deacetylation.

3.1.6. Acylation of *Xenopus* histone deacetylase HDACm.

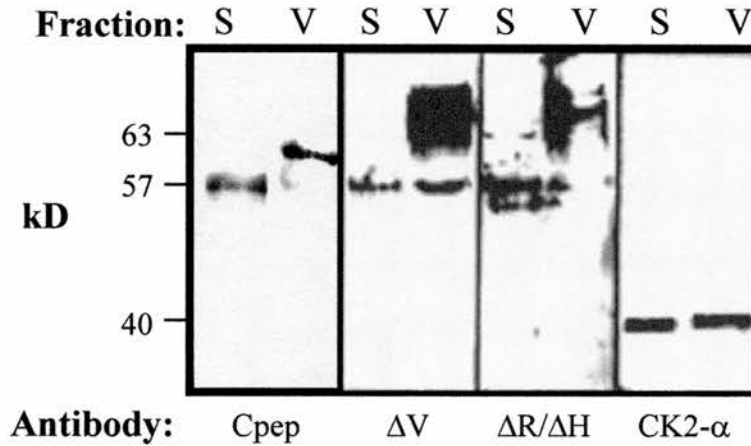
During the course of preliminary investigations into the distribution of the deacetylase during oogenesis, it became apparent that two forms of the deacetylase enzyme exist in the oocyte. The initial study was to determine if this phenomenon was real, or a result of cross reaction between the antisera and proteins other than the deacetylase. To determine this, the protein levels in soluble, nuclear and membrane vesicle fractions was studied using the $\Delta R/\Delta H$, ΔV and C-pep antibodies. The three different antibodies recognise the same pattern of bands; one at 57 kD and a second at 63 kD. To determine whether this represents a specific immunoreaction, the experiment was repeated

using anti-protein kinase CK2 antibodies. The results of this experiment show that this is a specific immunoreaction, the CK2 antibodies detect only the normal CK2 doublet, and this is of the predicted size in both soluble and membrane vesicle fractions (figure 27A). The vesicular material used in these experiments is difficult to analyse by SDS-PAGE due to the high lipid content of the fraction, however the band shift between soluble and vesicle associated material was duplicated upon detergent extraction of ovary tissue, confirming the existence of two forms of HDACm (figure 27B).

This finding confirms the value of the antibodies in recognising the deacetylase enzyme and indicates that there are two forms of the enzyme, one which is vastly enriched in nuclei and a second which is only found in the vesicle fraction of ovary. As the vesicle fraction contains lipid/hydrophobic material, then it would appear that the higher molecular weight form of the enzyme is most likely lipid or membrane associated.

It still remains unknown whether the 63 kD protein is actually related to the 57 kD protein. To determine this, the proteins were subjected to proteolytic digestion (figure 28C). Examination of the resulting pattern of banding demonstrates that many of the bands are shared between the two forms of the protein. This is further indication, when taken with the ability of two different antibodies to recognise it,

A



B

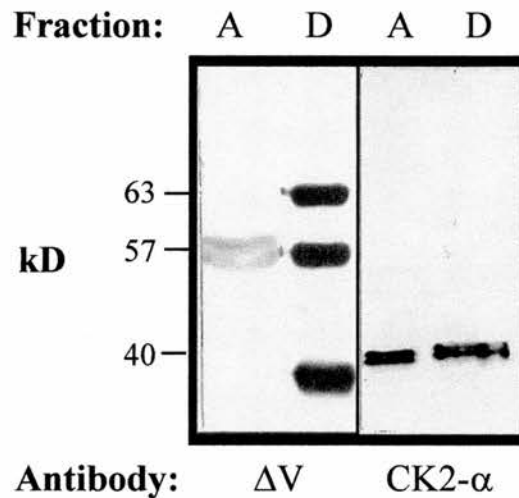


Figure 27. HDACm exist in a modified form in the cytoplasm. **(A)** Immunoblot of vesicle (V) and soluble (S) fractions of mature ovary, using Cpep, anti- ΔV , anti- $\Delta R/\Delta H$ and anti-Cpep. **(B)** Immunoblot of aqueous (A) and Triton X-114 detergent (D) fractions of mature ovary using anti- ΔV . These extracts are blotted with the antibodies raised against CK2- α as a control. The extra bands in extract D of the fraction immunoblotted with anti- ΔV are the unmodified HDACm (57 kD) and a common product of HDACm proteolysis (38 kD) as seen most frequently with the over expression of HDACm *in vivo*. (See section 3.3)

that the 63 kD protein is a modified form of the 57 kD histone deacetylase.

The most likely reason for the 63 kD protein being associated with the vesicle fraction is that HDACm is post-translationally modified. The most probable modification is by addition to the protein of a fatty acid moiety. Lipid modifications can be by either myristoylation, palmitoylation or isoprenylation [153,154]. On examining the amino acid sequence of HDACm and considering motifs recognised for modification in other proteins, the most likely to be involved in import of enzyme is palmitoylation or myristylation. To examine the existence of a modification of the enzyme of this nature, the vesicle fraction was treated with hydroxylamine (HA). This chemical is known to cleave palmioyl/myristoyl moieties from proteins. The results of this investigation show that incubation of the membrane vesicle material with increasing concentrations of HA reduces the amount of protein detectable in the 63 kD form and increases the amount of protein detected in the 57 kD form by immunoblotting with the anti-Cpep antibody (figure 28A). Vesicle material was also treated with calf intestinal phosphatase to see whether dephosphorylation produced the same band shift as hydroxylamine treatment, in case hydroxylamine has pleiotropic effects. The result is that there is no observable change in the proportion of protein detected in the 63 kD

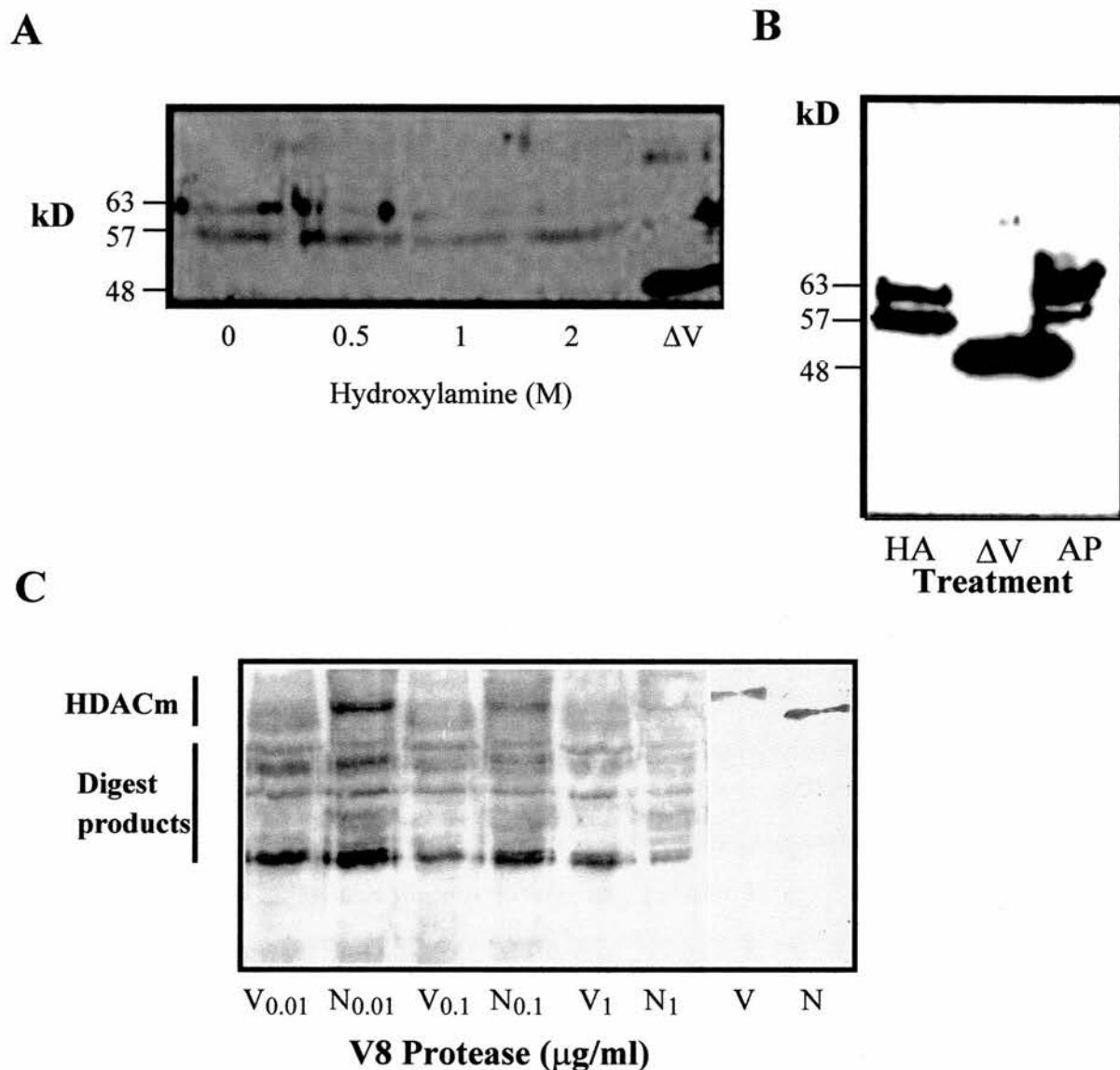


Figure 28. The cytoplasmic modification of HDACm is removed by treatment with hydroxylamine. **(A)** The level of the 63 kD form of HDACm in the vesicle fraction of mature ovary after treatment with increasing concentration of hydroxylamine (1 h at room temperature). Immunoblot performed with anti-Cpep. **(B)** Comparison of the effect of alkaline phosphatase (AP) treatment (1 IU calf intestinal phosphatase 1h at room temperature) and hydroxylamine (HA) treatment (1 M, 1 h at room temperature) on the level of the 63 kD form of HDACm in the vesicle. **(C)** Immunoblot of digested nuclear (N) and vesicle (V) material with V8 protease, using anti-Cpep. Digestion was carried out for 1 h at 37 C in 0.1% SDS and 5 M urea with increasing concentrations of protease.

form (figure 28B). Phosphatase treatment does not produce a shift in material from the 63 kD form to the 57 kD form, whereas a shift is observed upon HA treatment.

Upon incubating in increasing concentrations of HA, it can be seen that the enzyme changes from the 63 kD form to the 57 kD form in increasing amounts, therefore it would seem that the enzyme is post-translationally modified by fatty acylation. The two possible modifications occur only at specific amino acid motifs; palmitoylation can only occur at CAAX, CAC or CCX motifs with the cysteine being the site of addition for the ester-linked fatty acid moiety [154,155], myristylate is bound to N-terminal glycine residues through an amide link [154,156,157]. The deacetylase amino acid sequence contains no palmitoylation motifs, and whilst it contains 7 possible myristoylation sites none of these are at the N-terminus, therefore it would appear that neither of these modifications are likely.

3.2. HDACm and embryos

It is already known that histone acetylation is developmentally regulated, an observation made in sea-urchin, starfish and *Xenopus* [21,45,46]. In *Xenopus*, available histone H4 within the unfertilized egg is in the diacetylated form. Apart from the histone that is already incorporated into chromatin, stores of histone H3 and H4 are associated

with the chaperone proteins N1/N2 [24]. Incubation of oocytes with histone deacetylase inhibitors has no effect on the total amount of diacetylated histone H4 in the oocyte nucleus, a finding that complements the results presented in the preceding section i.e. the histone deacetylase HDACm has potential activity but is not active in the oocyte nucleus [11]. During the rapid cleavage divisions following fertilization, the stored acetylated histone is incorporated into newly synthesised chromatin. Deacetylation is reported to correspond to lengthening of the cell cycle, a point demonstrated neatly by Dimitrov *et al* (1993) by treating early embryos with butyrate, hyperacetylated histones appear for the first time at gastrulation [21]. Treatment of *Xenopus* embryos with TSA had a similar effect; it retarded normal development significantly, but only after the rapid cleavage divisions prior to MBT were completed [11]. Inhibition of HDAC activity in embryos by TSA delayed gastrulation and appeared to prevent normal mesoderm formation resulting in diminished mid-trunk and posterior development of the embryo [11]. TSA has a similar effect on starfish embryogenesis, it inhibits starfish development at gastrula before mesoderm formation [46]. The pattern of gene expression changes dramatically between MBT and gastrulation. At MBT the embryo initiates gene transcription. At this point the cells are totipotent and transcribe many genes that are normally lineage specific. Cell lineage-

specific patterns of expression are only established once gastrulation begins. These transitions are associated with changes in the type of linker histone present and the level of histone H4 acetylation [44]. Regulated histone deacetylation appears to play an important role at MBT and in executing cell differentiation during gastrula [11].

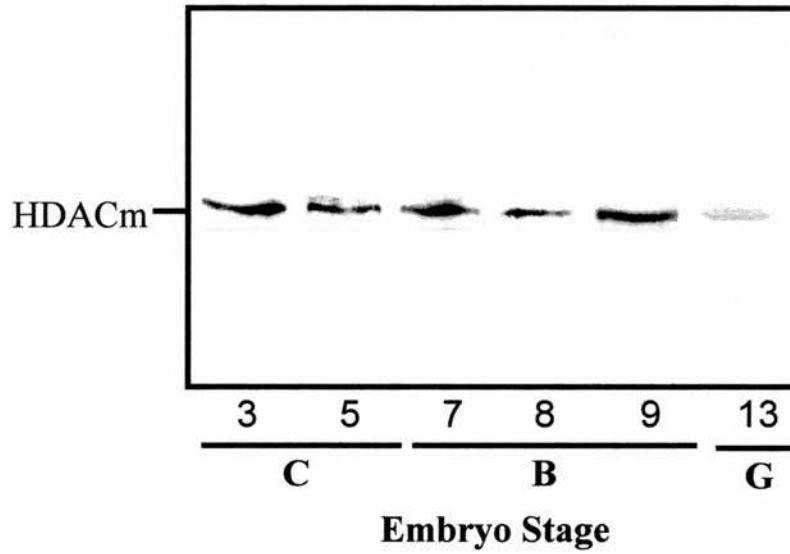
Histone deacetylases are maximally active in *Xenopus* embryos from some point post-MBT. The aim of this set of experiments was to identify the exact time of onset of histone deacetylase activity, the nature of the multimolecular complex in which the enzyme is found and subcellular location of HDACm. The time of activation is likely to be between MBT and the beginning of gastrula, for this reason the changes occurring around this time were looked at most closely.

3.2.1. Expression of HDACm and RbAp48 in early embryos.

It was established in a previous section (3.1.1) that levels of HDACm are highest in mature oocytes and remain high throughout the rapid cleavage divisions and blastula. The level of enzyme begins to diminish in gastrula stage embryos and is undetectable in tail bud stage embryos (figure 18). Measurement of the HDAC activity in these same samples showed that the profile of activity mirrored the amount of protein present (figure 25). As previous experiments have indicated that *in vivo* HDAC activity is detectable in post-blastula embryos by the

effect of inhibition, the first experiments conducted here were a more detailed investigation into the levels of HDACm and the previously identified associated protein RbAp48 in embryos at this stage in development. Cleavage stage embryos, early, mid and late blastula embryos plus gastrula embryos were assayed for these proteins by immunoblotting (figure 29). The profiles confirm the previous finding that HDACm is at its highest level in the cleavage embryos and throughout the blastula stages, the level of enzyme does not start to diminish until post blastula. However, the rate of decline after this point is rapid, within four cell cycles, i.e. the middle of gastrulation (stage 13), the enzyme level has dropped by almost 80%. The level of RbAp48 protein in the early embryo shows a similar pattern of expression. This protein is at peak levels in the embryo throughout the cleavage divisions and until the end of blastula. Protein levels drop considerably after this point, by midway through gastrulation (stage 13) the protein is at approximately 50% of its blastula level. There are two additional points to notice about the latter protein however; (i) the immunoblotted band appears as a doublet, (ii) the decline in the level of RbAp48 by stage 13 gastrula is nowhere near as great as the decline in HDACm over the corresponding time. RbAp48 and its closely related protein RbAp46 show great sequence similarity and are identical in the region against which the anti-serum used here has been raised. The

A



B

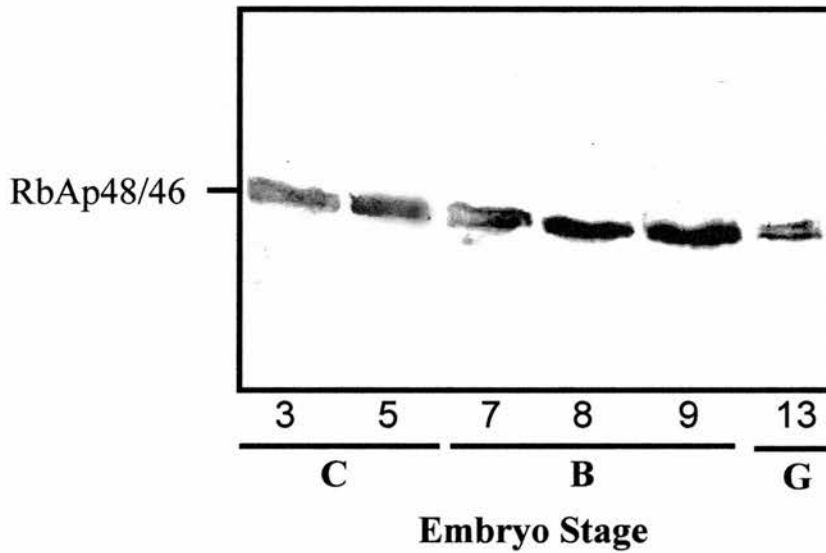


Figure 29. Levels of HDACm and RbAp48 protein in early embryogenesis. **(A)** Immunoblot, using anti-Cpep, of extracts from cleavage, blastula and gastrula stage embryos. Each track contains the protein equivalent of two embryos. **(B)** Immunoblot, using anti-RbAp48, of extracts from cleavage, blastula and gastrula stage embryos. Each track contains the protein equivalent of two embryos.

significance of expressing two closely related proteins that apparently have the ability to replicate each other's function is not known. The difference in the rate of decline in protein levels between HDACm and RbAp48 is of significance and probably is indicative of the multiple roles played by RbAp48 in a variety of chromatin remodelling complexes. This protein is reported to be involved in chromatin assembly as part of the CAC complex, it is involved in histone deacetylation and may also be involved in histone acetylation [27,28,158]. The decline in RbAp48 may be due to the loss of HDACm associated p48 only, its role in the mass deacetylation of chromatin now completed.

3.2.2. Location of HDACm and candidate deacetylase associated proteins within the embryo.

In oocyte nuclei, I have already demonstrated that HDACm and RbAp48 co-localise to the nuclear periphery but inside the lamin layer. In this location, the active enzyme complex is sequestered away from chromatin and stored, diacetylated histone H4. To study the distribution of these nuclear proteins and others within the cells of the early embryo of *Xenopus laevis*, alternative methods must be employed and physiological differences considered. The most important physiological difference between the cells in early stage embryos and somatic cells is

the regulation of DNA replication and chromosome segregation in mitosis. In somatic cells DNA replication and segregation are strictly regulated by a series of checkpoints in phases G1 and G2 of the cell cycle; chromosomes separate only after each has been successfully duplicated, and duplication cannot occur until the previous segregation is completed. S-phase and chromosome duplication cannot be initiated until a checkpoint indicating that segregation and cell growth are completed is passed in G1. Likewise, segregation cannot occur until a second checkpoint in G2 is passed successfully [147]. The pre-MBT divisions in *Xenopus* embryos do not contain G1 or G2 phases of the cell cycle. In these rapidly dividing cells growth and division are uncoupled, resulting in the so called reductive divisions of cleavage. In this situation each round of cell division proceeds in the absence of cell growth, producing successively smaller and smaller cells. In these cells, DNA replication occurs in a greatly altered fashion; each chromosome is surrounded by its own nuclear membrane to form a micronucleus, this structure is known as a karyomere. Inside the individual karyomeres, DNA replication takes place independently of the other chromosomes, as soon as all the chromosomes have been replicated cell division occurs. This system allows the early embryonic cells to cycle rapidly between S phase and M phase every 30 minutes, the necessary components for these cell divisions are stored in the oocyte in large

excess prior to fertilization to allow for the production of the 4 000 cell mid-blastula embryo. At the end of the cleavage divisions, when the embryos pass the MBT “normal” cell division is reinstated and with it the initiation of zygotic transcription.

Cleavage and blastula embryos have been looked at by three histological methods. In the first method, thin sections of formaldehyde fixed blastula stage embryos were immunostained using a variety of primary antibodies raised against HDACm and other nuclear proteins (figure 30). Anti-Cpep, anti-RbAp48, anti-MeCP2 and anti-mSin3 antibodies and FITC conjugated secondaries were used to immunostain these sections before viewing by confocal laser microscopy. The resulting images indicate that whilst HDACm, RbAp48 and MeCP2 are all associated with the nuclear envelope, *Xenopus* Sin3 is found distributed through out the blastula stage cells in a pattern that shows no predominant staining associated with nuclear structures. Sin3 does not seem to play a role specific to the nucleus and therefore, like the situation in the oocyte, only a small proportion of the Sin3 protein present is likely to be associated with HDACm.

The major drawback of this method of staining is that it does not allow easy visualization of individual karyomeres. To aid observation of the individual karyomeres two methods were tried of preparing these for histological examination. By the first method, a karyomere extract

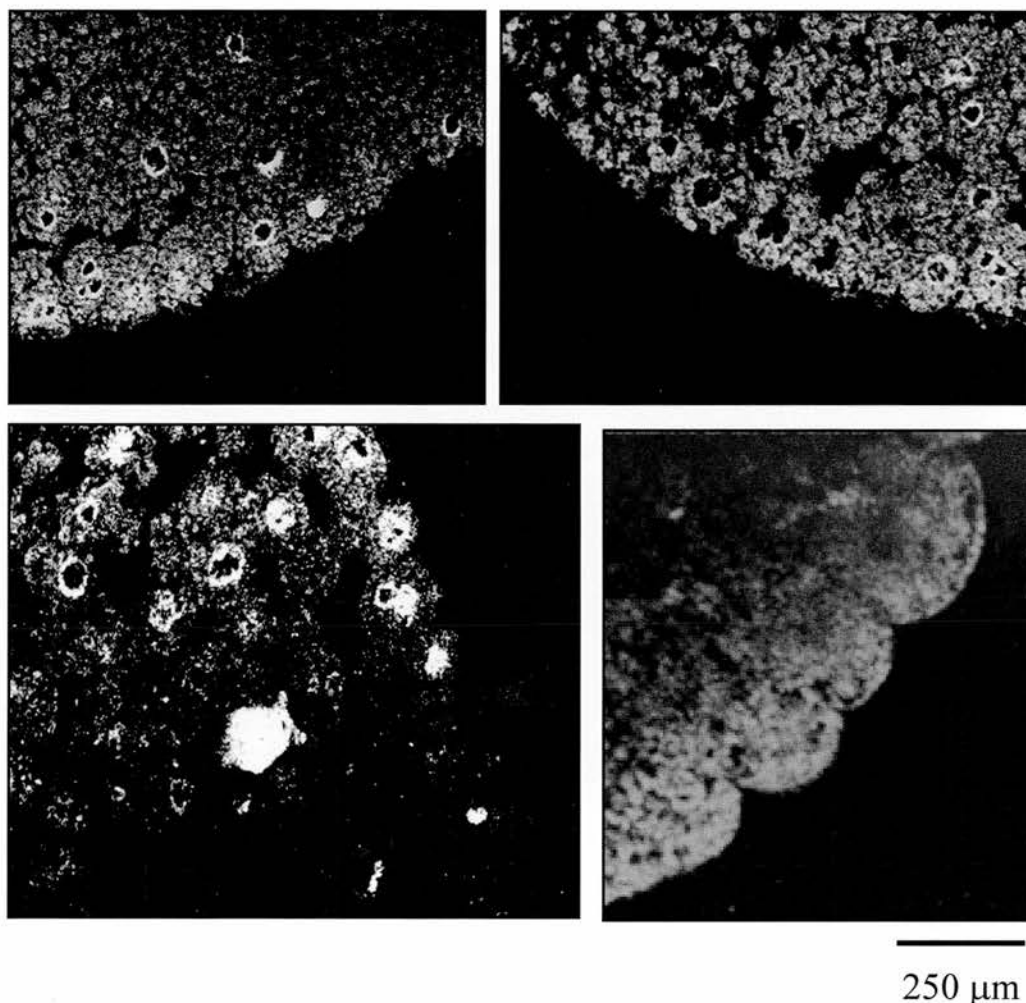


Figure 30. Localisation of nuclear proteins in sections of mid-blastula embryos. Immunostaining of karyomeres in sections of mid-blastula embryos using (I) anti-Cpep, (II) anti-RbAp48, (III) anti-MeCP2 and (IV) anti-sin3 antibodies. The fluorescent image is provided by fluorescein conjugated anti-rabbit IgG used as the secondary antibody. Material was viewed by confocal microscopy. The images shown are representative of several images seen on the sections. Staining in figures I-III appears to be quite specific, whilst the staining in figure IV appears to be general and throughout the cell. These sections were treated with ereochrome black (section 2.3.16) but despite this it is possible the image seen is the result of autofluorescence of yolk platelets.

was made and immunostained as described in section 2.3.19. By this method it was possible to demonstrate the co-localization of lamin B, HDACm, RbAp48 and DNA to the same particles (not shown). As this procedure spins the karyomeres flat, it is not possible to observe the structure of the karyomere or the nature of the interaction between the different components. The second method used for studying individual karyomeres involved squashing whole embryos once they had been fixed and immunostained (figure 31). These images are representative of a number of images seen through the centre of a mid-blastula karyomere using a scanning confocal laser microscope. The embryos had been arrested at S phase at this point in development by incubating with cycloheximide prior to fixing. By this method, it has been possible to study the distribution of HDACm, RbAp48 and MeCP2 within the karyomere. Immunostaining of whole mount karyomeres shows that HDACm and RbAp48 are located mainly around the internal margins of the karyomere during S-phase with very similar distribution (figure 31), much like the situation in the oocyte nucleus. These proteins lie internally in the nucleoplasm and are not detectable on the chromatin. The considerable overlap seen in the location of HDACm with respect to RbAp48 is yet again compatible with the proposition that the HDACm particles contain a subset of the nuclear RbAp48 molecules. This contrasts with the distribution of MeCP2, which appears

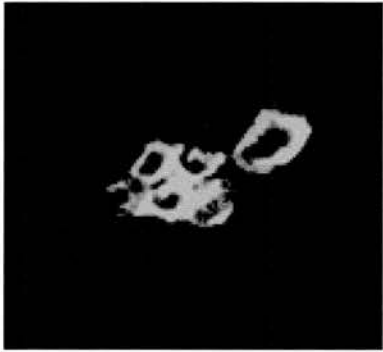
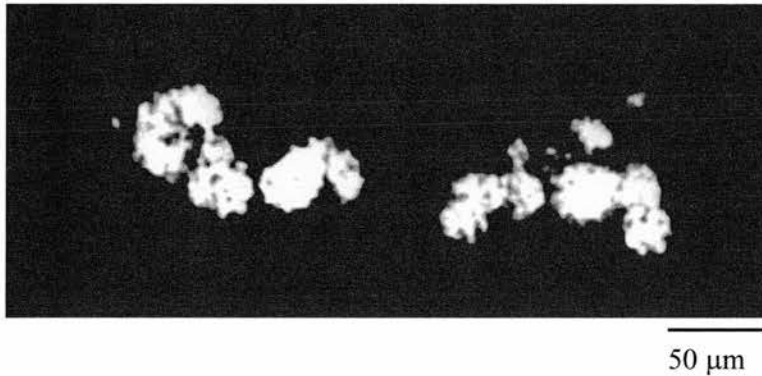
A**B****C**

Figure 31. Localisation of nuclear proteins in individual karyomeres of mid-blastula embryos. Immunostaining of karyomeres in whole-mount mid-blastula embryos using (A) anti-Cpep, (B) anti-RbAp48 and (C) anti-MeCP2 antibodies. Fluorescent image is provided by fluorescein conjugated anti-rabbit IgG used as the secondary antibody. Material was viewed by confocal microscopy, images shown are representative of several images seen through the approximate centre of the karyomeres. The embryos were all arrested at the same point of the cell cycle by incubating with 150 mg/ml cyclohexamide for 45 minutes prior to fixing.

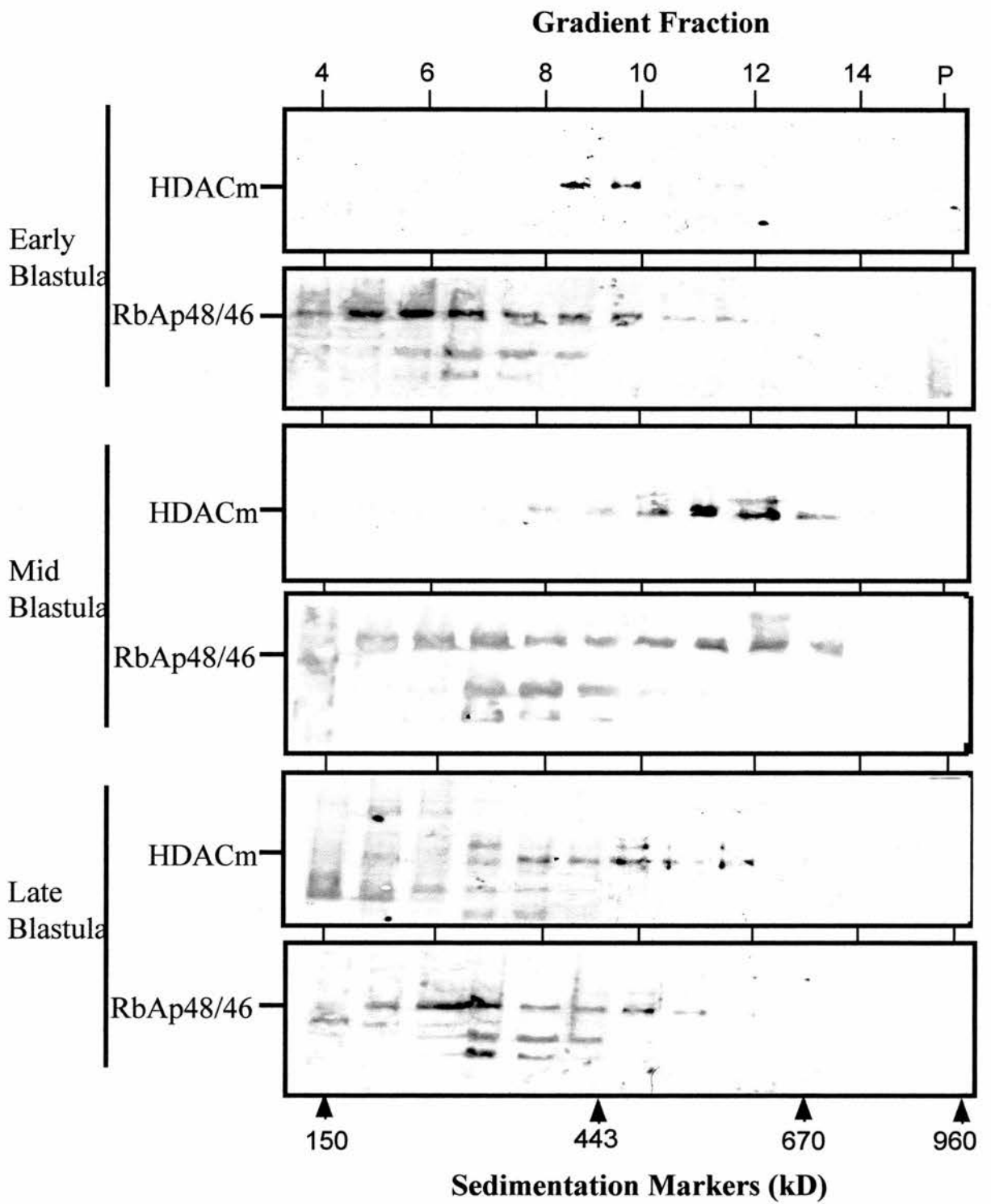
throughout the nucleoplasm in a fashion that indicates that it is located on the chromatin (figure 31). Sin3 was not detectable in a karyomere preparation of this type.

3.2.3. HDACm is a component of a multimolecular complex that changes in size through blastula.

Just as in *Xenopus* oocytes where HDACm activity is associated with protein complexes of approximately 300 kD as described in section 3.1 and Ryan *et al* [159], it was thought that the situation would be similar in embryos. Homogenates of early embryos show a heterodisperse sedimentation profile, indicating that some larger complexes may have formed by this stage in development. Some slower-migrating bands are detected at this stage in development, indicating that HDACm may be subject to protein modification at blastula [159]. Additionally, it has already been established that the HDACm sedimenting at a rate indicating it is in a particle of mass 300 kD is not a multimer of HDACm protein but is complexed with other proteins including RbAp48. The next step was to investigate sedimentation of HDACm and RbAp48 in early-, mid- and late-blastula embryos to see if they still co-migrate and if the size of the particles they are in are of the same size as those detected in large oocytes.

To obtain a measure of the relationship between molecular size and progress through blastula, a karyomere preparation was made as described in section 2.3.19 for early- mid- and late- blastula embryos. These samples were then separated under near-physiological conditions by rate-zonal centrifugation. The karyomere preparation was layered on a linear 10%-30% glycerol gradient and centrifuged for 18 hours at 30 000 rpm and 0°C in a Beckman SW55Ti rotor until the 19S marker reached the bottom of the tube. The gradients were then fractionated and analysed for HDACm and RbAp48 content by immunoblotting (figure 32). These immunoblots mark two important points. Firstly, the particle mass changes through blastula, increasing from approximately 450 kD in early blastula to approximately 600 kD by mid blastula before returning towards the 450 kD mark in late blastula embryos. Second, HDACm and RbAp48 overlap in their distribution in the early, mid and late blastula extracts, making it possible that HDACm particles still contain RbAp48. This is seen clearly with the different stages as the RbAp48 shifts through the gradient with the changes in the size of the HDACm containing particles. Protein complexes containing HDACm and Sin3 or HDACm and MeCP2 were also looked for, however the signal from the blots for Sin3 was too weak to be detected. The little MeCP2 that could be detected was found in a particle of

Figure 32. HDACm is found in complexes of differing sizes through mid-blastula. Detection of HDACm and RbAp48 in karyomere extracts from early, mid and late blastula embryos separated by rate sedimentation. The same gradient fractions were immunoblotted with anti-Cpep (HDACm) and anti-RbAp48 IgG. The position of the sedimentation markers are indicated (kD). Each gradient was loaded with the protein equivalent of 30 embryos. Protein complexes containing HDACm and Sin3 or HDACm and MeCP2 were also looked for, however the Sin3 signal from the blots was too weak to be detected. The little MeCP2 that could be detected was found in a particle of constant size throughout blastula. This particle sedimented at approximately 600 kD (not shown).



constant size throughout blastula. This MeCP2 particle sedimented with a peak of approximately 600 kD (not shown).

The continued association of RbAp48 with HDACm was investigated in more depth by immunoprecipitation. Anti-RbAp48 was chemically cross-linked to protein A beads. After incubation of the antibody beads with karyomere extracts from early-, mid- or late-blastula embryos, and after thorough washing to remove loosely associated protein, bound protein was eluted by washing with 0.1M glycine (pH 3.0). The eluate was immunoblotted for the presence of HDACm (figure 33). The result indicate that HDACm and RbAp48 are components of a common particle present in early-, mid- and late-blastula embryos. Immunoprecipitation conducted with oocyte nuclei extracts demonstrated that less than 20% of the total RbAp48 was bound to anti-Cpep beads but more than 80% of HDACm was bound to RbAp48. In embryos, the amount of HDACm associated with anti-RbAp48 beads remains at a constantly high level.

Immunoprecipitation of HDACm from a mid-blastula karyomere extracts with anti-RbAp48 beads pulls down two detectable forms of HDACm (figure 33). The slower migrating form of HDACm can be converted to the faster migrating 57 kD form by incubating the washed beads with a solution of alkaline phosphatase (2units/ml) for 30 minutes at room temperature. Therefore, HDACm would appear to be

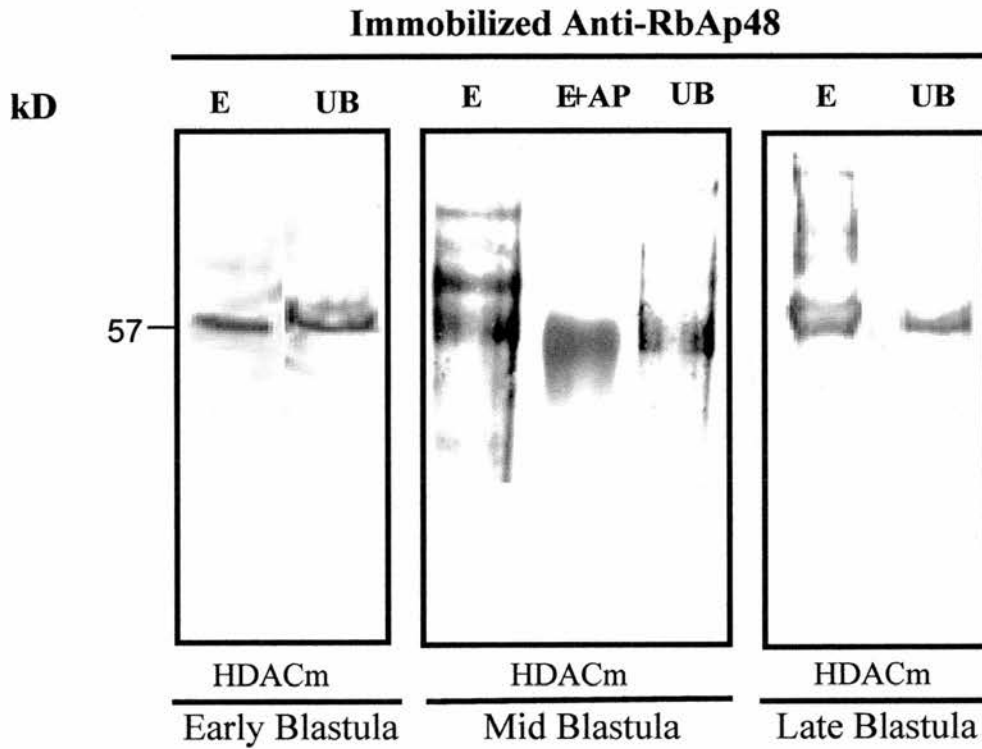


Figure 33. Co-precipitation of proteins associate with HDACm in embryos. Extracts from early, mid and late blastula embryos were incubated with anti-RbAp48 immobilized on protein A beads. Unbound (UB) and eluted (E) fractions were immunoblotted with anti-Cpep. Additionally, protein immobilized on the anti-RbAp48 beads was incubated with phosphatase prior to elution (E+AP). Immunoprecipitation was conducted with the protein equivalent of 30 embryos.

phosphorylated at mid-blastula. The HDACm containing particles increase in size progressively from late stage oocytes to blastula with the size of the multimolecular HDACm complex peaking at mid-blastula. This peak in sedimentation rate corresponds to the modification of HDACm. The progressive increase in HDACm particle size towards mid-blastula may well represent the steady assembly of a nuclear complex containing HDACm and RbAp48 post-fertilization that is aimed at creating a multimolecular complex with full activity. Phosphorylation of HDACm being the final modification of the complex that gives the complex *in vivo* activity.

3.2.4. Detection of *in vivo* HDACm activity.

Diacetylated histone H4 is found in two distinct populations during these early stages of development, firstly in storage particles with histone H3 and the chaperone proteins N1/N2 and secondly, in newly assembled chromatin. The proportion of the diacetylated histone in each population changes continually post-fertilization; the rapid cleavage divisions driving the flow of diacetylated histone H4 from the population of the stored material to the population incorporated in newly synthesised chromatin.

The two most likely schemes for the timing of deacetylation are as follows. Deacetylation may be continuous throughout early

development, a round of global deacetylation occurring at the end of each cell cycle. Alternatively, the initial deacetylation event may only occur at a point in development when all the stored histone has been incorporated into newly synthesised chromatin and possibly with the re-initiation of G1 and G2 phases of the cell cycle and the initiation of transcription from zygotic genes. This would involve 11 cycles of cell division going past with no deacetylation and in the absence of transcription. On or past MBT, as the cell cycle lengthens and the complex pattern of gene expression is initiated, the diacetylated histone H4, for example, would have to be deacetylated to organise all chromatin into the same “undifferentiated” state. This would be essential to allow cell type specific patterning of the chromatin to take place and allow cell differentiation.

The results presented to date would seem to rule out the first suggestion of continuous deacetylation through cleavage as deacetylase activity would have to rise through cleavage and peak at early blastula. This does not fit in with the results presented, with respect to the measured *in vitro* deacetylase activity (figure 25). Additionally, if deacetylation is to take place through cleavage and blastula, then the multimolecular complex of which HDACm is a member might be expected to remain at a constant size throughout this time of activity. The activity results and the results of the analysis of the HDACm

complex and its modifications lead to the preferred view that the deacetylase is active at MBT and onwards. To investigate deacetylation, examination of the levels of diacetylated histone H4 in total, and in the two populations, have been conducted in embryos staged between cleavage and gastrula.

Immunoblotting of embryo extracts from stage 3 (cleavage) to stage 13 (gastrula) embryos for the amount of diacetylated histone H4 shows that the level of this histone remains constant through the early cleavage divisions, the level of acetylated histone does not drop until the rapid cleavage divisions have been completed. The transition occurs between mid-blastula and late-blastula. Deacetylation appears to begin at the MBT (figure 34A). To analyse the two populations of diacetylated histone H4 around this point, further experiments have been conducted to study the two populations separately. Horseradish peroxidase immunostaining of whole-mount embryos at stages 3, 5, 7 and 8 shows that the population of diacetylated histone H4 stored in complex with N1/N2 is found in distinct punctate structures located deep within the cells (figure 34B). This is different from the distribution of HDACm and RbAp48, which are restricted entirely to the margins of karyomeres. The amount of immunostaining material in these punctate stores of histones can also be seen to diminish as development progresses, the diacetylated histone H4 is presumably moving from the

A

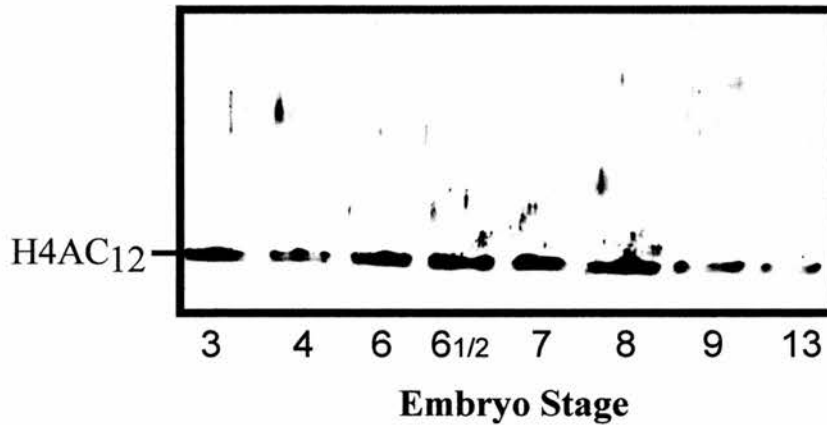
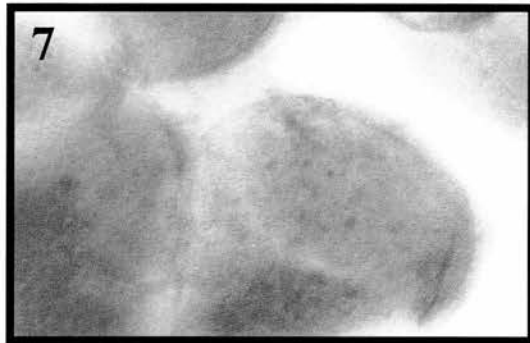
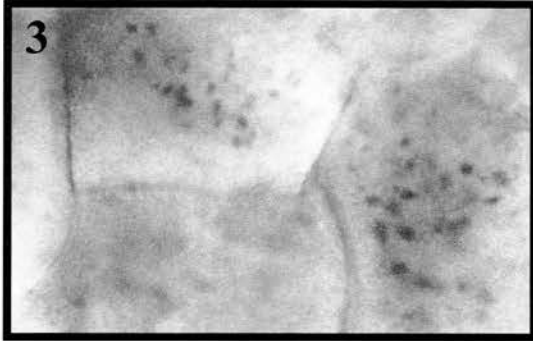


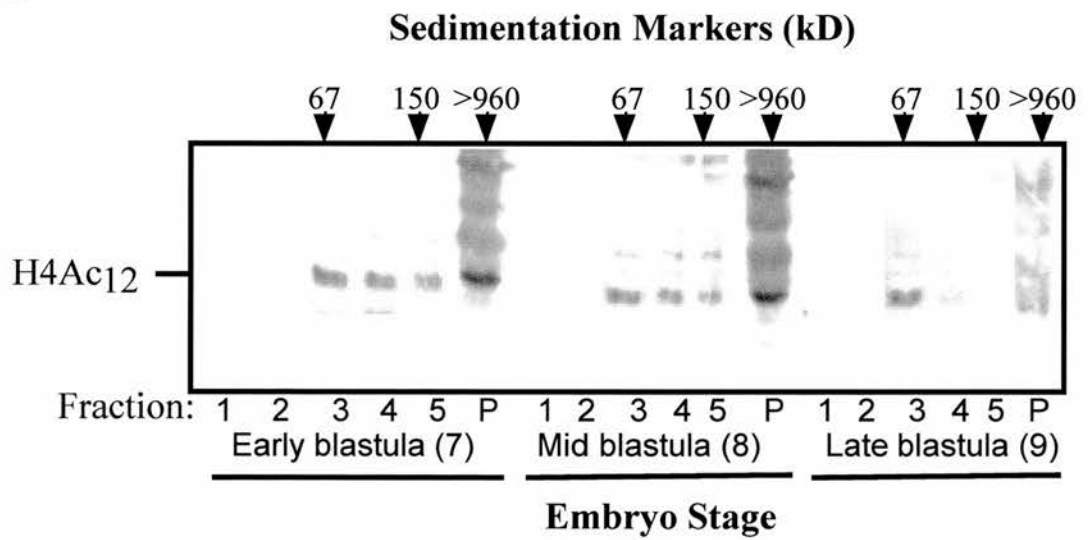
Figure 34. Histone acetylation state during early development. **(A)** Immunoblot, using anti-H4AC₁₂, to assess the amount of histone H4AC₁₂ stored in complex with N1/N2 and newly formed chromatin (total histone H4AC₁₂) in stage 3 to 13 embryos. Each track contains the protein equivalent of two embryos. **(B)** Immunostaining of whole mount *Xenopus* embryos viewed by light microscopy. Embryos were fixed at stage 3, 5, 7 and 8 and immunostained using anti-H4AC₁₂. The image is provided by horseradish peroxidase conjugated anti-rabbit IgG used as the secondary antibody and subsequent DAB reaction. The optical sections shown are representative of several images seen in the surface cells of the embryos. **(C)** Detection of histone H4AC₁₂ in early, mid and late blastula karyomere extracts separated by rate sedimentation, the protein equivalent of 30 embryos were loaded on the gradient. The positions of sedimentation markers are indicated (kD). The relevant fractions (1-5) and pelleted material (P) were probed with antibodies raised against histone H4AC₁₂. This antibody shows a high degree of cross reaction with material in the pellet, however it does react strongly with material corresponding in size to diacetylated histone H4. The nature of this cross-reacting material is unknown.

B



100 μ m

C



store and being incorporated into newly synthesised chromatin. Supernatants from early-, mid- and late-blastula embryos were separated under near physiological conditions by rate-zonal centrifugation on a linear 10% - 30% glycerol gradient until a 19S marker reached the bottom of the tube. Immunoblotting the fractionated gradients for the presence of K12 acetylated histone H4 clearly shows two populations of this histone (figure 34C). In early- and mid- blastula embryos there is a diminishing amount of acetylated histone associated with sedimenting complexes and a corresponding increasing amount associated with the pelleted material. This is consistent with the accumulation of acetylated histones into newly synthesised chromatin. Immunoblotting the gradient pellet from these two stages shows a seemingly large amount of cross-reaction with slower migrating material. That this cross-reaction is with chromatin associated material was confirmed by prior digestion with micrococcal nuclease, which resulted in the signal resolving to the H4 band position. The difference between the amount of protein in the two populations of diacetylated histone H4 between mid-blastula and late-blastula is apparent, the amount of stored (sedimenting) histone H4 is almost depleted (figure 34C). Histone H4 for further assembly of newly synthesised chromatin will come from the expression of zygotic genes. The amount of acetylated histone H4 in the chromatin is also greatly depleted, the

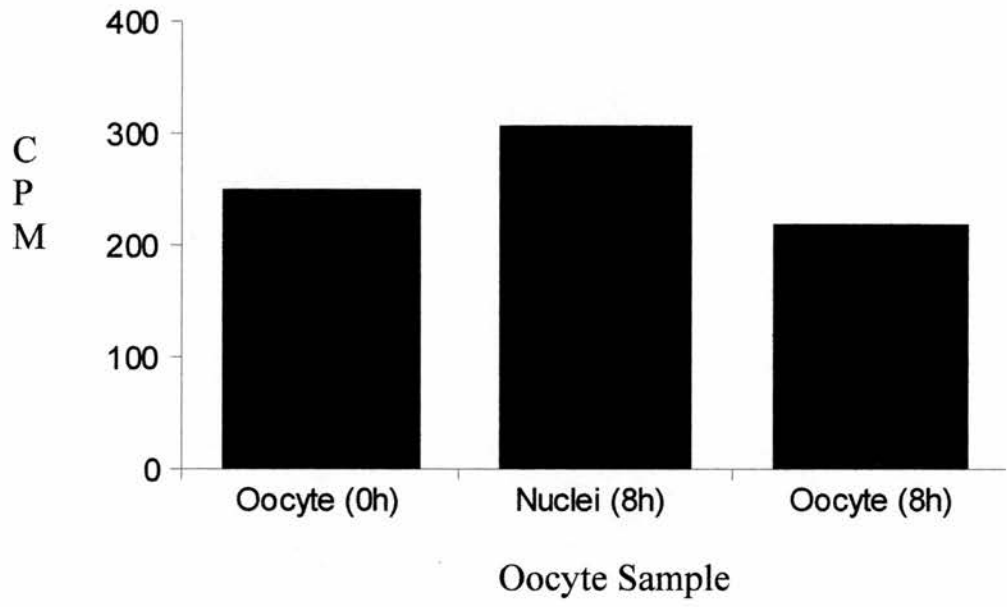
amount of acetylated histone H4 in the pelleted chromatin of the late-blastula embryo being no more than 10% of the amount in the chromatin of the mid-blastula embryo. The gradient analysis confirms the results of the previous two experiments; that whereas there is a progressive transfer of acetylated histone H4 from storage complexes to chromatin, the acetylation level in chromatin only falls between mid- and late-blastula.

There is one major drawback with the antibody-based techniques that have been used to assay *in vivo* HDACm activity in that they are only semi-quantitative. They would only detect a large drop in the amount of diacetylated histone H4 present in the embryo, not those that would occur in the embryo during the initial cleavage divisions. In early embryogenesis each cleavage division uses a small proportion of the total histone H4 store, whilst the final cleavage division theoretically uses 50% of the total histone H4 stored in the embryo, antibody techniques may not be sensitive enough to detect these smaller changes if present. To answer this question another way, I have tried to analyse *in vivo* HDAC activity by injecting acetylated histone H4 that has been labelled with ^3H -acetate. Labelling is carried out using an oocyte cytoplasmic extract as a source of HAT activity, purified histone H4 and ^3H -acetyl CoA as substrates. By this method it is possible to label histone H4 at the required sites (K5 and K12) for nuclear import,

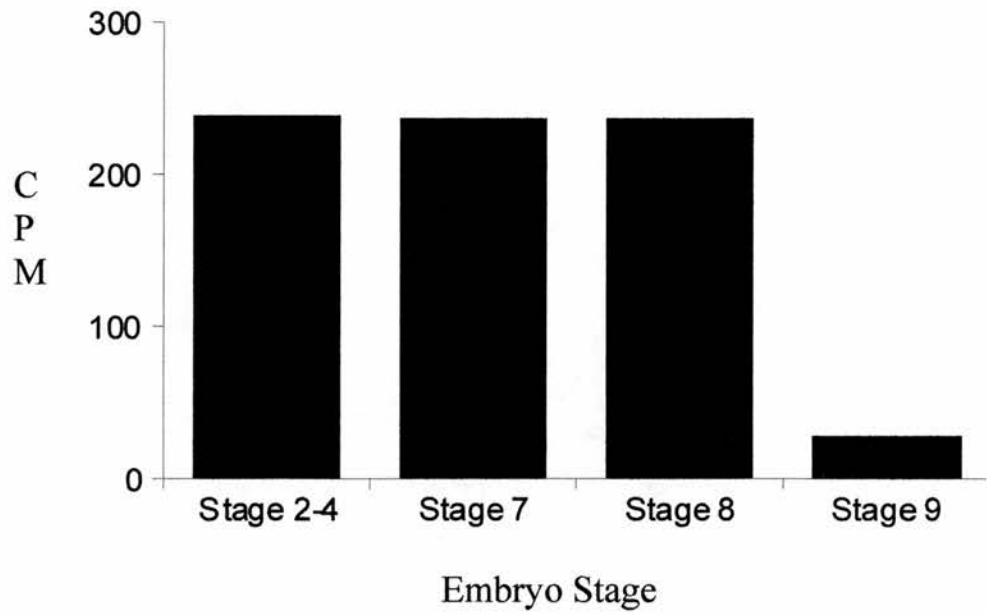
nuclear storage and incorporation into newly synthesized chromatin. This assay will only work if injected histone H4 is imported into the nucleus and stored away from HDAC activity. It is not feasible to confirm this in embryos, as it is difficult to isolate karyomeres intact, so nuclear uptake was investigated in oocytes (figure 35A). Oocytes were injected with labelled histone H4 and assayed for loss of radioactivity by precipitating protein in oocyte and nuclear extracts onto glass fibre filters with 20% TCA and counting in a scintillation counter. The analysis shows that by 8 hours post-injection all of the labelled histone is imported into the nucleus, and that it is stored in the nucleus in a manner that protects it from endogenous HDACm activity. Thus, nuclear import of injected histone H4 and protection from fortuitous deacetylation was demonstrated, at least in oocytes. Then embryos at the 2-4 cell stage were injected with ^3H -labelled acetylated histone H4 and assayed for *in vivo* HDAC activity throughout blastulation in the same manner as described for oocytes (figure 35B). No drop in the level of radioactivity could be detected in these embryos between the 2-4 cell stage and mid-blastula (stage 8) embryos, whereas between mid-blastula and late-blastula (stage 9) the amount of precipitable radioactivity drops by almost 90%. This agrees with the results of the previous investigation, indicating that histone deacetylase activity, of

Figure 35. *In vivo* assay of histone deacetylase activity in early embryos. It is possible to inject oocytes and embryos with histone H4 labelled with ^3H -acetyl groups using oocyte cytoplasmic HAT activity. This material can be used to measure histone deacetylase activity *in vivo* if it is imported into the nucleus post-injection. **(A)** To examine whether injected ^3H -labelled histone H4 is imported into the nucleus and stored away from HDACm in the same manner as native protein, oocytes were injected with ^3H -acetylated histone H4. Injected oocytes were analysed for precipitable radioactivity at the time of injection and 8 hours post injection. At this point a nuclear extract and a whole oocyte extract were analysed. Each sample contained the protein equivalent of 50 oocytes or 50 nuclei. **(B)** Having determined that injected histone H4 could be incorporated into the nuclear store and is not susceptible to fortuitous deacetylation, embryos at the 2-4 cell stages were injected with ^3H -acetylated histone H4. Injected embryos were analysed for radioactivity at the 2-4 cell stage and at stage 7, stage 8 and stage 9. Each sample contained the protein equivalent of 30 embryos. All measurements have been adjusted to remove the background counts.

A



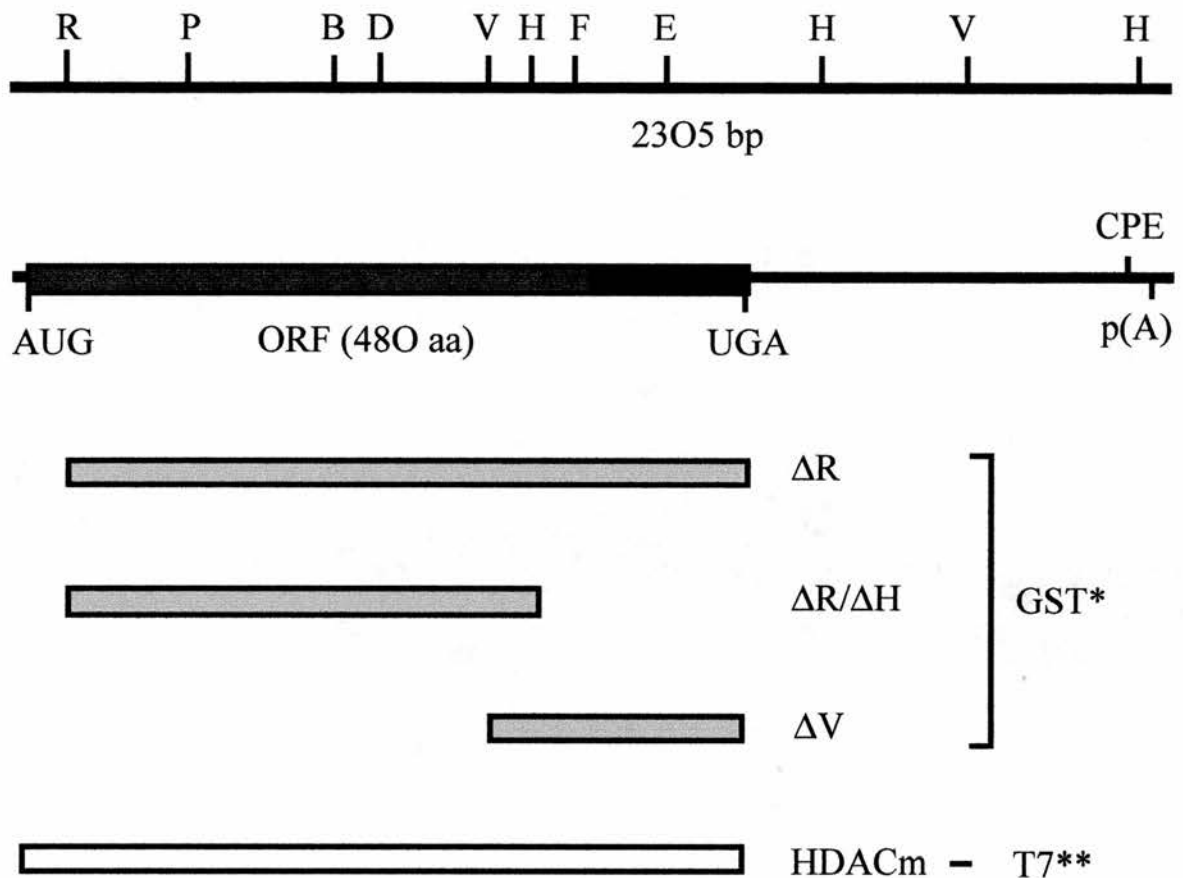
B



which HDACm activity must be the major component, is initiated *in vivo* only at MBT.

3.3. Expression of recombinant HDACm in oocytes

The experiments described so far have investigated the activity and distribution of endogenous HDACm. These experiments have demonstrated that endogenous histone deacetylase is a nuclear protein in both oocytes and early embryos. This enzyme has *in vitro* deacetylase activity. *In vivo* activity is only detectable after MBT with its accompanying transcriptional changes; HDAC activity cannot easily access the endogenous hyperacetylated chromatin present in transcriptionally active lampbrush chromosomes. HDACm would also appear to be post-translationally modified, with fatty-acylation anchoring the protein in the cytoplasm in smaller oocytes. To examine each of these features, and in light of the published work of Wong *et al* [160] that showed that histone deacetylase expressed from mRNA injected into the cytoplasm of *Xenopus* oocytes leads to strong repression of transcription from a DNA template injected into the nucleus, a number of epitope tagged clones and sub-clones were constructed from the original Ab21 clone (figure 36). The proteins resultant from expression of these clones allowed investigation of the individual properties of HDACm.



* ΔV is also available with an N-terminal GFP tag.

** HDACm is available with either an N-terminal T7 epitope tag or untagged in pBS vector.

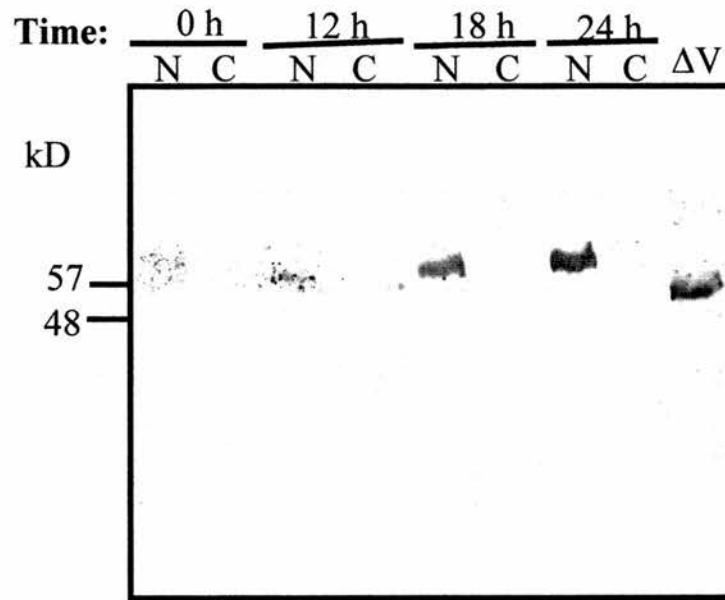
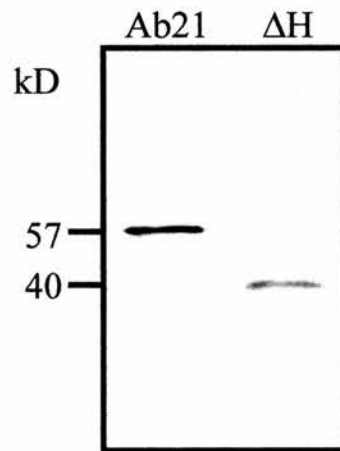
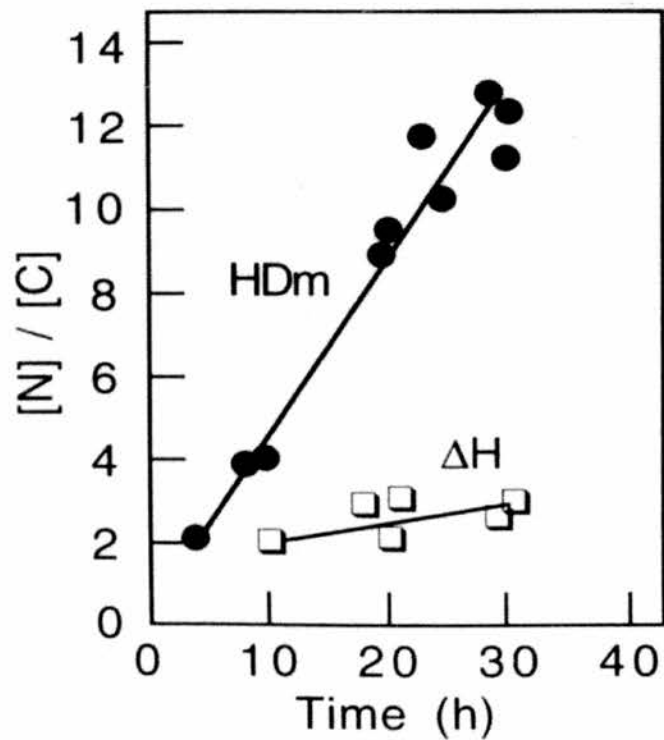
Figure 36. Map of Ab21 cDNA and its subclones. Restriction map of Ab21, the open reading frame and synthesized polypeptides (and their respective expression vectors). B, *BglIII*; D, *DraI*; E, *EaeI*; F, *FspI*; H, *HindIII*; P, *PstI*; R, *EcoRI*; V, *PvuII*. The open reading frame (ORF) consists of a conserved N-terminal region (cross-hatched) and a highly charged C-terminal region (filled). Subclones were used to produce glutathione S-transferase (GST) fusions and green fluorescent protein (GFP) fusions *in vivo* as indicated. A full length clone was used to produce Ab21 protein *in vitro* and a T7 HDACm fusion *in vivo* as indicated.

3.3.1. Injection of HDACm (Ab21) mRNA and protein.

The first property of HDACm to be investigated with these clones was that of post-translational modification of the enzyme by fatty-acylation. To test this idea attempts were made to induce this phenomenon by injecting Ab21 mRNA into the cytoplasm of stage IV oocytes. It was possible to follow the change in enzyme levels in the oocyte with time post-injection. The results of this experiment are shown in figure 37A. At zero time the level of detected protein reflects the amount of endogenous HDACm in the nucleus, by 24 hours post-mRNA injection the HDACm content of the nuclei is more than 10 times greater than normal, however HDACm is undetectable in the 63 kD form. Modification of translated protein could not be detected; this may be because the anchoring sites in the cytoplasm for modified enzyme to bind are already saturated by this point in oogenesis, or because the enzyme pathway involved in post-translationally modifying the protein are turned off by this point in oocyte development.

Injecting Ab21 fusion protein produced in the rabbit reticulocyte lysate system into mature oocytes produced similar results. Recombinant Ab21 protein and a truncated version lacking the carboxy-terminal domain (Δ H) were synthesised in reticulocyte lysate supplemented with ^{35}S -methionine to produce ^{35}S -labelled proteins (figure 37B) and injected into oocytes. Injection of the ^{35}S -labelled

Figure 37. Nuclear import of exogenous HDACm (Ab21 protein), using either Ab21 mRNA or protein expressed from mRNA in the rabbit reticulocyte lysate system. **(A)** Analysis of the levels of Ab21 protein in the nucleus and cytoplasm after cytoplasmically injecting oocytes with Ab21 mRNA. Samples were taken at 0, 12, 18 and 24 hours post injection and immunoblotted with anti-Cpep. Each track contains the equivalent of 2 ³⁵S-labelled cytoplasms or 10 ³⁵S-labelled nuclei. **(B)** Autoradiograph showing that ³⁵S-labelled Ab21 and its truncated form, ΔH, are substantially the only proteins synthesized from their respective RNA transcripts in the reticulocyte lysate system. **(C)** (Performed by J. Sommerville). Injection of ³⁵S-labelled recombinant proteins into the cytoplasm of stage V oocytes results in much higher levels of AB21 (filled circles) than Ab21ΔH (open squares) in the nucleus. Each point represents the nuclear:cytoplasmic ratio of concentration of radioactivity, [N]/[C], in a sample of five oocytes. Similar amounts of total radioactive protein were recovered from all samples injected with Ab21.

A**B****C**

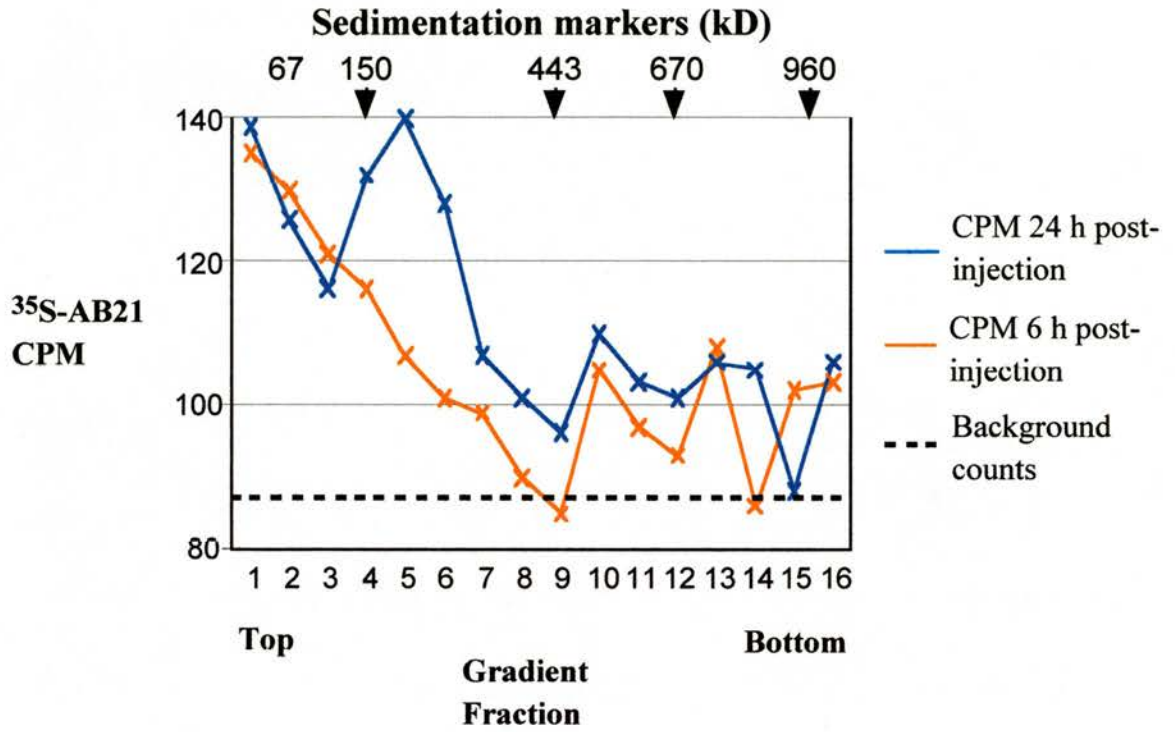
proteins into the cytoplasm of stage V oocytes resulted in a tenfold concentration of the protein in the nucleus after 24 hours, the kinetics of nuclear uptake being similar to those described for nucleoplasmin [116]. In contrast, ΔH failed to concentrate substantially in the nucleus, a result explained by the absence of the region containing a putative bipartite nuclear localisation signal (NLS) that shows a high degree of similarity to the NLS of *Xenopus* histone chaperone protein N1 (section 3.4). HDACm (Ab21) and ΔH synthesized in reticulocyte lysates were also assayed for enzyme activity, no activity was detected *in vitro* (results not shown). This suggests that HDACm is insufficient to generate activity; enzyme activity only being gained through association with other proteins.

Once in the nucleus, it has also been possible to investigate the interactions of this imported ^{35}S -Ab21 protein with other proteins in the nucleus. Nuclear extracts from stage V oocytes cytoplasmically injected with this recombinant protein were prepared at 6 hours and 24 hours after injection. These extracts were separated under near-physiological conditions by rate-zonal centrifugation. The clarified supernatants were loaded on linear 10%-30% glycerol gradients, which were centrifuged until the 19S marker approached the bottom of the tubes. The gradients were then fractionated and analysed for Ab21 content by measuring the amount of Ab21 present in each fraction (cpm). Post-injection nuclei

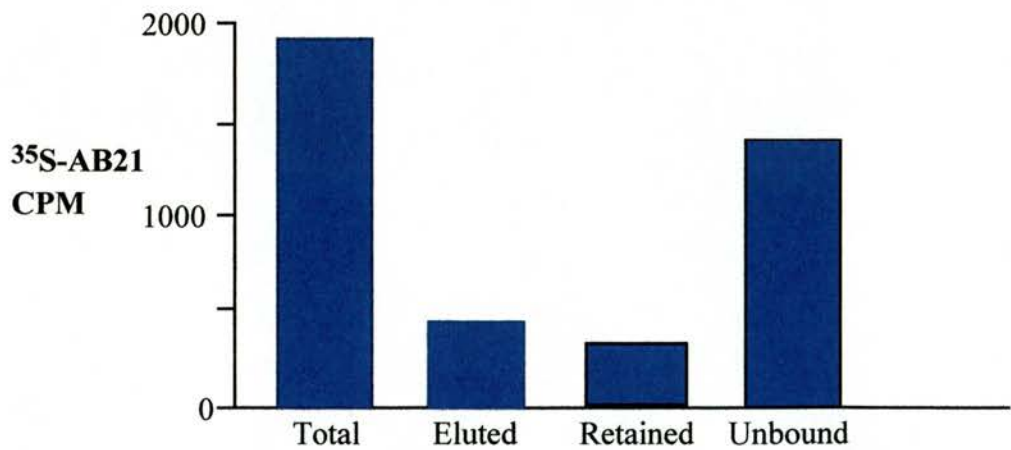
show Ab21 sedimenting over a broad range with peaks of approximately 60 kD after 6 hours and approximately 200 kD after 24 hours (figure 38A). The recombinant protein is beginning to accumulate in the nucleus 6 hours post injection and is present in soluble form, probably monomers of Ab21. 24 hours post injection, recombinant protein will be approaching peak levels in the nucleus (figure 37C) and is being incorporated into larger, multimolecular complexes. It is unlikely that the Ab21 found in the 200 kD particle 24 hours after injection consists of a tetramer of Ab21 protein. It is also possible that this protein may interact with the previously identified HDACm associated protein RbAp48. Immunoprecipitation of injected Ab21 from a nuclear extract with immobilized anti-RbAp48 antiserum was attempted to examine this possibility. The results indicate that this interaction is possible for at least some of the exogenous protein, as 40% of labelled protein was precipitated from the homogenate with anti-RbAp48 IgG immobilized on protein A Sephadex beads (figure 38B). The RbAp48 that exogenous HDACm interacts with is probably from a pool of free protein in the nucleus.

The effect of nuclear uptake of exogenous Ab21 on transcription was examined by John Sommerville by examining the level of transcription in injected oocytes. Non-injected oocytes and injected oocytes treated with TSA, continued to incorporate ³H-uridine into

Figure 38. Interactions of exogenous ^{35}S -labelled Ab21 protein (HDACm) in the oocyte. **(A)** Incorporation of exogenous labelled protein into protein complexes. Nuclei were isolated from oocytes injected with protein 6 hours and 24 hours post injection. 6 hours post injection, protein has entered the nucleus but is still soluble and not incorporated into larger complexes. 24 hours post injection, a great deal of the protein is still uncomplexed but a detectable proportion has become incorporated into larger complexes of approximate molecular mass 200 kD. **(B)** Immunoprecipitation of ^{35}S -labelled protein with immobilized anti-RbAp48. One quarter of the total labelled protein could be precipitated from the injected nuclei with the immobilized anti-RbAp48 IgG, demonstrating an interaction between the exogenous HDACm protein and endogenous RbAp48. Gradients were run with extracts equivalent to 50 nuclei isolated from injected oocytes, immunoprecipitations were also conducted with an extract equivalent to 50 nuclei isolated from injected oocytes. Measurements have been adjusted to take account of the background.

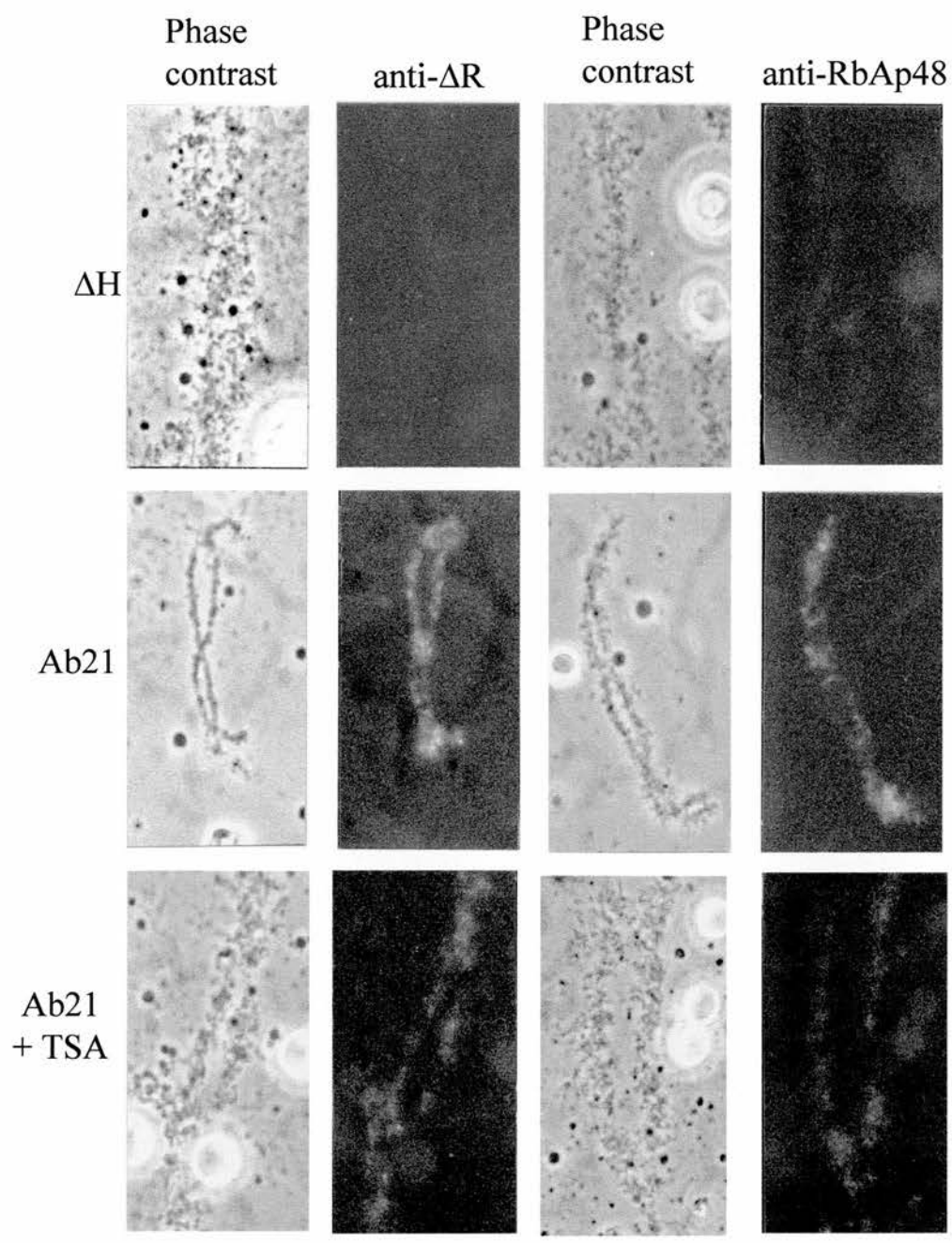
A**B**

Immunoprecipitation of ³⁵S labelled AB21 protein with immobilised anti-RbAp48



RNA up to 32 hours after injection, whilst non-treated oocytes injected with Ab21 failed to incorporate label much after 10 hours. By 10 hours after injection of Ab21, presumably sufficient *de novo* HDAC activity has accumulated in the nucleus to cause a run-down of RNA synthesis. Alternatively, the level of transcription in Ab21 injected oocytes could be analysed by observing their lampbrush chromosomes, the transcriptional activity of lampbrush chromosomes being related to the degree of loop extension from the axes of the chromosomes (figure 39). Lampbrush chromosomes from stage IV oocytes are not immunostained with any of the antibodies directed against HDACm or with anti-RbAp48, this situation is not changed by the injection of ΔH . Chromosomes isolated from oocytes 24 hour post-Ab21 injection are clearly immunostained with anti- ΔV . This immunostaining is not uniform throughout the chromatin, it shows reactive foci along the chromosome axes. These chromosomes also show extensive loop retraction and considerable foreshortening compared with chromosomes isolated from oocytes injected with ΔH . These changes are indicative of widespread inactivation of transcription. Incubation of oocytes injected with Ab21 protein with TSA (5 ng/ml) appears to inhibit loop retraction and chromosome condensation, whilst immunoreactivity remains. The immunostaining does seem fainter after treatment with TSA, however

Figure 39. Morphology and immunostaining of lampbrush chromosomes isolated from stage IV oocytes injected with recombinant proteins AB21 and AB21 Δ H. Oocytes were injected with similar amounts (approx. 10 pg) of recombinant protein. Chromosomes shown on the bottom row are representative of preparations made from injected oocytes treated with TSA. The various chromosome preparations were immunostained with either anti- Δ R (left-hand columns) or anti-RbAp48 (right-hand columns). Phase contrast partners of the immunofluorescent images are shown. Each panel shows a representative chromosomal bivalent. In the phase-contrast images, the chromosomes appear either extended, extending well out of the field shown, with fuzzy fringes of lateral loops (top and bottom rows), or contracted, contained within the field shown, with largely loop free chromomeric axes (middle row). The large refractile structures are nucleoli and the smaller, darker structures are snurposomes, neither of which show significant immunostaining. Preparations made by J. Sommerville



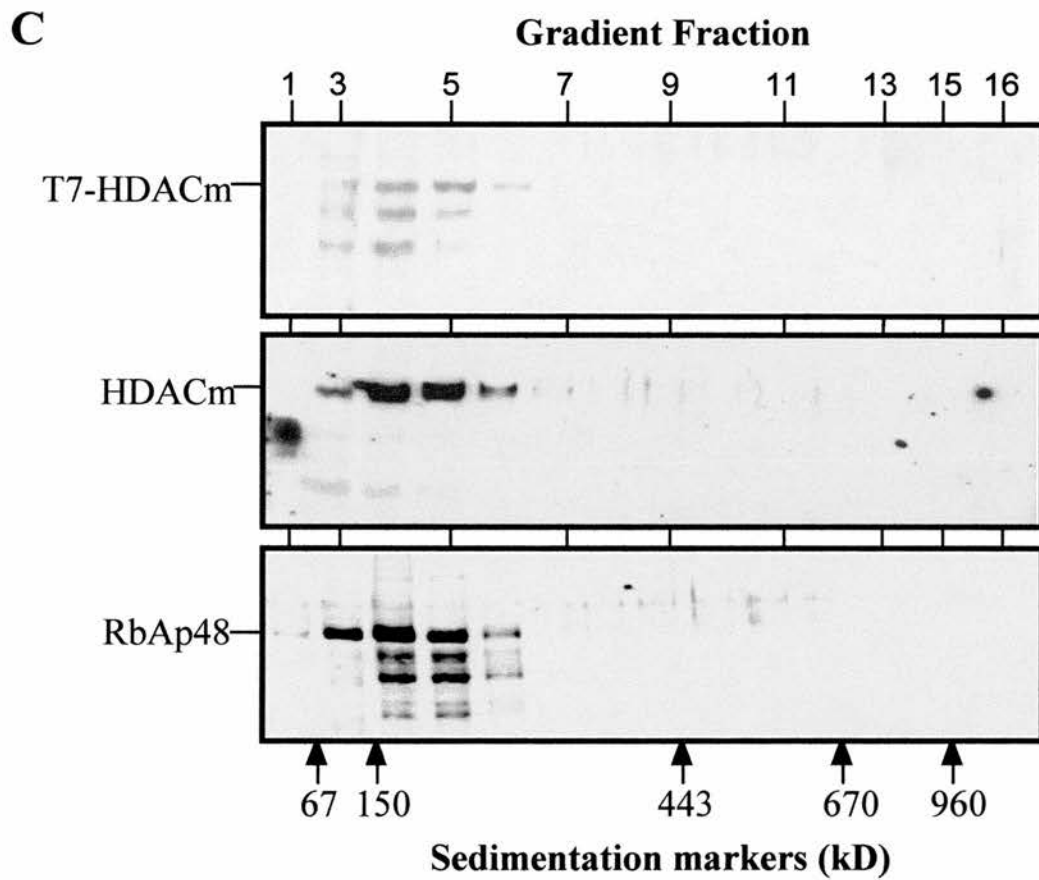
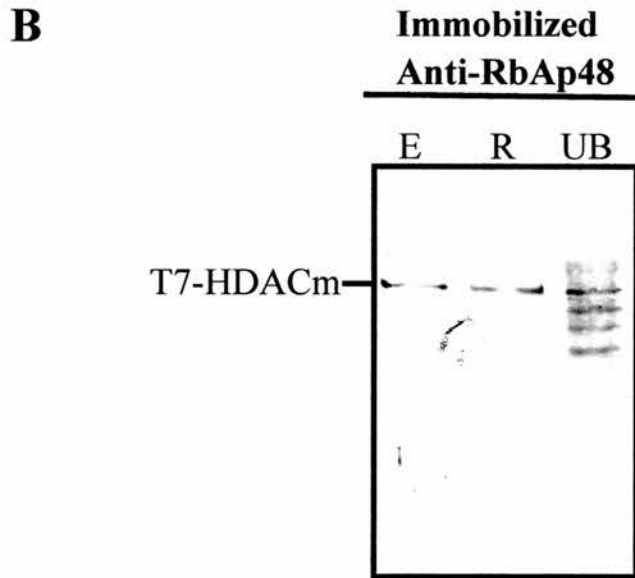
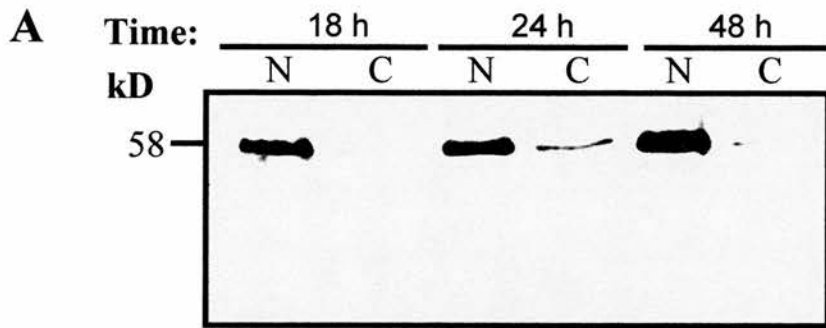
10 μm

this is probably due to the same amount of immunoreactive material being distributed over a larger surface area due to the lack of chromosome condensation. Since TSA is a highly specific inhibitor of HDAC activity in oocytes, it appears that the observed chromosome shortening is due to promiscuous activity of recombinant HDACm (Ab21). If exogenous HDACm is located on the chromosomes then it must be present in a complex as HDACm does not contain a DNA binding domain. Because the deacetylase complex contains RbAp48, a chromatin binding protein, this protein should also be detectable on the lampbrush chromosomes only after injection of Ab21. Anti-RbAp48 gives immunostaining patterns that are essentially the same as the pattern obtained with anti- ΔV . The chromosomes in non-injected oocytes are not immunoreactive, chromosomes in Ab21 injected oocytes are immunoreactive and condensed, whilst oocytes treated with TSA retain immunoreactivity but the signal is much fainter as the chromosomes are less condensed. These results are consistent with the idea that excess HDACm injected into oocytes is rapidly imported into the nucleus and associates with endogenous RbAp48. Protein complexes containing these two proteins are then free to interact with the chromatin of lampbrush chromosomes, resulting in premature loop retraction and chromosome condensation. This complex appears to have deacetylase activity, as indicated by its sensitivity to TSA.

3.3.2. Injection of T7 epitope tagged HDACm DNA

Injection of exogenous HDACm in the form of Ab21 message or recombinant protein is a useful tool but has one major drawback. Differentiation between endogenous and exogenous HDACm cannot be made using immunological techniques. To allow the study of the two populations by western blotting and immunostaining, the Ab21 cDNA was inserted into the pCGT plasmid. Injection of this plasmid into the oocyte nucleus allows the transcription of the insert as it is under the control of an eukaryotic (CMV) promoter. The gene product is a 58 kD protein with an amino terminal T7 tag that is detectable using a mouse monoclonal antibody. The product accumulates in the nucleus over time, although tiny amounts are detectable in the cytoplasm, in an unmodified form, 24 hours and 48 hours after injection (figure 40A). The T7-tagged protein also interacts with RbAp48; immobilized anti-RbAp48 IgG immunoprecipitated T7-Ab21 from a nuclear extract made from injected oocytes. However, only the full length product was precipitated by the immobilized antibody, degradation products of T7-Ab21 were left unbound (figure 40B). This degradation apparently removes the ability to bind endogenous RbAp48 from these proteins. Proteolysis probably takes place at the C-terminal of the protein, removing between 5 and 15 kD from the protein, because the degradation products retain their T7 tag. The site in HDACm through which it interacts with

Figure 40. Nuclear import of T7-Ab21 protein and its incorporation into protein complexes. **(A)** Analysis of the levels of T7-Ab21 protein in the nucleus and cytoplasm after injecting oocytes with pCGT7-Ab21 DNA. Samples were taken 18, 24 and 48 hours post injection. Each track contains the equivalent of 2 cytoplasm or 10 nuclei. **(B)** Nuclear extracts from stage VI oocytes injected with pCGT7-Ab21 DNA were incubated with anti-RbAp48 immobilised on protein A beads. Eluted (E), retained (R) and unbound (UB) fractions were immunoblotted with anti-T7. **(C)** Detection of T7-Ab21 protein, native HDACm and RbAP48 in an oocyte nuclear extract from stage VI oocytes injected with pCGT7-Ab21 DNA. Proteins in this extract were separated by rate sedimentation. The same fractions were immunoblotted with anti-T7, anti-Cpep and anti-RbAp48. The positions of sedimentation markers are indicated (kD). Gradient fractions probed with anti-T7 show that there is probably partial hydrolysis of this protein at some point in the process.



RbAp48 may be found in this region of the protein. As the largest degradation product has lost only the C-terminal 5 kD of protein, and with this the ability to interact with RbAp48, the binding site is likely to be found in this fraction of the protein.

Nuclear extracts from stage VI oocytes injected with the pCGT-Ab21 plasmid were prepared 24 hours after injection, these extracts were separated under near-physiological conditions by rate-zonal centrifugation. The clarified supernatants were loaded on linear 10%-30% glycerol gradients, which were centrifuged until the 19S marker approached the bottom of the tubes. The gradients were then fractionated and analysed for T7-Ab21, endogenous HDACm and RbAp48 by immunoblotting. Post-injection nuclei show all three proteins sedimenting over a fairly small range with a peak at approximately 200 kD (figure 40C). This is similar to the size of multimolecular complex detected for the ³⁵S-Ab21, but is significantly smaller than the size of complex in which the endogenous protein is normally detected (figure 22). Expression of exogenous protein appears to have disrupted the endogenous HDACm containing multimolecular complex, no HDACm containing particles with a molecular mass equivalent to 300 kD are detectable. This expression may even have disrupted the other complexes of which RbAp48 is a member as its sedimentation profile has also changed substantially.

The effects of this over-expression on enzyme activity and nuclear location of T7-Ab21 and RbAp48 have been studied by immunostaining hand-isolated nuclei and lampbrush chromosomes. Chromosomes isolated from oocytes 24 hours post injection are clearly immunostained with anti-T7. This immunostaining is not uniform throughout the chromatin. It shows reactive foci along the chromosome axes (figure 41). Overexpression of HDACm in the T7 tagged form can escape the restraints imposed on endogenous HDACm and can be seen to have deacetylase activity as it may result in premature loop retraction and chromosome condensation. However chromosome condensation does not occur in all injected oocytes, occasionally ectopic expression of T7-HDACm does not result in chromosome condensation (figure 41A(I)). Although the protein escapes the normal restraints and binds the lampbrush chromosomes, significant condensation is not seen. This may be because a threshold of activity has not been reached or there is a limited pool of some endogenous factor required for this phenomenon.

In an attempt to investigate the interaction of T7-Ab21 with RbAp48, advantage of having a mouse monoclonal antibodies directed against the T7 tag has been used to perform double labelling of the lampbrush chromosomes for this protein and RbAp48 or MeCP2 (figure 41A(ii)). Anti-RbAp48 gives an immunostaining pattern that is exactly the same as the punctate pattern obtained with anti-T7 (figure 41A).

A

kD

58



T7-Ab21

i

DAPI

anti-T7

Condensed
Chromosome



Uncondensed
Chromosome

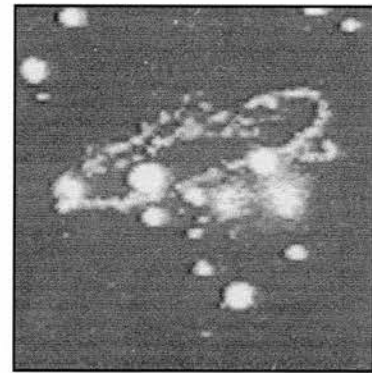
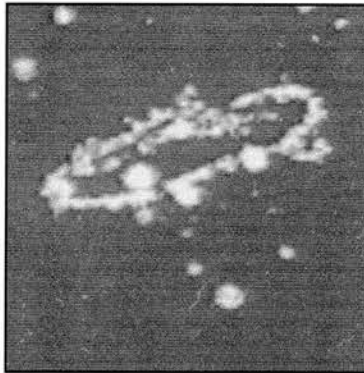


10 μ m

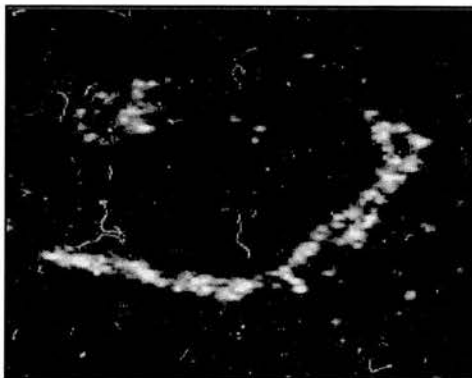
ii

anti-T7

anti-
RbAp48



anti-
MeCP2



10 μ m

B

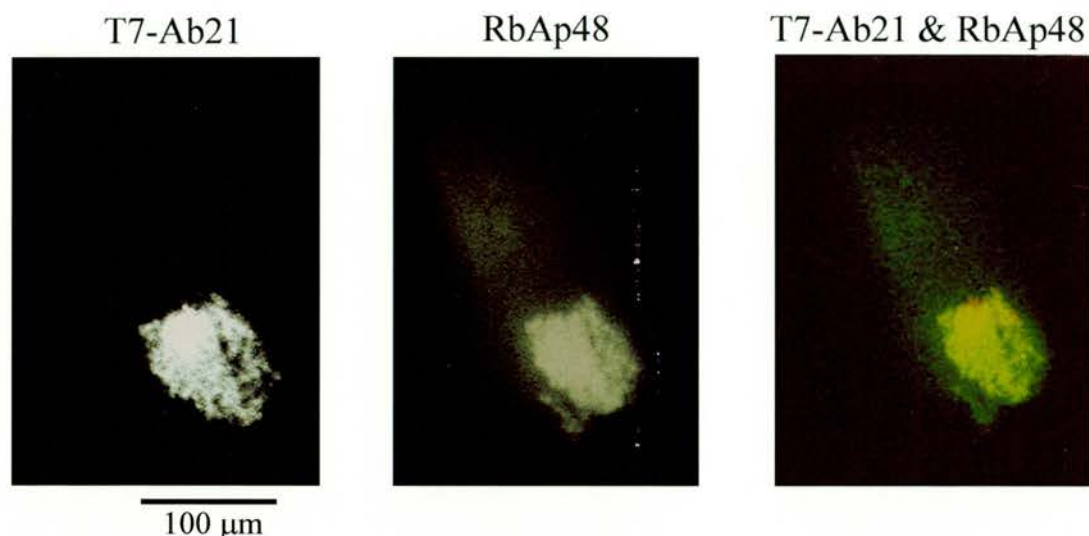


Figure 41. Nuclear location of T7–Ab21 protein. Expression of the correct protein is confirmed in an oocyte extract. **(A)** Morphology and immunostaining of lampbrush chromosomes isolated from stage IV oocytes injected with pCGT7–Ab21 DNA. **(i)** Ectopically expressed HDACm escapes the restraints imposed on endogenous protein and can bind chromatin. Binding can result in chromosome condensation (top row). However, just as frequently T7–HDACm can bind lampbrush chromosomes and not result in condensation (bottom row). **(ii)** The top row of chromosomes shows a representative chromosomal bivalent immunostained with anti-RbAp48 (FITC anti-rabbit 2°) and anti-T7 (TRITC anti-mouse 2°). The bottom row shows a representative chromosomal bivalent immunostained with anti-MeCP2 (FITC anti-rabbit 2°) and anti-T7 (TRITC anti-mouse 2°). The images were viewed through a dual channel confocal microscope. **(B)** Hand isolated nuclei viewed by confocal microscopy. Nuclei, of oocytes injected with pCGT7–Ab21, isolated under oil from stage VI oocytes, were fixed and immunostained with anti-RbAp48 (FITC anti-rabbit 2°) and anti-T7 (TRITC anti-mouse 2°). The optical sections and merged image shown are representative of several images seen through the approximate centre of the nuclei, at the optical level of the chromatin.

The chromosomes in T7-Ab21 injected oocytes are immunoreactive and condensed, consistent with the idea that excess HDACm injected into oocytes is rapidly imported into the nucleus and associates with endogenous RbAp48. As a control these same chromosomes were immunostained with anti-MeCP2. MeCP2 is a nuclear protein and is known to bind DNA [105,106]. Anti-MeCP2 gives an immunostaining pattern that is different to that observed with both anti-T7-Ab21 and anti-RbAp48. The chromosomes from T7-Ab21 injected oocytes are immunoreactive with anti-MeCP2, however the immunostaining is much more dispersed and is strictly restricted to the axes of the chromosome only. The effects of immunostaining hand isolated whole-mount nuclei with anti-T7 and anti-RbAp48 are presented in figure 41B. In non-injected oocyte nuclei HDACm is located around the internal margins of the nucleus, much the same as the situation with RbAp48 (figure 22D). These proteins are stored away from the chromatin. T7-Ab21 appears to be located on the chromatin, well within the oocyte nucleus, a different situation to that of endogenous HDACm. The nuclear location of RbAp48 is also altered remarkably in pCGT-Ab21 injected oocytes. This protein appears to have moved away from the nuclear periphery and followed exogenous deacetylase onto the chromatin, it is found with a distribution similar to that of T7-Ab21 (figure 41B).

These results indicate that exogenous HDACm can interact with endogenous RbAp48. This interaction may involve the C-terminal of the exogenous deacetylase and together these proteins are incorporated into a multimolecular complex with a molecular mass of approximately 200 kD. This multimolecular complex can bind chromatin and demonstrates changes to chromosomes associated with histone deacetylase activity.

3.3.3. Injection of DNA and protein from Ab21 sub-clones

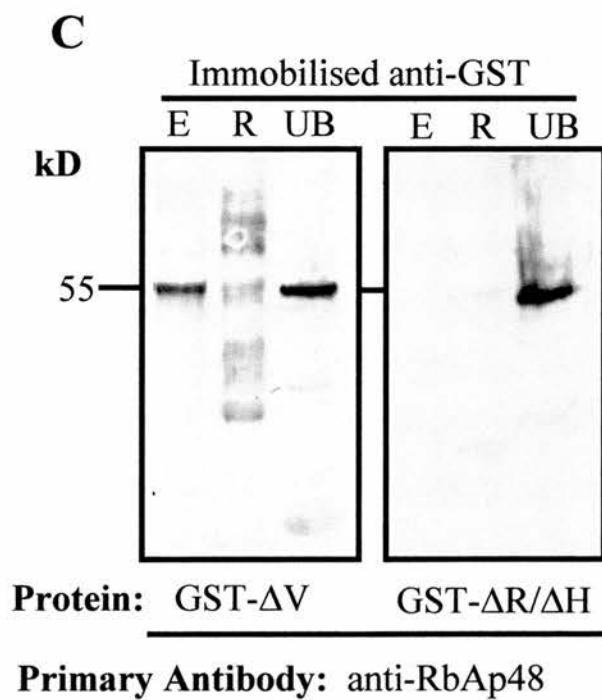
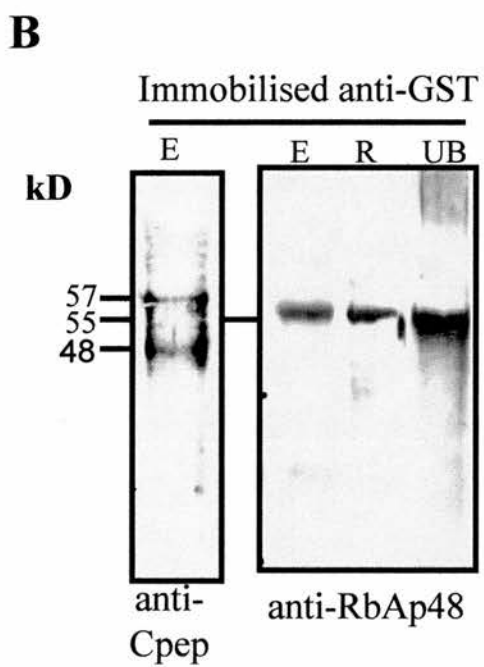
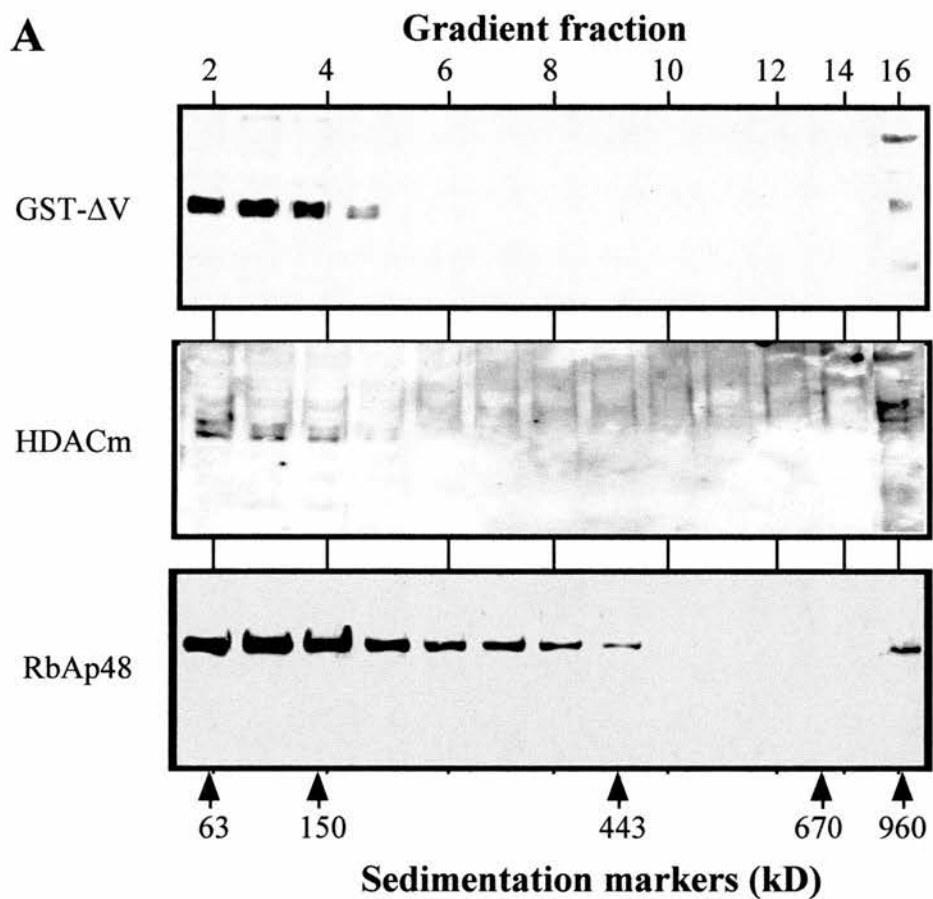
Studying whole length exogenous HDACm, either as Ab21 protein or as a T7 tagged protein is very useful as a method of investigating the protein as a whole. However, results presented above indicate that the variable region at the carboxy terminus of HDACm controls some of the *in vivo* functions of the protein, excluding activity [60]. To study the function of each portion of the HDACm protein, Dr. M. Lodomery constructed a series of GST tagged sub-clones; these are shown in figure 36. Cytoplasmic injection of GST- ΔV and GST- $\Delta R/\Delta H$, followed by immunoblotting hand isolated nuclei and cytoplasms taken at 12 hour time points post injection indicated that GST- ΔV accumulates in the nucleus with time, whilst GST- $\Delta R/\Delta H$ was retained in the cytoplasm. This result is similar to that produced by the

injection of Δ H recombinant protein into oocytes described in section 3.3.1. Experiments performed by Dr. A. Llinas with GST- Δ V and its truncated form, GST- Δ V-5, that has lost 5kD from the C-terminal of this fusion have confirmed that the amino acid sequence necessary for nuclear uptake is located in this terminal 5 kD region [161]. This region contains a sequence similar to the bipartite NLS found in nuclear chaperone N1 (section 3.4.2). Upon injection of the two fusion proteins, the GST- Δ V was imported into the nucleus but GST- Δ V-5 was not. The rate of nuclear uptake of GST- Δ V was reported to be further enhanced by the *in vitro* phosphorylation of the fusion protein with a cytoplasmic CK2 extract prior to injection.

Because GST- Δ V is rapidly imported into the nucleus it was desirable to examine its nuclear location, association with endogenous proteins and whether it could be incorporated into multimolecular complexes. Nuclear extracts from stage VI oocytes injected with bacterially expressed GST- Δ V were prepared 24 hours after injection, these extracts were separated under near-physiological conditions by rate-zonal centrifugation. The clarified supernatants were loaded on linear 10%-30% glycerol gradients, which were centrifuged until the 19S marker approached the bottom of the tubes. The gradients were then fractionated and the sedimentation of GST- Δ V, endogenous

HDACm and RbAp48 were analysed by immunoblotting (figure 42). Post-injection nuclei show the majority of all three proteins sedimenting over a small range with a peak at approximately 200 kD (figure 42A). This is similar to the size of multimolecular complex detected for the ³⁵S-Ab21 and T7-AB21, but is different from the size of complex in which the endogenous protein is normally detected (figure 22). Injection of this fusion protein appears also to have disrupted the endogenous HDACm containing multimolecular complex, no HDACm containing particles with a molecular mass equivalent to 300 kD are detectable. However, unlike the gradient analysis of injected ³²S-Ab21 protein and the T7-Ab21 plasmid, the GST-ΔV gradient series shows that a significant fraction of each protein investigated pellets, as does the chromatin. This is the first indication we have from gradient analysis of exogenous histone deacetylase and endogenous enzyme associating with the chromatin. A second difference between this series of gradients and that produced with the T7-Ab21 plasmid is that disruption of the RbAp48 profile is incomplete. This may be because there was less GST-ΔV protein injected into the oocytes than the T7-Ab21 plasmid produced in 24 hours, however this is unlikely because T7-Ab21 plasmid expressed at a low level. An alternative explanation could be that there are two RbAp48 binding sites in HDACm as suggested by Vermaak *et al* [152], only one of which is present in GST-

Figure 42. Nuclear import of GST- ΔV protein and its incorporation into protein complexes. **(A)** Detection of GST- ΔV fusion protein, native HDACm and RbAp48 in an oocyte nuclear extract from stage VI oocytes cytoplasmically injected with fusion protein. Proteins in this extract were separated by rate sedimentation. The same fractions were immunoblotted with anti-GST2 antibodies, anti-Cpep and anti-RbAp48. The positions of sedimentation markers are indicated (kD). **(B)** Nuclear extracts from stage VI oocytes cytoplasmically injected with GST- ΔV fusion protein were incubated with anti-GST immobilised on protein A beads. Eluted (E), retained (R) and unbound (UB) fractions were immunoblotted with anti-RbAp48. In a further experiment, the eluted fraction was reprobbed with anti-Cpep. **(C)** Nuclear extracts from stage VI oocytes were mixed *in vitro* with either GST- ΔV or GST- $\Delta R/\Delta H$. The mixture was then incubated with anti-GST immobilised on protein A beads. Eluted (E), retained (R) and unbound (UB) fractions from both mixtures were immunoblotted with anti-RbAp48.



ΔV . If RbAp48 binding is a matter of direct competition, the reduction in the number of RbAp48 binding sites in exogenous GST- ΔV would mean there is less competition for the RbAp48, explaining the incomplete disruption of RbAp48 containing complexes.

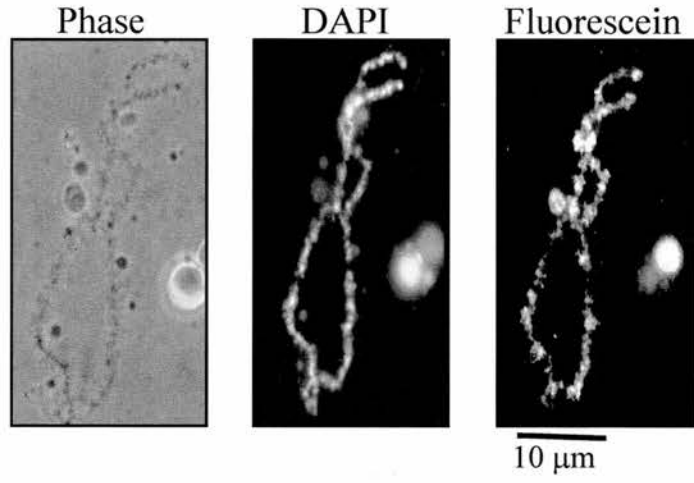
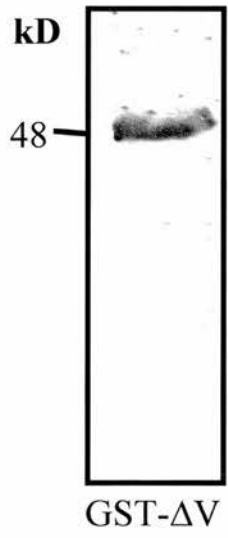
To investigate the association of GST- ΔV protein with endogenous RbAp48 a number of immunoprecipitations were performed (figure 42). Initially, immunoprecipitation from a nuclear homogenate made from stage VI oocytes injected with GST- ΔV protein was performed with immobilized anti-GST monoclonal antibodies. This antibody precipitated the fusion protein and RbAp48 (figure 42B). However, the immobilized anti-GST did not just precipitate the fusion protein and RbAp48; reprobing the eluted fraction with anti-Cpep IgG resulted in the detection of two immunoreactive bands in the immunoprecipitate (figure 42B). The faster migrating of these two bands corresponds in size to the GST fusion protein, the slower migrating immunoreactive band has a size consistent with endogenous HDACm. Further immunoprecipitations were performed *in vitro* with the two fusion proteins GST- ΔV and GST- $\Delta R/\Delta H$. These proteins were immobilized on anti-GST beads before being incubated in a nuclear homogenate made from nuclei hand isolated from stage VI oocytes. Immunoblotting the eluted bound and unbound fraction of this

experiment demonstrates the ability of GST- ΔV to bind RbAp48 *in vitro* as well as *in vivo*. It also confirms that the site through which interaction with RbAp48 is achieved is located in the C-terminal region of HDACm as GST- $\Delta R/\Delta H$ could not precipitate RbAp48 (figure 42C). This experiment had to be performed *in vitro* as cytoplasmically injected GST- $\Delta R/\Delta H$ does not enter the oocyte nucleus.

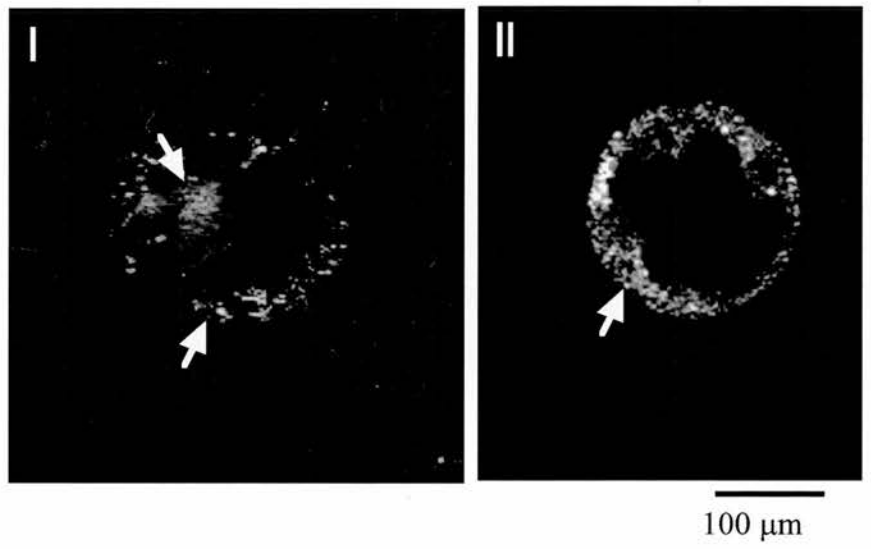
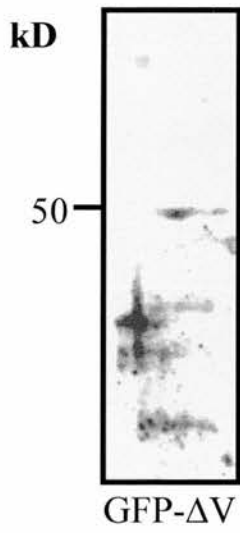
The effects of ΔV fusion proteins on enzyme activity have been studied by immunostaining lampbrush chromosomes. The nuclear location of imported ΔV has been studied by expressing GFP plasmid containing the ΔV insert in large oocytes. The product of expression from this plasmid is the ΔV protein with an N-terminal green fluorescent protein (GFP) tag. Chromosomes isolated from oocytes 24 hours post injection of GST- ΔV are immunostained with anti-GST antibody. This fluorescent staining is not uniform throughout the chromatin; like T7-tagged HDACm, it shows reactive foci along the chromosome axes. The chromosomes also show extensive loop retraction and considerable foreshortening (figure 43A). Loop retraction and chromosome foreshortening has been postulated at the result of HDAC activity. However GST- ΔV has no activity itself, this sub-clone does not contain the active site. Nuclear uptake of this protein and its incorporation into multimolecular complexes with both RbAp48 and

Figure 43. Nuclear location of GST- Δ V and GFP- Δ V fusion proteins. **(A)** Morphology and immunostaining of lampbrush chromosomes isolated from stage IV oocytes injected with GST- Δ V fusion protein. The panel shows a representative chromosomal bivalent. In the phase contrast image, the chromosome appears contracted and is contained within the field shown, with largely loop-free chromomeric axes. The DAPI image shows the DNA in the chromosome, whilst the immunostained image (using anti-GST) shows GST- Δ V going onto the chromosomes. **(B)** Hand isolated nuclei viewed by confocal microscopy of oocytes injected with GFP- Δ V. Nuclei were isolated under oil and viewed immediately. the fluorescent image is provided by the natural fluorescence of the GFP tag. The optical section shown are representative of several images seen through the nuclei (i) passing through the nucleus and chromatin, or (ii) through the nucleus away from the chromatin. Immunoblots, using anti-GST or anti-GFP, of tracks containing the equivalent of 10 nuclei from injected oocytes confirm the correct protein is present and is detectable.

A



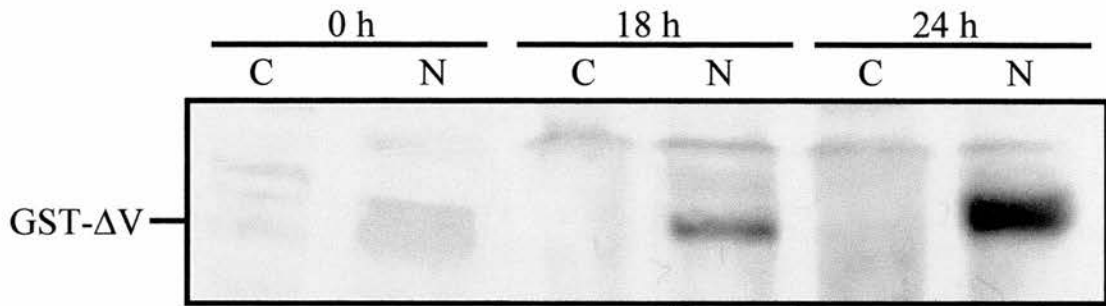
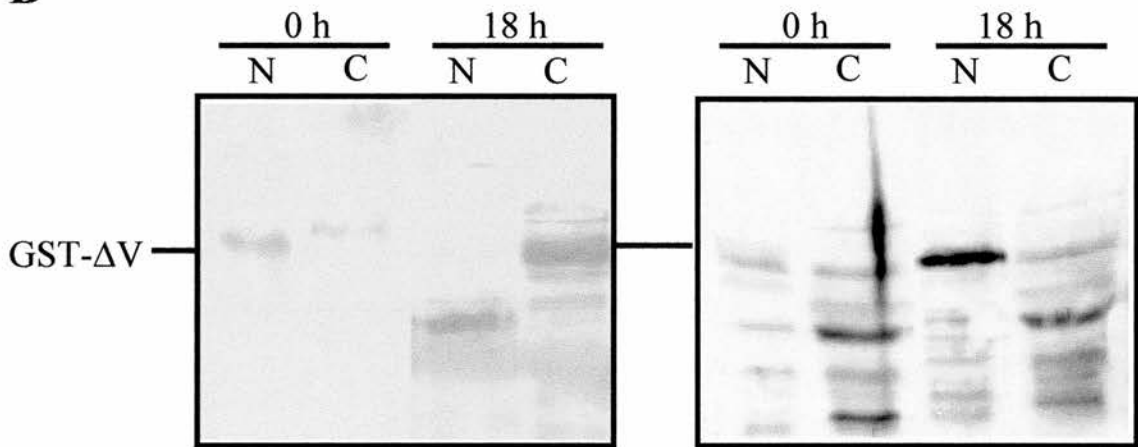
B



endogenous HDACm may allow the endogenous enzyme to overcome the normal constraints and leads to premature condensation of the lampbrush chromosomes.

The fluorescence of GFP- ΔV injected oocyte nuclei has been studied further by confocal laser microscopy (figure 43B). The advantage of this technique is that nuclei can be isolated and viewed in oil, there is no need to fix the nuclei, and this avoids all the artefacts that may be associated with fixing and immunostaining material. GFP- ΔV is found in two locations in the nucleus; at the nuclear periphery and in the centre of the nucleus, presumably in association with the chromatin. This is a combination of the locations at which endogenous enzyme (figure 22) and T7-tagged enzyme (figure 40) are found.

Nuclear import of GST- ΔV is not a simple process. This fusion protein does contain an NLS (section 3.4.2), but this alone is not enough to promote import. A well known nuclear transport protein is α -importin (appendix E), this protein has been demonstrated to bind GST- ΔV by Dr. A. Llinas (see section 3.4.1). However, it was not known if this protein was essential for nuclear import. To study the dependency of GST- ΔV on α -importin for nuclear import, the cytoplasms of stage VI oocytes were co-injected with GST- ΔV and anti- α -importin serum. The effects of this serum upon nuclear import are shown in figure 44.

A**B**

| | | |
|-----------------------|----------|----------|
| GST-ΔV: | + | + |
| anti-importin: | + | - |
| anti-p54: | - | + |

Figure 44. Nuclear import of GST-ΔV is dependent upon importin- α . **(A)** Cytoplasmically injected GST-ΔV accumulates in the oocyte nucleus over time. **(B)** Unlike the situation in **(A)**, cytoplasmically injected GST-ΔV is inhibited from accumulating in the nucleus if anti- α importin serum is co-injected with the fusion protein. This effect is not repeated if anti-p54 (RNA helicase) serum is co-injected with the fusion protein. Samples were taken 0 hours, 18 hours and 24 hours post injection. Each track is loaded with the protein equivalent of 2 cytoplasms or 10 nuclei.

Co-injection of GST- ΔV and anti-importin- α serum impedes nuclear import of GST- ΔV . Co-injection of GST- ΔV and an unrelated antibody raised against the RNA helicase Xp54 [162] had no effect upon the rate of nuclear import of GST- ΔV . Nuclear import of GST- ΔV appears to be dependent upon importin- α and the bipartite NLS, as such its import can be classified as following the “classical” pathway [163].

3.4. Phosphorylation of HDACm

Results presented so far indicate that HDACm can be phosphorylated. Alkaline phosphatase treatment of an oocyte extract reduces HDACm activity *in vitro* (figure 25D) and HDACm immunoprecipitated from mid-blastula embryos can be found in a phosphorylated form. The effect of alkaline phosphatase treatment on enzyme activity may be through the dephosphorylation of protein partners in the HDACm multimolecular complex. However, analysis of the primary structure of HDACm and other observations indicate that protein phosphorylation plays an important role in regulation of the enzyme subunit itself.

In the nuclei of large oocytes, HDACm is found in modified forms; four isoforms of this protein are observable (figure 45A). Incubation of stage VI oocytes with progesterone induces oocyte

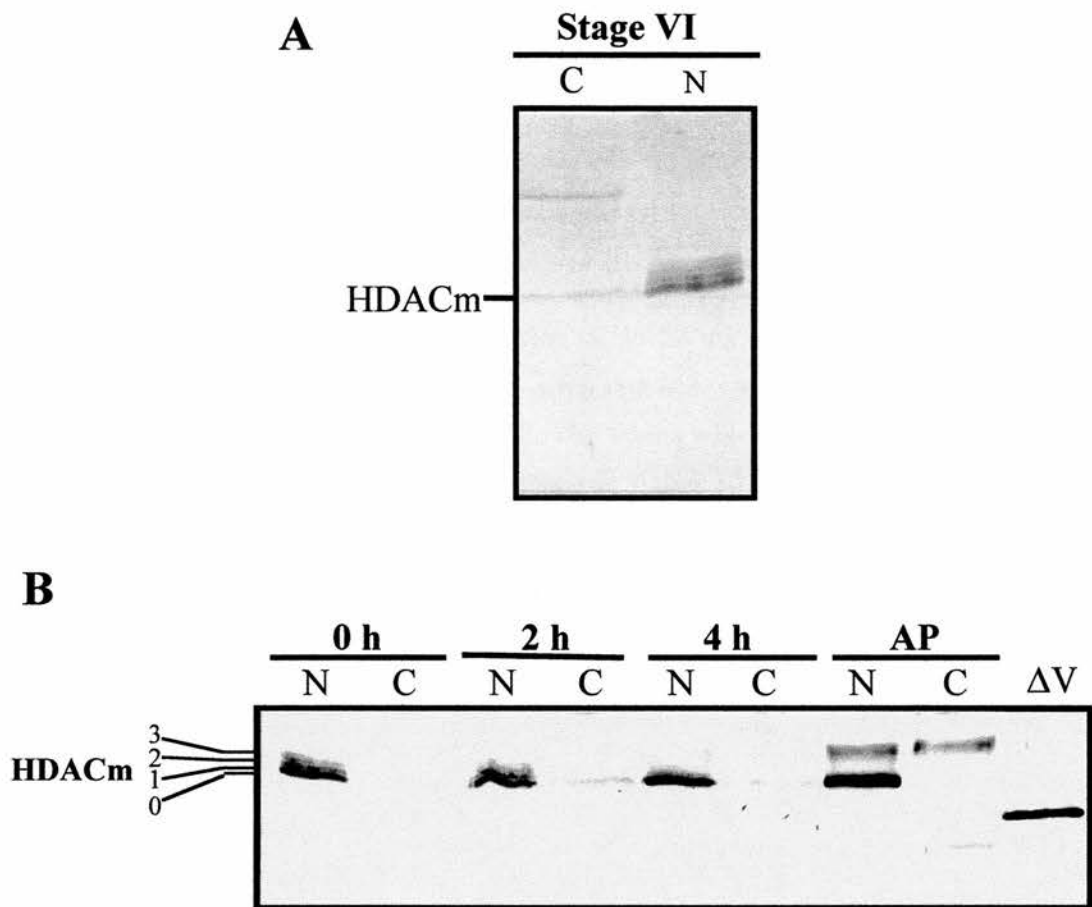


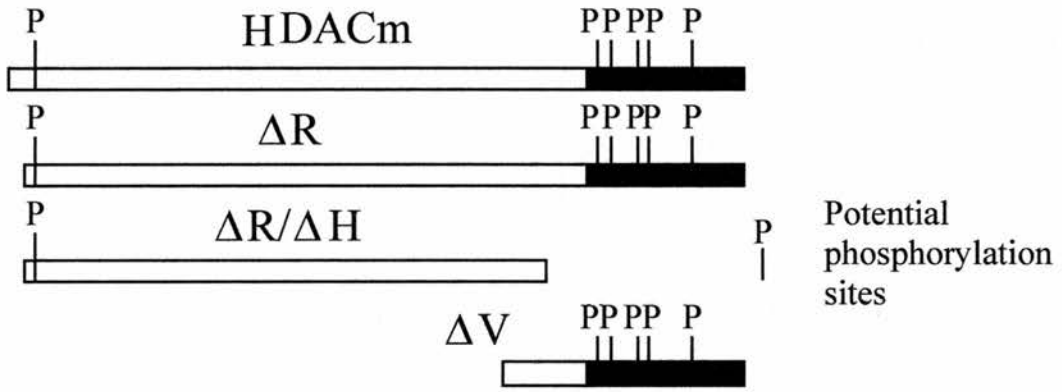
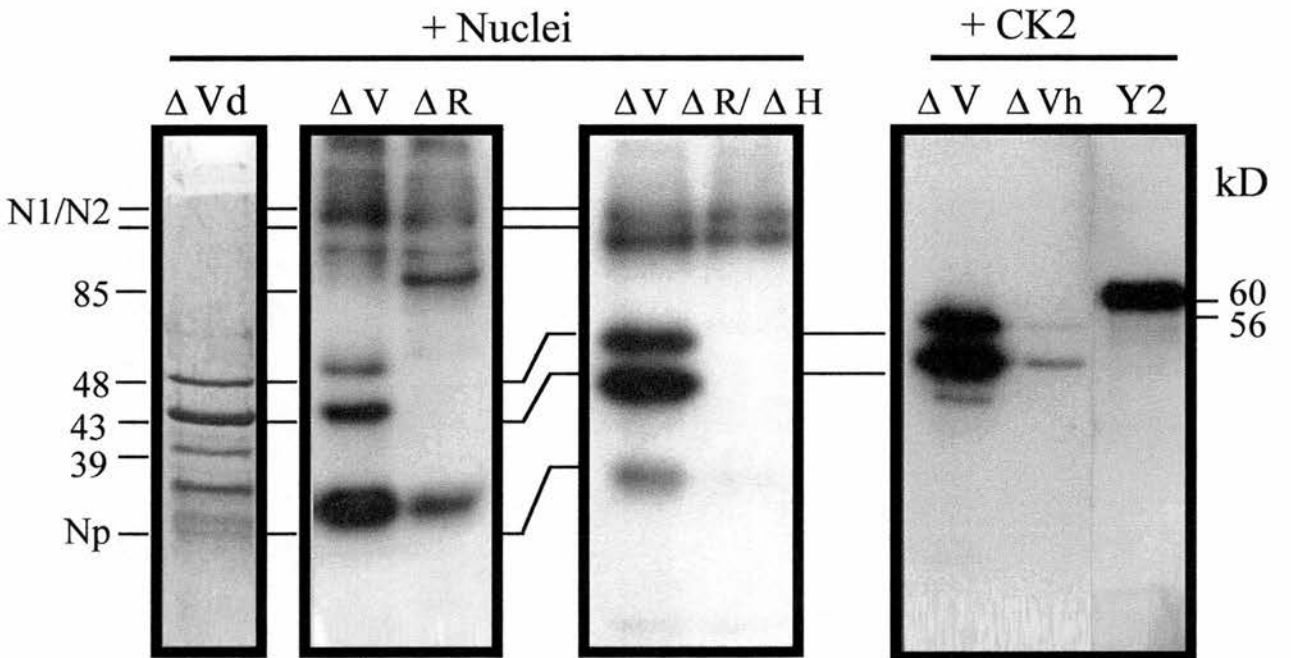
Figure 45. HDACm is phosphorylated in the nucleus of large oocytes, it is dephosphorylated as the oocyte matures in response to progesterone. **(A)** Immunoblot of nuclei and cytoplasm from stage VI oocytes. A number of isoforms of HDACm are present in the nuclei of stage VI oocytes. **(B)** Immunoblot showing isoforms of HDACm present in nuclei isolated from stage VI oocytes after treatment of oocytes with progesterone or alkaline phosphatase (AP). Oocytes were treated with 2 $\mu\text{g/ml}$ progesterone for 0, 2 and 4 hours before hand isolation of nuclei or isolated nuclei were treated with 1 IU phosphatase for 30 minutes at room temperature. Each track contains the protein equivalent of 10 nuclei or 2 cytoplasm.

maturation and resumption of meiosis I, it also reduces the number of detectable isoforms and the distribution of protein between them prior to breakdown of the geminal vesicle (figure 45B). As the oocyte matures, more material accumulates in the fastest migrating isoform. After 4 hours of incubation in progesterone almost all HDACm is in this single form, the slower migrating isoforms are no longer detectable. This phenomenon can be reproduced *in vitro* by incubating isolated nuclei from large oocytes in alkaline phosphatase. Incubation with alkaline phosphatase (0.1 IU/ μ l) for 30 minutes at room temperature shifts all HDACm protein into the fastest migrating isoform that resolves with an apparent molecular weight of 57 kD (figure 45B).

Analysis of the primary structure of this protein detects six regions that show a degree of similarity to consensus CK2 phosphorylation sites (S/T X X D/E). One of these sites is located near to the N-terminus of the protein, the five other sites are located in the C-terminal domain (figure 46A). Phosphorylation of GST fusion proteins $-\Delta R$, $-\Delta R/\Delta H$ and $-\Delta V$ was performed by Dr. A. Llinas [161]. The results of *in vitro* phosphorylation of GST fusion proteins $-\Delta R$, $-\Delta R/\Delta H$ and $-\Delta V$ with a nuclear CK2 extract and ^{32}P -ATP are shown in figure 45B. These fusion proteins contain: the entire protein excluding the N-terminal 5 kD (GST- ΔR – 85 kD), the majority of the N-terminus and

Figure 46. *In vitro* phosphorylation of HDACm fusion proteins. **(A)** Graphical representation of HDACm fusion proteins GST- Δ R, GST- Δ R/ Δ H and GST- Δ V showing varying lengths of HDACm and varying numbers of potential CK2 phosphorylation sites. **(B)** Autoradiograph showing the *in vitro* phosphorylation of HDACm GST fusion proteins by protein kinase CK2 with 32 P-ATP. This figure was prepared by Dr. A. Llinas. In the first five columns fusion protein was phosphorylated with a nuclear homogenate containing CK2. The GST- Δ Vd (degradation) track shows GST- Δ V phosphorylates under these conditions, as do breakdown products of the fusion protein at 43 and 39 kD. The second and third tracks contained GST- Δ V and GST- Δ R. The phosphorylation pattern shows that under these conditions there is efficient phosphorylation of fusion proteins containing the carboxy tail domain. The fourth and fifth tracks compare the level of phosphorylation of GST- Δ V with GST- Δ R/ Δ H and show that fusion proteins lacking the C-terminal phosphorylation sites do not get phosphorylated *in vitro*. N1/N2 and nucleoplasmin are also phosphorylated by protein kinase CK2 and 32 P-ATP under these conditions as they are present in the nuclear homogenate.

The material in columns 5-8 was phosphorylated using purified CK2. The GST- Δ V tracks show that a purified CK2 extract can phosphorylate GST- Δ V as well as the nuclear homogenate but that this phosphorylation is inhibited by the specific CK2 inhibitor heparin (h). A good control to indicate that phosphorylation is occurring by the action of CK2. As a second control, phosphorylation of the Y-box proteins FRGY2a/b with the CK2 extract was also investigated. These proteins only contain CK2 phosphorylation sites and are phosphorylated efficiently in this assay. This results supports the finding of the previous experiment i.e phosphorylation is most likely occurring through the action of CK2.

A**B**

the catalytic core (GST- Δ R/ Δ H – 60 kD) or the charged tail domain (GST- Δ V – 48 kD). GST- Δ R contains all 6 potential phosphorylation sites, GST- Δ R/ Δ H contains the N-terminal phosphorylation site only, whilst GST- Δ V contains the 5 C-terminal phosphorylation sites only.

Phosphorylation of GST- Δ V shows a number of bands, the largest at 48 kD (full length protein) plus others at 43 kD and 39 kD (figure 46B). These smaller proteins are the result of limited proteolysis from the C-terminal of the fusion protein. The 43 kD product is phosphorylated just as efficiently as the 48 kD protein, this means that the major phosphorylation sites lie beyond 5 kD from the C-terminus. Phosphorylation of GST- Δ R results in the detection of an 85 kD labelled protein, whereas GST- Δ R/ Δ H is not phospholabelled (figure 46B). Thus the N-terminal phosphorylation site is not phosphorylated *in vitro*. A number of other phosphoproteins are detected in these autoradiograph; the histone chaperones N1/N2 are detectable at 120/115 kD and nucleoplasmin is detectable at 35 kD, these act as useful internal size markers. There was no significant difference seen in the pattern of phosphorylation when using either a nuclear extract or CK2 activity isolated by affinity chromatography, apart from the presence of endogenous substrates. Kinase activity from both extracts was inhibited

by low concentrations of heparin and also showed activity towards the known CK2 substrate, FRGY2a/b.

Mapping of the CK2 sites in GST- ΔV that are phosphorylated *in vitro* was also performed by Dr. A. Llinas in collaboration with Dr. G. Kemp, the results are shown in figure 47. GST fusion - ΔV was phosphorylated using isolated CK2 and ^{32}P -ATP. The labelled protein was then digested with trypsin and the fragments were separated by fine-bore HPLC. The radiolabelled peptides were then sequenced. The results indicate that only three of the five C-terminal phosphorylation sites are phosphorylated *in vitro*, the detected phosphorylation sites are serines at positions 393, 421 and 423 of HDACm.

3.4.1. GST- ΔV phosphorylation, nuclear import and α -importin.

One feature of HDACm that is shared with the human and *Drosophila* homologues HDAC1 and RPD3, is the charged C-terminal domain. This domain contains the CK2 phosphorylation sites and a sequence similar to the bipartite nuclear localization site signal (NLS) which is contained in the *Xenopus* nuclear protein N1/N2 [164]. This sequence similarity may have biological significance because the two proteins have related function. HDACm deacetylates histone H4, whilst N1/N2 chaperones diacetylated histone H4 prior to incorporation into

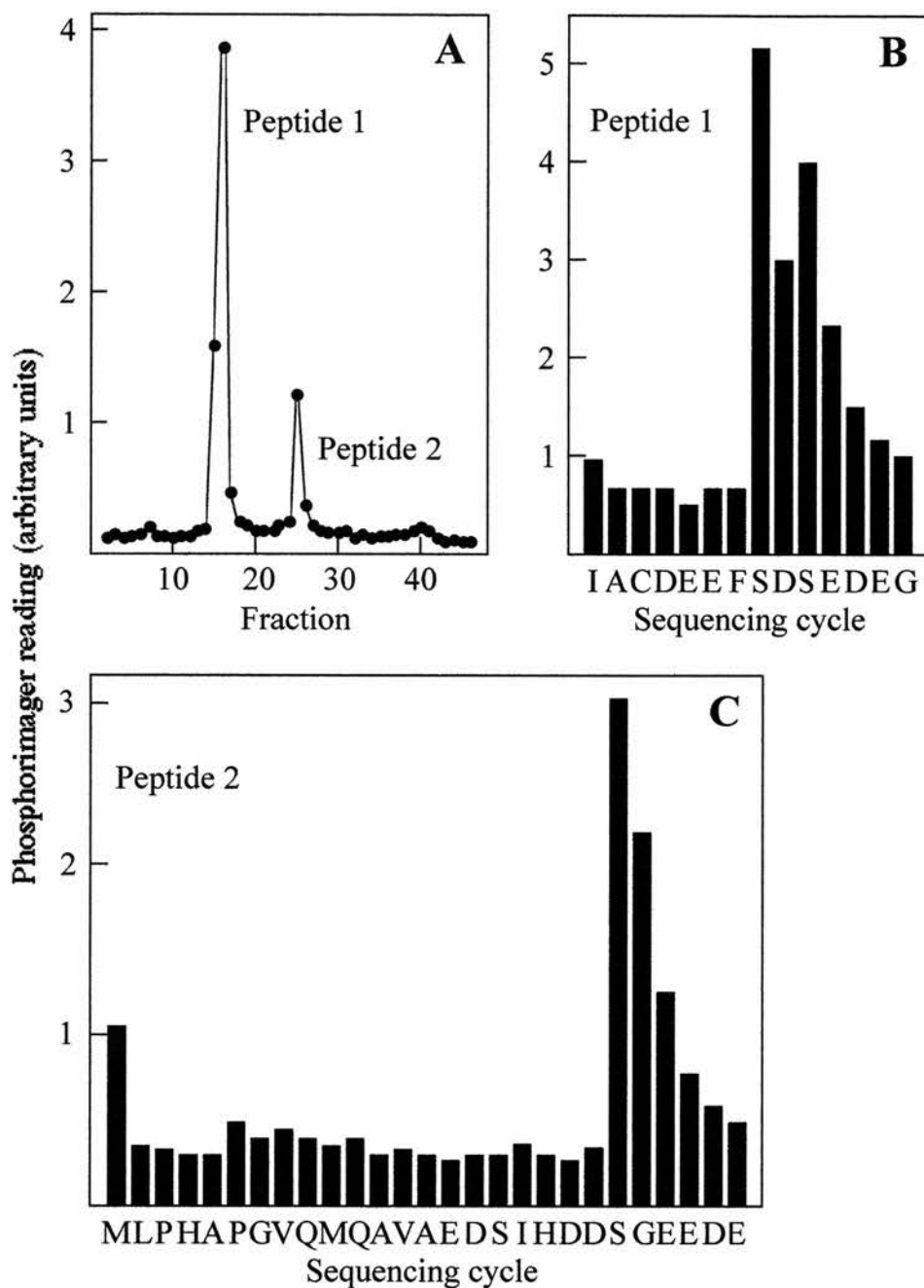


Figure 47. Peptide sequence of protein digest fragments of GST- Δ V that are phosphorylated *in vitro*. (A) Fine-bore HPLC separation of trypsin digested GST- Δ V after *in vitro* phosphorylation with 32 P-ATP shows radioactivity peaks in fractions 15 (peptide 1) and 26 (peptide 2). (B) Sequence of peptide1 shows that serine residues at positions 8 and 10 are radiolabelled. (C) Sequence of peptide 2 shows that the serine residue at position 22 is radiolabelled. These three residues are found at positions 421, 423 (peptide 1) and 393 (peptide 2) in the amino acid sequence of GST- Δ V. *In vitro* phosphorylation and trypsin digestion of GST-DV was performed by Dr. A. Llinas as part of the research for his Ph.D. HPLC separation and protein sequencing was performed by Dr. G. Kemp.

chromatin. A diagram summarising the primary structure, cleavage sites, phosphorylation sites and the proposed NLS of GST- Δ V is shown in figure 48A, a comparison of the primary structure of the HDACm NLS with the confirmed bipartite NLS in *Xenopus* N1 is shown in figure 48B. The requirement of this region for nuclear import of HDACm has been tested *in vivo* and described in section 3.3.1.

It has been demonstrated by Dr. A. Llinas [161] that phosphorylation of GST- Δ V increases the rate of nuclear uptake, creating a system very similar to that found when studying the nuclear import of nucleoplasmin, the efficient transport of which is dependent upon phosphorylation by CK2 [116].

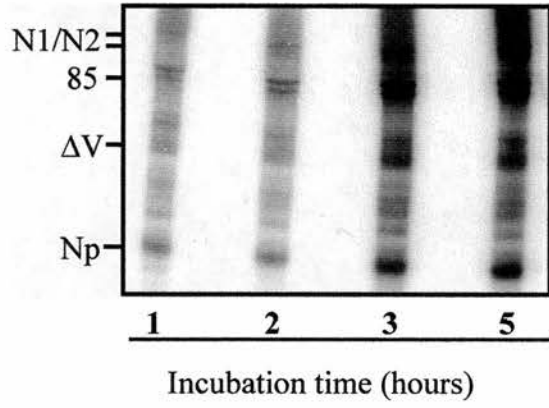
GST- Δ V can be imported into an isolated oocyte nucleus (under oil) from an extra-nuclear vesicle over a short period of time and the imported protein is phosphorylated (figure 49A). For import to occur the GST- Δ V outside the nucleus must be bound by importin- α (a reservoir of which is present inside the nucleus). Additionally, phosphorylation of the fusion protein must be a direct result of nuclear protein kinase activity, however the time of phosphorylation during the import process is not known. The import and phosphorylation of the fusion proteins in this system is unlikely to be due to altered physiology

or damage to the nucleus as previous experiments have demonstrated that under the conditions used an isolated nucleus retains *in vivo* structure and function for over 24 hours [135].

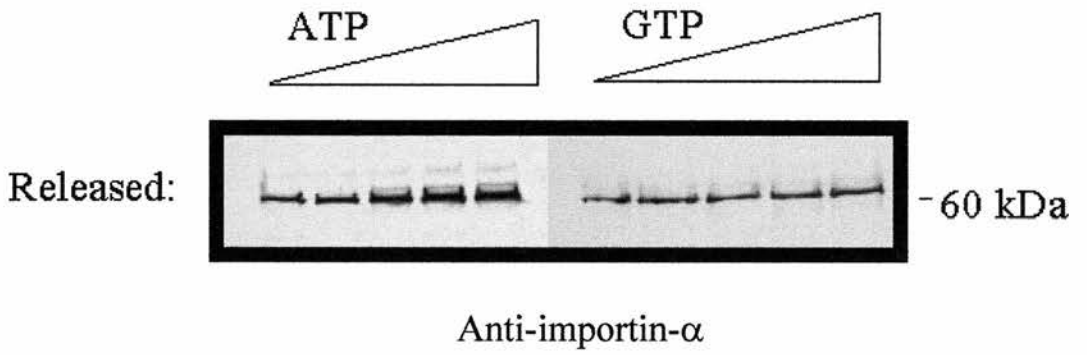
The role of phosphorylation has been investigated by a set of *in vitro* experiments by Dr. A. Llinas [161] and one of the roles of HDACm phosphorylation appears to be to regulate the interaction of HDACm with α -importin. These experiments demonstrated that, *in vitro*, phosphorylation of GST- ΔV was not required for binding to importin- α . However, phosphorylation of GST- ΔV is required for the release α -importin once bound. The key experimental results leading to this conclusion are shown in figure 49. Increasing concentrations of ATP but not GTP release increasingly large amounts of importin- α from immobilized GST- ΔV (figure 49B), and this release is inhibited by the protein kinase inhibitors DRB and quercetin but not by the non-inhibitory analogue, rutin (figure 49C). Phosphorylation of GST- ΔV would appear to occur post-import to liberate α -importin from fusion protein.

Figure 49. Nuclear import of GST- Δ V and the release of GST- Δ V from importin- α is dependent upon phosphorylation. **(A)** Autoradiograph showing incorporation of GST- Δ V into isolated nuclei in the phosphorylated form. Intact nuclei, hand isolated and under oil were incubated with a vesicle of GST- Δ V and 32 P-ATP. Under these conditions the nuclei can retain *in vivo* structure, composition and functions for up to 24 hours [126]. Nuclei were sampled at 1, 2, 3 and 5 hour time points. The autoradiograph show GST- Δ V accumulates in the nucleus with time, the nuclear phosphoproteins, nucleoplasmin (Np) and N1/N2, are also shown. Each track contains the protein equivalent of 10 nuclei. **(B)** (Performed by Dr. A. Llinas). The effect of increasing concentrations of ATP and GTP on the release of importin- α from immobilised GST- Δ V. Incubation of the immobilised fusion protein with increasing concentrations of ATP resulted in the release of correspondingly larger amounts of importin- α . Incubation of the immobilised fusion protein with increasing concentrations of GTP had no effect on the amount of importin- α released. **(C)** (Performed by Dr. A. Llinas). Immunoblot showing the effect of phosphorylation on the release of importin- α from GST- Δ V. Attempts were made to release importin- α from GST- Δ V immobilised on glutathione –Sepharose beads. Incubation of beads with the equivalent amount of CK2 as found in 1 stage VI nucleus releases no importin- α (track 1). Some importin- α is released upon incubation of the beads with 1 mM ATP (track 2). Incubation of the beads with 1 mM ATP and CK2 releases the majority of importin- α (track3). Release of importin- α is inhibited by the incubation of the beads with 1 mM ATP plus CK2 and 50 μ M DRB, the kinase inhibitor (track 4). This experimented is repeated with the kinase inhibitors quercetin (0.16 μ M) and rutin (0.16 μ M) in tracks 5 and 6 respectively. These do not inhibit release to the same extent as DRB.

A

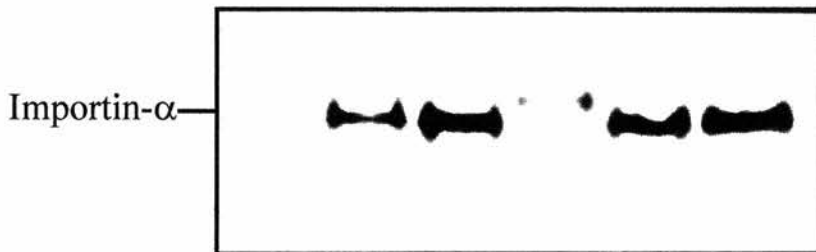


B



C

| | | | | | | |
|-------------------|---|---|---|-----|---|---|
| CK2: | + | - | + | + | + | + |
| ATP: | - | + | + | + | + | + |
| Inhibitor: | - | - | - | DRB | Q | R |

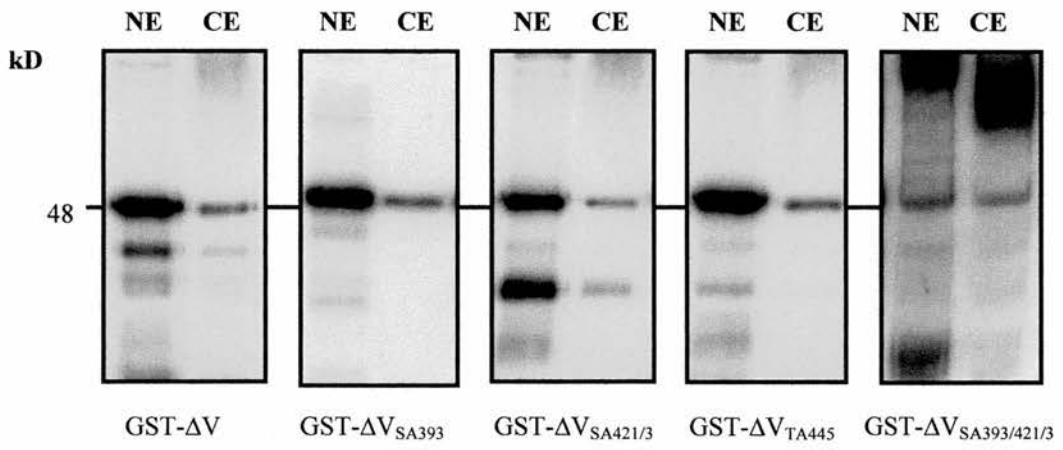
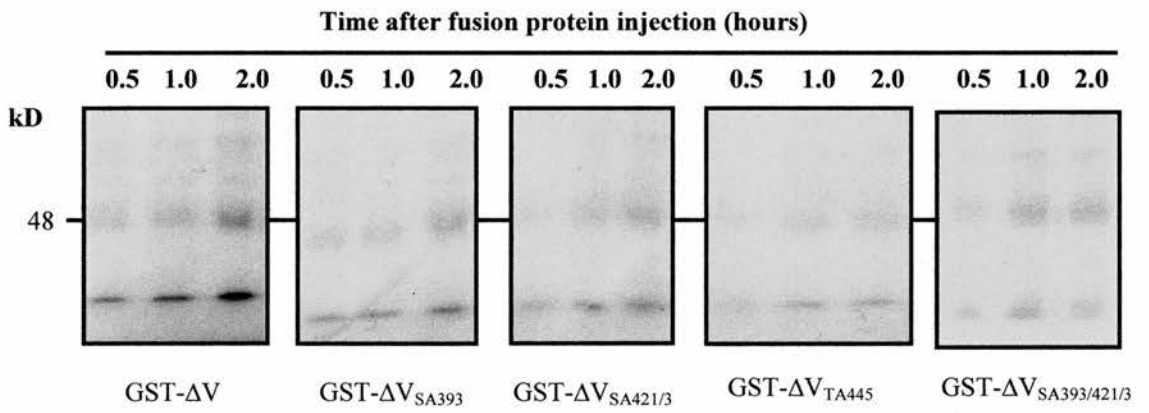
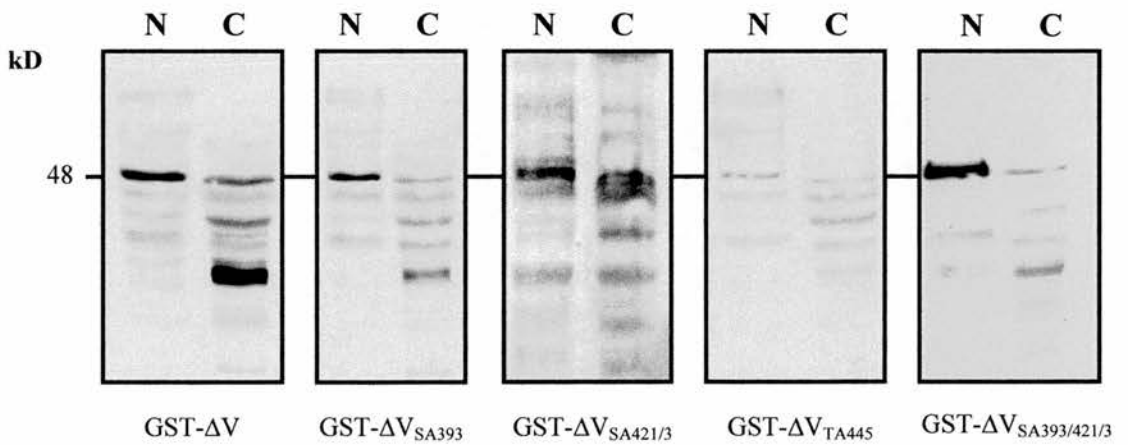


3.4.2. GST- Δ V and phosphorylation. Point mutation analysis of the *in vitro* and *in vivo* roles of phosphorylation on nuclear import and protein-protein interactions of GST- Δ V.

The aim of these experiments was to examine the role of phosphorylation in the nuclear import and protein-protein interactions of GST- Δ V. This work was conducted in collaboration with Dr. D. Smillie. Point mutations were introduced into GST- Δ V; serine (S) residues, known to be phosphorylated *in vitro*, were substituted by alanine (A) residues. The substitution mutations created were SA393, SA421/3 and SA393/421/3. A further substitution at position 445 (threonine (T) to alanine (A)) was made as phosphorylation at this position may play a role in regulating nuclear import *in vivo* but may not be phosphorylated *in vitro*.

The result of *in vitro* phosphorylation of these proteins with CK2 extracted from the nuclei and cytoplasm of large oocytes are shown in figure 50A. Each mutant protein was phospholabelled *in vitro*, but no mutant was phosphorylated as efficiently as GST- Δ V. The greatest differences in phosphorylation between GST- Δ V and the mutants are the reduction in the level of phospholabeling of SA421/3 with both kinase preparations and the marked decrease in the level of phospholabelling of SA393/421/3 with both kinase preparations. These

Figure 50. *In vitro* and *in vivo* phosphorylation of GST-ΔV fusion proteins. **(A)** *In vitro* phosphorylation of GST-ΔV and the point mutation proteins GST-ΔV_{SA393}, GST-ΔV_{SA421/3} and GST-ΔV_{TA445}. 0.1μg of fusion protein was incubated with a mix of ³²P-ATP and CK2 extract, equivalent to the amount present in 1 nucleus (NE) or 1 cytoplasm (CE) for 30 minutes. Samples were separated by SDS-PAGE and analysed by autoradiography. **(B)** *In vivo* phosphorylation of GST-ΔV and mutants in the nucleus of oocytes. Fusion protein was injected into oocyte cytoplasm in solution with ³²P-ATP. Nuclei were isolated from the injected oocytes 30 minutes, 1 hour and 2 hours post injection. These samples were separated by SDS-PAGE and analysed by autoradiography. Each track contains the protein equivalent of 10 nuclei. **(C)** Immunoblot, using anti-GST as primary, to study the level of fusion in the nucleus and cytoplasm of oocytes 20 hours after cytoplasmic injection. Each track contains the protein equivalent of 10 nuclei or 2 cytoplasm.

A**B****C**

reductions in labelling are presumably due to the substitution of residues susceptible to phosphorylation by residues that cannot be phosphorylated. The fact that SA393/421/3 is still phospholabelled, albeit at low level, by the kinase preparations also indicates that T445 can be phosphorylated *in vitro*, an event that was not detected in earlier experiments (figure 47).

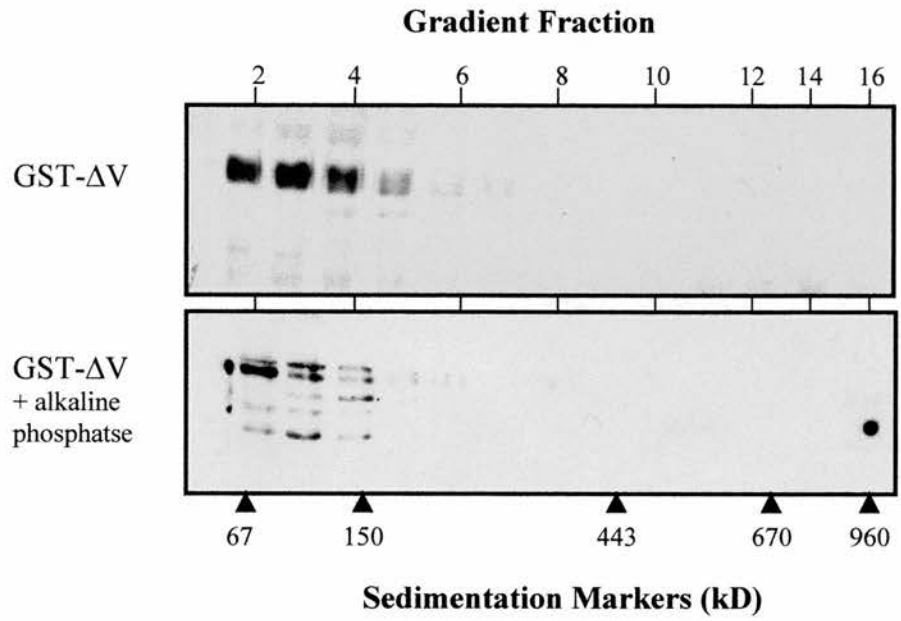
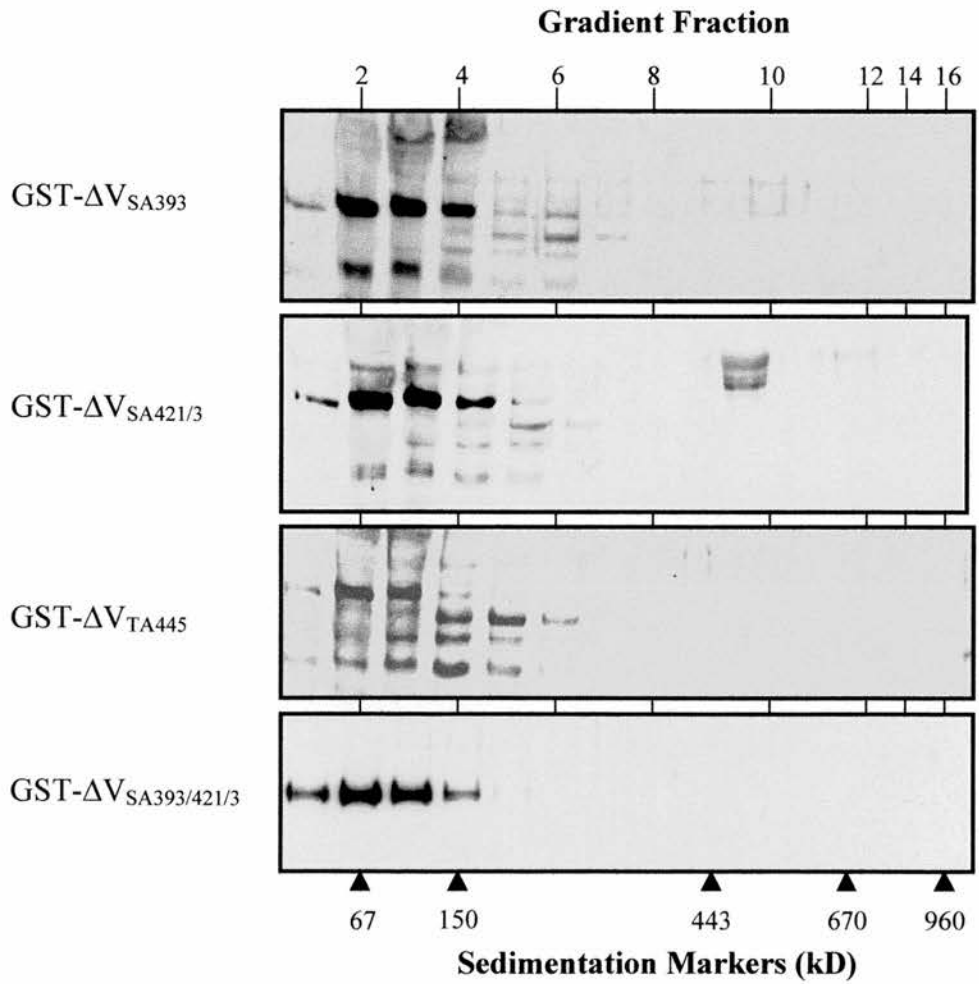
The *in vivo* situation is very different. Nuclear import and *in vivo* phosphorylation of GST- Δ V and the mutant forms has been analysed by a series of microinjection experiments. Fusion protein and ^{32}P -ATP were co-injected into the cytoplasm of large oocytes, nuclei were isolated from these oocytes over a short time course (0.5–2 hours) and analysed for labelled fusion protein by SDS-PAGE/autoradiography, the results are shown in figure 50B. GST- Δ V is labelled efficiently *in vivo* with labelled protein detectable in the nucleus within 30 minutes. The situation is similar with SA393, SA421/3 and SA393/421/3: labelled protein is detectable in the nucleus within the same time period but the level of radiolabelling is less than that of GST- Δ V. TA445 is not detectable in the nucleus in a phospholabelled form at two hours, whereas by this time labelling of the other fusion proteins is evident (figure 50B). There are a number of scenarios to account for the lack of radiolabelling of TA445. For instance, residue T445 in GST- Δ V may be

the predominant site for phosphorylation once protein has been imported into the nucleus, and whereas mutation of this site may not impede fusion protein import, no phospholabelling would be detected by autoradiography. Alternatively, phosphorylation of T445 may be essential for nuclear import. If this is so, removal of this site should prevent nuclear import. These two possibilities have been investigated by repeating the previous experiment and immunoblotting the nuclear and cytoplasmic fractions for GST-tagged protein, the results are shown in figure 50C. Twenty hours after injection, GST- Δ V, SA393, SA421/3 and SA393/421/3 are all found predominantly in the nucleus of injected oocytes, in contrast little TA445 fusion protein is detectable in the nucleus after the same time span. As residue T445 is located within the previously identified NLS, this finding supports the theory that this NLS is important for import. Additionally, phosphorylation of amino acid T445 within this motif appears to be essential for nuclear import; specifically, it may be necessary for release of the protein from importin- α once in the nucleus. The other notable point apparent from these immunoblots is that fusion protein retained in the cytoplasm is degraded rapidly, protein translocated to the nucleus exhibits lower levels of proteolysis.

Sedimentation analysis and immunoprecipitation were used to investigate the role of protein phosphorylation in the assembly of a

multimolecular complex once protein had entered the nucleus. Nuclear extracts were separated under near-physiological conditions by rate-zonal centrifugation. Clarified supernatants were layered on linear 10%-30% glycerol gradients that were centrifuged until a 960 kD (19S) marker approached the bottom of the tube. The gradients were then fractionated and analysed for GST content by immunoblotting. GST- ΔV can form small multimolecular complexes in oocyte nuclei; this complex is known to contain RbAp48 as well as this fusion protein (figure 42). Analysis of the fractions suggests that the fusion protein goes into a complex of molecular mass ≤ 200 kD and that within this complex GST- ΔV is phosphorylated. Treatment of the nuclear extract with alkaline phosphatase prior to sedimentation resolves the fusion protein to a well defined band but does not disrupt the complex once it has formed, however this treatment does seem to promote proteolysis (figure 51A). To investigate the importance of phosphorylation in the formation of this complex, rate-zonal sedimentation was performed on clarified nuclear homogenates made from oocytes injected with the mutant proteins under the same conditions as those described above. The results are shown in figure 51B. These immunoblots indicate that phosphorylation of the C-terminal of HDACm is not necessary for the assembly or maintenance of the multimolecular complex.

Figure 51. Mutant GST- Δ V fusion proteins can be components of multimolecular complexes. **(A)** GST- Δ V is found in a phosphorylated form in the nucleus and in this form is a component of a multimolecular complex. However, phosphorylation is not essential to the maintenance of this complex; treatment of an extract made from nuclei isolated from GST- Δ V injected stage VI oocytes 24 hours after injection with alkaline phosphatase (1 IU, 30 minutes, room temperature) dephosphorylates this extract. This protein sediments at the same rate as the phosphorylated form. **(B)** Mutant GST- Δ V fusion proteins sediment at the same rate as the wild type protein. Phosphorylation of the fusion protein does not seem to be essential to the formation of a multimolecular complex. As GST- Δ V_{T/A445} cannot be imported into the nucleus it was injected into the nucleus directly. Each gradient was loaded with an extract made from nuclei isolated from 50 injected stage VI oocytes.

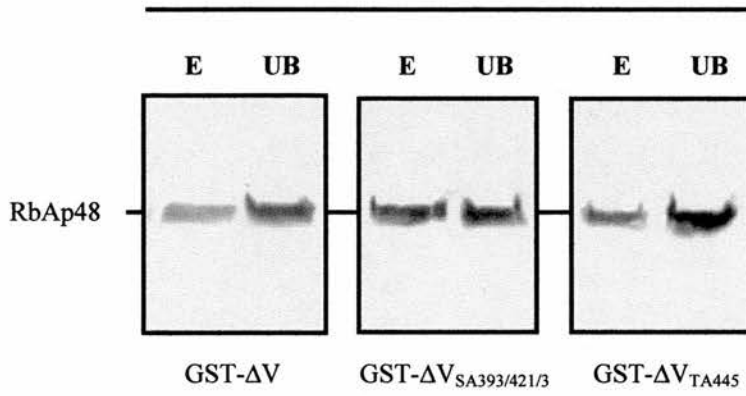
A**B**

In a second step, to confirm that RbAp48 was still forming part of this smaller complex, immunoprecipitations were performed on nuclear extracts made from oocytes injected with either GST- ΔV , SA393/421/3 or TA445. Anti-GST antibodies were immobilized on Protein A Sephadex beads and used to precipitate the fusion protein and any other protein bound to it, then this precipitated protein was analysed for the presence of RbAp48. The results are shown in figure 52. The eluted material was run next to a track containing the protein equivalent of 1/5 of the total unbound material or the protein equivalent of 10 nuclei. All three fusion proteins appear to co-precipitate RbAp48 with equal efficacy, each precipitating about 10% of the total RbAp48. This indicates that phosphorylation does not play a role in regulating the extent of the HDAC-RbAp48 interaction *in vivo*. Furthermore, as TA445 is not imported efficiently into the nucleus by the importin- α pathway, entry to the nucleus for this protein is limited to the small amount of protein that is imported, or can diffuse across the nuclear envelope. Despite this barrier to import, the small amount of TA445 protein that enters the nucleus still forms part of a multimolecular complex of the same size as that in which GST- ΔV is found. Therefore TA445 may integrate into this complex without going through the standard import pathway. It is unlikely that there is pre-assembly of the

Figure 52. Mutant GST- Δ V fusion proteins and their interaction with RbAp48. **(A)** Oocytes were injected with GST- Δ V, GST- Δ V_{SA393/421/3} and GST- Δ V_{TA445}. Nuclei were collected from 50 of these oocytes 20 hours after injection and homogenised. This homogenate was then used in an immunoprecipitation experiment. Anti-GST antibodies were immobilised on protein A Sephadex beads, these beads were then incubated with the nuclear homogenate described above. Protein specifically bound to these beads was then eluted **(E)** and analysed for the presence of RbAp48 by Western blotting. The amount of protein in the eluate was compared to the amount of protein remaining in the unbound fraction **(UB)** by running 1/5 of the unbound material (the protein equivalent of 10 nuclei) along side the eluted fraction. **(B)** As a control, the experiment was repeated using a nuclear homogenate supplemented with 5 μ g GST. The eluted and unbound material was probed for the presence of, **(i)** GST itself and, **(ii)** RbAp48, positive controls of 1 μ g GST and 10 nuclei were also run.

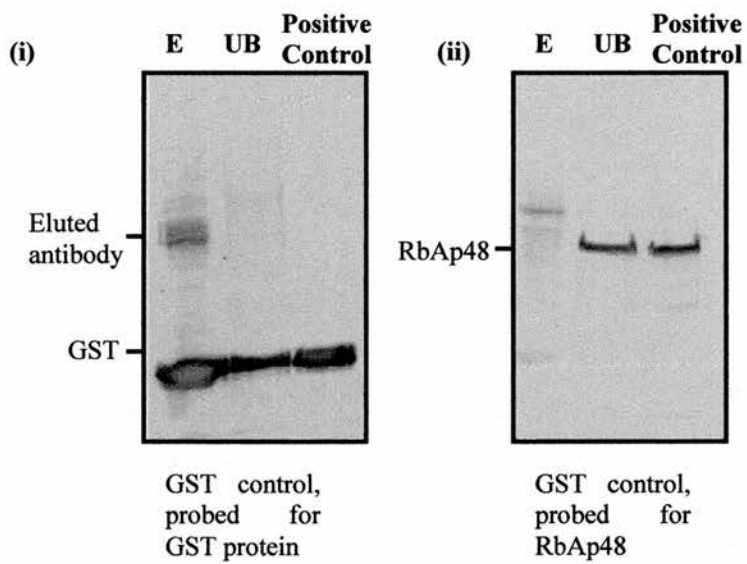
A

Immobilized anti-GST antibody



B

Immobilized anti-GST antibody



complex in the cytoplasm (the complex would be too large to enter the nucleus by diffusion). Additionally, the protein modification associated with importin- α mediated nuclear import does not appear to be essential for the formation of the complex in the nucleus.

In summary, *in vitro* dephosphorylation of GST- ΔV does not lead to disassembly of the complex, therefore phosphorylation is not essential for maintenance of the multimolecular complex once formed. Neither is phosphorylation essential to form the complex, hence all the mutants form part of a multimolecular complex. However, there may be other effects caused by the loss of key phosphorylation sites. Loss of phosphorylation at T445 as a result of the T/A substitution mutation may result in increased susceptibility of fusion protein to cytoplasmic proteases, as witnessed by degradation of TA445 *in vivo* (figure 50C) and degradation of GST- ΔV *in vitro* upon phosphatase treatment (figure 51A). However, breakdown of TA445 *in vivo* may be due to its long-term retention in the cytoplasm (figure 50C). Protein degradation may occur because nuclear import is impaired, resulting in greater exposure to protein degradation by cytoplasmic proteases. *In vitro* degradation of GST- ΔV after treatment with alkaline phosphatase may be due to the action of proteases in the calf intestinal phosphatase extract or release of sequestered nuclear proteases upon homogenisation. To test this,

GST- Δ V was incubated with alkaline phosphatase and a nuclear extract, either separately or in combination. Incubation in a nuclear extract, in the presence and absence of alkaline phosphatase, caused extensive proteolysis of the fusion protein (not shown). This activity was inhibited by the addition of protease inhibitors. Incubation of fusion protein with alkaline phosphatase alone resulted in no detectable proteolysis of the fusion protein. It seems unlikely that phosphorylation of T445 is important for protein stability.

Discussion

Histone deacetylase HDACm is unique within this class of enzymes because it is the only deacetylase so far identified whose expression is limited to early development. The reasons for this limited expression are many, but to understand these it is necessary to understand the complex nature of gene expression during early *Xenopus* development.

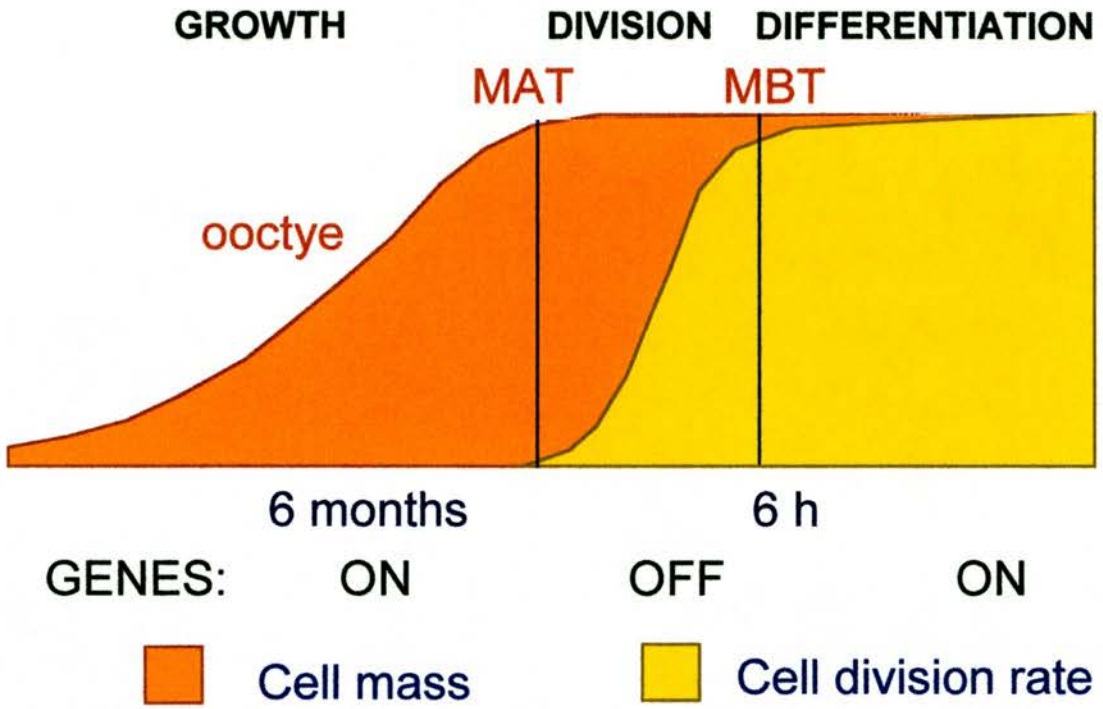
Over the period of development I have been looking at histone acetylation has multiple roles, coupling chromatin assembly with replication [165] as well as acting as a potential regulator of gene expression in the oocyte and early embryo. In *Xenopus* oocytes, transcription occurs at a high level with RNA synthesis taking place on the lampbrush chromosomes [166]. The genes being transcribed at this stage are those necessary for regulating oocyte growth and development, and those necessary for the protein store that will see the embryo through the cleavage divisions [110]. During oogenesis, expression of genes encoding the proteins necessary for the cleavage divisions are up-regulated and the genes encoding the core histones are especially active [110]. At this stage histone H4 is synthesised and stored in the diacetylated form in the nucleus of the growing oocyte [11,21,111]. The effect of over-expression of HDACm during this phase of development is suppression of transcription [159]. On studying the effect of over-expressing HDACm on transcription of specific

genes, it has been shown that 5S rRNA expression is reduced (John Sommerville, personal communication).

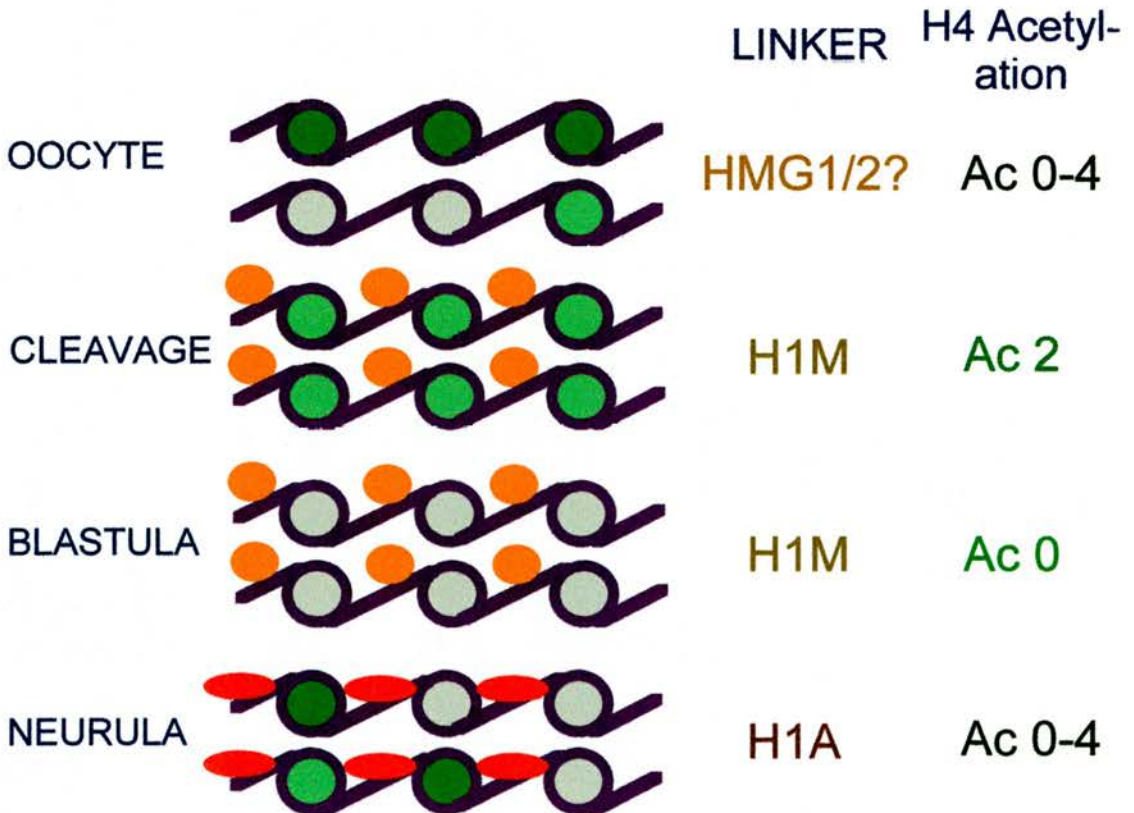
Putting these events onto a time scale puts the process into perspective. It takes approximately six months for an oocyte to grow from stage I to stage VI in the ovary of a mature female animal, RNA synthesis occurs throughout this period and protein synthesis is from these maternal messages only (figure 53A). Upon oocyte maturation and the re-initiation of meiosis I, transcription is halted [167], fertilization of the egg results in the completion of meiosis II and initiates the rapid cell divisions of cleavage [122]. Progression through cleavage occurs with the chromosomes in structures called karyomeres and in the absence of transcription from zygotic genes (figure 53A) [147,168]. At the start of cleavage each chromosome becomes surrounded by nuclear envelope, forming micronuclei or karyomeres. In these structures prereplication centres gather on the condensed chromosome during anaphase, DNA replication then initiates autonomously in each karyomere at early telophase before nuclear reconstruction and mitosis completion. Thus, during early development the chromosomes behave as structurally and functionally independent units. This atypical system of replication disappears abruptly after thirteen divisions and defines a novel transition that affects both the

Figure 53: The relationship between gene expression, histone H4 acetylation and linker histone type during early development. **(A)** The level of gene expression changes throughout oogenesis and the early stages of embryogenesis. Gene expression is turned on during oogenesis as genes required for completion of early development are expressed from the maternal genome. This expression is turned off upon oocyte maturation and the resumption of meiosis, it remains turned off post-fertilization until the cleavage divisions are completed and MBT is passed (approx. 6 hours). Expression of genes from zygotic chromosomes, and with this cell differentiation, occurs post-MBT. Initially, cell lineage specific genes are pleiotropically transcribed, only with embryo gastrulation are cell-lineage specific patterns of expression established. **(B)** The changes in gene activity are associated with changes in the acetylation of histone H4 and the type of linker histone associated with the nucleosome. In the oocyte, gene transcription is widespread and occurring at a high level. At this time histone H4 is found in a variety of acetylation states, including hyperacetylated at active gene loci. Upon fertilization, gene expression is turned off. The entire genome is replicated every 30 minutes, chromatin assembly of nucleosomes containing diacetylated histone H4 from the nuclear store begins as replication progresses. At MBT the chromatin is deacetylated, after this point there is a wave of locus specific de novo acetylation. This results is coupled to gene reactivation and the pleiotropic transcription of zygotic genes post-blastula and cell-lineage specific patterns of gene expression in gastrula stage embryos. Changes in histone H4 acetylation are accompanied by changes in linker histone type, a transition that can also effect gene transcription. Accumulation of histone H1 in the embryonic chromatin between MBT and neurulation results in the transcriptional repression of the many cell-line specific genes pleiotropically expressed post-MBT. Figures courtesy of J. Sommerville.

A



B



replication and the transcription programs of development. This transition occurs at the MBT.

The mid-blastula transition introduces G1/G2 phases to the cell cycle of the embryo, with this comes the lengthening of the cell cycle and the initiation of a complex pattern of gene expression from the zygotic chromosomes (figure 53A) [21,111,121,169]. Many cell-lineage-specific genes are pleiotropically transcribed at MBT, only with gastrulation of the embryo are cell-lineage specific patterns of expression established [39].

The changes in gene activity detected through this period of development are associated with changes in the acetylation status of core histones and the type of linker histone bound to the nucleosome (figure 53B). In the oocyte, gene transcription is widespread and occurs at a high level. At this time, histone H4, for instance, is found in a variety of acetylation states, this allowing transcription factors a high level of access to the genes required for the production of the mRNA and stores (hyperacetylated sites), whilst blocking unnecessary transcription (hypoacetylated sites) (figure 53B) [32]. Oocyte chromatin is patterned to promote transcription of the required set of genes. Upon fertilization, gene expression is turned off and transcription repressed as the nature of the cell cycle is altered. The entire genome is replicated every 30 minutes and chromatin assembly is coupled to replication

[170,171]. Each chromosome is replicated individually inside its karyomere [147]; chromatin assembly begins as replication progresses, with nucleosomes containing diacetylated histone H4 from the nuclear store being deposited on this newly synthesised chromatin (figure 53B) [21]. This situation persists until the embryo passes through the MBT. By the time the embryo passes MBT, histone H4 in the chromosomes is completely deacetylated. This is thought to remove any epigenetic imprint due to variation in the pattern of histone acetylation from the chromatin. As a result, the chromosomes in each cell of the embryo will be identical. A wave of *de novo* histone acetylation occurs post-MBT and with this the pleiotropic expression of lineage-specific genes follows (figure 53B) [11,39]. In the early gastrula embryo, chromatin is again epigenetically patterned; acetylation of histone H4 is varied as cells commit to different cell fates [172]. The changes in histone H4 acetylation occur over a similar time scale as changes in linker histone type. The changes in the type of linker histone associated with the core nucleosome can also effect gene transcription [39,112,113,114]. Accumulation of histone H1 in embryonic chromatin between MBT and neurulation results in the repression of transcription from many of the cell-line specific genes pleiotropically expressed at MBT [172,173], as well as being associated with repression of 5S RNA expression [169].

4.1. HDACm and its activity in early development

In all of the samples tested from *Xenopus* oocytes and early embryos, there is a correlation between the amount of the 57 kD HDACm protein detected and the level of HDAC activity assayed *in vitro*. This relationship is apparent throughout early development and from sedimentation analysis of nuclear extracts. As 50% of total HDAC activity in a nuclear extract can be immunoprecipitated by antibodies directed against the C-terminal peptide of HDACm, this indicates that HDACm is the major source of HDAC activity present in oocytes. No crossreacting bands are detected on immunoblotting soluble extracts from oocytes with antibodies directed against regions of HDACm conserved in all other histone deacetylases described. A number of isoforms of HDACm are detectable by Western blotting in oocytes and embryos, it has been demonstrated that HDACm can be both acylated and phosphorylated. These modifications can be removed *in vitro* to resolve the modified protein as a 57 kD protein.

4.1.1. HDACm activity in oogenesis and pre-MBT embryogenesis

The presence of HDACm-containing complexes that exhibit HDAC activity within the nucleus presents a problem for oocytes. Each stage VI oocyte contains the same amount of active enzyme as 4 000 embryonic cells at blastula.

Oocytes contain two sources of HDAC substrate. They contain approximately 21 ng of stored diacetylated histone H4 that will be required for chromatin assembly in pre-MBT embryos [174], and histone H4 in lampbrush chromosomes, the transcriptional activity of which is reflected by the widespread occurrence of hyperacetylated histone H4 within this chromatin [175]. The consequences of unregulated histone deacetylase activity would spell disaster for further development. Deacetylation of oocyte chromatin would result in a complete stop in transcription and a depleted store of the chromatin assembly factors required for the cleavage divisions, whilst deacetylation of diacetylated histone H4 stored in the nucleus would produce a reservoir of histone not suitable for incorporation into newly synthesised chromatin.

In vivo neither of these events is encountered. On immunostaining lampbrush chromosomes using antibodies which recognize specifically the four different acetylation sites in the N-terminal tail of histone H4, three of the sites (K8, K12 and K16) are found to be acetylated at multiple foci within the chromatin [32,175]. This acetylation is stable, incubation with the HDAC inhibitor sodium butyrate does not increase the signal given by immunostaining [32,175]. Additionally, the N1/N2-histone H3/H4 complex that stores the diacetylated histone H4 in the nucleus protects the histones from

premature deacetylation by HDACm. I have shown that diacetylated histone H4 stored in this form is not an accessible substrate for HDACm (figure 26).

The fact that the lampbrush chromosomes are not deacetylated *in vivo* despite the nuclei containing HDAC activity suggests that HDACm may be sequestered away from the chromatin until activity is required during embryogenesis. This argument is supported by the fact that oocyte and embryo extracts have immediately available HDAC activity *in vitro*, this would not be so if activity were controlled through the regulated expression of inhibitory factors. Li *et al* claim an association of nuclear HDAC with nuclear matrix material in chicken immature erythrocytes [76]. Whilst I have nothing to indicate HDACm associates with the nuclear matrix, evidence for the compartmentalisation of HDACm through oogenesis and pre-MBT embryogenesis comes from the immunoreactivity of oocyte nuclei and embryo karyomeres to HDACm antibodies (figures 22 & 31). This antibody reacts with material located around the internal margins of these nuclear structures and not throughout the nucleoplasm: chromatin also remains unstained. The HDACm/RbAp48 complex appears to be associated with the lamin layer inside the nucleus, it may even be anchored here by some unknown interaction between a member of the HDACm containing complex and a nuclear envelope protein.

The reason for this accumulation in the nucleus is unknown, but the anchoring on the nuclear envelope may act as a way of distributing the complex through the cells of the pre-MBT embryo in association with components of the nuclear envelope. Alternatively, HDACm may have a role to play in deacetylating proteins other than histone H4 (section 4.3.2).

4.1.2. HDACm activity in post-MBT embryogenesis

The experiments performed in section 3.2.4 allow us to pinpoint the time of initial histone deacetylase activity. Deacetylation of histone H4 occurs at MBT. Prior to these investigations it was known that at MBT all histone H4 incorporated in chromatin is deacetylated. There are two theories as to when deacetylation may occur. The first suggests there is a round of deacetylation at the end of each round of cell division [21], the second suggests deacetylation occurs at MBT itself and that all the chromatin in the embryo is deacetylated at the same time. The results I have obtained support the latter of these two theories. The next question to answer is, does the histone deacetylase HDACm have a secondary function post MBT? The answer is that we do not know. The level of acetylation of histone H4 is the balance between HAT activity and HDAC activity, incubation of *Xenopus* embryos in TSA results in the accumulation of hyperacetylated histone

during gastrula and leads to a delay in the completion of gastrulation and defects in mesoderm formation [11,21]. We know that HDACm is present in the embryo until neurula, and the above work by Dimitrov *et al* [21] and Almouzni *et al* [11] tells us that histone deacetylases are active in the embryo post-MBT and are essential for the correct development and establishment of a stable state of differential gene activity. However, it is not known whether the HDAC inhibited by the TSA is HDACm or a zygotic HDAC expressed post-MBT. We know that HDACm activity is inhibited by TSA (5 ng/ml) in oocyte and embryo extracts, but so might be the activity of another HDAC. A second point about these experiments is how necessary is the pre-MBT deacetylation of histone H4 to embryo development? The development of treated embryos was not affected until the formation of mesoderm during gastrulation [11]. Deacetylation may not be essential for the re-initiation of gene expression, but it may be essential for determining cell fate in a gastrula stage cell. Lack of deacetylation during gastrulation may result in genes that should have been silenced remaining active. This may slow the rate at which cells commit to their fate and stop cells committing to specific mesoderm cell fates, resulting in the observed phenotypic effects.

4.2. The HDACm complex through early development

In several respects, the HDAC complexes described here are similar to the HDAC-A complexes described for *S. cerevisiae* [14,71]. In yeast, distinct types of complex are found: HDAC-A, which has an estimated mass of approximately 350 kD, deacetylates all core histones, and is strongly inhibited by TSA; and HDAC-B, which has a mass of approximately 600 kD and is relatively insensitive to TSA. In large oocytes (stage V/VI), most of the 57 kD antigen and HDAC activity recovered are found in the same peak of material sedimenting with a mass of about 300 kD (figures 21 & 22). HDAC activity in oocyte extracts show sensitivity to TSA comparable to that of yeast HDAC-A, with 80% inhibition of activity at a concentration of 0.5 ng/ml TSA. In eggs and through the pre-MBT embryo, the HDACm complex increases in molecular mass. Upon maturation of the oocyte the complexes gain in mass to approximately 400-450 kD. The complex continues to increase in size through the cleavage divisions to peak at approximately 600 kD in the mid-blastula embryo. This complex deacetylates the newly synthesised chromatin at MBT. This complex is closer in size to yeast HDAC-B, however its activity still exhibits sensitivity to TSA comparable to that of yeast HDAC-A [71].

4.2.1. The complex contains multiple copies of HDACm

Several different types of large multiprotein complex containing HDAC activity have been isolated from vertebrate cells and described [176,177]. In the cells studied, the complexity of much of the HDAC particle is due to the need to target the activity to specific genes. Targeting is possible through interaction with a number of corepressors. Human HDAC1/2 can be targeted to specific sites by interacting with a range of transcriptional corepressors through mSin3 [95,176,177]. At other times HDAC1/2 deacetylases can be targeted to E-box promoters by interaction with RB, this interaction being mediated by RbAp48 [102,104]. Other groups report HDAC activity being coupled to ATPase-dependent chromatin remodelling complexes containing Snf2-related factors [149]. Some of these complexes seem to contain two molecules of HDAC [177,178]. The presence of two molecules of HDAC per complex may be a specific requirement for activity, especially if you consider that this is a feature not only of these complex described for human HDAC1 and HDAC2, but also those found in yeast and chicken erythrocytes [70,71,75,76]. Some evidence to support the idea of there being two molecules of HDACm in the multimolecular complex found in large oocytes has been generated. Injecting full length exogenous HDACm protein results in lampbrush chromosome condensation (figures 38 and 40). Injection of GST- ΔV ,

the truncated form of the protein that contains only the C-terminal third of the protein, can also result in lampbrush chromosome condensation (figure 41). The GST- ΔV protein lacks the active site present in the full length protein, but it may still be able to target deacetylase activity to the lampbrush chromosomes. This would be possible if GST- ΔV is forming part of a multimolecular complex containing endogenous HDACm. Direct evidence of this interaction comes from the immunoprecipitation of GST-tagged material from oocytes injected with GST- ΔV protein by immobilized RbAp48 antibodies (figure 42). In this experiment both GST- ΔV and endogenous HDACm are precipitated, a result that is only possible if HDACm and GST- ΔV are interacting with each other, because the native protein is not GST-tagged. The reason for two molecules of HDAC per multimolecular complex is not known.

4.2.2. The RbAp48 and HDACm interaction

Of all the HDAC associated proteins that it has been possible to examine, only one has been found that co-sediments, shows coincident immunolocalization and coprecipitates with HDACm. This protein is RbAp48. RbAp48 is a member of the conserved family of Msi-1-like WD repeat proteins [178]. This protein contains seven highly conserved

WD-40 motifs; each consists of a four stranded, twisted β sheet that takes on a “propeller blade” conformation that can bind both HDAC and histones simultaneously [179,180].

The reports of Ahmad *et al* [183], Hassig *et al* [177] and Vermaak *et al* [152] have described the sites within the respective histone deacetylases studied that bind RbAp48. These workers have traced the p48-binding region to specific areas in HDAC proteins.

(A) HDACm interacts with two molecules of RbAp48

Ahmad *et al* mapped two regions important to RbAp48 binding by chicken HDAC 2, these are found between amino acid residues 82-180 and 245-314 and bind to WD repeats in the N-terminal and C-terminal of RbAp48 [183]. More importantly Vermaak *et al*, studying the HDACm homologue xRPD3, have demonstrated that xRPD3 interacts with two molecules of RbAp48 and that the interaction with RbAp48 occurs at the N- and C- terminals of xRPD3, with Sin3 coordinating this interaction [152] (figure 54B).

The interaction of RbAp48 with HDACm has not been studied in great depth, although a number of observations about this interaction have been made. It has been possible to immunoprecipitate RbAp48 with the fusion protein GST- ΔV but not with the fusion protein GST- $\Delta R/\Delta H$, and it has been demonstrated that C-terminally degraded T7-

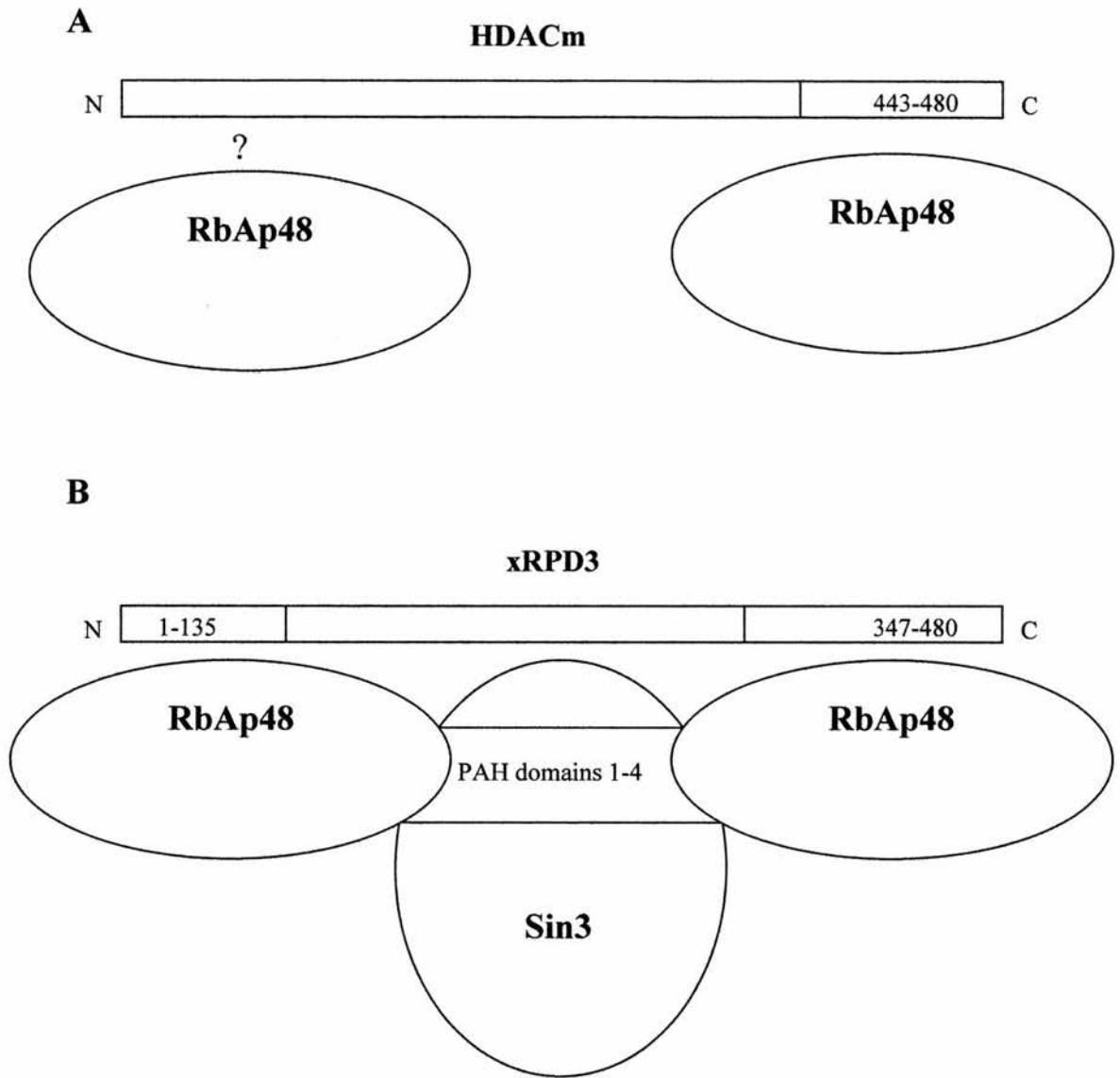


Figure 54: The domains of HDACm that interact with RbAp48 compared with the domains of xRPD3 that interact with RbAp48. **(A)** By analysing RbAp48 binding with sub-clones of HDACm it has been possible to positively identify the location of one RbAp48 binding domain in the C-terminal domain of this protein. It is also possible that a second binding site may exist in the N-terminal domain. **(B)** This is similar to the RbAp48 binding sites identified in xRPD3 by Vermaak *et al* [152] using similar deletion techniques. They have located RbAp48 binding sites between amino acids 1-135 and 347-480. It is thought that RbAp48 binding at these sites in xRPD3 is mediated through Sin3. Sin3 binds xRPD3 at an unknown site and it is thought it mediates RbAp48 binding through the PAH domains. A similar Sin3 interaction has not been detected in HDACm [159]. Further interactions through the PAH domains of Sin3 are thought to mediate MeCP2 binding [106].

Ab21 protein does not bind RbAp48 (figures 39 and 42). This indicates the importance of the C-terminal domain of HDACm in the interaction with RbAp48. There may be some evidence for the existence of a second RbAp48 binding site in HDACm. Injection of excess exogenous HDACm completely disrupts the sedimentation profile of native HDACm and RbAp48 (figure 40), whilst injection of excess GST- Δ V does not completely disrupt the sedimentation profile of native RbAp48 (figure 42). In effect, these experiments are binding competition assays. Exogenous protein binds RbAp48, the more you add the more disruption of endogenous RbAp48 containing complexes there is as the equilibrium is forced towards binding exogenous protein. As equal amounts of both proteins were injected, the only plausible explanation for the difference in effect is that the full-length exogenous protein contains more RbAp48 binding sites than GST- Δ V, and one of these must be in the conserved core of HDACm (figure 54A). However, the fact that GST- Δ V can bind RbAp48 *in vitro* whilst GST- Δ R/ Δ H cannot may indicate that the interaction is synergistic in nature and requires binding of RbAp48 at the C-terminal before RbAp48 binding is possible at the N-terminal. This correlates with part of the results reported by Vermaak *et al* [152], but it was not possible to detect Sin3 in our complex.

(B) The interaction of HDACm and RbAp48 is dependent on zinc

Hassig *et al* traced the specific residues responsible for the HDAC interaction with RbAp48 to residues D174, D179 and H199 in human HDAC 1 [177]. These residues do not coincide with the RbAp48 binding domain identified in the C-terminal domain of HDACm (figures 40 & 42). However, upon sequence alignment of the amino acid sequence of human HDAC 1 with HDACm it is apparent that the mutated sites are conserved in many acetyl-metabolizing enzymes [60]. There is evidence to suggest that these enzymes are dependent upon zinc ions for activity [159]. The residues in HDAC 1 identified as being essential for binding RbAp48 by Hassig *et al* [177] are also those that have previously been predicted as being necessary for the co-ordination of Zn^{2+} ion binding [66]. Substitution at these sites may not alter the structure of the RbAp48 binding domain, instead the mutations may prevent Zn^{2+} incorporation and with this prevent HDAC 1 from assuming the tertiary structure required to bind RbAp48.

The importance of Zn^{2+} to both HDACs and RbAp48 has been demonstrated by a number of groups. HDAC 1 activity can be inhibited by the zinc chelator 2-mercaptopyridine N-oxide in the micromolar range [177]. I have presented evidence here (section 3.1.5, figure 25D) of HDACm being 80% inhibited by 1 mM $ZnCl_2$, whilst Mg^{2+} has no effect on activity, indicating that high concentration of Zn^{2+} may be

specifically disrupting HDACm. Sensitivity to Zn^{2+} ions has previously been demonstrated with yeast HDAC [71]. Additionally, the potent HDAC inhibitor TSA, which was used as a ligand in the cloning of the original HDAC, is now thought to act in part through a metal chelation mechanism involving a functionally critical hydroxamic acid [177]. RbAp48 is also dependent upon Zn^{2+} ions; RbAp48 can bind at least 3 Zn^{2+} [178]. These ions are probably necessary for the propeller structure of the WD repeats to be formed correctly, Zn^{2+} binding may stabilize the structure of RbAp48 to allow the protein-protein interactions that are important for its many roles in chromatin assembly and remodelling.

The intriguing point of this is that the majority of Zn^{2+} binding proteins, such as the zinc finger transcription factors, mediate DNA binding as part of a transcription activation or repression complex. Neither HDACm nor RbAp48 demonstrates an ability to bind DNA directly. This is not an insurmountable problem if HDAC activity pre-MBT is targeted in the manner described in section 4.2.3B as then DNA binding activity is not required. However, during the establishment of cell-specific patterns of gene expression this method of HDAC targeting is not feasible, at this time DNA binding is necessary and must be mediated through a DNA-binding transcription factor. Despite this change in requirements, RbAp48 is still found in complex with

HDACm. In this context RbAp48 might be acting as an adapter rather than as an HDAC targeting factor. How this situation is resolved *in vivo* is not known, but what is apparent is the dependence of both RbAp48 and HDACm on Zn^{2+} .

4.2.3 *Xenopus* oocyte HDAC complexes

(A) Differences in opinion

A number of HDAC containing complexes have been described in early *Xenopus* development. The first of these is the HDACm/RbAp48 described previously by J. Ryan *et al* [156], the others are the MeCP2 containing complex described by Jones *et al* [106] and the Snf2 containing complex described by Wade *et al* [149]. The latter complexes contain both RbAp48 and the histone deacetylase xRPD3 (appendix F). The complex that consists primarily of MeCP2, Sin3 and xRPD3 and has a molecular mass of approximately 700 kD may recruit HDAC to methylated DNA [106]. The complex containing Snf2 ATPase activity has six major subunits, including Mi-2, RbAp48 and xRPD3, and an estimated molecular mass of 1.0-1.5 MD [149]. It has not been possible to detect either MeCP2 or Sin3 in our complex; there is no overlap in sedimentation, coincidence in immunostaining of nuclear material or coprecipitation with HDACm or RbAp48, the proteins do not even show similar patterns of expression during

oogenesis (figure 22). Even the nuclear/cytoplasmic distribution of these proteins can be different i.e. Sin3B is distributed equally between the nucleus and the cytoplasm (figure 22). The interesting thing about the differences between these complexes is that the two *Xenopus* HDACs, HDACm and xRPD3, are 97% identical and 99% identical (figure 55). However, this is not a surprise as xRPD3 was cloned using primers directed against the HDACm sequence. These proteins may well be expressed from pseudoalleles of the same gene in the tetraploid species *Xenopus laevis*.

The apparent discrepancy in HDAC particle size can be explained by a number of considerations. First, the efficacy of our HDAC antibody compared with the HDAC antibody used by the Wolffe laboratory may be lower, making it difficult to detect small populations of HDAC containing complexes in glycerol gradients. Second, large particles may be preferentially selected by multistep chromatography as used by Jones *et al* and Wade *et al* [106,149], whereas our approach has been to show the nature of HDACm in material contained in intact nuclei. Unfortunately I did not have the necessary equipment with which to recreate the chromatography experiments performed by the Wolffe laboratory. However, on making oocyte extracts of the type described in these reports [106,149,152] and running a 10%-30% glycerol gradient I have found that there was no

Comparison of amino acid sequences of *Xenopus laevis* histone deacetylases HDACm and XRPD3

| | | |
|---------------------|---------------------|---------------------|
| MAL <u>S</u> QGTKKK | VCYYDGDVG | NYYYGQGHM |
| MAL <u>T</u> LGTKKK | VCYYDGDVG | NYYYGQGHM |
| KPHRIRMTHN | LLLNYGLYRK | MEI <u>Y</u> RPHKAS |
| KPHRIRMTHN | LLLNYGLYRK | MEI <u>F</u> RPHKAS |
| AE <u>E</u> MTKYHSD | DYIKFLRSIR | PDNMSEYSKQ |
| AE <u>D</u> MTKYHSD | DYIKFLRSIR | PDNMSEYSKQ |
| MQRFNVEDC | PVFDGLFEFC | QLS <u>T</u> GGSVAS |
| MQRFNVEDC | PVFDGLFEFC | QLS <u>A</u> GGSVAS |
| AVKLNKQQT | ISVNWSGGLH | HAKKSEASGF |
| AVKLNKQQT | ISVNWSGGLH | HAKKSEASGF |
| CYVNDIVLAI | LELLKYHQRV | VYIDIDIHHG |
| CYVNDIVLAI | LELLKYHQRV | VYIDIDIHHG |
| DGVEEAFYTT | DRVM <u>S</u> VSFHK | YGEYFPGTGD |
| DGVEEAFYTT | DRVM <u>T</u> VSFHK | YGEYFPGTGD |
| LRDIGAGK GK | YYAVNY <u>P</u> LRD | GIDDES YEAI |
| LRDIGAGK GK | YYAVNY <u>A</u> LRD | GIDDES YEAI |
| FKPVM <u>T</u> KVME | MFQPSAVVLQ | CGADSLSGDR |
| FKPVM <u>S</u> KVME | MFQPSAVVLQ | CGADSLSGDR |
| LGCFNLTIKG | HAKCVEFIKT | FNL <u>P</u> MLLGG |
| LGCFNLTIKG | HAKCVEFIKT | FNL <u>L</u> MLLGG |
| GGYTIRNVAR | CWTYETAVAL | DSEIPNELPY |
| GGYTIRNVAR | CWTYETAVAL | DSEIPNELPY |
| NDYFEYFGPD | FKLHISPSNM | TNQNTNEYLE |
| NDYFEYFGPD | FKLHISPSNM | TNQNTNEYLE |
| KIKQRLFENL | RMLPHAPGVQ | MQA <u>I</u> PEDSYH |
| KIKQRLFENL | RMLPHAPGVQ | MQA <u>V</u> AEDSIH |
| DDSGEED <u>E</u> ED | PDKRISIRSS | DKRIACDEEF |
| DDSGEED <u>D</u> ED | PDKRISIRSS | DKRIACDEEF |
| SDSEDEGEGG | RKNVANFKKV | KRVKTEEEKE |
| SDSEDEGEGG | RKNVANFKKV | KRVKTEEEKE |
| GEDKKDVKEE | EKAKDEKTDS | KRVKEETKSV |
| GEDKKDVKEE | EKAKDEKTDS | KRVKEETKSV |

Xenopus laevis XRPD3
Xenopus laevis HDACm

X amino acid
substitution

Figure 55: Comparison of amino acid sequence of *Xenopus* histone deacetylase HDACm with xRPD3. These two enzymes have been cloned from mRNAs synthesized and expressed in the oocytes of *Xenopus laevis*. The primary structures of these two proteins are 96% identical and 99% similar, however the multimolecular protein complexes of which these proteins are part show distinct differences in size and composition.

significant difference in the size of the HDACm containing complex in the oocyte extract compared with a nuclear extract. The greatest problem with the oocyte extract was trying to detect specific proteins, I found the level of background reaction with specific antibodies raised against HDACm and RbAp48 was very high with an oocyte extract compared with a nuclear extract.

The xRPD3 complexes have also been isolated from whole oocyte homogenates under conditions vastly different to those found *in vivo*, not only are subcellular compartments disrupted and their contents allowed to mix but the repeated chromatographic steps alter the ionic conditions to which the cellular components are exposed. These disruptions may promote interactions with the HDAC that are not normally possible in the oocyte. Evidence to support the idea of extranuclear interactions comes from the sedimentation analysis of progesterone matured oocytes (figure 21). HDACm containing particles of the size detected in *Xenopus* eggs by Wade *et al* [149] have not been detected by me in oocytes or embryos. However, sedimentation analysis of progesterone matured oocytes (figure 21) shows that breakdown of the nuclear envelope upon maturation releases HDACm in complex with RbAp48 into contact with the cytoplasm. The release results in the assembly of a larger, multimolecular complex. This is presumably due to the interaction of the nuclear complex with additional components

present in the cytoplasm only. This increase in the molecular mass of the complex may be the first step in incorporating HDACm-RbAp48 into an active complex that will deacetylate the newly synthesised chromatin in the embryo at the MBT. Following maturation the complex continues to increase in size until a fully active complex is assembled and active at MBT.

(B) Differences resolved.

The discrepancy in complex composition is intriguing but it is possible to explain the difference in a more rational manner than the difference in complex isolation techniques. The 300 kD I identified was isolated by looking at endogenous protein [159]. This complex contains HDACm and RbAp48 and a number of other unidentifiable sub-units (figure 54A). It has histone deacetylase activity *in vitro* (figure 25), but this activity is suppressed in the oocyte *in vivo* (figure 26). The 300 kD HDACm complex may well represent a minimal active complex i.e. a storage form that can be added to, or adapted, for specific functions as required. Various types of large complex are most likely assembled, when required, from simpler units.

In the experiments in which the Mi-2 containing complex [149] and the MeCP2 containing complex [106] were identified, xRPD3 was over-expressed. Experiments by myself (figures 38, 40 & 42) and

Vermaak *et al* [152] have shown that over-expression of HDAC in an oocyte can effect the size of the HDAC containing complex. The core unit of the HDAC complexes by the Wolffe Laboratory is very similar to basic complex that I have described (figure 54B). It is possible that by over-expressing xRPD3 in oocytes the Wolffe laboratory is inducing the formation of a range of the possible complexes containing HDAC that can be formed later in development but which are not normally formed in the oocyte.

The reason for the existence of different types of HDAC complex during development is as follows. It is thought that RbAp48/46 may target an HDAC complex to the nucleosome [152]. Members of the RbAp48/46 family of proteins are integral subunits of three types of protein complex known to be involved in the nucleosome assembly pathway. These are the B-type HAT that acetylates newly synthesised histone (RbAp46), histone tetramer assembly factor CAF-1 (RbAp48) and the histone deacetylases (RbAp48/46) [181]. These proteins can bind selectively to histone H4 with the same specificity, the RbAp48/46 binding site lying in helix 1 of histone H4. However, binding can only occur if the histone is not incorporated into nucleosomes or if the histone tetramer has not been assembled on the DNA [181].

The mode of histone H4 binding by RbAp48 has important implications for chromatin assembly and the timing of histone

deacetylation if HDACm activity is directed through RbAp48 targeting. Incorporation of diacetylated H4 into new chromatin is mediated through the CAF-1 complex, NAP-1 and ATP [28,29]. Several residues within helix 1 of histone H4 make important interactions with the nucleosomal DNA, whilst others are important for heterodimerisation of the histone proteins, thus it seems unlikely that the core nucleosome can be formed whilst p48 is bound to helix 1 of histone H4 [181]. This would also predict the need to displace RbAp48 from the nucleosome core (histone tetramer) post-deposition before chromatin assembly can be completed. If HDAC activity were to be targeted to the tetramer by RbAp48, the time of deacetylation would need to be at the time of deposition, prior to the formation of mature nucleosomes. This method of deacetylating histone H4 would be restricted to use on newly synthesised chromatin only e.g. the deacetylation of chromatin that removes epigenetic imprinting from the embryo at MBT. This would require only a simple complex with the purpose of general (non-specific) deacetylation of the entire genome. The complex I have isolated by studying endogenous protein may perform this function.

The role of RbAp48 in the complex outside this time i.e. post-MBT, where the role of the complex is to remodel and establish tissue specific patterns of gene expression in chromatin is unknown. This process involves deacetylation of mature chromatin in which the

histone H4-RbAp48 binding site is protected. RbAp48 may have a role in co-ordinating formation of a different complex containing a DNA binding protein, such as *Xenopus* transcription factor EED [182]. This protein contains a zinc finger DNA binding domain and five WD-40 repeats through which this transcription factor can interact with histone deacetylases and targets enzyme activity to tissue specific sites [182]. An alternative theory has been suggested by Verreault *et al* [181], nucleosome-remodelling factors associated with the HDAC may assist in peeling the DNA off the histone octomer prior to RbAp48/46 binding to allow deacetylation This would predict a requirement for ATP-utilizing components in nucleosome remodelling complexes. This type of specifically targeted gene repression complex containing HDAC activity may well be the type of complex that has been formed by over-expression of xRPD3 in the experiments performed by the Wolffe Laboratory [106,149]. MeCP2 may target the HDAC-RbAp48 containing complex to the requisite site for deacetylation and gene silencing and Mi-2 may provide the ATPase activity.

On the balance of probability, it is likely that both groups are right. The complex containing endogenous HDAC that I detect in oocytes is the form in which most HDACm is found during early development. The complexes detected by Wade and Jones [106,149]

may exist *in vivo*, but not at the time in development at which their existence is induced by over-expression of xRPD3.

4.3. Regulation of HDACm subcellular location and nuclear import in oocytes

Regulation of endogenous protein within the nucleus of large oocytes has already been discussed (4.1.1). Evidence for the involvement of protein modifications in controlling nuclear accumulation of HDACm has also been gathered and may provide proof of further compartmentalization of HDACm during early development. Extraction of soluble HDACm from *Xenopus* oocytes can be difficult. A substantial amount of HDACm is retained in the pelleted material of an oocytes homogenate upon low speed centrifugation (figure 27); this material is recovered more efficiently when extraction is performed with an organic solvent (1,1,2-trichlorotrifluoroethane) that solubilizes membranous material. It has also been observed that small oocytes are immunostained around the oocyte membrane with anti-HDACm IgGs (figure 20), HDACm is associated with the oolemma and vesicular structures close to the perimeter of the cytoplasm. These structures may be responsible for the anchorage of HDACm in the cytoplasm. Evidence gathered supports the theory that

the modification that locates HDACm to these sites is fatty-acylation of HDACm (figure 28).

4.3.1. Acylation and cytoplasmic retention

Cytoplasmic retention of HDACm may be a developmental adaption unusual for deacetylases. Protein acylation is a frequently detected modification, however it is normally restricted to proteins involved in signal transduction. It is either associated with membrane bound proteins, such as transmembrane receptors, the α - subunit of tripartite G proteins and monomeric G proteins such as p21^{ras} [137,154,155,156,157] or alternatively it is used as a method for anchoring proteins involved in second messenger cascades in the cytoplasm i.e. cAMP-dependent protein kinase [184]. The possibility of an HDAC playing a role in signal transduction is not one that has been considered before, however it does contain two putative receptor tyrosine kinase phosphorylation sites (Y333 and Y336). These residues in the C-terminal domain of HDACm might be target sites for the many tyrosine kinases activated during signal transduction [184]. Binding of ligand by a receptor tyrosine kinase could in turn activate the intracellular kinase domain and lead to phosphorylation of the HDACm at specific tyrosine residues. For this to be possible HDACm would have to contain an SH2 domain so that it could bind to the

phosphorylated tyrosine kinase [185], however no such motif is recognized in the primary structure. It may be possible for HDACm to bind the tyrosine kinase through an adapter protein, such as Grb2 (growth factor receptor-bound protein 2), that contains both SH2 and SH3 domains [184]. Phosphorylation of the receptor tyrosine kinase would in turn allow recruitment of further proteins involved in the signalling cascade to this site, one such group of factors recruited to autophosphorylated receptor tyrosine kinases are phospholipases, such as phospholipase C [186], phosphorylation of these proteins up regulates their enzyme activity [184]. Binding of HDACm to activated receptor tyrosine kinases could result in phosphorylation of HDACm at the tyrosine residues and may in turn be the signal for the recruitment of phospholipases to the tyrosine kinase. Phosphorylation of the lipase would result in its upregulation and cleavage of the acyl moiety from HDACm, leaving it free to be imported into the nucleus.

4.3.2. Phosphorylation and nuclear uptake

Retention of nuclear factors in the cytoplasm can occur by a number of pathways (figure 56). The most common methods of regulating cytoplasmic retention are through either a cytoplasmic retention domain (CRD) or through suppressing an NLS [119]. Protein phosphorylation of sites near an NLS has dual roles. It has been linked

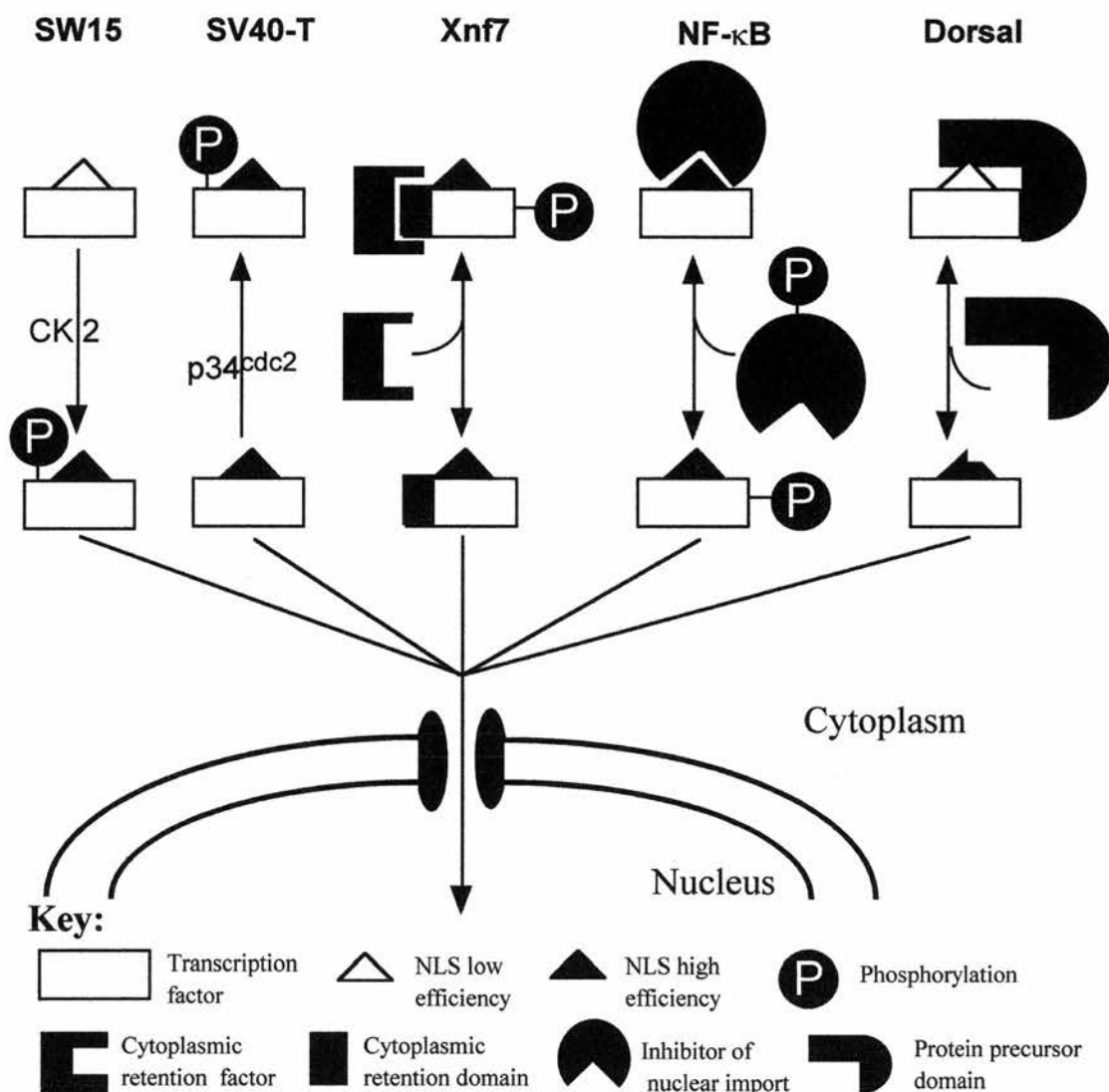


Figure 56. Mechanisms by which nuclear factors may be retained in the cytoplasm. NLS driven nuclear import can be modulated by phosphorylation at sites near or within the NLS. This phosphorylation can have a positive effect upon the rate of nuclear import (SW15 driven by phosphorylation by CK 2) or a negative effect upon nuclear import (SV40 large T antigen inhibited by phosphorylation by p34^{cdc2}). Cytoplasmic retention can be achieved by a nuclear factor containing a CRD that itself interacts with a cytoplasmic anchoring partner (as with xnf7). The NLS may be masked by intermolecular interaction with an inhibitor protein. This is the case with NF-κB and I-κB, the interaction between the two being down-regulated by phosphorylation. Finally, the NLS may be masked by a domain of the protein precursor masking the NLS. Upon the signal for the continued processing of the protein the precursor domain is cleaved, exposing the NLS and allowing import. Figure based on Vandromme, M., Gauthier-Rouviere, C., Lamb, N. & Fernandez, A. (1996) TIBS. 21, 59-64.

to the cytoplasmic retention and enhanced import of nuclear proteins e.g. phosphorylation of SV40 large T-antigen by cyclin-dependent kinase p34^{CDC2} inhibits nuclear import by “masking” the NLS, whilst phosphorylation of the same protein by protein kinase CK2 stimulates nuclear import [119]. Alternatively, phosphorylation of sites surrounding a CRD may stimulate cytoplasmic retention. *Xenopus* nuclear factor 7 (xnf7) is one of the most widely studied proteins in early *Xenopus* development; the MAP kinase and cyclin dependent kinase signal transduction pathways regulate nuclear uptake of xnf7 [187]. Like HDACm, xnf7 is a maternally expressed protein with *in vivo* function in the nucleus [188]. It is anchored in the cytoplasm between maturation of the oocyte and MBT [189]. Nuclear uptake of xnf7 is under the control of a CRD. Phosphorylation of xnf7 results in cytoplasmic retention by promoting the formation of a 670 kD complex between xnf7 and a cytoplasmic anchor via the CRD, nuclear uptake only occurs upon dephosphorylation of the protein at MBT [188]. Unlike xnf7, nuclear localization of HDACm seems to be under the control of deacylation and an NLS.

Enhanced import of nuclear proteins as a result of phosphorylation has been observed with a variety of proteins, including SV40 large T-antigen, nucleoplasmin and nucleolin [116,190,191,192]. This phenomenon also appears to apply to nuclear uptake of exogenous

HDACm and the GST- ΔV protein. The GST- ΔV fusion protein is phosphorylated at multiple sites by the protein kinase CK2. It also contains a putative bipartite NLS in the C-terminus domain that shows a high degree of similarity to the NLS found in nuclear protein N1 (figure 47). It was hypothesised that the function of the NLS could be regulated by phosphorylation of the CK2 sites, with preliminary data indicating that phosphorylation might accelerate nuclear import (John Sommerville, unpublished data). This would be in line with the results published by other groups, who have demonstrated that the nuclear import of proteins such as nucleolin, nucleoplasmin and SV40 large T antigen may be increased by phosphorylation [116,117,118]. In the case of SV40 large T-antigen, the rate of import can be increased 40-fold by phosphorylation at specific sites [190]. Phosphorylation of HDACm at residue T445 plays an important role in nuclear import. This residue is found in a CK2 consensus phosphorylation site within the bipartite NLS and substitution of this residue by alanine inhibits nuclear import *in vivo* (figure 49). Phosphorylation of this site in HDACm has the same stimulus upon uptake as that of phosphorylation of the NLS in cyclin B1 [193] and of phosphorylation of the CcN motif found in SV40 large T antigen. However, unlike SV40 large T antigen, HDACm does not contain a consensus CDK/p34^{cdc2} phosphorylation site to down-regulate the rate of uptake [118,193,194].

It is interesting to note that the nuclear proteins HDACm and N1 share such similarities in their bipartite NLS sequences and the method for modulating their nuclear import, because the function of the two proteins are also related. These proteins function during the early development of *Xenopus* embryos and are involved in chromatin assembly. N1/N2 acts as the chaperone for the stored acetylated histones H3/H4 that are incorporated into newly synthesised chromatin during the cleavage divisions [151], whilst HDACm deacetylates these histones later in the developmental process once they have been incorporated into nucleosomes.

The mechanism by which protein import is enhanced by CK2-phosphorylation is unknown. It is thought that phosphorylation may effect the interaction with NLS binding proteins, such as importin- α , or by enhancing docking with the nuclear pore complex (NPC). The results generated previously by microinjection of GST- ΔV and its truncated form indicate that the NLS is essential for import [159]. Inhibition of the nuclear import of GST- ΔV by co-injecting the importin- α antibody indicates that import is facilitated through importin- α (figure 44). Information generated from binding studies and the site-specific mutants indicate that phosphorylation has a complicated involvement in the binding and release of importin- α

(figures 49 & 50). The results obtained indicate that regulation of the binding of importin- α to the NLS may be dependent upon phosphorylation of T445 in the C-terminal region of HDACm, as mutation of threonine to alanine at this site impairs import. However, importin- α must be dissociated from its substrate and converted into a form that has low affinity for the NLS sequence once the NLS containing protein has been imported to prevent export [195]. It is not known whether phosphorylation at T445 is necessary for binding to importin- α or release from importin- α once the protein has been imported into the nucleus. The data produced to date indicates that phosphorylation of the C-terminus of GST- ΔV is by a nuclear CK2, as GST- ΔV is phosphorylated and imported into the nucleus in the absence of the cytoplasm in experiments using only physiologically active nuclei under oil (figure 49). As the CK2 has been shown to be associated with the internal membrane of the oocyte nucleus [161], the phosphorylation event must occur inside the nucleus. It is not known which sites are being phosphorylated in this import experiment, however from the results of the substitution mutations experiments, it would be reasonable to predict that phosphorylation of T445 plays a role. The role of phosphorylation at S393 and S421/3 are as yet unknown, but they appear to play no role in regulating nuclear uptake

or the interaction between the NLS and importin- α . RbAp48 binds GST- ΔV and its mutant forms with the same affinity, phosphorylation or dephosphorylation of the carboxyl tail domain appears not to affect the binding of RbAp48 to this domain (figures 51 & 52). Phosphorylation of these CK2 sites may be necessary to bind additional components of the multimolecular HDACm complex, or to anchor the nuclear HDACm complex to the nuclear lamina.

If phosphorylation of T445 does promote the disassociation of HDACm and importin- α , other factors that reverse importin- α binding to the NLS must be taken into account. The association of importin- α with an NLS has been shown to be dependent upon the presence of Ran-GDP but not Ran-GTP [163,196]. Ran-GTP present in the nucleus is necessary for the interruption of the importin- α/β interaction and export of importin- α [196]. Protein acetylation is now known to be a common protein modification under the control of the HATs and HDACs, in contrast to the previous assumption that it is involved purely in regulating histone acetylation [197]. Acetylation of importin- α is known to be influential in nuclear import. The human importin- α , Rch 1, is acetylated *in vitro* by the histone acetyltransferase CREB-binding protein (CBP) and can be detected in an acetylated form *in vivo* [198]. The acetylation site in importin- α is found within the importin- β

binding domain (IBB) [198,199,200]. Acetylation of importin- α is necessary for efficient interaction between importin- α and importin- β [198]. It is not known where in the oocyte importin- α is acetylated; however, in oocytes the predominant acetyltransferase is the cytoplasmic HAT 1 responsible for acetylation of newly synthesised histone H4 [158,181]. Deacetylation of importin- α may convert this protein into the isoform that has a low affinity for the NLS sequence.

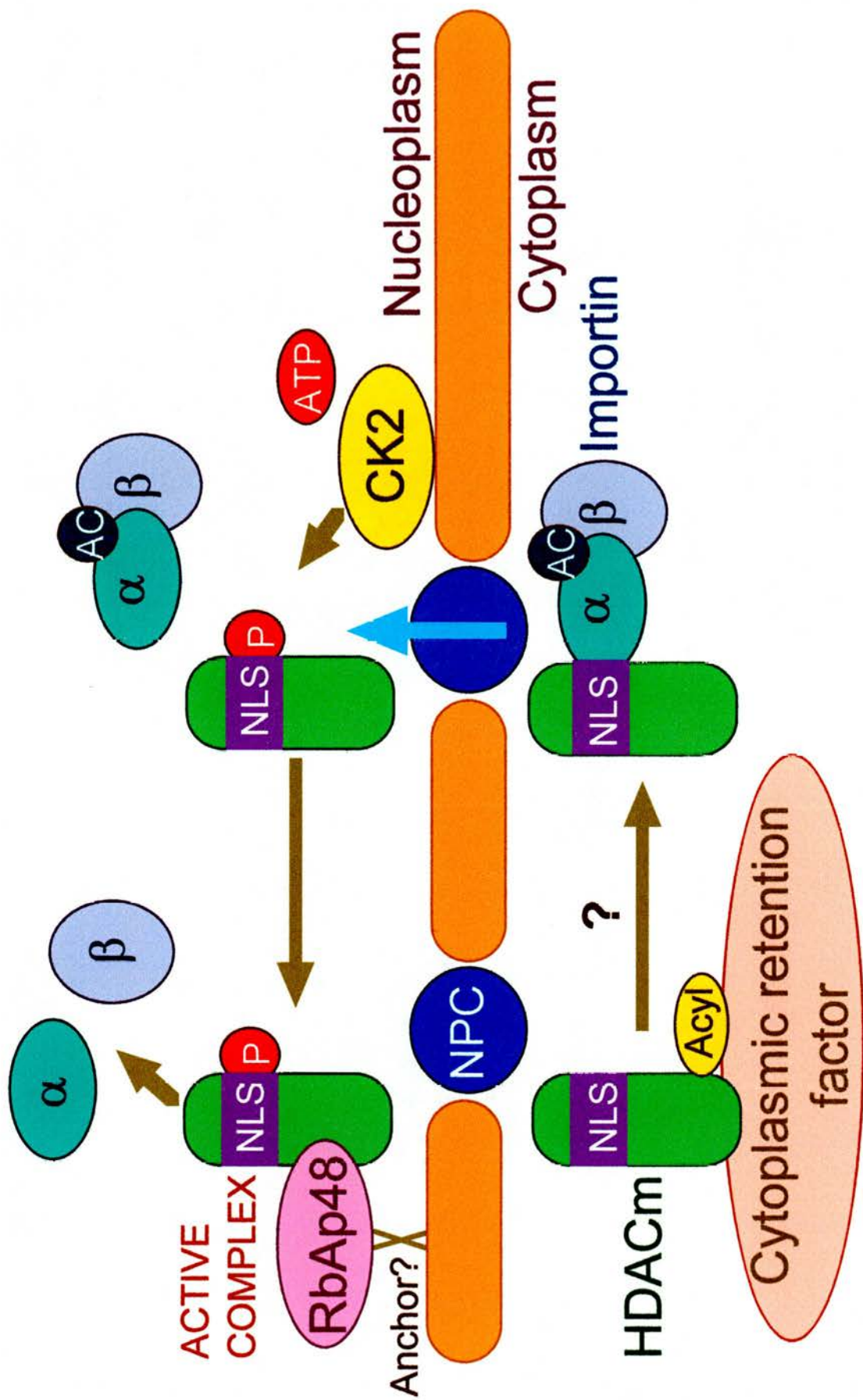
Importin- α should bind the HDACm NLS in the cytoplasm. Acetylation of importin- α in the cytoplasm would then promote binding of importin- β and formation of a stable HDACm-importin- α/β complex capable of import through the NPC. Upon entering the nucleus a complex series of events would promote the dissociation of the import complex. Ran-GTP would promote the dissociation of importin- α/β dimer and prepare importin- α for export. Concurrently nuclear CK2, a protein that has been shown to be localized to an internal layer of the nuclear envelope [161], could phosphorylate T445 in the NLS of HDACm. Phosphorylation would release importin- α from the NLS and allow the formation of the multimolecular complex containing HDACm and permit its anchoring to the nuclear lamina. Deacetylation of importin- α by HDACm located at the nuclear periphery may also occur during this process and result in the conversion of importin- α to an

isoform with a low affinity for any NLS. Importin- α would be exported as previously described [163,195,196] in complex with the cellular apoptosis susceptibility gene product (CAS) and Ran-GTP. This scheme is summarised in figure 57. If correct, this scheme would explain the presence of HDACm in a potentially active form around the internal margin of the nuclear envelope during a phase of development where the need for enzyme activity is not apparent upon initial investigation. It also offers a possible explanation for the correlation between enzyme phosphorylation and enzyme activity during oogenesis and embryogenesis. Enzyme phosphorylation has been demonstrated to relate to enzyme activity (figure 25), at the time of detectable *in vivo* activity in oocytes (pre-maturation), and mid-blastula embryos, HDACm is phosphorylated. This protein is dephosphorylated, and therefore deactivated, at the crucial times during early development when ectopic activity upon chromatin would be detrimental i.e. upon progesterone induced oocyte maturation.

4.4. Over-expressing HDACm during oogenesis

With the analysis of lampbrush chromosomes it has been possible to demonstrate HDAC activity in oocytes of recombinant HDACm and protein fragments expressed in oocytes as T7 tagged fusion proteins or expressed in bacteria as GST fusion proteins (3.3.2 & 3.3.3). In

Figure 57: Regulation of HDACm nuclear import and importin- α binding by acylation, phosphorylation and acetylation. Acylation of HDACm retains the protein in the cytoplasm, possibly by anchoring it to a cytoplasmic retention factor, this may be the oocyte membrane. An unknown signal triggers removal of the acyl moiety and levels HDACm free for import via the importin- α pathway. Interaction of importin- α with importin- β may be promoted by the cytoplasmic acetylation of importin- α . Once this complex is formed it docks with the NPC and import is actively driven, a GTP requiring step. Inside the nucleus HDACm is further phosphorylated by a nuclear kinase, this promotes the dissociation of importin- α from HDACm and allows the formation of the multimolecular complex containing RbAp48. This complex is somehow linked to the inner margin of the nuclear membrane, probably to the lamin layer. In this position HDACm has *in vivo* activity but is separated from the acetylated histone substrates. It is in a position to deacetylate imported proteins and acetylated factors of the import pathway, such as importin- α ; deacetylation of importin- α being required for export in complex with CAS and Ran-GTP.



contrast, HDACm (Ab21) synthesized by the reticulocyte lysate system fails to generate any activity *in vitro* (3.3.1). These observations suggest that HDACm alone is insufficient to generate activity i.e. that catalytic activity can only be gained through association with other proteins. Other results presented here (figures 25, 33 & 45) suggest that phosphorylation of HDACm may also be required for *in vivo* activity.

Injection of additional recombinant HDACm or expression of exogenous HDACm from DNA/RNA templates in oocytes appears to be sufficient for the generation of HDAC activity *in vivo*. The corresponding location of exogenous HDACm and endogenous RbAp48 on chromatin (figures 39, 41 & 43) suggests that both are required for the *de novo* activity observed. These results are not at odds with the HDAC activity recorded on minichromosomes after injection into oocytes of RNA encoding HDAC protein [160]. It can only be concluded that recombinant HDACm escapes the restraints imposed on endogenously expressed HDACm and that its uncontrolled activation can lead to premature condensation of lampbrush chromosomes.

4.5. Summary

- The *Xenopus laevis* protein HDACm is a histone deacetylase enzyme with a similar sequence and inhibitor sensitivity to HDAC 1.

- Expression of this protein is from a maternal mRNA synthesised and stored in the oocyte. This message persists through early development, being detectable in embryos until neurula.
- HDACm protein expression and enzyme activity follow a common pattern. Enzyme and HDAC activity are first detectable in pre-vitellogenic oocytes, they both increase continually through oogenesis to peak in stage VI oocytes. HDACm and HDAC activity are both associated with the nuclear material.
- Nuclear import is facilitated through a pathway utilising a putative bipartite NLS present in the C-terminal domain of HDACm recognized by the receptor importin- α .
- Once in the nucleus, HDACm forms part of a multimolecular complex of approximate molecular weight 300-360 kD. This complex also contains retinoblastoma associated protein RbAp48.
- This complex is retained at the internal margin of the nuclear envelope. In this location the enzyme is inhibited from deacetylating acetylated histone H4 incorporated into the chromatin, however it may be able to deacetylate acetylated proteins as they are imported into the nucleus e.g. importin- α . The nuclear store of diacetylated histone H4 is protected from deacetylation by binding the chaperone proteins N1/N2.
- In the early embryo, levels of HDACm remain high and the enzyme is still located at the internal margins of the karyomere.

- HDACm and RbAp48 are still part of what may be the same multimolecular complex in early embryos. The size of the multimolecular complex containing HDACm and RbAp48 increases through the cleavage divisions to peak in size at approximately 600 kD in mid-blastula stage embryos.
- The peak in complex size corresponds to the time of detected *in vivo* activity i.e. at MBT with the deacetylation of chromatin synthesized during the reductive cleavage divisions.
- Endogenous HDACm is post-translationally modified. This protein can be acylated and phosphorylated. Acylation appears to anchor the protein in the cytoplasm of small oocytes by linking the enzyme to vesicular material. Fatty-acylation may anchor HDACm to the oolemma or cortical granules located around the periphery of the oocyte. The specific nature of the acylation and the region of the protein within which the modification takes place are unknown.
- Phosphorylation of HDACm at consensus CK2 sites appears to have pleiotropic effects on enzyme behaviour. Phosphorylation is required for activity. This modification is detectable *in vivo* in stage V/VI oocytes and mid-blastula embryos. Dephosphorylation of HDACm removes its ability to generate activity and occurs naturally upon progesterone induced maturation of the oocyte.

- Phosphorylation of residue T445 in the C-terminal domain is required to promote nuclear import of HDACm. This modification appears to regulate the interaction between the NLS in HDACm and importin- α . It is unknown if phosphorylation of this site within the NLS up-regulates or down-regulates the interaction with importin- α . Phosphorylation at sites (S393 and S421/3) adjacent to this site does not effect nuclear import of HDACm.
- The level of phosphorylation does not influence the interaction between HDACm and RbAp48.
- Over-expression of HDACm or fragments of this protein have failed to generate activity on their own. They require the presence of other factors to generate activity.
- However, over expression of HDACm in *Xenopus* oocytes is sufficient to recruit HDAC activity to chromatin *in vivo*. This procedure also recruits RbAp48 to the same locations as HDACm on endogenous chromatin, suggesting both proteins are required for the observed activity.
- Ectopically expressed HDACm escapes the restraints placed upon its endogenous counterpart and has uncontrolled activity that leads to premature condensation of lampbrush chromosomes and the inhibition of mRNA synthesis.

4.6. Further work

There is still a great deal of work to be conducted in this area. All of the HDACm associated proteins, bar RbAp48, remain to be identified. One of the primary objectives has got to be the identification of these factors and the recreation of enzyme activity *in vitro*. To achieve this, all the components of the complex need to be identified and cloned. As a starting point to this investigation, RbAp48 should be cloned and expressed in the reticulocyte lysate with HDACm to examine the theory of a "minimum complex" consisting of RbAp48 and HDACm being sufficient to target HDAC activity to acetylated histone H4. This initial investigation could then be built upon with the identification and cloning of additional factors and their addition to the reticulocyte lysate system. Identification of additional proteins would involve the large scale isolation of stage VI oocyte nuclei and affinity chromatography of the extract with immobilized TSA or anti-Cpep columns.

The putative NLS lying in the C-terminal domain of HDACm needs to be investigated to demonstrated its ability to target nuclear import of normally non-nuclear proteins and to identify the functional lysine residues in the bipartite sequence. The creation of a chimeric protein consisting of the NLS fused to a carrier peptide normally retained in the cytoplasm would be a useful tool to aid this

investigation. To avoid the problem of nuclear import of this chimera by diffusion through the NPC, the protein must have a molecular weight of at least 45 kD [118]. Once created, site-specific mutants could be introduced into the NLS to examine the role of specific residues, singly and in combination, in the import process. The work of Kleinschmidt and Seiter on N1/N2 [117] could be used as a template for this work. The end point of this study would be to transfer these mutations into the full length HDACm protein along with the site specific mutants created to study the role of phosphorylation in nuclear import. Work with these full-length mutants would best be conducted by transfecting cells of a *Xenopus* cell line, such as XTC2, with the mutants transferred into a eukaryotic expression vector such as the pCGT vector. This would allow fast and accurate analysis of the influence of the various mutants upon nuclear import. Use of this plasmid has the additional benefit of allowing ectopically expressed HDACm to be detected without cross-reaction with endogenous HDAC by making use of the T7 tag. Use of cells for this type of investigation is of further help because it also permits the addition of factors, such as the phosphatase inhibitor okadaic acid, to the medium and the investigation of the influence protein modifications have upon nuclear import.

Appendices

Appendix A: HDACm amino acid and DNA sequences

NCBI ACCESSION: X78454

Amino acid sequence:

Number of amino acids: 480

MALTLGTKKK VCYYYDGDVG NYYYGQGHM KPHRIRMTHN LLLNYGLYRK MEIFRPHKAS AEDMTKYHSD
DYIKFLRSIR PDMNSEYSKQ MQRFNVEDC PVFDGLFEFC QLSAGGSVAS AVKLNKQQTD ISVNWSSGLH
HAKKSEASGF CYVNDIVLAI LELLKYHQRV VYIDIDIHGG DGVEEAFYIT DRVMTVSFHK YGEYFPGTGD
LRDIGAGK GK YYAVNYALRD GIDDES YEAI FKPVMSKVME MFQPSAVVLQ CGADSLSGDR LGCFNLTIKG
HAKCVEFIKT FNLPLMLGG GGYTIRNVAR CWYETAVAL DSEIPNELPY NDYFEYFGPD FKLHISPSNM
TNQNTINEYLE KIKQRLFENL RMLPHAPGVQ MQVAEDSIH DDSGEEDEDD PDKRISIRSS DKRIACDEEF
SDSEDEGEGG RKNVANFKKV KRVKTEEEKE GEDKKDVKEE EKAKDEKIDS KRVKEETKSV

DNA base sequence:

BASE COUNT:

679 a 410 c 544 g 672 t

```
1 gcggaaggaa aatggcgctg actctaggaa caaagaagaa agtgtgctac tactatgatg
61 gtgatgttgg aaattattat tatgggtcaag ggcacccat gaaacctcat agaattcgca
121 tgacacacaa cctgctgctc aactatggac ttaccgaaa aatggaaatc tttagccccc
181 acaaagccag cgccgaggat atgacaaaat atcacagtga tgattatatac aaattcctgc
241 gctccatacg accagacaat atgtccgaat acagtaaaaca gatgcagaga ttaaatgttg
301 gtgaggactg tcctgtgttt gatggcctat ttgagtcttg ccagctctct gcagggggtt
361 ttgttagcaag tctgtttaa ctaaacaaac agcagactga catttcagt aactggctg
421 gtggccttca tcatgcaaag aaatctgagg catctggttt ttgttatgtc aacgatattg
481 tccttgccat cctggaacta ctaaagtatc accagagagt tegtatatatt gatatagaca
541 ttcaccacg tgatgggtgt gaggaggcat ttacacaac cgatagggtt atgactgtgt
601 ccttccataa gtagggagag tattttcctg gaactggaga tctgagagat atgggtgcag
661 ggaaaggcaa atactatgct gtaaattatg ccttacggga tgggattgac gatgagtcct
721 atgaagcaat ttttaaacca gtaatgtcca aagttatgga aatgtttcag cccagtgacag
781 tggctcttaca gtgcggagca gattcattat ctggggatag actgggatgc ttcaatttga
841 ccattaaggg acatgcgaag tgtgtggagt ttataaagac cttaacttg ccactgttga
901 tgttaggagg tggaggttac actatccgga atgtggctcg ttgctggaca tatgaaacag
961 ctgtggctct ggactctgag atccccaatg agcttccata taatgattat tttgaatatt
1021 ttgggtccgga cttcaagctt cacatcagcc catccaacat gactaatcag aacactaatg
1081 aatatctgga gaaaattaag cagcgcctct ttgagaactt gcgatgctc ccccatgctc
1141 ctggagttca gatgcaagcc gttgcagagg actccataca cgatgacagt ggtgaagaag
1201 atgaagatga tcccgacaag cgtatttcaa ttcggtcatc agataaaagg attgcctgtg
1261 atgaggagtt ctcagattct gaggatgaag gggaggaggg tcgcaaaaac gtggccaatt
1321 tcaaaaaagt aaaacgggtt aaaactgaag aggaaaagga aggagaggac aagaaagatg
1381 ttaaagaaga ggagaagct aaagatgaga agacggatag caaacgggta aaagaagaga
1441 ccaaatcagt ctgatccttc aactatgggg agaaaaatccg aagaccaaac taattctcat
1501 ggttttata tttgtatatg ccctgtacag agccctacta tgaatataa gtccacacat
1561 tctaaattat ttctgtccca ctggttgagg gggggtgaag tggctcgtgt agtggattaa
1621 gcttcacatc ttttaccttt ttttaagatt cacatctggt acctttttac cagatgtttc
1681 cagctctttg gctttttttt tttttttgac caaaaacttt ccatgttttc ctgtgcctct
1741 gtaatcttcg gtggtgcaat gcattacgga tttatttccc tgctcccttc tatacacact
1801 ttgctgtcag actacagact tttgctacag tacatgaaat atgtacactt atgctcagga
1861 tcaggcata tgcacttat gctcaggatc aggcagtgg aaggaggtgg gttccagctg
1921 tcttccaaat gaatttgaga gggttacctt gagggatgga agggggaagc tgaagctcct
1981 cttaaactaa actatcagg gattccctgt tcacttaatg ctgctaacc cctccagat
2041 tagttcatga agcagatttt tagatgtgtg gaaacctggg ccacagttac cttataatgg
2101 ggattgtggg gatttgaat ttgggtttct gcctttaatc ttagtgggtt ggagagtgc
2161 tggattcatg gagtgaagaa aatggagaat ttttatgtct aattttgtg atgggaaatt
2221 tctttttttt tttttttatg gttgagttgt agaaaagctt tgtaataaaa tctggtactt
2281 atacaaaaaa aaaaaaaaaa aaaaa
```

Appendix B: *Xenopus* RbAp48 amino acid and DNA sequences

NCBI ACCESSION: AF073787

Amino acid sequence:

Number of amino acids: 425

MADKEAAFDD AVEERVINEE YKIWKNTPF LYDLVMTHAL EWPSLTAQWL SDVTRPDGKD
FSIHRLVLGT HTSDEQNLHV IASVQLPNDQ AQFDASHYDS EKGEFGGFGS VSKIEIEIK
ITHDGEVNRA RYMPQNPCI I ATKPTSDVL VFDYTKHPSK PDPSGECNPN LRLRGHQKEG
YGLSWNPMLS GNLLSASDDH TICLWDISAV PKEGKVVDK TIFTGHTAVV EDVSWHLLHE
SLFGSVADDQ KLMIWDTRSN NTSKPSHSVD AHTAEVNCLS FNPYSEFILA TGSADKTVAL
WDLRNLKLLK HSFESHKDEI FQVQWSPHNE TILASSGTR RLNVWDLSKI GEEQSPEDAE
DGPELLEFIH GGHTAKISDF SWNPNEPWI CSVSEDNIMQ VWQMAENIYN DEDTEGGVDP
EGQGS

DNA base sequence:

BASE COUNT: 546 a 443 c 464 g 519 t

1 ggcacgagac caccagtagt gaaagacttc cgtaaccatg tctacggcct accgtaacca
61 cgtgacgtcc attttagccg gctcttggca gacgcccact tgtgacgaaa ggtctcttga
121 ttggtgactt ctgcacaatt cttattgggt cttgttggcg ccaagtgtgc ggctcggaaa
181 cacgggggag gcgggaaaca atagcaggag gagcacgccc ggtcaccgtg ggaggagtca
241 gaagaagaac cggggaacgt gagtctggct gctgacttag agagcaagtc gagtcgtgaa
301 aacagtaaaag tatccgtccc tggatttact atggctgata aagaagctgc gttcagtgat
361 gcgggtggagg aacgagtcac aaatgaagag tataaaatat ggaagaaaaa cacccttcc
421 ctgtatgatc tggatgatgc ccatgccttg gagtggccta gcctcactgc tcagtggctc
481 tcagatgta ccagaccgga tgggaaagat ttcagcatcc acagactggt actgggaaca
541 cacacttctg atgaacagaa tcacctggtg attgctagcg tgcagcttcc taatgatgat
601 ctccaatttg atgcttccca ctatgacagt gaaaaaggag agtttggagg ctttggctct
661 gtgagtggga aaatagaaat cgagatcaaa ataactcatg acggagaggt gaacagagct
721 cgttacatgc cacagaatcc atgcattatt gccacaaaaa ctccaaccag tgacgttctt
781 gtgtttgact acaccaaaca cccatctaaa ccagatcctt ctggtgagtg taatccaaat
841 ctccgacttc gaggccacca aaaggagggc tatggcttat cctggaatcc caacctaatg
901 ggcaacctgc ttagtgcttc agacgaccat acaatatgcc tgtgggatat cagtgtgta
961 cctaaggagg gcaaagtggg ggatgcaaag accttttca cagggcacac tgcagtgggt
1021 gaggatgtat cttggcattt attgcatgaa tctctctttg gatcagttgc agatgatcag
1081 aaactgatga tctgggacac ccgatcaaac aacacatcaa agcccagcca ctcagtagat
1141 gctcacacag ctgaagtgaa ctgtctgtca tttaaccctt acagtgagtt catattggca
1201 actgggtcag ctgacaagac tgttgcatca tgggacctgc gcaatctgaa attaaagttg
1261 cattcatttg aatctcaaaa agatgaaatc ttccaggctc agtggctctc acataatgag
1321 accattcttg atccagtgag aactgaccgt agactaaatg ttgggattt aagtaaata
1381 ggagaagagc agtctcctga agatgcagaa gatggtcccc ctgaacttct gtttattcat
1441 ggtggtcaca cagccaagat atcagacttc tcatggaatc ctaatgaacc atgggtgatc
1501 tgttctgtat ctgaagataa tatcatgcag gtctggcaaa tggcggaaaa catttataat
1561 gatgaagata cagagggtgg tgttgatcca gagggtaaac gtcctaaac aaagataac
1621 tgttctgtct gtttcttgca aaaacagaga ttgtgtcttc tgcattccagc acttagacat
1681 cggccattca atgctgcaca gagctgcttc tggctcctcc tcttcccccc tgcgttctaa
1741 tctcgttttc actggttttt ttgaggaatc cccttttatt ttatatatat atatatatat
1801 atatatatat tgttatttta tataaaatc tcattttaac catgtatct ctggcagggt
1861 gtttttataa tctgggaggg ggagagagag cccttgtct gactcacggg ctggattccc
1921 ccagtgcctt ccaactgcatc agatatcaag aataattccc cccccccc tc

Appendix C: *Xenopus* MeCP2 amino acid and DNA sequences

NCBI ACCESSION: AF106951

Amino acid sequence:

Number of amino acids: 467

MAAAPSGEER LEEKSEDQDL QQQKDKPPKL RKVKKDKKDE EEKQEPFHSS EHQPGEPADE
GKADMSESAE ENLAVPESSA SPKQRRSVIR DRGPMYEDPT LPEGWTRKLLK QRKSGRSAGK
FDVYLINPNG KAFRSKVELI AYFQKVGDTL LDPNDFDFTV TGRGSPSRRE QKQPKKPKAP
KSSVSGRGRG RPKGSIKKVK PPVKSEGVQV KRVIKSPGK LLVKMPYSGT KEASDATTSQ
QVLVIKRGGR KRKSETDPSA APKKRGRKPS NVSLAAAAAE AAKKKAIKES SIKPLLETVL
PIKKRKTRET ISVDVKDTIK PEPLTPVIEK VMKGQNPAS PESRSTEGSP KIKTGLPKKE
LQQHHHHHHH HHHHHHSESK ASATSPEPET SKDNIGVQEP QDLSVKMCKE EKLPESDGCA
QEPAKTQPAD KCRNRAEGER KDIVSSVPRP TREEPVDTRT TVTERVS

DNA base sequence:

BASE COUNT: 597 a 333 c 377 g 321 t

1 ggacagag aaaatggccg ctgcgccgag cggagaggag agactggaag aaaaatctga
61 ggatcaagat cttcaaggac aaaaagataa accaccaaaa ctcaggaaag taaaaaaga
121 caagaaggat gaggaagaaa agcaggaacc atttcattcc tctgagcatc agccccgaga
181 acctgcagat gaagggaag ctgatatgtc tgaaagtgtc gaggaaaacc ttgctgttcc
241 tgaatcttct gcctctccca aacagaggcg gtctgttatt agagacaggg gtcccatgta
301 cgaagaccct actcttctcg aaggctggac acgaaaactc aagcaaagaa aatctggctc
361 ttctgctgga aaattgatg tatatttaat caaccctaat ggaaaagctt ttcggctcaa
421 agttgagctt atagcatact tccaaaaggt aggggacaca tctctagacc ctaatgattt
481 tgacttcaact gtaactggga gagggagccc gtctcgaagg gaacagaagc aaccgaaaaa
541 gcctaaagct ccaaaatctt ctgtatcagg gagaggaaga ggaagacctt aaggaaat
601 aaaaaaagt aagccacctg taaaatctga aggagtacaa gtcaaaaggg tgatagagaa
661 gagtccggga aaacttttgg taaaatgccc ttattctgga actaaagagg catcagatgc
721 aacaacgtca caacaggttt tggtcattaa aagaggcggt cgtaaaagaa aatcagaaac
781 tgatccatct gcagctccta aaaaaagggg gagaaaagcca agcaactgta gcttggctgc
841 tgcagcagca gaagcagcaa agaaaaaagc aatcaaagag tcttccatca agcctctttt
901 agagactgtg ttaccaataa agaaacgcaa gaccagggag actatcagtg tagatgtaaa
961 agatacaata aaaccagagc ctcttacacc tgttatagaa aaagtcatga aaggacaaaa
1021 ccctgcaaaa agtccagaaa gcagaagcac agagggtagc ccaaaaatta aaactggctt
1081 gccgaaaaaa gagctgcagc agcaccatca tcatcatcac caccaccatc accatcatca
1141 ctccgaatct aaggcatctg ccaccagtcc agagccagag acttcaaagg acaacattgg
1201 ggttcaggag ccccaggact taagtgtcaa aatgtgtaaa gaggagaagc taccagaaag
1261 tgatggctgt gctcaggagc cagccaagac tcagcctgct gataaatgta gaaaccgagc
1321 agaagggtgaa agaaaagaca ttgtttcatc tgtccctaga ccaacaagag aagagcccgt
1381 ggacaccaga acaacggtga cagaaagagt tagctgactt taaaaggatt agcaggatct
1441 ggttgtttct ttctcgggca cctgtgtgtc tgttgcact gtctttctc atcgactgaa
1501 attttctaa tcgtaaaaca gttaaaatt aactaaggca gctctggctc cttctttgtg
1561 tgggtagggc tctgacaagg cttccctata aatgaaagta agaaaaaaaa aaaaaaaaaa
1621 aaaaaaa

Appendix D: *Xenopus* Sin3 amino acid and DNA sequences

NCBI ACCESSION: AF154112

Amino acid sequence:

Number of amino acids: 1275

```
MKRRLEPEEA AAYPPQPRRI AESFAHTRV LAPAPPTYEP PPDAMQPTAG IQYSVAPGYQ
VSAVPQSSGG HGQASLTAVH GSHHNTVPV THGGPAVQSH AHSTPPAAPA QGQQFQRLKV
EDALSYLDQV KLQFGSQPV YNDFLDIMKE FKSQSIDTPG VISRVSQLFK GHPELIMGFG
AFLPPGYKIE VQTNDLVNVT TPGQVHQITT HGLQPPIPQA PPSQPSAPP IPSPVHPTPQ
PPPAKISKPM QSQAHPTNQ QSTPIQYPSR SPSPAQPHTP GPLAHATPTA TAATPTMQNN
QPVEFNHAIN YVNIKKNRFQ GQPDYKSF EILHTYQKEQ RNAKEAGGNY TPALTEQEVY
AQVARLFKNQ EDLLSEFGQF LPDANSSVLL SKTTAEKVES VRNDHGGTVK KPQLNNKQQR
PNQNGCQIRR HSGTGVTTPV KKKPKILIPK DQSLADANKH GAGAESQFFD KVRKALRSAE
AYDNFLRCLV IFNQEVISRS ELVQLVSPFL AKFPELFTWF KNFLGYKESS HMESFPKERA
TEGIAMEIDY ASCKRLGSSY RALPKVFQPP KCTGRTPLSK EVLNDTWVSF PSWSEDSTFV
SSKKTQYEEH IYRCEDERFE LDVVLETNLA TIRVLETVQK KLSRLSAEDQ AKFRLDNTLG
GTSEVIHRKA LQRIYADKAA DIIDGLKKNP AVAVPIVLKR LKMKEEWEWRE AQRGFNKIWR
EQNEKYLLKS LDHQGINYKQ IDTKVLRSKS LLNEIESIYD ERQEQVSEDN SGISSGPHLT
LTYDDKQILD DAASLIHVV KRQTGIQKED KYKIKQIVYH FIPDLLFSQR GELSDVEEEE
EEETVEAEDG VTKKHNGVGV GGGSSPPKAK LMFNGTAAQK WRGMEDAYNL FYVNNWYIF
LRLHQILCSR LLRIYNQAEK QVEEEMRERE WEREVLGLKR DKNSAAIQL RLKEPMDIEA
EDYNPAFLDM VRNLLDGNMD SNQYEDSLRE MFTIHAFTTF TMDKLIQSIV RQLQHIVSDE
ICVQVTELYL SESNTNATGG LLSTQASRNL NEANYQRKAE QLMSDENCfk LMFSQSRGQV
QLTIELLDTE EENSDDPAET ERWSYIERY MNCDSSTPEV REHLAQKPVF LPRNLRIRK
CQRGREQQEK DGSGKRALEN LESLDKLQCK FKLNSYKMYV VIKSEYMYR RTALLRAQQS
HERVSKRLHQ RFQSWLRKWN VEHVSHEMAS ESRKWLMGEG VEGMVPCTTS RDSEILNFVD
INKYRVKYGA AFKTP
```

DNA sequence:

BASE COUNT: 1352 a 1022 c 1052 g 1095 t

```
1 ggcacgagcg gagatccagt gctcgtctaa ttctcgcggt cgaggtggcg tttggcgaac
61 aaaaaggcca tcaactggtgc ttgactatgt tctcaggatg aagcggcgat tggacgagcc
121 agaggcagct gcctatccac ctacgccccg caggattgct gaatctttg cccacacgca
181 tcgtgtactt gcccctgctc ctccaacata tgagcctcct cctgatgcta tgcagccac
241 tgcgggcatt cagtactctg tagcccctgg ataccaggtc tcagcagtc ctcagagctc
301 tggaggccat ggccaggcat cacttacagc agtgcatggt agtcatcacc acaacacgcc
361 tgtgccaacc catggaggac ctgctgtgca gagtcatgct cattcaacc cacctgctgc
421 acctgcacaa ggacaacagt tccagaggct aaaggtggag gatgctcttt cgtacctga
481 ccaggtaaaa ctgcagttt gtagccagcc acaggtgtac aatgactttc ttgacataat
541 gaaagaattc aagtcacaga gtattgacac accaggggtc ataagccggg tgtctcaact
601 cttcaaaggt catccagagc taatcatggg ctttggcgct ttcttgccac ctggatacaa
661 gatagaggtg caaacaatg acttggttaa tgtaacaact ccagggcaag tacaccagat
721 tacaacacat ggtctgcagc ctccaattcc tcaagctcct ccaccatcac agccatctgc
781 cccgccatt ccatcaccag tgcaccgac tcctcagcct ccgccagcta aatcagcaa
841 gccaatgcag tcccaggctc acaccccaac aatcagcaa agcacaccta tacagtaccc
901 atctccacga tetccaccag cacaccgca cacaccagga ccttggcaca atgctacacc
961 caccgcaact gcagcaactc ctacaatgca gaacaaccag ccagttgaat tcaaccacgc
1021 tattaactat gtaacaaga tcaagaaccg atttcaaggc cagccagaca tttacaagtc
1081 tttccttgag attctgcaca catatcagaa ggaacaacgc aatgctaaag aagcaggggg
1141 taattacaca ctagccctga ccgagcagga ggtctatgcc caggtagcaa gacttttaa
1201 aaaccaggag gacctgttat cagaatttgg ccaattttt ccagatgcca acagctctgt
1261 gcttttgagc aaaacaacag ctgaaaaagt tgaatctgta agaatgatc acggtgttac
1321 tgtgaagaag ccacaactta acaataagca gcagaggccc aatcagaatg gctgccaat
1381 tagaagacac tctgggactg gagtacacc tcctgttaag aagaacctta aattcttat
1441 ccctaaagac cagtcactgg cagatgccaa caaacatgga gcaggagcag aatcacagtt
```

1501 ttttgacaag gttcggaaag cactgcgagg tgcagaggca tacgataact tcctaagatg
1561 tcttgtgatc ttcaatcaag aagtaatttc ccggtccgag ctagtccagc tgggtgtctcc
1621 attcctagct aagttcccag agctgtttac atggtttaaa aatttcttgg gttacaaaga
1681 gtccctccac atggagagct tccccaaaaga gcgagctact gagggtattg ccatggagat
1741 tgactatgcc tcatgtaagc gtttggggtc gagttaccgg gctttgccaa aagtcttcca
1801 gcagccaaaa tgcactggca gaacaccact cagtaaagag gttttgaatg acacttgggt
1861 gtcttttcca tcttggctag aagactctac ttttgtgagc tctaaaaaga cacagtacga
1921 ggaacacatt taccgatgtg aagacgagag atttgagttg gacgtgggtat tagaaaccaa
1981 cctggctacc attcgtgttc tggagactgt tcagaagaaa ctttcacggc tttctgcgga
2041 ggaccaggcc aaattcagac tagacaatac acttggaggg acatctgagg tcatcccaccg
2101 caaggcttta cagaggatata atgcggataa agctgctgat ataatagatg gtctaaagaa
2161 aaaccctgct gtcgctgtac ccattgtcct aaagaggttg aaaaatgaagg aggaggagtg
2221 gcgggaagca cagcgtgggt ttaataagat ctggcgggaa cagaacgaga agtactatct
2281 taactctctg gatcatcagg gtatcaacta caaacagatt gatacaaagg tgttattcgtc
2341 caagagtctc cttaatgaga ttgagagcat ctatgatgag cggcaggaac aagtttcaga
2401 agacaactct gggatctctt ctggcccaca cctcacactc actatgatg acaaacagat
2461 actggacgat gtagcctcac ttatcatcca ccatgtaaaa cgacagacty gcatacaaaa
2521 ggagacaaa aaattcagac agcagattgt ctatcatttt atcccggatt tactttttc
2581 tgcagctggg gagctctctg atgtagagga agaagaggag gaagaaacag tggaggctga
2641 agatggcgtt acaaaaaaac acaatggagt gggggttggg ggcggtagta gtcctccaaa
2701 ggctaagttg atgtttggaa atacagcagc acaaaagtgg cgtggatagg aggatgcata
2761 caaccctttt tatgtgaaca ataactggta catattcctt cgcctacatc agatattatg
2821 ttcccggctt cttcgcactc acaaccaggc agagaagcaa gtggaggaag agatgagggga
2881 aagggaatgg gaaagagagg tactgggact aaagagggac aaaaatgaca gcgcagctat
2941 acagcttcca ctaaaagaac caatggacat agaggctgaa gattataatc cagcattcct
3001 agacatgggt cggaaacctgc ttgatgggaa catggactcc aatcagatg aggatcttt
3061 gcgagagatg tttaccatcc atgcctttac caccttactc atggacaagc tggattcagag
3121 cattgttaga cagctccagc acatagtcag tgatgaaatc tgtgtgcagg tgactgaact
3181 gtacctttct gagagcaata ccaatgccac aggaggctcg ttaaccactc aggcttcacg
3241 taactgaat gagggcaaac accagcgtaa agctgagcag ctaatgtcag atgagaattg
3301 cttcaagctg atgttctccc agagtcgtgg acaggctccag ttaacaattg aactactgga
3361 cactgaggaa gaaaattctg atgaccagc ggagaccgag cgctggtctg attacattga
3421 gaggtacatg aactgtgact ccacttctcc agaagtccga gagcaccttg cacaaaaacc
3481 tgtgttctg cctagaaact tgcgcagaat aagaaagtgc cagaggggca gggagcagca
3541 agagaaagat gggagtggaa agcgtgcact ggagaacttg gagagccttg ataagctca
3601 gtgcaagttt aaactgaatt cttacaagat ggtctatgtg ataaaatctg aggactacat
3661 gtatcggcga actgcccctg tgcgggcaca gcagtcccac gaacgagtg gcaaacgatt
3721 gcaccagcgc ttccagtcct ggctgagaaa atggaatgtt gaacatgta gccatgaaat
3781 ggcctctgaa agcagaaagt ggctgatggg ggaggaggtt gagggaaatg tgcctgttac
3841 cactagtaga gactctgaga tcctgaactt tgtggacatt aataagtatc gagtcaagta
3901 tggggcagcc ttcaaaaccc cataacattt ttaaactgaa gaatacatta aaaaaacagc
3961 aacctgagaa ctctgagatt gatctgaaga gcattgcttg ctgtctaaac cagaaggatg
4021 gtcatcaaaag gcatgactag gcctcaacc ttgaaatagag aatttatgaa cctcttctg
4081 tgccagagga ctggagaaat ggtacagtgt tactgaaatt gtccttctt cctgccattt
4141 tgtcccagta aatccacttt gccacccttc tgtaaataca tgcgtgtaca gaatgtcaac
4201 aagggctctg ttgattaatt tcttgtacc catattgcat attatttat aacaggatc
4261 attagtttta tgttagatgt ctttgaaca tagtaatggg ggaagggaca tcttagaag
4321 ccacaccctc cccgggggag tctgttgaga agagtgggtt taatatatat atgtgtgtgt
4381 gtatatatgt atgtatatat atatatatat atatatatat atatatatat atatatatat
4441 atgtatatat gtgtatatat atatatattt cttcccttga ctgtcttctc aatgtgtttt
4501 attttcttt cccaccctt t

Appendix E: *Xenopus* importin- α amino acid and DNA sequences

NBCI ACCESSION: L36339

Amino acid sequence: Number of amino acids: 522

```

MPTTNEADER MRKFKNKGKD TAE LR RRR RVE VSVELRKAKK DEQILKRRNV CLPEELILSP
EKNAMQSVQV PPLSLEEIVQ GMNSGDPENE LRCTQAARKM LSRERNPPLN DIIEAGLIPK
LVEFLSRHDN STLQFEAWA LTNIASGTS D QTKSVVDGGA IPAFISLISS PHLHISEQAV
WALGNIAGDG PLYRDALINC NVIPPLLALV NPQTPLGYLR NITWMLSNLC RNKNPYPPMS
AVLQILPVL T QLMHHDDKDI LSDTCWAMSY LTDGSNDRID VVVKTGIVDR LIQLMYSPEL
SIVTPSLR TV GNIVTGTDKQ TQAAIDAGVL SVLPQLLRHQ KPSIQKEAAW AISNIAAGPA
PQIQQMITCG LLSPLVDLLN KGDFKAQKEA VWAVTNYTSG GTVEQVVQLV QCGVLEPLL N
LLTIKDSKTI LVILDAISNI FLAAEKLGEQ EKLC LLVEEL GGLEKIEALQ THDNH MVYHA
ALALIEKYFS GEEADDIALE PEMGKDAYTF QVPMQKESF NF
    
```

DNA base sequence: BASE COUNT: 515 a 334 c 390 g 434 t

```

1 gttgcaaatc cgaagaatct gtagaaccga tcaaaatgcc gaccacaaat gaagcagatg
61 agaggatgag gaagttaag aacaaaggca aagacacggc ggaattgagg cgcagaagag
121 tggaaagtcag tgtggagctt aggaaggcaa agaaggatga acagatattg aagaggagaa
181 atgtatgctt accagaagag ctgattctct ctccagaaaa gaatgctatg cagagtgtgc
241 aggttcctcc actttctctg gaagaaattg tgcaaggaaat gaattctggt gatcctgaaa
301 atgaactcag gtgtacacaa gctgcaagga aaatgctatc cagagagagg aatcctccat
361 taaatgatat aatagaagca ggattgattc caaagctggt ggaattcctg agccgtcatg
421 ataacagcac cctgcagttt gaagctgcct gggcactgac caacattgct tctgggacct
481 ctgaccagac gaagtctggt gtggatggag gcgccattcc tgcctttata tcaattattt
541 cttcaccaca ccttcacatc agtgaacaag cagtatgggc tctgggaaat attgctggtg
601 atggcccact gtatagagat gctctaatac actgcaatgt gatcccacct ctgttggctc
661 tggttaacct ccagactccg ttgggttatt tgaggaatat tacatggatg ctatccaacc
721 tttgtcgaaa caagaatcca taccctccca tgtcggctgt cctgcaaat ctaccagtat
781 tgacacaact tatgcatcac gacgacaaag acattttgtc tgatacttgc tgggcaatgt
841 cttatcttac tgatggctca aatgatagaa ttgatgttgt ggtgaagact gggattgtgg
901 atcgtctaat tcaattgatg tacagtccag aactaagat agtgacacca tcaactgcgtg
961 ctgttggaaa tattgtcact ggcacagaca aacagaccca agcggccatt gatgctggtg
1021 tcctgtctgt gttgccacaa cttttacgac accagaagcc aagcattcag aaggaagcag
1081 catgggcaat aagtaacatt gctgcagggc cagctcccca gatccagcaa atgatcactt
1141 gtggattgct ttctccttta gtggatcttc tcaataaggg agacttcaag gccagaaaag
1201 aagcagtttg ggctgtaaca aactacacca gtggaggaac tgtggagcaa gtggttcagc
1261 tggtagcttg tggagttttg gaacccttc tgaatctact aactattaag gacagcaaaa
1321 ctattcttgt aattctggat gccatttcca acattttctt ggctgcagag aaacttggtg
1381 agcaggagaa actttgctta cttgttgaag aactaggagg acttgaaaaa attgaggctc
1441 tacaactca tgacaatcac atggtttatc atgcagcttt ggctctaata gaaaaatct
1501 tctcaggaga ggaggcggat gacattgctt tagagccaga gatgggaaag gatgcctaca
1561 cctttcaggt cccaaatag caaaaagagt ctttcaattt ctgaattatg aaacataatt
1621 tacagttggt aaattaaaaa taataaaagc atgtaaattt gaatttaca gtt
    
```

Appendix F: *Xenopus* RPD3 amino acid and DNA sequences

NCBI ACCESSION: AF020658

Amino acid sequence:

Number of amino acids: 480

MALSQGTKKK VCYYDGDVG NYYYGQGHM KPHRIRMTHN LLLNYGLYRK MEIYRPHKAS
AEEMTKYHSD DYIKFLRSIR PDMSEYSKQ MQRFNVEDC PVFDGLFEFC QLSTGGSVAS
AVKLNKQQT D ISVNWSGGLH HAKKSEASGF CYVNDIVLAI LELLKYHQRV VYIDIDIHHG
DGVEEAFYTT DRVMSVSFHK YGEYFPGTGD LRDIGAGK GK YYAVNYPLRD GIDDES YEAI
FKPVMTKVME MFQPSAVVLQ CGADSLSGDR LGC FNLTIKG HAKC VEFIKT FNL PMLMLGG
GGYTIRNVAR CWTYETAVAL DSEIPNELPY NDYFEYFGPD FKLHISPSNM TNQNTNEYLE
KIKQRLFENL RMLPHAPGVQ MQAIPEDSVH DDSGEEDEED PDKRISIRSS DKRIACDEEF
SDSEDEGEGG RKNVANFKKV KRVKTEEEKE GEDKKDVKEE EKAKDEKTDS KRVKEETKSV

DNA sequence:

BASE COUNT: 470 a 278 c 375 g 364 t

1 ggcacgaggc cgaaggaaaa tggcgctgag tcaaggaaca aagaagaaag tgtgctatta
61 ctatgatggt gatgttgaa attattatta tggacagggg cacccaatga aacctcatag
121 aattcgatg acacacaacc tgctgctcaa ctatggactt taccggaaaa tggagatcta
181 tagaccacac aaagccagtg cagaggagat gacaaagtat cacagtgatg attatatcaa
241 attcctgccc tccatacgac cagacaatat gtctgaatac agtaaacaga tgcagagatt
301 taatgttggg gaggactgtc ctgtgtttga tggcctatgt gagtctgccc agctctctac
361 aggaggctct gtagcaagtg ctgttaaact aaacaaacaa cagacggaca tttcagtgaa
421 ctggctctgg ggccttcac atgccaagaa atctgaggca tctggttttt gttatgtcaa
481 cgatattgtc cttgccatcc tggaaactact taagtatcac cagagagttg tgtatattga
541 catagacatt caccacggtg atgggtttga ggaggcattt tacacaactg atagggttat
601 gtcagtgtct ttccacaagt atggagagta tttccctgga actggagatc tgagagatat
661 tgggtgcagg aaagcacaat actatgctgt gaattacccc cttcgggatg ggattgatga
721 tgagtcctat gaagcaattt ttaaacagtg gatgacaaa gttatggaga tgttccagcc
781 aagtgcagtg gtcctacagt gtggagcaga ttcattatct ggggatagac ttggatgctt
841 caatttgacc atcaaaggac atgccaagtg tgtggagttc ataaagacct ttaacttgcc
901 aatgctgatg ctaggagggtg gcggttacac tatcaggaat gtggctcggt gctggacata
961 tgaacgggct gtggctctgg actccgagat acctaagtag cttccataca atgattattt
1021 tgaatatttt ggaccggact tcaaacttca catcagttca tccaacatga ccaatcagaa
1081 cactaatgaa tatctggaga aaatcaagca gcgcctcttt gagaacttgc gcatgctccc
1141 ccatgctcca ggagttcaga tgcaagccat cccagaggac tctgtacatg atgacagtg
1201 tgaagaagat gaagaagatc ctgacaagcg catttccatt cggatcatccg ataaaaggat
1261 tgcgtgcgac gaggagtctc cagattctga ggatgaaggg gagggagggtc gcaaaaacgt
1321 ggccaatttc aaaaaagtaa aacgggttaa aactgaagag gaaaaggaag gagaggacaa
1381 gaaagatggt aaagaagagg agaagctaa agatgagaag acggatagca aacgggttaa
1441 agaagagacc aatcagttc gatccttcaa ctatggggag aaaaatcc

Bibliography

- [1] **Kossel, A.** (1928). *The Protamines and Histones*. Longmans, London.
- [2] **Stedman, E. & Stedman, E.** (1947). *The chemical nature and functions of components of cell nuclei not histone but protein*. Cold Spring Harb. Symp. 12, 224-36.
- [3] **Watson, J.D. & Crick, F.H.C.** (1953). *A structure for deoxyribosenuclei acids*. Nature. 171, 737-738.
- [4] **Fitzsimmons, D.W. & Wolstenholme, G.E.W.** (1976). *The structure of chromatin*. CIBA Found. Symp. 28, 368.
- [5] **Avery, O.T., MacLeod, C.M. & McCarthy, M.** (1944). *Studies on the chemical nature of the substance inducing transformation of pneumococcal types*. J. Exp. Med. 79, 137-158.
- [6] **Bradbury, E.M.** (1992). *Reversible Histone modifications and the chromosome cell cycle*. BioEssays. 14, 9-15.
- [7] **Hayes, J.J. & Wolffe, A.P.** (1992). *The interaction of transcription factors with nucleosomal DNA*. BioEssays. 14, 597-602.
- [8] **Han, M. & Grunstein, M.** (1988). *Nucleosome loss activates yeast downstream promoters in vivo*. Cell. 55, 1137-1145.
- [9] **Megee, P.C., Morgan, B.A., Mittman, B.A. & Smith, M.M.** (1990). *Genetic analysis of histone H4: essential role of lysines subject to acetylation*. Science. 247, 4932-4934.
- [10] **Roth, S.Y. & Allis, C.D.** (1992). *Chromatin condensation: does histone H1 dephosphorylation play a role?* TIBS. 17, 93-98.
- [11] **Almouzni, G.A., Khochbin, S., Dimitrov, S. & Wolffe, A.P.** (1994). *Histone acetylation influences both gene expression and development of Xenopus laevis*. Dev. Biol. 165, 654-669.

- [12] **Wade, P.A., Pruss, D. & Wolffe, A.P.** (1997). *Histone acetylation: chromatin in action*. TIBS. 22, 128-132.
- [13] **Sternglanz, R.** (1996). *Histone acetylation: a gateway to transcription activation*. TIBS. 21, 357-358.
- [14] **Rundlett, S.E., Carmen, A.A., Kobayashi, R., Bavykin, S., Turner, B.M. & Grunstein, M.** (1996). *HDA1 and RPD3 are members of distinct yeast histone deacetylase complexes that regulate silencing and transcription*. Proc. Natl. Acad. Sci. USA. 93, 14503-14508.
- [15] **Wang, B-C. & Rose, J.** (1994). *The octomeric histone core of the nucleosome. Structural issues resolved*. J. Mol. Biol. 236, 179-188.
- [16] **Wolffe, A.P.** (1995). *Histones and transcriptional control*. In: *Eukaryotic Gene Transcription*, (Goodbourn, S., Ed.), pp 34-40. IRL Press. Oxford.
- [17] **Avents, G. & Moudrianakis, E.N.** (1995). *The histone fold: a ubiquitous architectural motif utilized in DNA compaction and protein dimerisation*. Proc. Natl. Acad. Sci. USA. 92, 11170-11174.
- [18] **Luger, K., Mäder, A.W., Richmond, R.K., Sargent, D.F. & Richmond, T.J.** (1997). *Crystal structure of the nucleosome core particle at 2.8Å resolution*. Nature. 389, 251-260.
- [19] **Rhodes, D.** (1997). *The nucleosome core all wrapped up*. Nature. 389, 231-233.
- [20] **Crane-Robinson, C.** (1997). *Where is the globular domain of linker histone located on the nucleosome?* TIBS. 22, 75-77.
- [21] **Dimitrov, S., Almouzni, G., Dasso, M. & Wolffe, A.P.** (1993). *Chromatin transitions during early *Xenopus* embryogenesis: changes in histone H4 acetylation and in linker histone type*. Dev. Biol. 160, 214-227.

- [22] **Travers, A.A.** (1994). *Chromatin structure and dynamics*. BioEssays. 16, 657-662.
- [23] **Almouzni, G. & Mechali, M.** (1988). *Assembly of spaced chromatin promoted by DNA synthesis in extracts from Xenopus eggs*. EMBO. J. 7, 665-672.
- [24] **Dilworth, S.M., Black, S.J. & Laskey, R.A.** (1987). *Two complexes that contain histones are required for nucleosome assembly in vitro: role of nucleoplasmin and NI in Xenopus egg extracts*. Cell. 51, 1009-1018.
- [25] **Almouzni, G., Clark, D.J., Mechali, M. & Wolffe, A.P.** (1990). *Chromatin assembly on replicating DNA in vitro*. NAR. 18, 5767-5774.
- [26] **Bulger, M., Ito, T., Kamakaka, R.T. & Kadonaga, J.T.** (1995). *Assembly of regularly spaced nucleosome arrays by Drosophila chromatin assembly factor 1 and a 56-kDa histone binding protein*. Proc. Natl. Acad. Sci. USA. 92, 11726-11730.
- [27] **Tyler, J.K., Bulger, M., Kamakaka, R.T., Kobayashi, R. & Kadonaga, J.T.** (1996). *The p55 subunit of Drosophila chromatin assembly factor 1 is homologous to a histone deacetylase-associated protein*. Mol. Cell Biol. 16, 6149-6159.
- [28] **Verreault, A., Kaufman, P.D., Kobayashi, R., Stillman, B.** (1996). *Nucleosome assembly by a complex of Caf-1 and acetylated histones H3/H4*. Cell. 87, 95-104.
- [29] **Kaufman, P.D.** (1996). *Nucleosome assembly: the CAF and the HAT*. Curr. Opin. Cell Biol. 8, 369-373.
- [30] **O'Neill, L.P. & Turner, B.M.** (1995). *Histone H4 acetylation distinguishes coding regions of the human genome from heterochromatin in a*

differentiation-dependent but transcription-independent manner. EMBO. J. 14, 3946-3957.

[31] **Hayes, J.J., Clark, D.J. & Wolffe, A.P.** (1991). *Histone contributions to the structure of DNA in the nucleosome.* Proc. Natl. Acad. Sci. USA. 88, 6829-6834.

[32] **Sommerville, J., Baird, J. & Turner, B.M.** (1993). *Histone H4 acetylation and transcription in amphibian chromatin.* J. Cell. Biol. 120, 277-290.

[33] **Moretti, P., Freeman, K., Coodly, L. & Shore, D.** (1994). *Evidence that a complex of SIR proteins interacts with the silencer and telomere-binding protein RAP1.* Genes & Development. 8, 2257-2269.

[34] **Hecht, A., Strahl-Bolsinger, S. & Grunstein, M.** (1996). *Spreading of transcriptional repressor SIR3 from telomeric heterochromatin.* Nature. 383, 92-96.

[35] **Hecht, A., La roche, T., Strahl-Bolsinger, S., Gasser, S.M. & Grunstein, M.** (1995). *Histone H3 and H4 N-termini interact with SIR3 and SIR4 proteins: a molecular model for the formation of heterochromatin in yeast.* Cell. 80, 583-592.

[36] **Vettesse-Dadey, M., Grant, P.A., Hebbes, T.R., Crane- Robinson, C., Allis, C.D. & Workman, J.L.** (1996). *Acetylation of histone H4 plays a primary role in enhancing transcription factor binding to nucleosomal DNA in vitro.* EMBO. J. 15, 2508-2518.

[37] **Turner, B.M. & Fellows, G.** (1989). *Specific antibodies reveal ordered and cell-cycle-related use of histone-H4 acetylation sites in mammalian cells.* Eur. J. Biochem. 179, 131-139.

- [38] **Turner, B.M.** (1989). *Acetylation and deacetylation of histone H4 continue through metaphase with depletion of more-acetylated isoforms and altered site usage.* Experimental Cell Research. 182, 206-214.
- [39] **Patterson, D. & Wolffe, A.P.** (1996). *Developmental roles for chromatin and chromosomal structures.* Dev. Biol. 173, 2-13.
- [40] **Steger, D.J. & Workman, J.L.** (1996). *Remodelling chromatin structure for transcription: what happens to the histones?* BioEssays. 18, 875-884.
- [41] **Bartsch, J., Truss, M., Bode, J. & Beato, M.** (1996). *Moderate increases in histone acetylation activates the mouse mammary tumour virus promoter and remodels its nucleosome core.* Proc. Natl. Acad. Sci USA. 93, 10741-10746.
- [42] **Turner, B.M.** (1993). *Decoding the nucleosome.* Cell. 75, 5-8.
- [43] **De Rubertis, F., Kadosh, D., Henchoz, S., Pauli, D., Reuter, G., Struhl, K. & Spierer, P.** (1996). *The histone deacetylase RPD3 counteracts genomic silencing in Drosophila and Yeast.* Nature. 384, 589-591
- [44] **Patterson, D. & Wolffe, A.P.** (1996). *Developmental roles for chromatin and chromosomal structures.* Dev. Biol. 173, 2-13.
- [45] **Chambers, S.A.M. & Shaw, B.R.** (1984). *Levels of histone H4 diacetylation decreases dramatically during sea urchin embryonic development and correlate with cell doubling rate.* J. Biol. Chem. 259, 13458-13463.
- [46] **Ikegami, S., Ooe, Y., Shimizu, T., Kasahara, T., Tsuruta, T., Kijima, M., Yoshida, M. & Beppu, T.** (1993). *Accumulation of multiacetylated forms of histones by trichostatin A and its developmental consequences in early starfish development.* Roux's Arch. Dev. Biol. 202, 144-151.
- [47] **Grabher, A., Brosch, G., Sendra, R., Lechner, T., Eberharder, A.,**

- Georgieva, E.I., López-Rodas, G., Franco, L., Dietrich, H. & Loidl, P.** (1994). *Subcellular localisation of enzyme involved in core histone acetylation.* *Biochem.* 33, 14887-14895.
- [48] **López-Rodas, G., Georgieva, E.I., Sendra, R. & Loidl, P.** (1991). *Histone acetylation in Zea mays I.* *J. Biol. Chem.* 266, 18745-18750.
- [49] **Parthun, M.R., Widom, J. & Gottschling, D.E.** (1996). *The major cytoplasmic histone acetyltransferases in yeast: links to chromatin replication and histone metabolism.* *Cell.* 87, 85-94.
- [50] **Kleff, S., Andrulis, E.D., Anderson, C.W. & Sternglanz, R.** (1995). *Identification of a gene encoding a yeast histone H4 acetyltransferase.* *J. Biol. Chem.* 270, 24674-24677.
- [51] **Brownell, J.E., Zhou, J., Ranalli, T., Kobayashi, R., Edmondson, D.G., Roth, S.Y. & Allis, C.D.** (1996). *Tetrahymena histone acetyltransferase A: a homologue to yeast Gcn5p linking histone acetylation to gene activation.* *Cell.* 84, 843-851.
- [52] **Wolffe, A.P. & Pruss, D.** (1996). *Targeting chromatin disruption: transcription regulators that acetylate histones.* *Cell.* 84, 1-20.
- [53] **Sobel, R.E., Cook, R.G. & Allis C.D.** (1994). *Non-random acetylation of histone H4 by a cytoplasmic histone acetyltransferase as determined by novel methodology.* *J. Biol. Chem.* 269, 18576-18582.
- [54] **Perry, C.A., Allis, C.D. & Annunziato, A.T.** (1993). *Parental nucleosomes segregated to a newly replicated chromatin are under acetylated relative to those assembled de novo.* *Biochem.* 32, 13615-13623.
- [55] **Kiermaier, A. & Eilers, M.** (1997). *Transcriptional control: calling in histone deacetylase.* *Curr. Biol.* 7, R505-R507.

- [56] **Hay, C.W. & Candido, E.P.M.** (1983). *Histone deacetylase. Association with a nuclease resistant, high molecular weight fraction of HeLa cell chromatin.* J. Biol. Chem. 258, 3726-3734.
- [57] **Wolffe, A.P.** (1996). *Histone deacetylase: a regulator of transcription.* Science. 272, 371-373.
- [58] **Vidal, M. & Gaber, R.F.** (1991). *RPD3 encodes a second factor required to achieve maximum positive and negative transcriptional states in Saccharomyces cerevisiae.* Mol. Cell. Biol. 11, 6317-6327.
- [59] **Taunton, J., Hassig, C.A. & Schreiber, S.L.** (1996). *A mammalian histone deacetylase related to the yeast transcriptional regulator Rpd3p.* Science. 272, 408-411.
- [60] **Ladomery, M. Lyons, S. & Sommerville, J.** (1997). *Xenopus HDm, a maternally expressed histone deacetylase, belongs to an ancient family of acetyl-metabolising enzymes.* Gene. 198, 275-280.
- [61] **Grundy, F.J., Waters, D.A., Takova, T.Y. & Henkin, T.M.** (1993). *Identification of genes involved in utilization of acetate and acetoin in Bacillus subtilis.* Molecular Microbiology. 10, 259-271.
- [62] **Jenkins, L.S. & Nunn, W.D.** (1987). *Genetic and molecular characterization of the genes involved in short-chain fatty acid degradation in Escherichia coli: the ato system.* J. Bacteriology. 169, 42-52.
- [63] **Leipe, D.D. & Landsman, D.** (1997). *Histone deacetylases, acetoin utilization proteins and acetylpolyamine amidohydrolases are members of an ancient protein superfamily.* Nucleic Acids Research. 25, 3693-3697.

- [64] **Carstea, E.D., Miller, S.P.F., Christakis, H. & O'Neill, R.R.** (1993). *Analogues of Butyric acid that increase the expression of transfected DNAs.* Biochem. Biophys. Res. Comm. 192, 649-656.
- [65] **Yoshida, M., Horinouchi, S. & Beppu, T.** (1995). *Trichostatin A and Trapoxin: novel chemical probes for the role of histone acetylation in chromatin structure and function.* BioEssays. 17, 423-430.
- [66] **McCaffery, P.G., Newsome, D.A., Fibach, E. et al** (1997). *Induction of γ -Globin by histone deacetylase inhibitors.* Blood. 90, 2075-2083.
- [67] **Minucci, S., Horn, V., Bhattacharyya, N., Russanova, V., Ogryzko, V.V., Gabriele, L., Howard, B.H. & Ozato, K.** (1997). *A histone deacetylase inhibitor potentiates retinoid receptor action in embryonal carcinoma cells.* Proc. Natl. Acad. Sci. USA. 94, 11295-11300.
- [68] **Miyashita, T., Yamamoto, H., Nishimune, Y., Nozaki, M., Morita, T. & Matsushiro, A.** (1994). *Activation of the mouse cytokeratin A (endo A) gene in teratocarcinoma F9 cells by the histone deacetylase inhibitor Trichostatin A.* FEBS Letters. 353, 225-229.
- [69] **Chen, W.Y., Bailey, E.C., McCune, S.L., Dong, J.Y. & Townes, T.M.** (1997). *Reactivation of silenced, virally transduced genes by inhibitors of histone deacetylase.* Proc. Natl. Acad. Sci. USA. 94, 5798-5803.
- [70] **Sanchez Del Pino, M.M., López-Rodas, G., Sendra, R. & Tordera, V.** (1994). *Properties of the yeast nuclear histone deacetylase.* Biochem. J. 303, 723-729.
- [71] **Carmen, A.A., Rundlett, S.E. & Grunstein, M.** (1996). *HDA1 and HDA3 are components of a yeast histone deacetylase (HDA) complex.* J. Biol. Chem. 271, 15837-15844.

- [72] **Pederson, T.** (1998). *Thinking about a nuclear matrix*. Journal Mol. Biol. In press.
- [73] **Brosch, G., Georgieva, E.I., López-Rodas, G., Lindner, H. & Loidl, P.** (1992). *Specificity of Zea mays is regulated by phosphorylation*. J. Biol. Chem. 267, 20561-20564.
- [74] **López-Rodas, G., Brosch, G., Golderer, G., Lindner, H., Gröbner, P. & Loidl, P.** (1992). *Enzymes involved in the dynamic equilibrium of core histone acetylation of Physarum polycephalum*. FEBS letters. 296, 82-86.
- [75] **Hendzel, M.J., Delcuve, G.P. & Davie, J.R.** (1991). *Histone deacetylase is a component of the internal nuclear matrix*. J. Biol. Chem. 266, 21936-21942.
- [76] **Li, W., Chen, H.Y. & Davie, J.R.** (1996). *Properties of chicken erythrocyte histone deacetylase associated with the nuclear matrix*. Biochem. J. 314, 631-637.
- [77] **Holmes, S.G. & Broach, J.R.** (1996). *Silencers are required for inheritance of the repressed state in yeast*. Genes & Dev. 10, 1021-1032.
- [78] **Enomoto, S. & Berman, J.** (1998). *Chromatin assembly factor 1 contributes to the maintenance, but not the re-establishment, of silencing at the yeast silent mating loci*. Genes & development. 12, 219-232.
- [79] **Stone, E.M. & Pillus, L.** (1998). *Silent chromatin in yeast: an orchestrated medley featuring sir3p*. BioEssays. 20, 30-40.
- [80] **James, T.C. & Elgin, S.C.R.** (1986). *Identification of a non-histone chromosomal protein associated with heterochromatin in Drosophila melanogaster and its gene*. Mol. Cell. Biol. 6, 3862-3872.
- [81] **Elgin, S.C.R.** (1990). *Chromatin structure and gene activity*. Curr. Opin. Cell. Biol. 2, 437-445.

- [82] **Zink, B. & Paro, R.** (1989). *In vivo binding pattern of a trans regulator of homeotic genes in Drosophila melanogaster.* Nature. 337,468-471.
- [83] **Klar, A.J.S & Bonaduce, M.J.** (1991). *swi6, a gene required for mating-type switching, prohibits meiotic recombination in the mat2-mat3 "cold spot" of fission yeast.* Genetics. 129, 1033-1042.
- [84] **Moehrle, A & Paro, R.** (1994). *Spreading the silence: epigenetic transcriptional regulation during Drosophila development.* Dev. Genet. 15, 478-484.
- [85] **Locke, J., Kotarski, M.A. & Tartof, K.D.** (1988). *Dosage dependent modifiers of position effect variegation in Drosophila and a mass action model that explains their effect.* Genetics. 120, 181-188.
- [86] **Orlando, V. & Paro, R.** (1993). *Mapping Polycomb-repressed domains in the bithorax complex using in vivo formaldehyde cross-linked chromatin.* Cell. 75, 1187-1198.
- [87] **Moore, G.D., Sinclair, D.A. & Grigliatti, T.A.** (1983). *Histone gene multiplicity and position effect variegation in Drosophila melanogaster.* Genetics. 105, 327-344.
- [88] **Mottus, R, Reeves, R. & Grigliatti, T.A.** (1980). *Butyrate suppression of position effect variegation in Drosophila melanogaster.* Mol. Gen. Genet. 178, 465-469.
- [89] **Kadosh, D. & Struhl, K.** (1998). *Targeted recruitment of the Sin3-Rpd3 histone deacetylase complex generates a highly localized domain of repressed chromatin in vivo.* Mol. Cell Biol. 18, 5121-5127.

- [90] Ayer, D.E., Lawrence, Q.A. & Eisenman, R.N. (1995). *Mad-Max transcriptional repression is mediated by ternary complex formation with mammalian homologues of yeast repressor Sin3*. Cell. 80, 767-776.
- [91] Sommer, A., Hilfenhaus, S., Menkel, A., Kremmer, E., Seiser, C., Loidl, P. & Lüscher, B. (1997). *Cell growth inhibition by the Mad/Max complex through recruitment of histone deacetylase activity*. Curr. Biol. 7, 357-365.
- [92] Schreiber-Agus, N., Chin, L., Chen, K., Torres, R., Rao, G., Guida, P., Skoultchi, A.I. & DePinho, R.A. (1995). *An amino-terminal domain of Mxi1 mediates anti-myc oncogenic activity and interacts with a homologue of the yeast transcriptional repressor SIN3*. Cell. 80, 777-786.
- [93] Stillman, D.J., Dorland, S. & Yu, Y. (1994). *Epistasis analysis of suppressor mutations that allow HO expression in the absence of the yeast SWI5 transcriptional activator*. Genetics. 136, 781-788.
- [94] Wolffe, A.P. (1997). *Sinful repression*. Nature. 387, 16-17.
- [95] Heinzl, T., Lavinsky, R.M., Mullem, T-M, Söderstrom, M., Laherty, C.D., Torchia, J., Yang, W.M., Brard, G., Ngo, S.D., Davie, J.R., Seto, E., Eisenman, R.N., Rose, D.W., Glass, C.K. & Rosenfeld, M.G. (1997). *A complex containing N-CoR, mSin3 and histone deacetylase mediates transcriptional repression*. Nature. 387, 43-48.
- [96] Dhordain, P., Albagli, O., Lin, R.J., Ansieau, S., Quief, S., Leutz, A., Kerckaert, J.P., Evans, R.M & Leprince, D. (1997). *Corepressor SMRT binds the BTB/POZ repressing domain of the Lz3/BCL6 oncoprotein*. Proc. Natl. Acad. Sci. USA. 94, 10762-10767.

- [97] **Nomura, T., Khan, M.M., Kaul, S.C., Dong, H.D., Wadhwa, R., Colmenares, C., Kohno, I. & Ishii, S.** (1999). *Ski is a component of the histone deacetylase complex required for transcriptional repression by Mad and thyroid hormone receptor.* Genes Dev. 13, 412-423.
- [98] **Hu, X. & Lazar, M.A.** (2000). *Transcriptional repression by nuclear hormone receptors.* TEM. 11, 6-10.
- [99] **Ghosh, A.K., Steele, R. & Ray, R.B.** (1999). *MBP-1 physically associates with histone deacetylase for transcriptional repression.* Biochem. Biophys. Res. Comm. 260, 405-409.
- [100] **Wong, C-W. & Privalsky, M.L.** (1998). *Transcriptional repression by the SMRT-mSin3 corepressor: multiple interactions, multiple mechanisms, and a potential role for TFIIB.* Mol. Cell. Biol. 18, 5500-5510.
- [101] **Brehm, A., Miska, E.A., McCance, D.J., Reid, J.L., Bannister, A.J. & Kouzarides, T.** (1998). *Retinoblastoma protein recruits histone deacetylase to repress transcription.* Nature. 391, 597-601.
- [102] **Magnaghi-Jaulin, L., Groisman, R., Naguibneva, I., Robin, P., Lorain, S., Le Villain, J.P., Troalen, F., Trouche, D. & Harel-Bellan, A.** (1998). *Retinoblastoma protein represses transcription by recruiting a histone deacetylase.* Nature. 391, 601-604.
- [103] **Vermaak, D. & Wolffe, A.** (1998). *Dissection of a functional deacetylase in frogs.* 15th International Workshop on the Cell Nucleus. Meeting abstract, p77.
- [104] **Luo, R.X., Postigo, A.A. & Dean, D.C.** (1998). *Rb interacts with histone deacetylase to repress transcription.* Cell. 92, 463-473.

- [105] **Nan, X., Ng, H-H., Johnson, C.A., Laherty, C.D., Turner, B.M., Eisenman, R.N. & Bird, A.** (1998). *Transcriptional repression by the methyl-CpG-binding protein MeCP2 involves a histone deacetylase complex.* Nature. 393, 386-389.
- [106] **Jones, P.L., Veenstra, G.J.C., Wade, P.A., Vermaak, D., Kass, S.U., Landsberger, N., Strouboulis, J. & Wolffe, A.P.** (1998). *Methylated DNA and MeCP2 recruit histone deacetylase to repress transcription.* Nature genetics. 19, 187-191.
- [107] **Razin, A.** (1998). *CpG methylation, chromatin structure and gene silencing – a three-way connection.* EMBO J. 17, 4905-4908.
- [108] **Bird, A.** (1995). *Gene number, noise reduction and biological complexity.* Trends Genet. 11, 94-100.
- [109] **Jones, P.A.** (1985). *Altering gene expression with 5-Azacytidine.* Cell. 40, 485-486.
- [110] **Woodland, H.R.** (1990). *Regulation of protein synthesis in early amphibian development.* J. Reprod. Fert. Suppl. 42, 215-224.
- [111] **Chambers, S.A.M. & Ramsey-Shaw, B.** (1987). *Histone modifications accompanying the onset of developmental commitment.* Dev. Biol. 124, 523-531.
- [112] **Hock, R., Moorman, A., Fischer, D. & Scheer, U.** (1993). *Absence of somatic histone H1 in oocytes and preblastula embryos of Xenopus laevis.* Dev. Biol. 158, 510-522.
- [113] **Dworkin-Rastl, E., Kandolf, H & Smith, R.C.** (1994). *The maternal histone H1 variant, HIM (B4 protein), is the predominant H1 histone in Xenopus preblastula embryos.* Dev. Biol. 161, 425-439.

- [114] **Nightingale, K., Dimitrov, S., Reeves, R. & Wolffe, A.P.** (1996). *Evidence for a shared role of HMG1 and linker histones B4 and H1 in organising chromatin.* EMBO J. 15, 548-561.
- [115] **Bouvet, P., Dimitrov, S. & Wolffe, A.P.** (1994). *Specific regulation of chromosomal 5S rRNA transcription in vivo by histone H1.* Genes Dev. 8, 1147-1159.
- [116] **Vancurova, I., Paine, T.M., Lou, W. & Paine, P.L.** (1995). *Nucleoplasmin associates with and is phosphorylated by casein kinase II.* J. Cell Science. 108, 779-787.
- [117] **Kleinschmidt, J.A. & Seiter, A.** (1988). *Identification of domains involved in nuclear uptake and histone binding of protein N1 of Xenopus laevis.* EMBO. J. 7, 1605-1614.
- [118] **Jans, D.A.** (1995). *The regulation of protein transport to the nucleus by phosphorylation.* Biochem. J. 311, 705-716.
- [119] **Vandromme, M., Gauthier-Rouvière, C., Lamb, N. & Fernandez, A.** (1996). *Regulation of transcription factor localization: fine-tuning of gene expression.* TIBS. 21, 59-64.
- [120] **Dumont, J.N.** (1977). *Oogenesis in Xenopus laevis.* J. Morph. 136, 153-180.
- [121] **Gilbert, S.F.** (1994). *Developmental Biology*, 4th Ed. Sinauer Associates, Inc. Massachusetts.
- [122] **Ferrell, J.E. Jr.** (1999). *Xenopus oocyte maturation: new lessons from a good egg.* BioEssays. 21, 833-842.

- [123] **Nieuwkoop, P.D. & Faber, J.** (eds). (1956). *A systematical and chronological survey of the development from the fertilized egg till the end of metamorphosis*. North-Holland Publishing company.
- [124] **Severne, Y., Schaffner, W. & Rusconi, S.** (1988). Metal binding 'finger' structures in the glucocorticoid receptor defined by site-directed mutagenesis. *EMBO J.* 7, 2503-2508.
- [125] **Tanaka, M. & Herr, W.** (1990). Differential transcriptional activation by Oct-1 and Oct-2-interdependent activation domains induce Oct-2 phosphorylation. *Cell.* 60, 375-386.
- [126] **Jones, D.S.C. & Schofield, J.P.** (1990). A rapid method for isolating high quality plasmid DNA suitable for DNA sequencing. *Nucleic Acids Research.* 18, 7463.
- [127] Ready-To-Go™ PCR beads instructions. Pharmacia Biotech.
- [128] Nucleon easiCLONE KIT instruction booklet (version 1.1). Scotlab bioscience.
- [129] **Boyle, J.S., Lew, A.M.** (1995). An inexpensive alternative to glassmilk for DNA purification. *Trends in Genetics.* 11, 8.
- [130] Ready-To-Go™ T4 DNA ligase instructions. Pharmacia Biotech
- [131] Instructions on Transformation of Competent Novagen *E.coli*. Novagen
- [132] mMessage mMachine instruction manual. Ambion.
- [133] **Williams, J.A., Langeland, J.A., Thalley, B.S.** (1995). *Expression of foreign proteins in E.coli using plasmid vectors and purification of specific polyclonal antibodies*. In: *DNA cloning 2. Expression systems*. 2nd ed. (Glover, D.M. & Hames, B.D. eds). pp41-42. IRL Press, Oxford.

- [134] **Smith, L.D., Xu, W. & Varnold, R.L.** (1991). Oogenesis and oocyte isolation. In: *Methods in cell biology* (Kay, B.K. & Peng, H.B. eds) 36, pp 47-51. Acad. P., NY.
- [135] **Paine, P.L., Johnson, M.E., Lau, Y-T., Tluczek, L.J. & Miller, D.S.** (1992). The oocyte nucleus isolated in oil retains in vivo structure and function. *BioTechniques*. 13, pp 238-245.
- [136] **Evans, J.P. & Kay, B.K.** (1991). Biochemical fractionation of oocytes. In: *Methods in cell biology* (Kay, B.K. & Peng, H.B. eds) 36, pp 142-143. Acad. P., NY.
- [137] **Gutierrez, L., Magee, A.I., Marshall, C.J. & Hancock, J.F.** (1989). Post-translational processing of p21^{ras} is two-step and involves carboxyl-methylation and carboxy-terminal proteolysis. *EMBO. J.* 8, 1093-1098.
- [138] **Evans, J.P. & Kay, B.K.** (1991). Biochemical fractionation of oocytes. In: *Methods in cell biology* (Kay, B.K. & Peng, H.B. eds) 36, 138-139. Acad. P., NY.
- [139] **Colman, A.** (1984). Translation of eukaryotic messenger RNA in *Xenopus* oocytes. In: *Transcription and translation, a practical approach* (Hames, B.D. & Higgins, S.J. eds) pp 275-282. Acad. P., NY.
- [140] **Degtyarev, M.Y., Spiegel, A.M. & Jones, T.L.Z.** (1993). The G protein α_s subunit incorporates [³H]palmitic acid and mutation of cysteine-3 prevents this modification. *Biochemistry*. 32, 8057-8061.
- [141] **Cummings, A., Barrett, P. & Sommerville, J.** (1989). Multiple modifications in the phosphoproteins bound to stored messenger RNA in *Xenopus* oocytes. *Biochemica et Biophysica Acta*. 1014, 319-326.

- [142] **See, Y.P. & Jackowski, G.** (1990). SDS gel electrophoresis. In: *Protein structure, a practical approach* (Rickwood, D & Hames, B.D. eds). pp 8-9. IRL Press, Oxford.
- [143] **Williams, J.A., Langeland, J.A., Thalley, B.S.** (1995). Expression of foreign proteins in E.coli using plasmid vectors and purification of specific polyclonal antibodies. In: *DNA cloning 2. Expression systems*. 2nd ed. (Glover, D.M. & Hames, B.D. eds). pp39-40. IRL Press, Oxford.
- [144] ECL Western blotting detection reagents and ECL Western blotting analysis system instruction booklet. Amersham Life Science Ltd.
- [145] **Klymkowsky, M.W. & Hanken, J.** (1991). Whole mount staining of *Xenopus* and other vertebrates In: *Methods in cell biology* (Kay, B.K. & Peng, H.B. eds) 36, p431. Acad. P., NY.
- [146] **Denegre, J.M., Ludwig, E.R. & Mowry, K.L.** (1997). Localized maternal proteins in *Xenopus* revealed by subtractive immunization. *Devel. Biol.* 192, 446-454.
- [147] **Lemaitre, J-M & Mechali, M.** (1998). Dynamics of the genome during early *Xenopus laevis* development: karyomeres as independent units of replication. *J. Cell Biol.* 142, 1159-1166.
- [148] **Fagotto, F. & Gumbiner, B.M.** (1994). β -catenin localization during *Xenopus* embryogenesis: accumulation at tissue and somite boundaries. *Development.* 120, 3667-3679.
- [149] **Wade, P.A., Jones, P.L., Vermaak, D. & Wolffe, A.P.** (1998). A multiple subunit Mi-2 histone deacetylase from *Xenopus laevis* cofractionates with an associated Snf2 superfamily ATPase. *Curr. Biol.* 8, 843-846.

- [150] **Ng, H-H. & Bird, A.** (2000). *Histone deacetylases: silencers for hire.* *TIBS.* 25, 121-126.
- [151] **Kleinschmidt, J.A., Fortkamp, E., Krohne, G., Zentgraf, H. & Franke, W.W.** (1985). *Co-existence of two different types of soluble histone complexes in nuclei of Xenopus laevis oocytes.* *J. Biol. Chem.* 260, 1166-1176.
- [152] **Vermaak, D., Wade, P.A., Jones, P.L., Shi, Y-B. & Wolffe, A.P.** (1999). *Functional analysis of the SIN3-Histone deacetylase RPD3-RbAp48-histone H4 connection in Xenopus oocyte.* *Molec. Cell. Biol.* 19, 5847-5860.
- [153] **Zhang, Y., LeRoy, G., Seelig, H.P., Lane, W.S. & Reinberg, D.** (1998). *The dermatomyositis-specific autoantigen Mi2 is a component of a complex containing histone deacetylase and nucleosome remodelling activities.* *Cell.* 95, 279-289.
- [154] **McIlhinney, R.A.J.** (1990). *The fats of life: the importance and function of protein acylation.* *TIBS.* 15, 387-391.
- [155] **Milligan, G., Parenti, M. & Magee, A.I.** (1995). *The dynamic role of palmitoylation in signal transduction.* *TIBS.* 20, 181-186.
- [156] **Mumby, S.M., Heukeroth, R.O., Gordon, J.I. & Gilman, A.G.** (1990). *G-protein α -subunit expression, myristoylation and membrane association in COS cells.* *Proc. Natl. Acad. Sci. USA.* 87, 728-732.
- [157] **Parenti, M., Viganó, M.A., Newman, C.M.H., Milligan, G. & Magee, A.I.** (1993). *A novel N-terminal motif for palmitoylation of G-protein α subunits.* *Biochem. J.* 291, 349-353.
- [158] **Imhof, A., Wolffe, A.P.** (1999). *Purification and properties of the Xenopus Hat1 acetyltransferase: Association with the 14-3-3 proteins in the oocyte nucleus.* *Biochemistry.* 38, 13085-13093.

- [159] **Ryan, J., Llinas, A.J., White, D.A., Turner, B.M. & Sommerville, J.** (1999). *Maternal histone deacetylase is accumulated in the nuclei of Xenopus oocytes as protein complexes with potential enzyme activity.* J. Cell. Sci. 112, 2441-2452.
- [160] **Wong, J., Patterson, D., Imhof, A., Guschin, D., Shi, Y.B. & Wolffe, A.P.** (1998). Distinct requirements for chromatin assembly in transcriptional repression by thyroid hormone receptor and histone deacetylase. *EMBO J.* 17, 520-534.
- [161] **Llinas, A.J.** (1998). *The activities of protein kinase CK2 in oogenesis of Xenopus Laevis.* PhD Thesis. University of St. Andrews Library.
- [162] **Ladomery, M., Wade, E. & Sommerville, J.** (1997). *Xp54, the Xenopus homologue of human RNA helicase p54, is an integral component of stored mRNP particles in oocytes.* NAR. 25, 965-973.
- [163] **Kohler, M., Haller, H. & Hartmann, E.** (1999). Nuclear protein transport pathways. *Expt. Nephrol.* 7, 290-294.
- [164] **Dingwall, C. & Laskey, R.A.** (1991). *Nuclear targeting sequence – a consensus?* Trends Biochem. Sci. 16, 478-481.
- [165] **Kaufman, P.D. & Botchan, M.R.** (1994). *Assembly of nucleosomes: do multiple assembly factors mean multiple mechanisms.* Curr. Opin. Genet. Devel. 4, 229-235.
- [166] **Callan, H.G., Gall, J.G. & Berg, C.A.** (1987). *The lampbrush chromosomes of Xenopus laevis; preparation, identification and distribution of 5S DNA sequences.* Chromosoma. 95, 236-250.

- [167] **La Marca, M.J., Strobel-Fidler, M.C., Smith, L.D. & Keem, K.** (1975). *Hormonal effects on RNA synthesis by stage VI oocytes of Xenopus laevis*. *Devel. Biol.* 47, 384-393.
- [168] **Newport, J.W. & Kirschner, M.W.** (1982). *A major developmental transition in early Xenopus embryos I. Characterization and timing of cellular changes at the mid blastula stage*. *Cell.* 30, 675-686.
- [169] **Lund, E. & Dahlberg, J.E.** (1992). *Control of 4-8S RNA transcription at the midblastula transition in Xenopus laevis embryos*. *Genes & Devel.* 6, 1097-1106.
- [170] **Almouzni, G. & Wolffe, A.P.** (1993). *Replication coupled chromatin assembly is required for the repression of basal transcription in vivo*. *Genes & Devel.* 7, 2033-2047.
- [171] **Almouzni, G. & Wolffe, A.P.** (1995). *Constraints on transcriptional activator function contribute to transcriptional quiescence during early Xenopus embryogenesis*. *EMBO J.* 14, 1752-1765.
- [172] **Rupp, R.A.W. & Weintraub, H.** (1991). *Ubiquitous Myo D transcription at the mid-blastula transition precedes induction-dependent Myo D expression in presumptive mesoderm of Xenopus laevis*. *Cell.* 65, 927-937.
- [173] **Steinbach, O.C., Wolffe, A.P. & Rupp, R.** (1997). *Accumulation of somatic linker histones causes loss of mesodermal competence in Xenopus*. *Nature.* 389, 395-399.
- [174] **Adamson, E.D. & Woodland, H.R.** (1974). *Histone synthesis in early amphibian development. Histone and DNA syntheses are not co-ordinated*. *J. Molec. Biol.* 88, 263-285.

- [175] **Turner, B.M., O'Neill, L.P. & Allan, I.M.** (1989). *Histone H4 acetylation in human cells: Frequency of acetylation at different sites defined by immunolabelling with site-specific antibodies.* FEBS Letts. 253, 141-145.
- [176] **Hassig, C.A., Fleischer, T.C., Billin, A.N., Schreiber, S.L. & Ayer, D.E.** (1997). *Histone deacetylase activity is required for full transcriptional repression by mSin3A.* Cell. 89, 341-347.
- [177] **Hassig, C.A., Tong, J.K., Fleischer, T.C., Owa, T., Grable, P.G., Ayer, D.E. & Schreiber, S.L.** (1998). *A role for histone deacetylase activity in HDAC1-mediated transcriptional repression.* Proc. Natl. Acad. Sci. USA. 95, 3519-3524.
- [178] **Kenzior, A.L. & Folk, W.R.** (1998). *AtMSI4 and RbAp48 WD-40 repeat proteins bind metal ions.* FEBS Letts. 440, 425-429.
- [179] **Lambright, D.G., Sondek, J., Bohm, A., Skiba, N.P., Hamm, H.E. & Sigler, P.B.** (1996). *The 2.0 angstrom crystal structure of a heterotrimeric G protein.* Nature. 379, 311-319.
- [180] **Sondek, J., Bohm, A., Lambright, D.G., Hamm, H.E. & Sigler, P.B.** (1996). *Crystal structure of a G(A) protein beta gamma dimer at 2.1 angstrom resolution.* Nature. 379, 369-374.
- [181] **Verreault, A., Kaufman, P.D., Kobayashi, R. & Stillman, B.** (1997). *Nucleosomal DNA regulates the core-histone-binding subunit of the human Hat1 acetyltransferase.* Current Biology. 8, 96-108.
- [182] **van der Vlag, J. & Otte, A.P.** (1999). *Transcriptional repression mediated by the human polycomb-group protein EED involves histone deacetylation.* Nature genetics. 23, 474-478.

- [183] **Ahmad, A., Takami, Y. & Nakayama, T.** (1999). *WD repeats of the p48 subunit of chicken chromatin assembly factor-1 required for in vitro interaction with chicken histone deacetylase 2*. J. Biol. Chem. 274, 16646-16653.
- [184] **Bolander, F.F.** (1994). *Molecular endocrinology*. 2nd Ed. Acad. Press. London.
- [185] **Songyang, Z., Shoelson, S.E., Chaudhuri, M., Gish, G., Pawson, T., Haser, W.G., King, F., Roberts, T., Ratnofsky, S. & Lechleider, R.J.** (1993). *SH2 domains recognize specific phosphopeptide sequences*. Cell. 72, 767-778.
- [186] **Weiss, A.** (1993). *T cell antigen receptor signal transduction: A tale of tails and cytoplasmic protein-tyrosine kinases*. Cell. 73, 209-212.
- [187] **Li, X., Shou, W., Kloc, M., Reddy, B.A. & Etkin, L.D.** (1994). *Cytoplasmic retention of Xenopus nuclear factor 7 before the mid blastula transition uses a unique anchoring mechanism involving a retention domain and several phosphorylation sites*. J. Cell. Biol. 124, 7-17.
- [188] **El-Hodiri, H.M., Shou, W. & Etkin, L.D.** (1997). *Xnf7 functions in dorsal-ventral patterning of the Xenopus embryo*. Devel. Biol. 190, 1-17.
- [189] **Li, X., Shou, W., Kloc, M., Reddy, B.A. & Etkin, L.D.** (1994). *The association of Xenopus nuclear factor 7 with subcellular structures is dependent upon phosphorylation and specific domains*. Expt. Cell. Res. 213, 473-481.
- [190] **Rihs, H-P, Jans, D.A., Fan, H. & Peters, R.** (1991). *The rate of nuclear cytoplasmic protein transport is determined by a casein kinase II site flanking the nuclear localization sequence of the SV40 T-antigen*. EMBO J. 10, 633-639.
- [191] **Jans, D.A. & Jans, P.** (1994). *Negative charge at the casein kinase II site flanking the nuclear localization signal of the SV40 large T-antigen is*

mechanistically important for enhanced nuclear import. Oncogene. 9, 2961-2968.

[192] Schwab, M.S. & Dreyer, C. (1997). *Protein phosphorylation sites regulate the function of the bipartite NLS in nucleolin.* Eur. J. Cell Biol. 11, 857-866.

[193] Li, J., Meyer, A.N. & Donoghue, D.J. (1997). *Nuclear localization of cyclin B1 mediates its biological activity and is regulated by phosphorylation.* Proc. Natl. Acad. Sci. USA. 94, 502-507.

[194] Bürglin, T.R., Mattaj, I.W., Newmeyer, D.D., Zeller, R. & De Robertis, E.M. (1987). *Cloning of nucleoplasmin from Xenopus laevis oocytes and analysis of its developmental expression.* Genes & devel. 1, 97-107.

[195] Görlich, D. & Mattaj, I.W. (1996). *Nucleocytoplasmic transport.* Science. 271, 1513-1518.

[196] Stochaj, U. & Rother, K.L. (1999). *Nucleocytoplasmic trafficking of proteins: with or without Ran?* BioEssays. 21, 579-589.

[197] Kouzarides, T. (2000). *Acetylation: a regulatory modification to rival phosphorylation?* EMBO J. 19, 1176-1179.

[198] Bannister, A.J., Miska, E.A., Görlich, D. & Kouzarides, T. (2000). *Acetylation of importin- α nuclear import factors by CBP/p300.* Current Biology. 10, 467-470.

[199] Mattaj, I.W. & Conti, E. (1999). *Snail mail to the nucleus.* Nature. 399, 208-210.

[200] Cingolani, G., Petosa, C., Weis, K. & Müller, C.W. (1999). *Structure of importin- β bound to the IBB domain of importin- α .* Nature. 399, 221-229.